UMTRI-85-55-3

Experimental Data for Development of Finite Element Models: Head/Thoraco-Abdomen/Pelvis

Volume III : PELVIS

Guy S. Nusholtz
Patricia S. Kaiker

Contract Number:
DOT-HS-7-01636

FINAL TECHNICAL REPORT
DECEMBER 1985

UMTRI The University of Michigan
Transportation Research Institute

Technical Report Documentation Page

1. Report No.	2. Government Accession No.	3. Recipient's Catalog No.

4. Title and Subtitle	5. Report Date
Experimental Data for Development of Finite Element Models Head/Thoraco-Abdomen/Pelvis: Vol.III Pelvis	December 31, 1985
	6. Performing Organization Code
7. Author(s) Guy S. Nusholtz and Patricia S. Kaiker	8. Performing Organization Report No. UMTRI-85-55-3
9. Performing Organization Name and Address Biosciences Division, Transportation Research Institute, The University of Michigan, 2901 Baxter Road, Ann Arbor, MI 48109	10. Work Unit No.
	11. Contract or Grant No. DOT-HS-7-01638
12. Sponsoring Agency Name and Address National Highway Traffic Safety Administration Department of Transportation, Seventh and E Streets, S.W., Washington, DC 20590	13. Type of Report and Period Covered July 1977 - Dec. 1983
	14. Sponsoring Agency Code

15. Supplementary Notes

Experimental data.

16. Abstract

Validation of biomechanical computer models of impact biodynamics cannot be accomplished without descriptive experimental data. The research program, therefore, involved data gathering on the kinematics and damage response of three human cadaver subsystems: the head, the thoraco-abdomen, and the pelvis. 14 unembalmed human cadavers were utilized in 68 dynamic impact tests. The research program entailed 14 head impacts (6 subjects), 41 thoraco-abdominal impacts (11 subjects), and 13 pelvis impacts (10 subjects). In addition, the thoraco-abdominal tests were supplemented with static three-point bending tests conducted on rib specimens from 5 of the dynamically tested cadavers.

17. Key Words	18. Distribution Statement
Impact Biomechanics, Head, Thoraco-Abdomen, Pelvis, Experimental Data	

19. Security Classif. (of this report)	20. Security Classif. (of this page)	21. No. of Pages	22. Price
		309	

TABLE OF CONTENTS - PELVIC SERIES

LIST OF FIGURES - PELVIC SERIES

Figure

LIST OF TABLES - PELVIC SERIES

Table

CHAPTER 3

EXPERIMENTAL DATA FOR DEVELOPMENT OF FINITE ELEMENT MODELS - PELVIS

Contract No. DOT-NHTSA-C-HS-7-01636 UM Acct. No. 015651

1.0 INTRODUCTION

The research program, Experimental Data for Development of Finite Element Models, involved data gathering on the kinematic response of three human cadaver subsystems: 1) the pelvis, 2) the head, and 3) the thoraco-abdomen. Each impact target investigation is presented as a self-contained chapter in this final report. This chapter presents the pelvis series, Chapter 1 presents the head series, and Chapter 2 presents the thoraco-abdomen series.

The research program utilized 14 cadavers in 68 dynamic impact tests. For the pelvis subsystem experiments, 10 subjects received a total of 13 impacts; for the head series, 6 subjects received a total of 14 impacts; and for the thoraco-abdomen, 11 subjects received a total of 41 impacts.

2.0 BACKGROUND

Pelvic injuries of varying type and severity have been found to occur in a significant number of automotive accidents [16-17,20,30,32]. Investigations of trauma of the pelvis resulting from impact in an automotive environment have been documented primarily through accident investigation methods. There have only been a limited number of biomechanical studies attempting to research pelvic impact trauma under laboratory conditions. One of the earliest of these studies was conducted by Evans and Lissner in 1955 [11], and consisted of impacts to the denuded pelvis in the inferior-superior direction. Although no fracture tolerance data were obtained, it was concluded from this study that the pelvis exhibited elastic behavior and failed due to tensile

stresses in various structural members. Ten years later a study of the behavior of the knee-femur-pelvis complex in an automotive impact environment was reported by Patrick, et al. [26]. In this series of tests, an impact sled was used to apply femoral-axis impacts to the knee of embalmed cadavers. The lowest applied load found to cause pelvic injury was 7.1 kN, and loads ranging from 8.5 kN to 17 kN were found to cause multiple fractures of the pelvis. It was suggested that a maximum force criterion (of about 6.2 kN) should be the threshold level for injury of the patella/femur/pelvis complex. A similar study using unembalmed cadavers was reported by Melvin and Nusholtz in 1980 [22]. A single pelvis fracture was found to occur at an applied load of about 20 kN, however loads up to 26 kN were applied with no resulting pelvis injury [22].

A recent biomechanical study of pelvic impact in an automotive environment was documented first in 1979 [28] and more completely in 1980 [7] by Cesari and Ramet. The goal of the research was to supply data for design of side door padding by impacting cadavers laterally to the pelvis and recording the force/injury relationships observed. It was suggested from this study that the pelvic response to impact is characterized by velocity of impact, maximum force, and force impulse. Admissible force tolerance for females was documented as 5-7 kN (1100-1600 lb) and for males as 7-13 kN (1600-2900 lb) [7,28]. These studies essentially characterized the injury tolerance of the pelvis using maximum force and force impulse indicators.

To further investigate the kinematic and injury response of the pelvis in automotive environment impacts, a series of tests involving indirect impacts to the pelvis has been conducted by the Biomechanics

Department at UMTRI [23]. The tests were conducted using unembalmed cadavers and two types of impact facilities: a linear pendulum impactor and a pneumatic impactor. Indirect loads were delivered to the acetabulum of the pelvis by impacting the femur either axially or laterally. This allowed loads to be delivered to the acetabulum in either anterior-to-posterior or right-to-left directions. The cadavers were instrumented to measure pelvic triaxial accelerations in all tests, while in some tests three-dimensional motion of the pelvis was recorded with nine accelerometers. Additionally, triaxial accelerations of the right and left femurs and thoracic vertebra T8 were measured. Photographic targets on the pelvis and femurs were used for photokinemetric analysis of motion due to the impact. The conclusions were:

(1) Complete description of three-dimensional motion is invaluable to the understanding of pelvic response.

(2) The complex nature of the response of the femur/pelvis/soft tissue system, the variability of subjects, and resulting damage patterns may preclude the determination of a single tolerance criterion such as maximum force or peak acceleration response.

(3) In lateral impacts, energy-absorbing and load-distributing materials are effective means of transmitting greater amounts of energy to the pelvis without ensuing damage.

(4) The nature of the impactor/femur/pelvis interaction, as well as the biometrics of the population at large are critical factors in understanding the response of the pelvis to impact and subsequent damage patterns.

The work being reported in this document is a continuation of those experiments which investigated the results of indirect impacts to the pelvis summarized above [23]. Appendix F is the earlier research article [23].

3.0 ANATOMICAL CONSIDERATIONS

The bony pelvis (Figure 1) consists of two large, flat, irregularly shaped hip (innominate) bones that join one another at the pubic symphysis on the anterior midline. Posteriorly, the wedge shaped sacrum completes the pelvic ring forming a relatively rigid structure.

In the adult, each hip bone is formed by the fusion of three separate bones, the ilium, ischium, and pubis, which join at the acetabulum. The ilium forms the broad upper lateral part of the hip bone and the upper portion of the acetabulum. Its upper curved edge is the iliac crest. The prominence on this crest is known as the anterior-superior iliac spine. Posteriorly, the crest ends in the posterior iliac spine, adjacent to its articulation with the sacrum, the sacroiliac joint. The ischium forms part of the acetabulum and has a superior ramus that ends below in the ischial tuberosity. From there the inferior ramus ascends to join with the inferior ramus of the pubic bone. Together this bar of bone is frequently referred to as the ischio-pubic ramus or inferior pubic ramus. The body of the pubic bone forms the anterior part of the acetabulum. From here the superior pubic ramus passes to the midline where it joins its fellow of the opposite side through the pubic symphysis. Beneath the superior pubic ramus, the inferior pubic ramus joins the inferior ischial ramus. The posterior-lateral bony pelvis is covered by multiple muscle layers, buttock fat and skin. The iliac crest is relatively free of heavy musculature. The

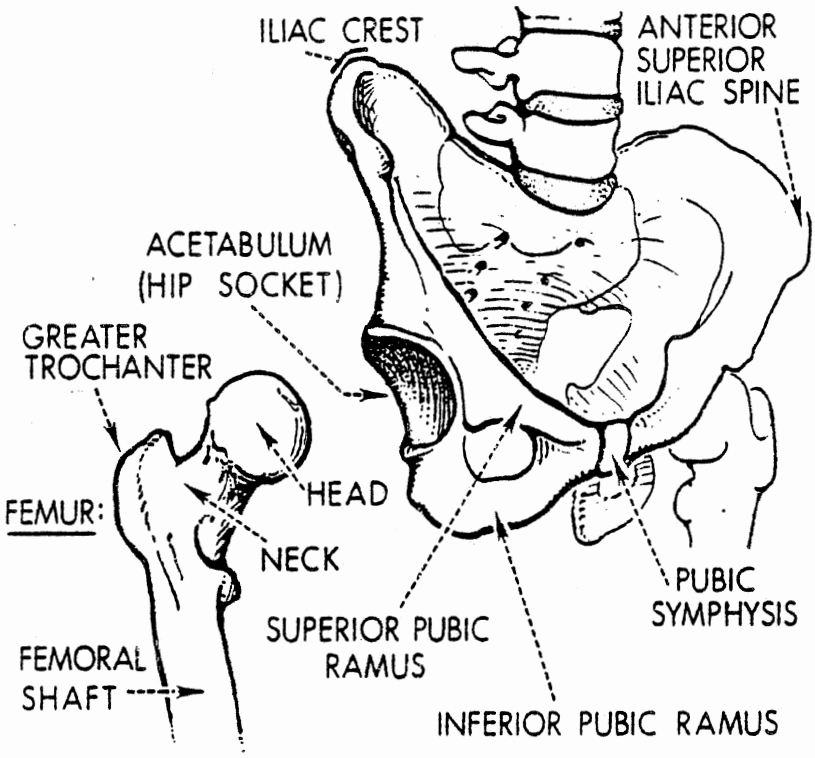

A. Pelvic Anatomy

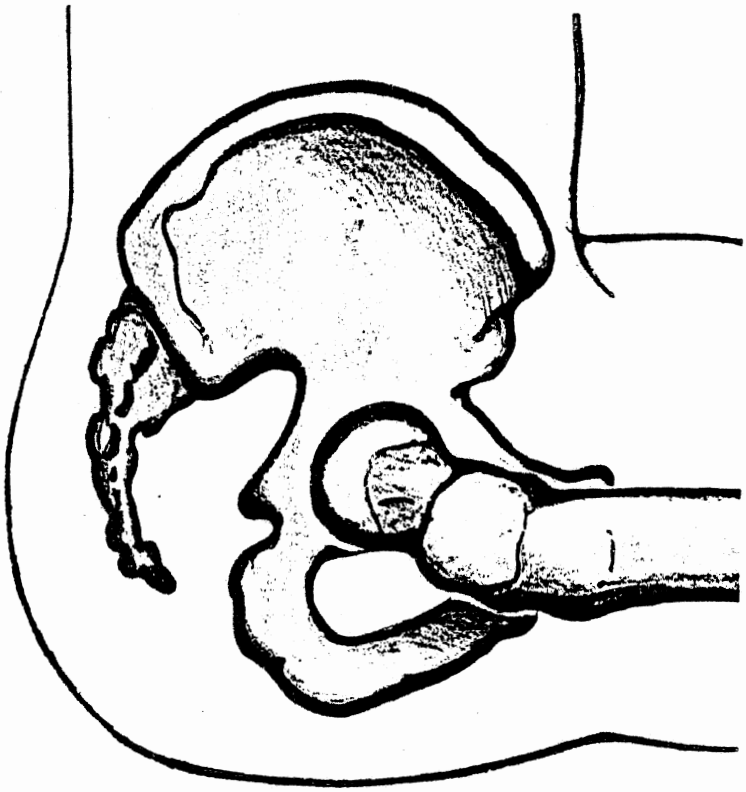

B. Pre-Impact Position

Figure 1

rounded head of the femur articulates with the acetabulum and is held within the socket by ligaments. On the lateral upper femur is the greater trochanter, a large bony prominence, to which muscles attach.

4.0 GOAL OF PELVIC SERIES IMPACT TESTING

The goal of the pelvic test series was to investigate the relationship between selected kinematic parameters and resultant tissue damage caused by blunt indirect impact to the pelvis of the unembalmed human cadaver[1] as a surrogate model for living humans. The kinematic parameters selected were force/angular and translational accelerations and velocities. A series of laboratory techniques precisely defined the selected kinematic and injury parameters. The impacting surface was padded with various materials to produce different force-time and load distribution characteristics. High speed photokinemetrics were obtained using standard techniques. Assessment of tissue damage was obtained by gross autopsy observations.

Two series of pelvic impacts were conducted. In the first series, 5 cadavers were subjected to an indirect lateral pelvic impact delivered by a 25 kg mass using either a linear or a pneumatic ballistic pendulum impactor. An additional subject received duplicate impacts. The right hip was impacted 8 cm anterior to the trochanterion landmark. This provided indirect loading of the acetabulum in the right-to-left direction. Impact force and triaxial acceleration at three points on the pelvis were recorded. The three triaxial accelerometer clusters used to document three-dimensional motion were mounted on a magnesium

---

[1]The protocol for the use of cadavers in this study was approved by the University of Michigan Medical Center and followed guidelines established by the U.S. Public Health Serivce and those recommended by the National Academy of Sciences, National Research Council.

plate rigidly affixed to the pelvis. In the second test series, 4 cadavers were subjected to a similar indirect lateral pelvic impact delivered by a 20 kg mass pneumatic impactor. Three subjects received a single impact, while another received triplicate impacts. Only impact force was recorded for the second test series.

Impact load and pelvic acceleration data are presented in this chapter as functions of both time and frequency in the form of mechanical impedance. Injury descriptions based on gross autopsy are provided. The kinematic response of the pelvis during and after impact is presented to indicate the similarities and differences in response of the pelvis for various load levels. While the impact response data cannot prescribe a specific tolerance level for the pelvis, they do indicate variables which must be considered and some potential problems in developing an accurate injury criterion.

5.0 METHODOLOGY:

5.1 Methods and Procedures of Impact Testing:

5.11 Subjects - 10 unembalmed male cadavers were tested. The cadavers were obtained by UMTRI from the University of Michigan Medical School Department of Anatomy. Following transfer to UMTRI, the cadavers were stored for a short time at 4° C until subsequent use. The cadavers were sanitarily prepared, anatomically measured, and examined radiologically prior to the installation of accelerometer hardware. See Table 1 for subject biometrics.

The execution and coordination of the testing sequence was guided by the use of a detailed protocol which is included in Appendix B in Chapter 2 [1-32]. The testing sequence is outlined below and additional information about application of specific techniques is available elsewhere [1,15,21-24,31]. Six groups of procedures are associated with the impact testing-data gathering-analysis activities. They are: 1) pre-test preparation, 2) instrumentation surgery, 3) trial test, 4) impact testing, 5) post-test autopsy and injury coding in DOT format, and 6) data analysis and report.

5.12 Pre-test Preparation - The arrival of a test subject cannot be predicted more than a half a day in advance. Generally, preparation for a test sequence begins the day a subject is received. The subject requires a day and a half of preparation, which is sufficient time to set up the impact lab and run equipment checks which include a trial test. The areas requiring special preparation are outlined below.

Table 1. Biometric Data

Cadaver No.	Test No.	Cause of Death	Age	Stature cm	Waist Breadth cm	Hip Breadth cm	Weight Kg
000	82E008	Cardiac arrest	60	184	29.2	25	52
020	82E028	Cardiac arrest	67	180	24	36	77
040	82E049	Myocardial infarction	65	169	32	33.5	87
050	82E051 82E052 82E053	Coronary thombosis	60	180	-	-	67
060	82E067	Cardiac arrest	60	170	23	28.6	67
070	82E071	Cardiac arrest	61	181	-	-	55
080	83E087 83E088	Pulmonary edema	44	171	25	31.4	72
079	83E091	Myocardial infarction	62	176	-	31.5	76
090	83E093	Cerebral contusion	51	180	-	30	68
100	83E109	Cardiac arrest	60	182	31.3	33.9	77

Morgue - Cadaver subjects are stored there at 4°C in coolers until subsequent use.

Anatomy Lab - Sanitary preparation, anthropometry [30-31], and surgical instrumentation of the test subject is done in the Anatomy Lab. All tools, materials, and instrumentation equipment necessary to prepare the subject are constructed or laid out in advance. Included in the setup are surgical instruments, measuring equipment, gauze and toweling, accelerometer mounting hardware, support harnesses and clothing for the cadaver subjects.

Radiology Lab - The table and X-Ray head are positioned and a sufficient supply of film is loaded into the X-ray cassettes. Adequate film is loaded so that the test sequence can be completed without interruption. Each subject is X-rayed here when it is received to check for structural integrity and surgical implants.

Dark Room - Chemicals are mixed for X-Ray developing. Labels for X-Rays are prepared. Courier forms and packaging for the 16 mm high-speed films are readied.

Physiology Lab - 16 mm high-speed films are chemically hypersensitized in order to obtain better image clarity in an oven at 30-35°C with forming gas for 24 hours.

Impact Lab - Test facilities, recording equipment, and accelerometers must be assembled, wired, and trial tested. In addition, a portable cart containing equipment for instrumenting the subject with accelerometers is prepared. Impact padding and support materials for the subject are

assembled near the impact device. The high-speed cameras are readied. All electrical equipment is connected to a power source.

Impact Lab and Instrumentation Room Electronics - The input/output voltage characteristics of all analog tape channels are checked by calibration at predetermined voltage levels. The tape channel calibrations are determined when the test pulses are played back off tape through a computer routine.

All accelerometers are labeled and wired through a patch panel into the Instrumentation Room. From there, the signals are passed through amplifiers if necessary and wired to their designated channels as input to the analog tape recorders. Amplifiers are adjusted for the proper gain. Accelerometer excitation voltages are set on the amplifers, and their piezoresistive nature also requires that balancing be perfor med. Instrumentation Room wiring cannot be completed until the timer unit and the devices it operates, such as high-speed cameras, lights, and ropecutters, are connected and set for the proper control, delay and run times. Final wiring is completed in the Instrumentation Room and the impacting device is prepared for a trial test.

5.13 Surgery - In the Anatomy Lab the test subject is surgically instrumented with the required test hardware. The hardware consists of a pelvic accelerometer mount.

Nine-Accelerometer Pelvic Plate - The nine-accelerometer plate (Figure 2) is installed in the following manner. Four lag bolts are screwed into the posterior-superior iliac spines,

within the dimensions of the magnesium plate to be mounted. Quick setting dental acrylic is molded around the bolts to form a securing medium, and the accelerometer plate is placed into the acrylic.

5.14 Trial Test - To insure that all mechanical and electronic equipment is functioning and wired appropriately for the test design, trial tests of the equipment are performed on the day before the test, allowing sufficient time to locate and correct system defects. Accelerometers, amplifiers, umbilical cables, and recorders are tested by suspending a rubber cyclinder weighing approximately 20 pounds in front of the designated impactor with all the necessary accelerometers taped to it. A preliminary check of the accelerometers and amplifiers is made to insure proper balancing and noise levels. The striker is then manually released and the rubber cylinder impacted. The signals from all accelerometers are recorded on the analog tape recorders. All channels are played back immediately on the brush chart recorder for inspection purposes. The striker accelerometer is also tested in this procedure. The timerbox, cameras, lights, ropecutter and velocity probe are tested individually. Triaxial clusters are then labeled for their specific point of attachment to the subject and placed in protective sleeves.

Three classes of operations take place before and during impact that are necessary for the documentation of the impact event: events associated with recording of electromechanical accelerometer output, events associated with photometrics documentation, and events associated with the impacting device.

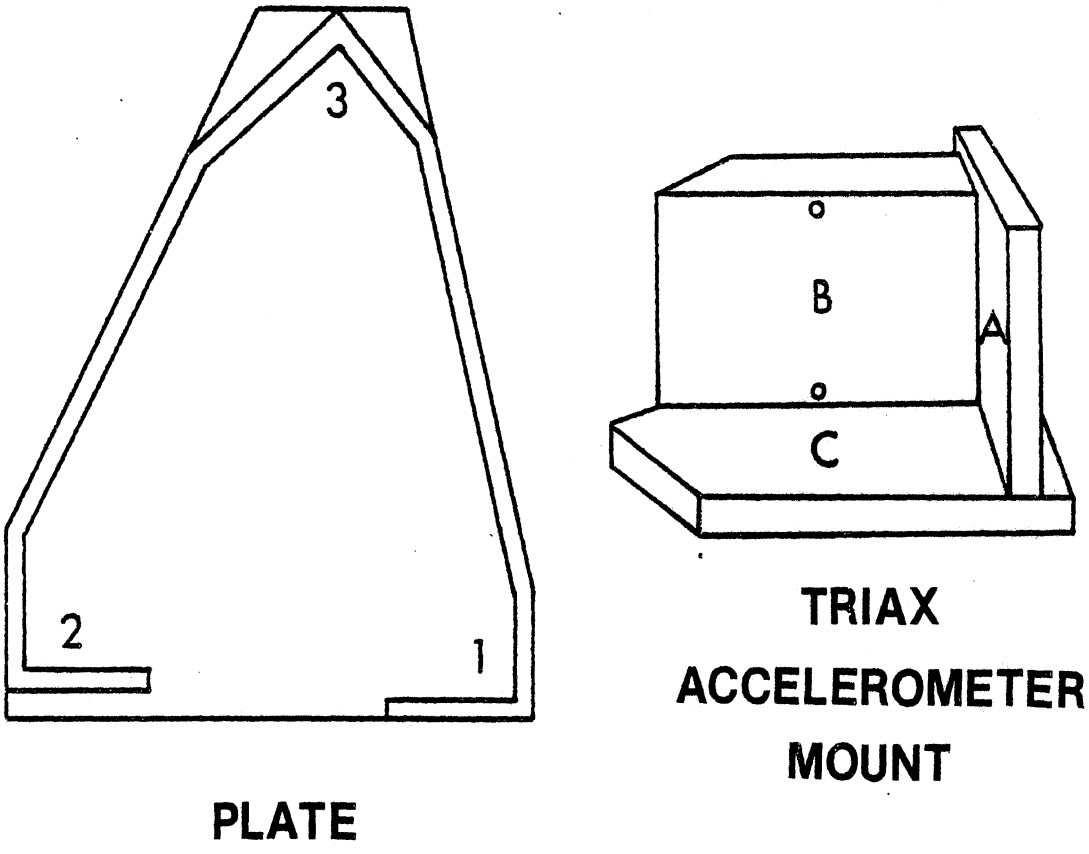

Figure 2

Nine-Accelerometer Pelvic Plate

Timing - The impact test event sequence is initiated by an operator-controlled manual switch and is thereafter controlled by signals generated by a specially constructed timing unit. The synchronization of the events associated with these signals is such that the lights are fully illumniated and the cameras are powered and running at the preset speed when the impact test takes place. In addition, the cameras are sequenced such that they are operational for the minimum amount of time. This economizes the amount of effort associated with photokinemetric documentation (changing film, etc.) and allows for a smoother running test sequence.

The recording equipment must be at operational speed before the striker is released. During the impact event, the output of the piston accelerometer must be fit into a "corridor" or window so that the pre-impact acceleration from rest and the post-impact acceleration from end-of-stroke are not recorded. The striker must be released so that impact will occur within the assigned time corridor. A sychronizing contact strobe, which places simultaneous electrical and photographic signals on the analog tape and high-speed film, must occur near the beginning of impact.

Equipment - The basic test equipment includes the timing control unit, a signal conditioning device for the force signal, the accelerometer patch panels, the accelerometers, the impacting device, cameras, the photographic lights, and the restraints (hoists). Each piece that plays a significant role in the data acquisition is described below.

Linear Pendulum Impacts -- The linear pendulum impact device (Figure 3) consisted of a free-falling pendulum as an energy source which struck a 25 kg impact piston. The impactor, guided by a set of Thompson linear ball bushings, was brought to impact velocity prior to impact and traveled up to 25 cm before being arrested. Axial loads were measured with either a load cell or a Setra model 111 accelerometer. Impact conditions between tests were controlled by varying impact velocity and the type and depth of padding on the impact piston surface. The piston excursion and the distance the piston traveled from the point of contact to the point of arrest ranged from 3 to 20 cm. The velocity of the piston was measured by timing the pulses from a magnetic probe which sensed the motion of targets on the piston.

For the first series tests conducted with this device, the subject was placed in a restraint harness and suspended in a seated position. Indirect lateral impacts to the acetabulum were delivered by impacting the trochanteric region of the right femur, along the axis of the neck of the femur.

Pneumatic Ballistic Pendulum Impacts - The UMTRI ballistic pendulum impact device (Figure 4) consisted of an air reservoir, a ground and honed cylinder, and a carefully fitted piston mechanically coupled to a ballistic pendulum. The piston, propelled by compressed air through the cylinder from the air reservoir chamber, served to accelerate the ballistic pendulum. The 10-150 kg mass of the ballistic pendulum was set at 25 kg for these tests. The piston was arrested at the end

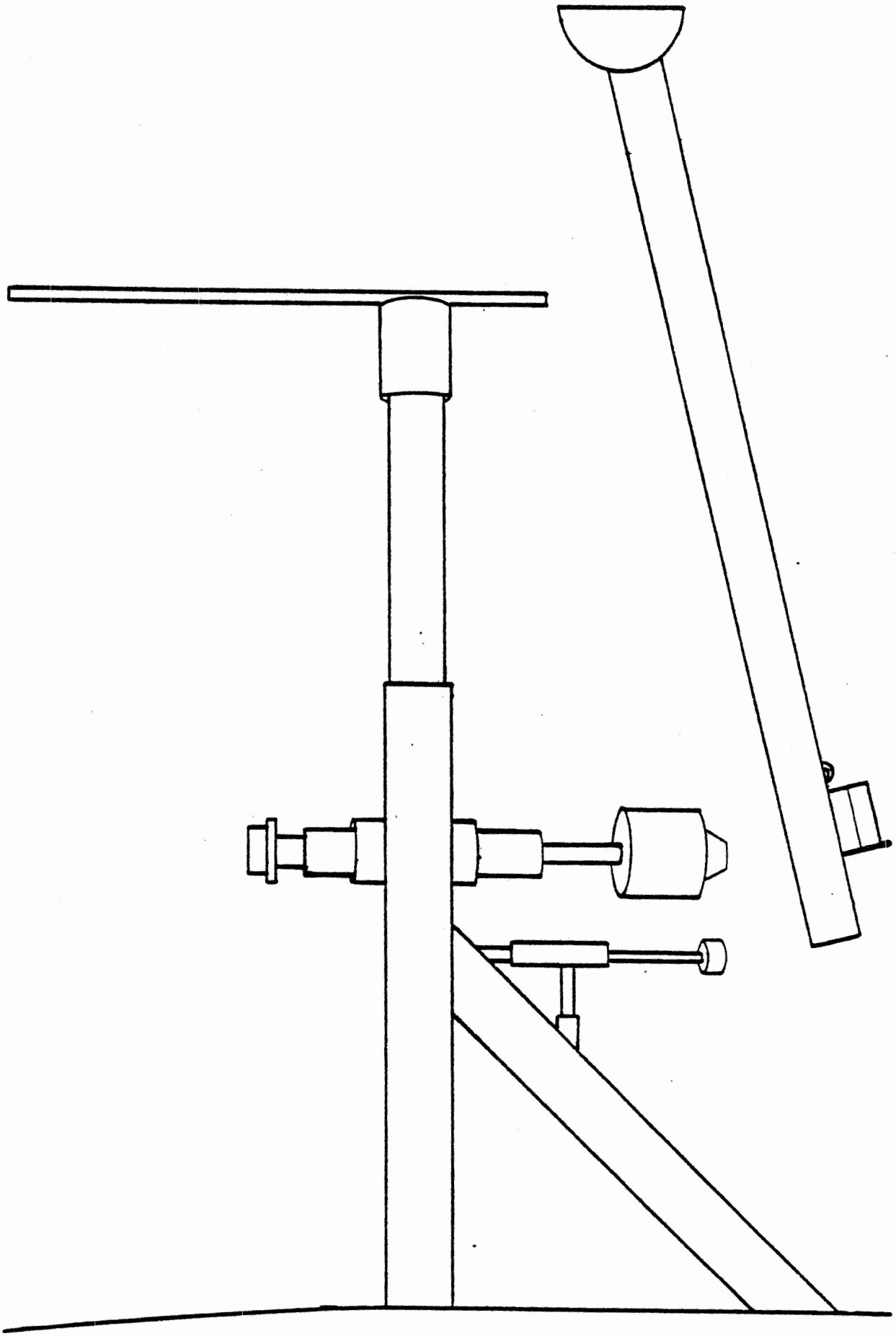

Figure 3

Linear Pendulum Impact Device

of its travel, allowing the ballistic pendulum to become a free-traveling impactor. The ballistic pendulum was fitted with an inertia-compensated load cell.

For the first series tests conducted with this device, the subject was placed in a restraint harness and suspended in a seated position similar to the linear pendulum impacts. An indirect lateral impact to the acetabulum was delivered by impacting the right hip 8 cm anterior to the trochanterion landmark, along the axis of the neck of the femur.

Pneumatic Impacts -- The cannon pneumatic impact device (Figure 5) consisted of an air reservoir which was connected to a honed steel cylinder. A driver piston was propelled down the cylinder by the pressurized air in the reservoir. The driver piston contacted a striker piston affixed with a piezoelectric accelerometer and a piezoelectric load washer, in order to determine the acceleration-compensated contact loads applied to the test subject. The mass, velocity, and stroke of the striker piston could be varied to provide the desired impact conditions for a particular test. For the second series tests conducted with this device, a 20 kg mass was selected. The velocity of the impactor was measured by timing the pulses from a magnetic probe which sensed the motion of targets on the impactor.

For the cannon tests, the subject was suspended by a body harness and an overhead pulley system while seated on blocks of balsa wood upon a mobile table. Impacts were delivered indirectly to the pelvis via the right hip as described above.

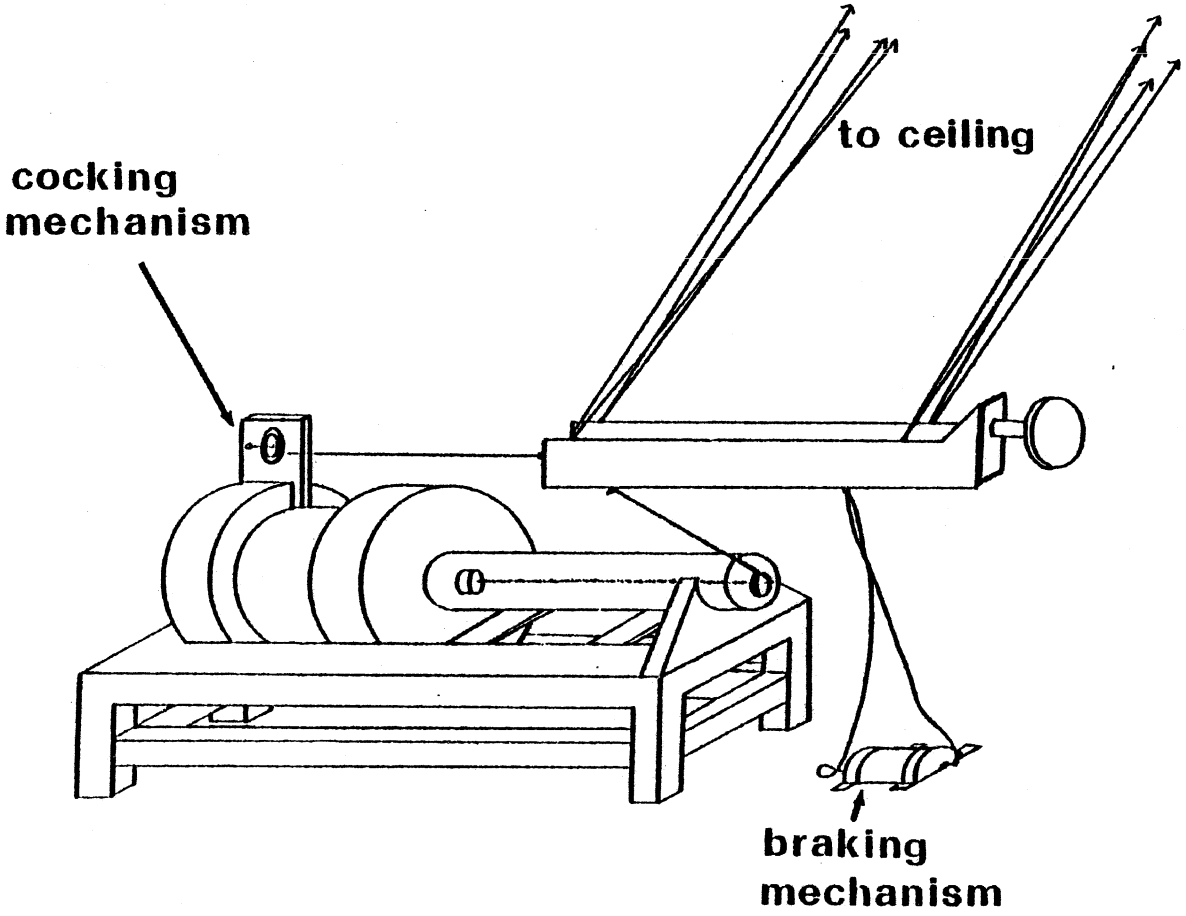

Figure 4

Pneumatic Ballistic Pendulum Impact Device

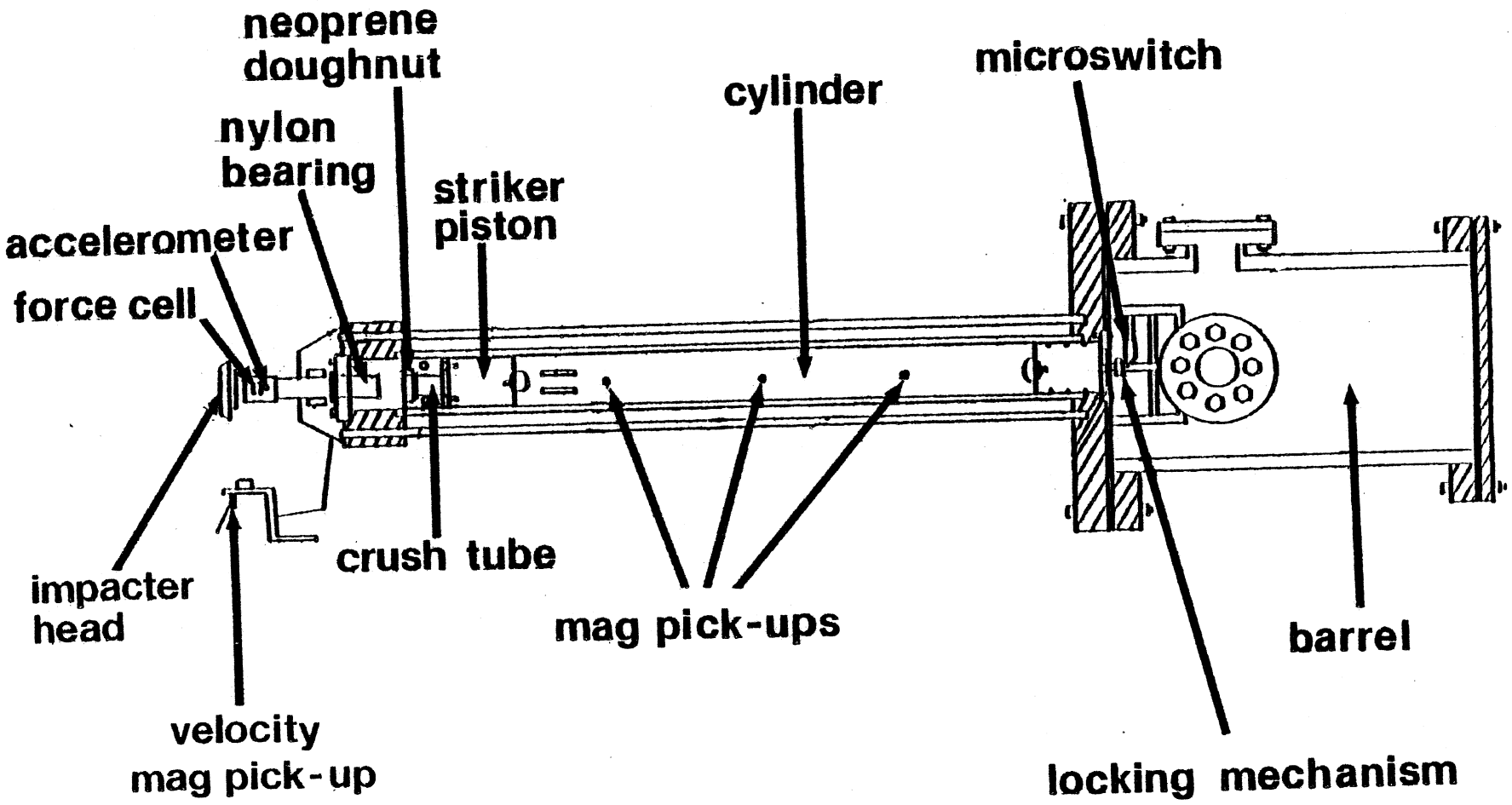

Figure 5

Cannon Pneumatic Impact Device

Data Handling - All accelerometer time-histories (impact force, impactor acceleration, nine pelvic accelerations) were recorded unfiltered on either a Honeywell 7600 or 9600 FM Tape Recorder. All data was recorded at 30 ips. The analog data on the FM tapes was played back for digitizing through the appropriate anti-aliasing analog filters. The analog-to-digital process for all data, results in a digital signal sampled at 6400 Hz equivalent sampling rate. Raw transducer time-histories were digitally filtered with a Butterworth filter at 1650 Hz, 4th order.

Acceleration Measurement -- Accelerations were measured in three orthogonal directions at three sites on the pelvis proximal to each other with Endevco 2264-2000 piezoresistive accelerometers. The three triaxial accelerometer clusters were secured to a single mounting platform on the pelvis. The location of the center of gravity of the pelvis, the coordinate system of the triaxial clusters, and the nine-accelerometer array are shown in Figure 6.

Photokinemetrics System - The motion of the subject was determined from high-speed (1000 frames per second) film by following the motion of single-point phototargets on the pelvis and impactor piston. For selected impacts, a Hycam camera operating at 3000 frames per second provided a close-up lateral view of the pelvis. A Photosonics 1B camera provided an overall lateral view at 1000 frames per second.

Analytical photogrammetry was used in these experiments to describe the geometry of anatomical structures and their motion

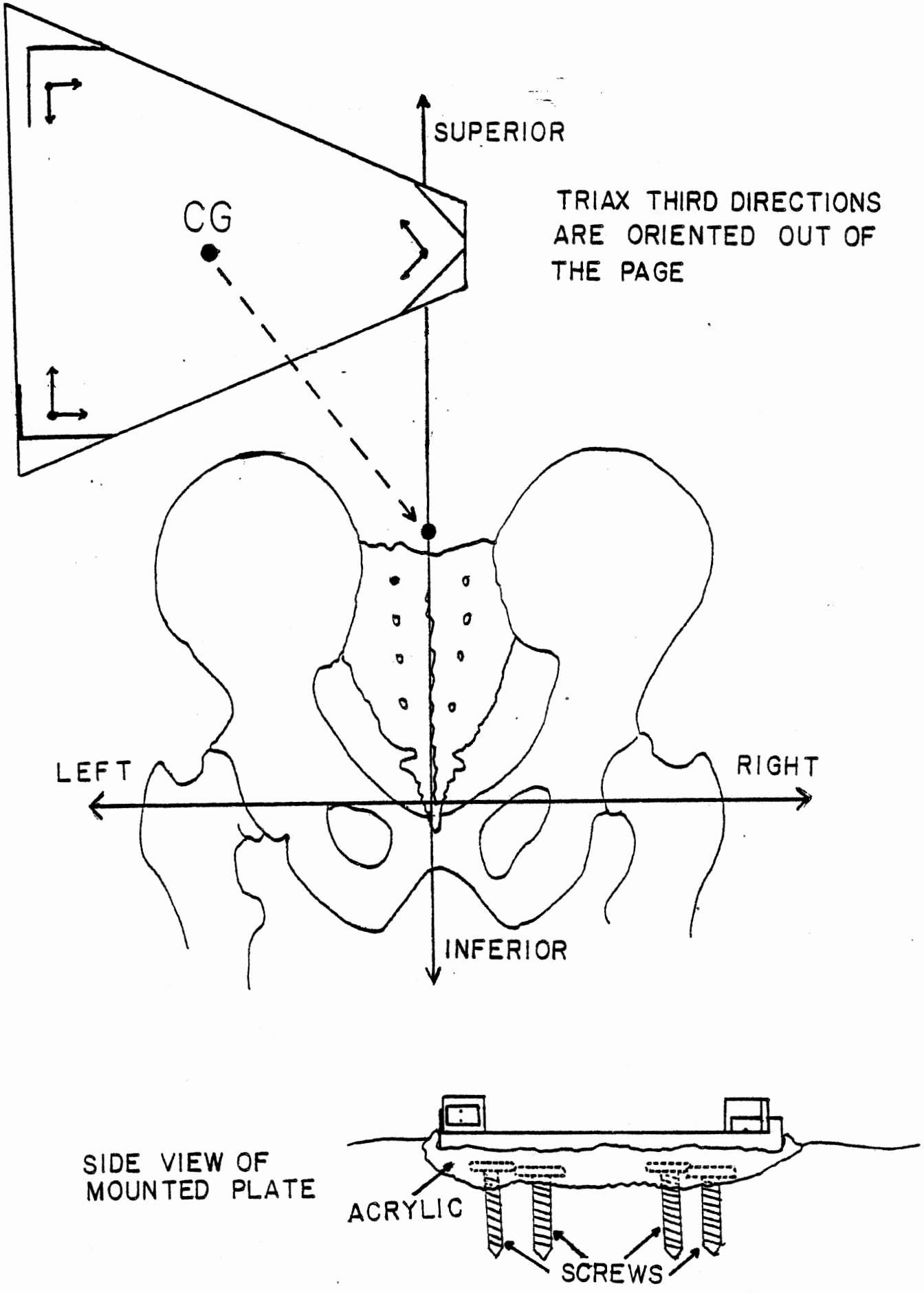

Figure 6

Accelerometer Coordinate System

in the laboratory reference frame. The objective space coordinates of points of interest were obtained once the coordinates of well-defined points in an image space and the calibration translation and rotations were specified. The points in an image space were obtained with photographic equipment and were preserved on film.

Motion of the pelvis in space was obtained by measuring the time-history of the position of a photographic target which had a well-defined position and orientation, relative to a predefined anatomical landmark. Defined descriptors such as position, velocity, and acceleration were associated with rigid body motion in object space. Once these motion descriptors were determined and digitized, they could then be used to characterize the dynamic response of the subject under study and to assist in understanding injury mechanisms.

In these tests the chosen descriptors were based upon anatomical structures in a two-dimensional image space produced by a camera. The descriptors were restricted to the two-dimensional plane of the film and thus did not take into account rotations and translations which moved objects in and out of the plane of gross whole body motion.

Test Subject Preparation - The unembalmed cadavers were stored at 4°C prior to testing. The cadaver was X-Rayed as part of the structural damage evaluation and anthropomorphic measurements were recorded. Next, the cadaver was instrumented, sanitarily dressed and transported to the testing

room where the accelerometers are attached. The subject was positioned. Pre-test photographs were taken. The subject was then impacted.

5.15 Initial Test Conditions - For all tests in both series, the subject was placed seated in a restraint harness which was in turn suspended from the ceiling. (See Figure 7.) The impactor was either rigid and unpadded or padded with a variety of materials in different padding combinations of Ensolite, A-L Ensolite, styrofoam, energy absorbing foam, or APR paddings. Table 2 presents a summary of initial conditions and padding. The target area for all impacts in both test series was 8 cm anterior to trochanterion centered on the greater trochanter of the right femur. Impact occurred in the right-to-left direction.

5.16 Post-Test Autopsy - After impact testing, the test subject was brought to the Anatomy Lab for autopsy. A gross autopsy was performed. All injuries were recorded in the test protocol on charts and brief descriptions were also written in the protocol. 35 mm still photographs in color and in black and white were taken of all significant tissue damages. These were later coded according to the AIS-80 scheme and reported in DOT format. Occasionally, knowledgeable medical professionals were consulted when more descriptive information might better characterize the observed tissue damages than the AIS-80 coding permits. All of this information was used in the analysis and reconstruction of mechanisms of injury and is included in the written reports to the sponsor.

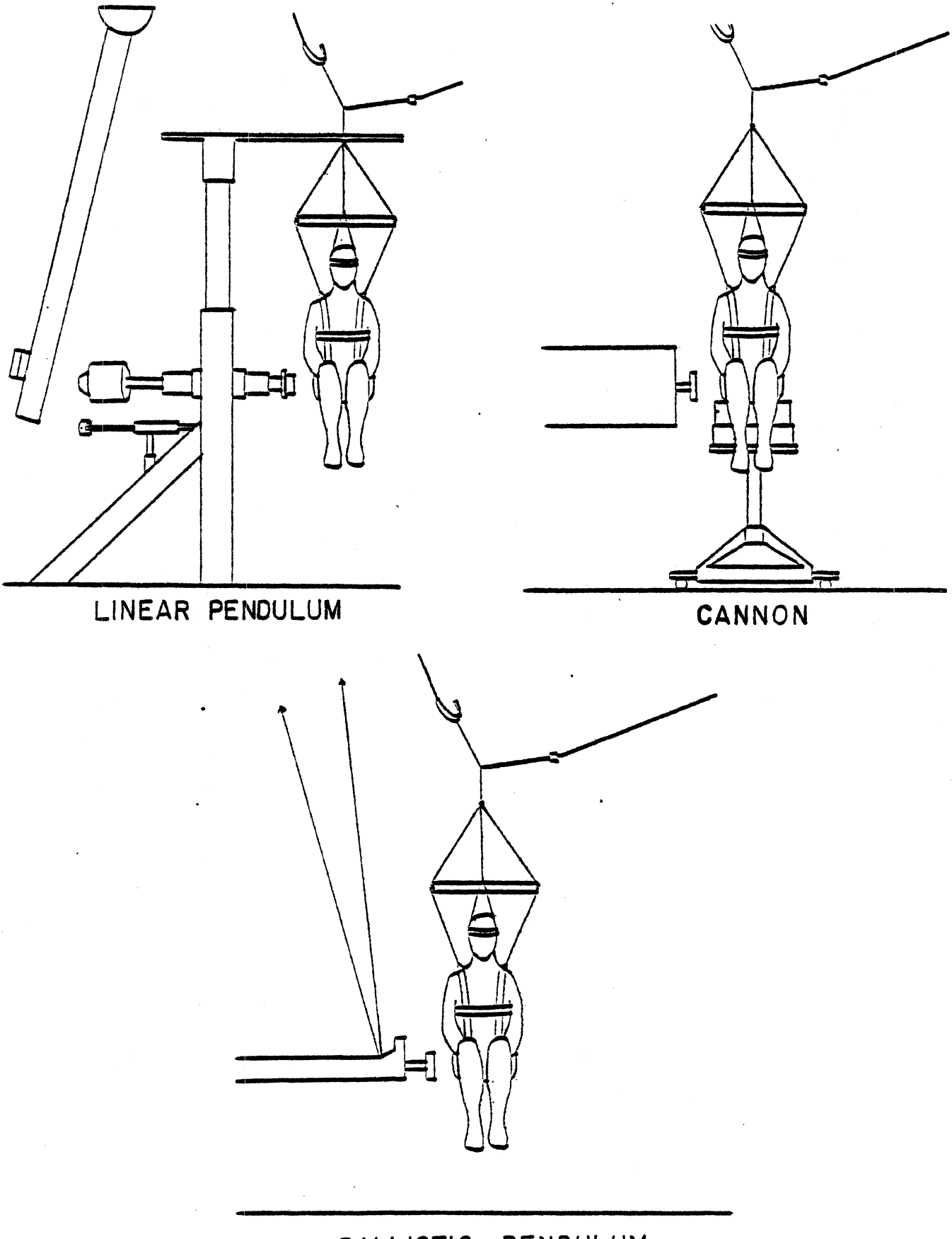

Figure 7

Initial Test Conditions

5.2 Data Analysis and Report - The techniques used to analyze the results are outlined below. Additional information can be found in [1,15,21-24,31].

5.21 Force-Time Duration Determination - In order to define the pulse duration, a standard procedure was adopted which determined the beginning and end of the pulse. The procedure was to first determine the peak and the time at which it occurs. Next, the left half of the pulse, defined from the point where the pulse started to rise until the time of the peak, was least-squares fitted with a straight line. This rise line intersected the time axis at a point which was taken as the formal beginning of the pulse. For those tests which exhibited multimodal signals, the least-squares line was fitted from where the pulse started until the time of the first significant peak. A similar procedure was followed for the right half of the pulse, i.e., a least squares line was fitted to the fall section of the pulse which was defined from the peak to the point where the first pulse minimum occurred. The formal end of the pulse was then defined as the point where the fall line intersects the time axis. In many cases, however, the formal end of the pulse as defined was not the end of contact between the impactor and the subject. In these instances, two durations were used: one to indicate the end of the most significant aspect of the force-time-history and one to indicate the end of the contact.

5.22 Frame Fields - One method for analyzing the motion of a material body such as the pelvis is to analyze the motion of a

point on that body. In the case of the tests performed in this research program, the point chosen was midway between the posterior-superior iliac spines. The motion of this point was analyzed using the concept of a moving frame discussed elsewhere [15] and briefly summarized here.

A vector field is a function which assigns a uniquely defined vector to each point along the path generated by a moving point. Similarly, any collection of three mutually orthogonal unit vectors emanating from each point on the path is a frame field. Thus, any vector defined on the path (for example, acceleration) may be resolved into three orthogonal components of any well defined frame field.

In biomechanics research, frame fields are frequently used which are defined based on anatomical reference frames. The anatomical references frames used are shown in Figure 8. The frames are based on the anatomical orientation of a standing test subject. The inferior-superior direction of the femur is roughly equivalent to the minus anterior-posterior direction of the pelvis for a seated subject. Other frame fields such as the Principal Direction Triad [15] or Frenet-Serret frame [15], which contain information about the motion embedded in the frame field, have also been used to describe the motion resulting from impact.

A very effective tool for analyzing the motion of the pelvic points of interest as they move along paths in space, is the concept of a moving frame [15]. The path generated as each

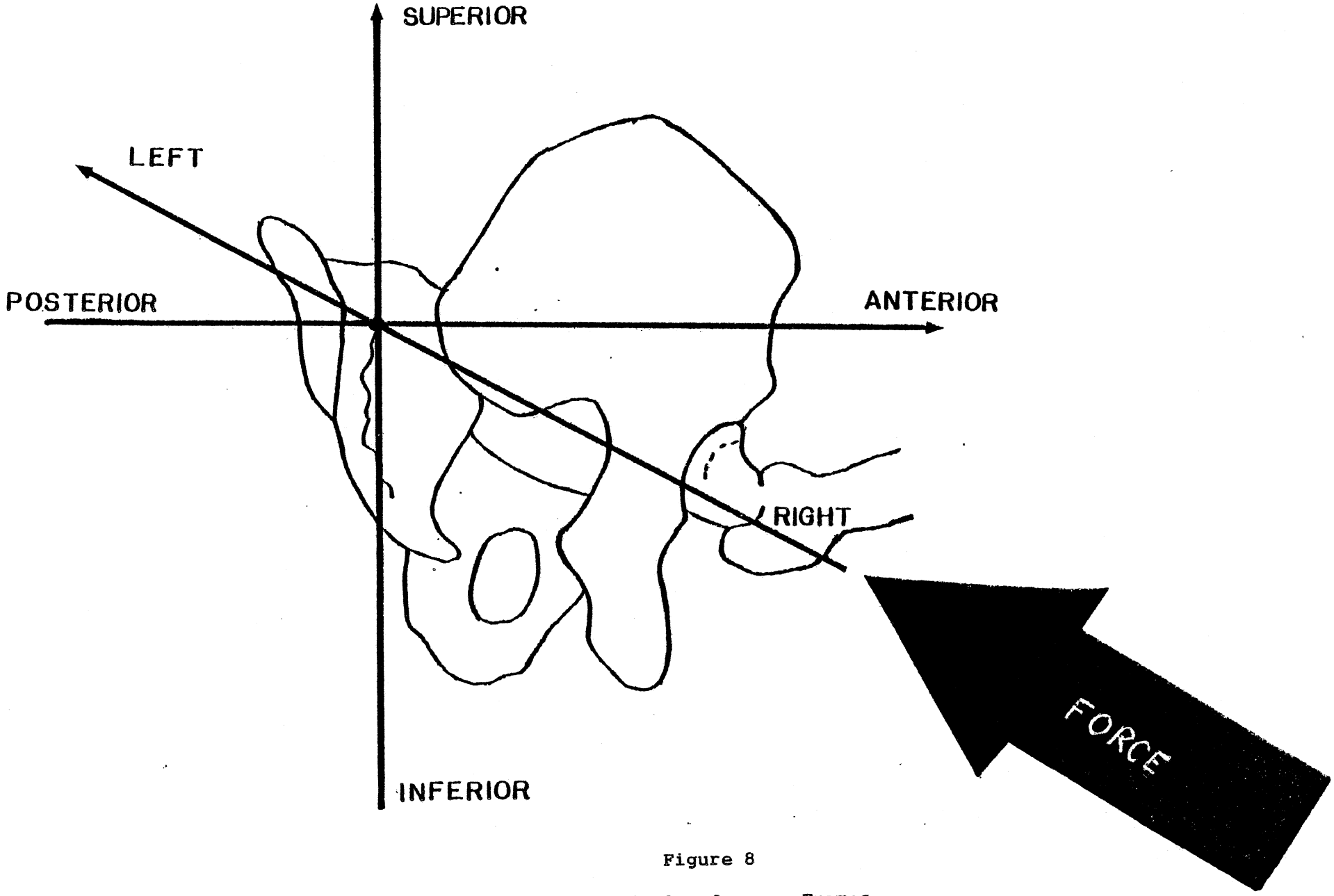

Figure 8

Anatomical Reference Frames

point travels through space is a function of time and velocity. A vector field is a function which assigns a uniquely defined vector to each point along a path. Thus, any collection of three mutually orthogonal unit vectors defined on a path is a frame field. Therefore, any vector defined on the path (for example, acceleration) may be resolved into three orthogonal components of any well-defined frame field, such as the laboratory or anatomical reference frames. Changes in a frame field with time (for example, angular acceleration of the frame field) are interpreted as vectors defined on the curve and are also resolved into three components.

The Frenet-Serret Frame [15] consists of three mutually orthogonal vectors T, N, B. At any point in time a unit vector can be constructed that is co-directional with the velocity vector. This normalized velocity vector defines the tangent direction T. A second unit vector N is constructed by forming a unit vector co-directional with the time derivative of the tangent vector T, since the derivative of a unit vector is normal to the vector. To complete the orthogonal frame, a third unit vector B (the unit binormal) can be defined as the cross product T x N. This procedure defines a frame at each point along the path of the point of interest. Within the frame field, the linear acceleration is resolved into two distinct types. The tangent acceleration Tan(T) is always the rate of change of speed (absolute velocity) and the normal acceleration Nor(N) gives information about the change in

direction of the velocity vector. The binormal direction Bin(B) contains no acceleration information.

5.23 Transfer Function Analysis - For blunt impacts, the relationship between impact force and the motion resulting at various points of the impacted system can be expressed in the frequency domain through the use of a transfer function. This input-output function is a complex-valued function in the frequency domain and can be expressed by a magnitude and a phase at a given frequency. Transfer functions can be determined from the Fourier transforms of the input-output response time-histories or from the spectral densities of the input and output response signals.

A transformation of simultaneously monitored accelerometer time-histories can be used to obtain the frequency-response functions of impact force and accelerations of remote points. When the frequency-response functions have been obtained, another transfer function of the form:

$$(Z)(iw) = (w)\ \ (F)[F(t)]/(F)[A(t)]$$

can be calculated from the transformed quantities where the definitions are the same as above.

This particular transfer function is the mechanical transfer impedance which can be defined as the ratio between simple harmonic driving force and corresponding velocity of the point of interest. Mechanical transfer impedance [15] is a complex valued function which for the purpose of presentation will be described by its magnitude and its phase angle.

In the case of a force and an acceleration, such as impact force and acceleration of a given point, a transformation of the form:

$$(X)(iw) = (F)[F(t)]/(F)[A(t)]$$

can be calculated from the transformed quantities, where w is the given frequency, F[F(t)] and F[A(t)] are the Fourier transforms of the impact force time-history and the acceleration time-history, respectively.

5.24 The Coherence Function $cxy^2(w)$, is a measure of the quality of a given transfer function at a given frequency.

$$cxy^2(w) = \frac{|Gxy(w)|^2}{Gxx(w)Gyy(w)}$$

where Gxx(w) and Gyy(w) are the power spectral densities of the two signals, respectively. Power Spectral Density is a Fourier transform of each signal's auto-correlation. $|Gxy(w)|^2$ is the Cross-Spectral Density function squared. Cross-Spectral Density is the Fourier transform of the cross-correlation of the two signals and w at the given frequency. By definition, $0 \leq cxy^2(w) \leq 1$. Values of $cxy^2(w)$ near 1 indicate that the two signals may be considered causally connected at that frequency. Values significantly below 1 at a given frequency indicate that the transfer function at that frequency cannot accurately be determined. In the case of an input-output relationship, values of $cxy^2(w)$ less than 1 indicate that the output is not attributable to the input and is perhaps due to extraneous noise. The coherence function in the

frequency domain is analogous to the correlation coefficient in the time domain. For more information on this measure see [15]. The coherence function was used to determine the useful range of the data in the frequency domain.

6.0 RESULTS

The tables presented on the following pages and the graphs in Appendix H represent the data considered most pertinent in discussing the test results. Appendix F contains preliminary research published in the Stapp Car Crash Conference Proceedings. Appendix G contains a manuscript submitted to the Journal of Biomechanics which discusses only the impacts conducted with the cannon impactor. The data for the whole test series in presented in Appendix H. Table 1, presented earlier in the text, contains biometric data of all test subjects. Initial pelvic test conditions are presented in Table 2. A summary of gross autopsy results is presented in Table 3. Impact test summaries containing force linear and angular accelerations are presented in Table 4. Table 5 lists the accelerometer response peaks.

Table 2. Initial Test Conditions

Cadaver No.	Test No.	Impactor	Padding	Velocity m/s
000	82E008	25 kg linear pendulum	2.5 cm Ensolite 1.3 cm Styrofoam	8.4
020	82E028	25 kg linear pendulum	0.5 cm Ensolite	8.4
040	82E049	25 kg linear pendulum	2.5 cm Ensolite 2.5 cm Styrofoam	8.6
050	82E051	20 kg cannon	5.0 cm Foam 2.5 cm A.L. Ensolite	20.0
050	82E052	20 kg cannon	2.5 cm Styrofoam	22.0
050	82E053	20 kg cannon	2.5 cm Styrofoam	26.0
060	82E067	25 kg linear pendulum	No Padding	6.0
070	82E071	20 kg cannon	7.5 cm A.L. Ensolite 2.5 cm Styrofoam	26.0
080	83E087	25 kg ballistic pendulum	15 cm APR pads	7.0
080	83E088	25 kg ballistic pendulum	No Padding	7.2
079	83E091	20 kg cannon	2.5 cm Styrofoam 2.5 cm Ensolite	10.2
090	83E093	20 kg cannon	2.5 cm Styrofoam 2.5 cm Ensolite	9.2
100	83E109	25 kg ballistic pendulum	15 cm APR pads	9.2

Table 3. Injuries

Cadaver No.	Test No.	Injuries
000	82E008	None
020	82E028	Vertical separation fracture of ischio-pubic ramus. Horizontal fracture of acetabulum extending 5 cm into superior pubic ramus, including crushing of superior aspect of acetabulum.
040	82E049	None
050	82E051 82E052 82E053	None
060	82E067	None
070	82E071	Separational fracture of ilio-pubic ramus into acetabulum. Fracture of inferior pubic ramus. Fracture of pubic rami at symphysis pubis.
080	83E087 83E088	None
079	83E091	None
090	83E093	None
100	83E109	None

TABLE 4
IMPACT SUMMARY RESPONSE

Cadaver No.	TEST NUMBER	FORCE N	ANG ACC P-A(I) rd/s/s	ANG ACC R-L(J) rd/s/s	ANG ACC I-S(K) rd/s/s	LIN ACC P-A(I) G	LIN ACC R-L(J) G	LIN ACC I-S(K) G	VELOCITY m/s
000	82E008	11700	4040	18200	7490	52.5	85.3	35.5	8.4
020	82E028	14000	7190	21000	11500	36.2	78.5	57.4	8.4
040	82E049	13400	2570	4650	3060	13.5	37.9	10.1	8.6
050	82E051	2820	-	-	-	-	-	-	20.0
050*	82E052	2550	-	-	-	-	-	-	22.0
060	82E067	-	2670	2310	2050	15.5	38.3	23.5	6.0
070	82E071	45700	-	-	-	-	-	-	26.0
080	83E087	4750	436	905	751	5.2	10.7	4.8	7.0
080	83E088	4330	777	688	417	4.7	10.4	7.3	7.2
079	83E091	12000	-	-	-	-	-	-	10.2
090	83E093	26400	-	-	-	-	-	-	9.2
100	83E109	15200	1640	1010	1520	14.7	6.7	8.4	9.2

*Loss of data for 82E053 (Velocity=26 m/s).

Table 5
Pelvic Impact Accelerometer Response Peaks

Test No.	Force N	ANG ACC P-A(I) rd/s/s	ANG ACC R-L(J) rd/s/s	ANG ACC I-S(K) rd/s/s	LIN ACC P-A(I) G	LIN ACC R-L(J) G	LIN ACC:I-S(K) G
82E008	12000	4000	18000	-7500	53	85	36
82E028	14000	-7200	-21000	11000	36	79	57
82E049	13000	2600	-4600	-3100	14	38	-10
82E051	2800	-	-	-	-	-	-
82E052	2500	-	-	-	-	-	-
82E053	LOSS OF DATA	-	-	-	-	-	-
82E067	-	2700	-2300	2000	-16	38	-24
82E071	46000	-	-	-	-	-	-
83E087	4800	440	900	690	-5.2	-11	5.0
83E088	4300	-780	690	420	-4.7	-10	-7.3
83E091	12000	-	-	-	-	-	-
83E093	26000	-	-	-	-	-	-
83E109	15000	-1600	-1000	1500	15	-7.0	8.4

7.0 DISCUSSION

The results presented in this paper have been obtained from a series of pelvis injury research programs conducted during the past five years. The data is presented in abbreviated form to represent the trends which are felt to be important factors in pelvis impact response.

The response of the pelvis can be interpreted as the response of a material body (the pelvis) in contact with other material bodies (the femur, spine, soft tissue, and abdominal organs). The degree to which each of the material bodies interacts with the pelvis is dependent upon the amount of available impactor energy and how it is transmitted to the pelvis.

7.1 Force-Time Histories - Several distinct events occurred in all the force time-histories and could be used as event markers. They are: the beginning of impact noted as E1, the peak force noted as E2, and the end of impact noted as E3.

7.2 Transfer Functions -- The transfer functions generated from the impact force and accelerations include the effects of padding and subject response. The response of the pelvis under dynamic lateral loads requires the description of several material bodies: the impactor, the femur, the soft tissue and the pelvis. The ball and socket nature of the interface of the acetabulum and the head of the femur, as well as the difficulty of impacting through the effective center of mass of the pelvis-femur complex, suggest that an instability will generally result due to asymmetric loading of the acetabulum during impact. This type of interaction, as well as the effects of damage produced during loading, can lead to a wide range of responses.

The accelerometer mounting platform was anchored to the pelvis through the use of lag bolts and dental acrylic. This may have added to the lateral stiffness of the pelvis by reducing the differential movement between the two innominate bones during impact, consequently simplifying the gross whole body motion of the pelvis. The degree to which the accelerometer plate stiffens the pelvis is undetermined. No damage was observed as a result of the lag bolts indicating that the accelerometer platform was not a significant load path. There was also a section of soft tissue between the mounting plate and the boney pelvis which may have dampened the pelvic structures' response as reflected in the acceleration signals.

In tests 82E008, 82E028, 82E049, 83E087, 83E088 and 83E109, the three-dimensional motion of the pelvis showed that the direction, magnitude, phasing, and waveform of the motion descriptors obtained from the nine-accelerometer analysis did not follow a consistent pattern. These differences occurred primarily in both angular and linear accelerations in those directions perpendicular to the impactor motion. Examples are Figures 9 and 10 for 82E028, and Figures 11 and 12 for 82E049. Both the linear and angular variables differ significantly during the E1 to E2 interval even though the gross overall motion as obtained from both the nine accelerometer analysis and the high-speed movies are the same. Variables representing this trend are the relative magnitude and phasing of the resultant and tangential acceleration, with no clear relation between peak force and acceleration or when it will occur in the force time-history. This is consistent with research program results from other research acceleration data [7]. Figure 13 depicts some of the waveforms that support this observation.

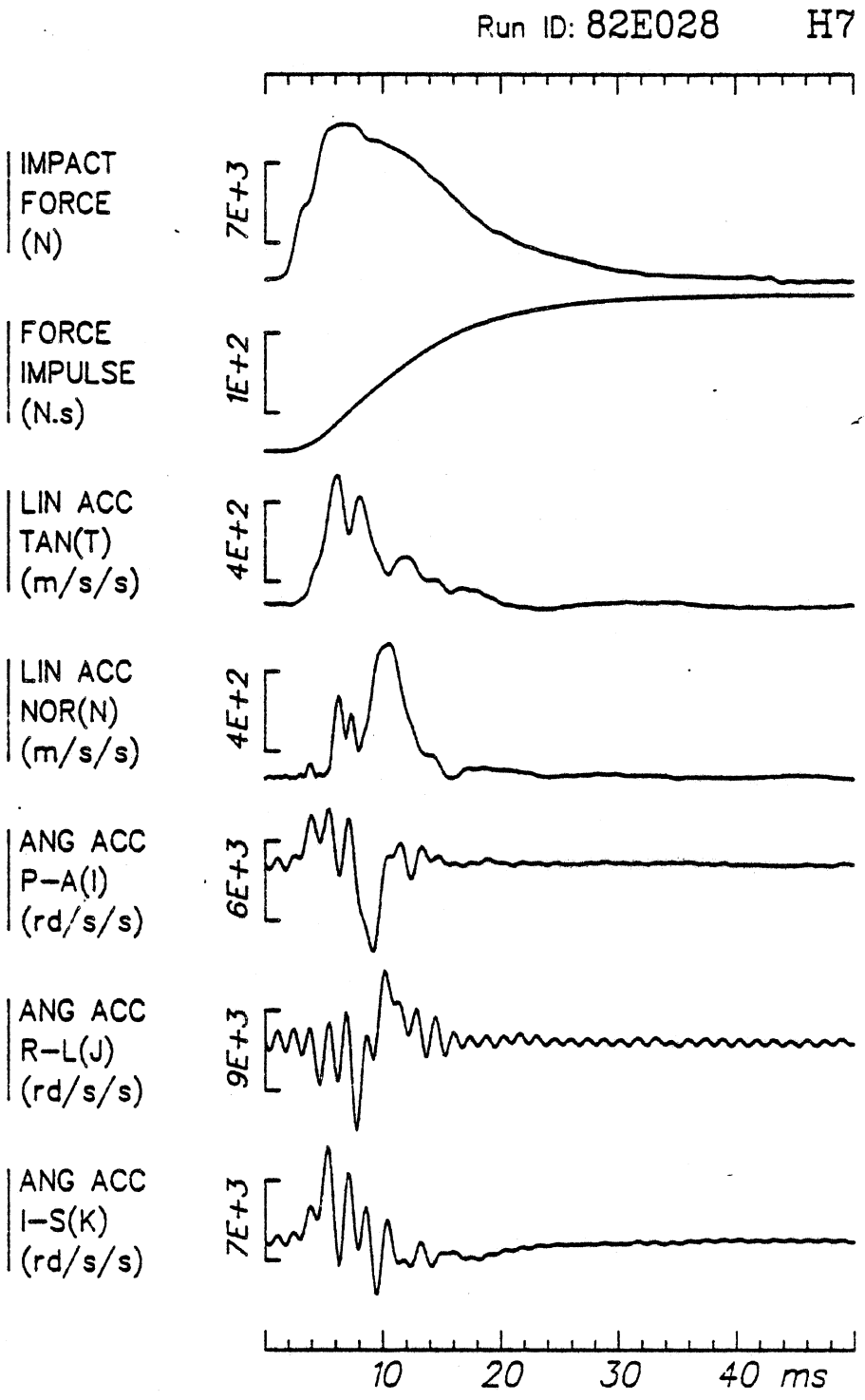

Test 82E028

Figure 9

Angular Acceleration

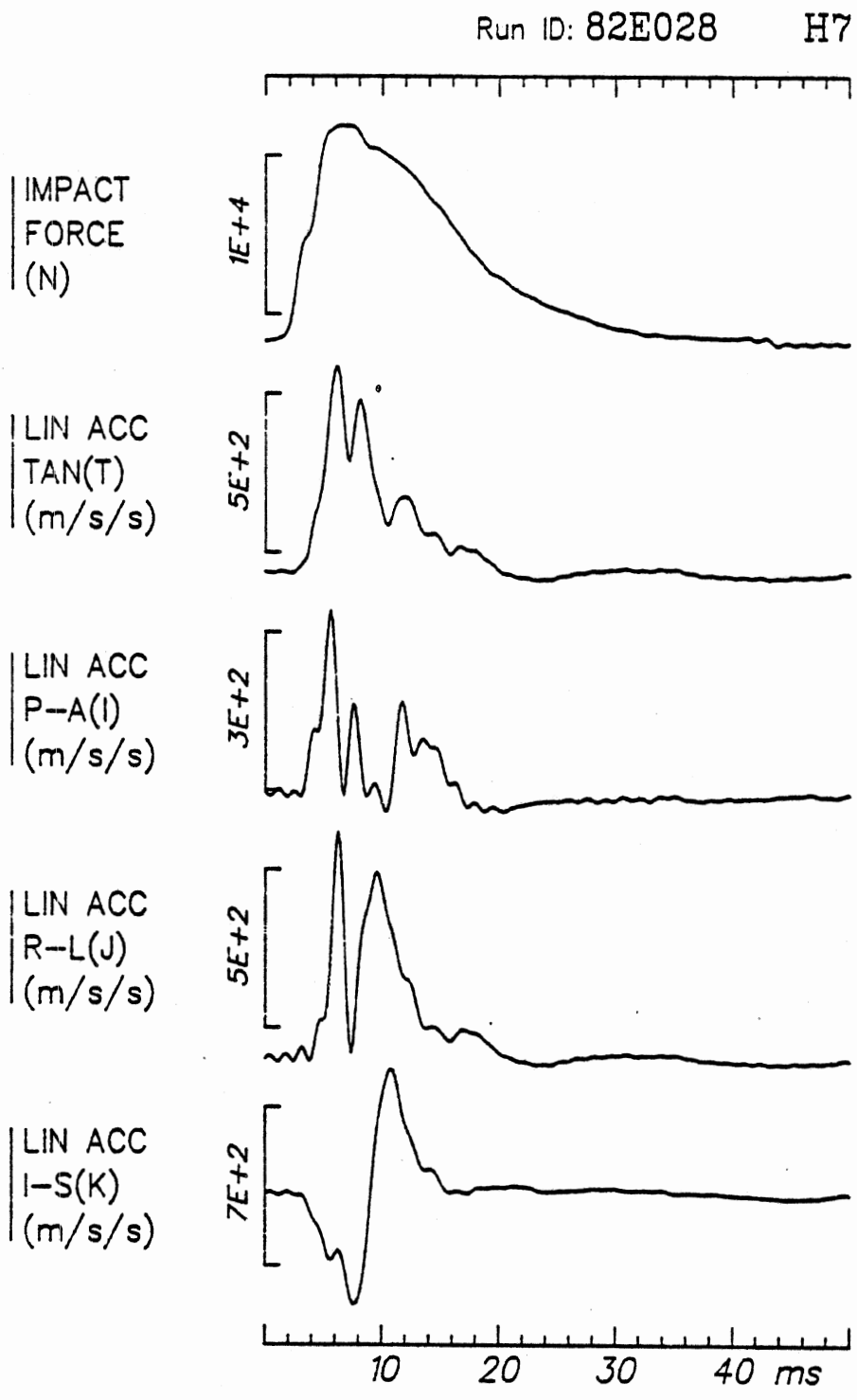

Test 82E028

Figure 10

Linear Acceleration

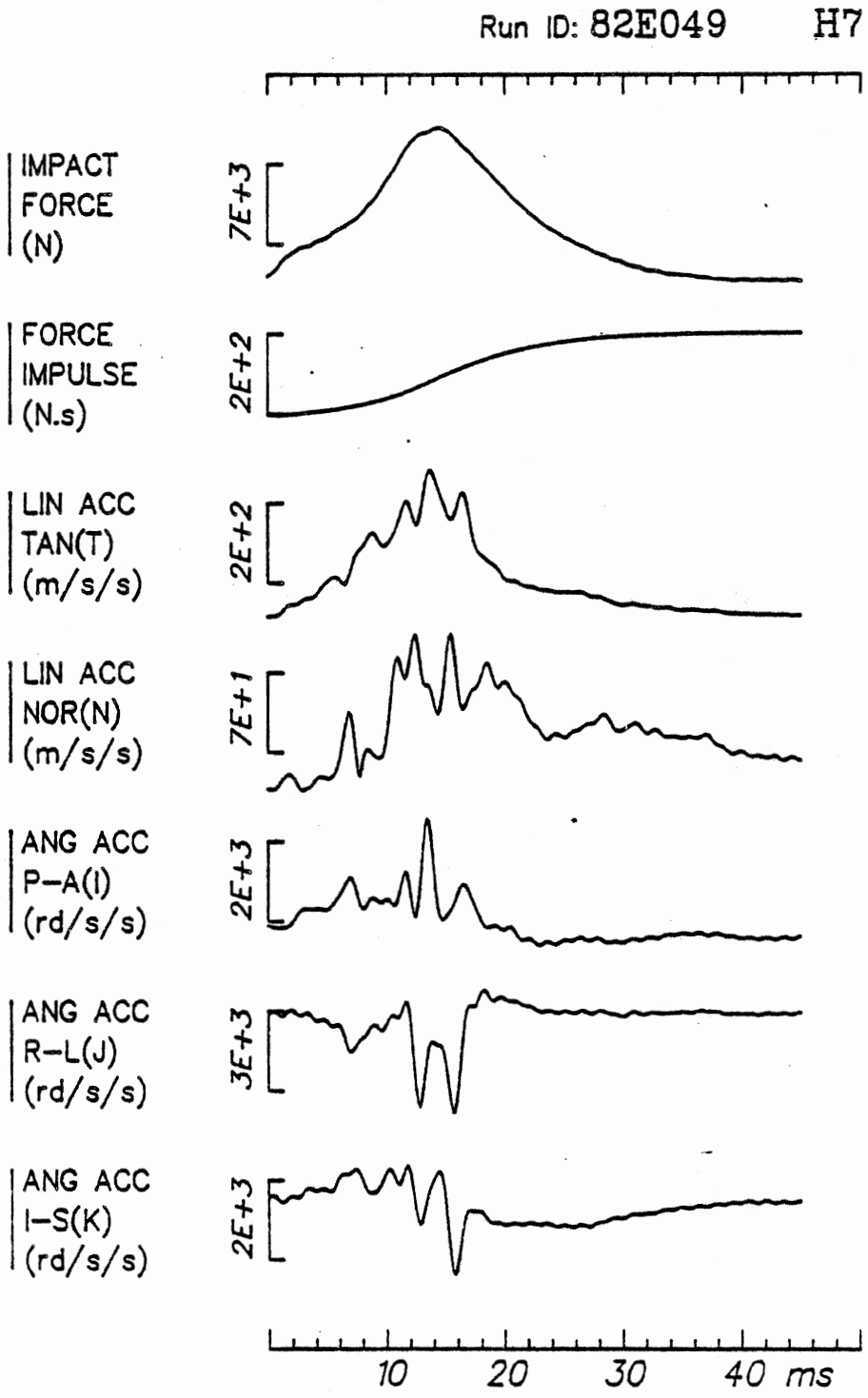

Figure 11
Angular Acceleration

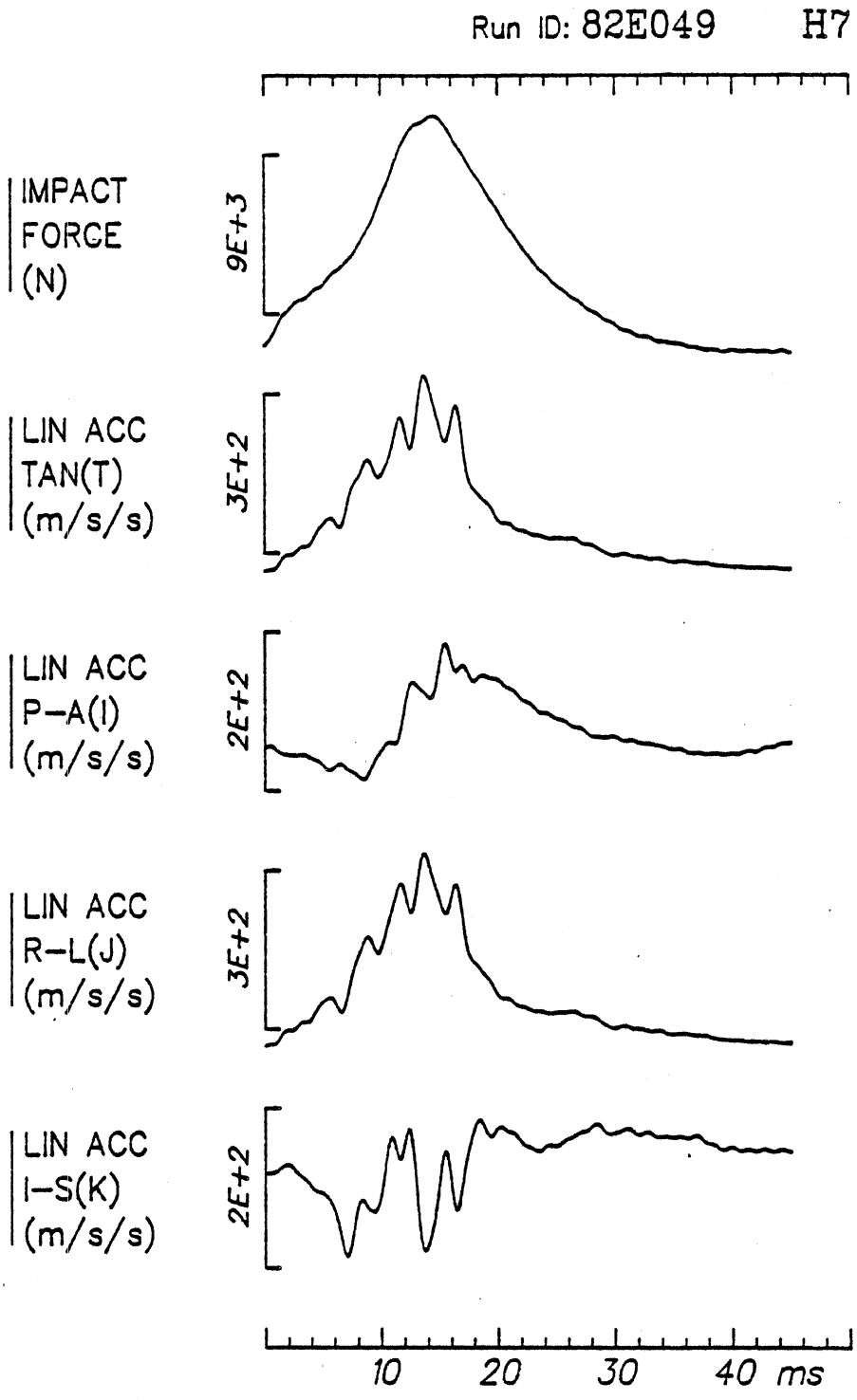

Figure 12

Linear Acceleration

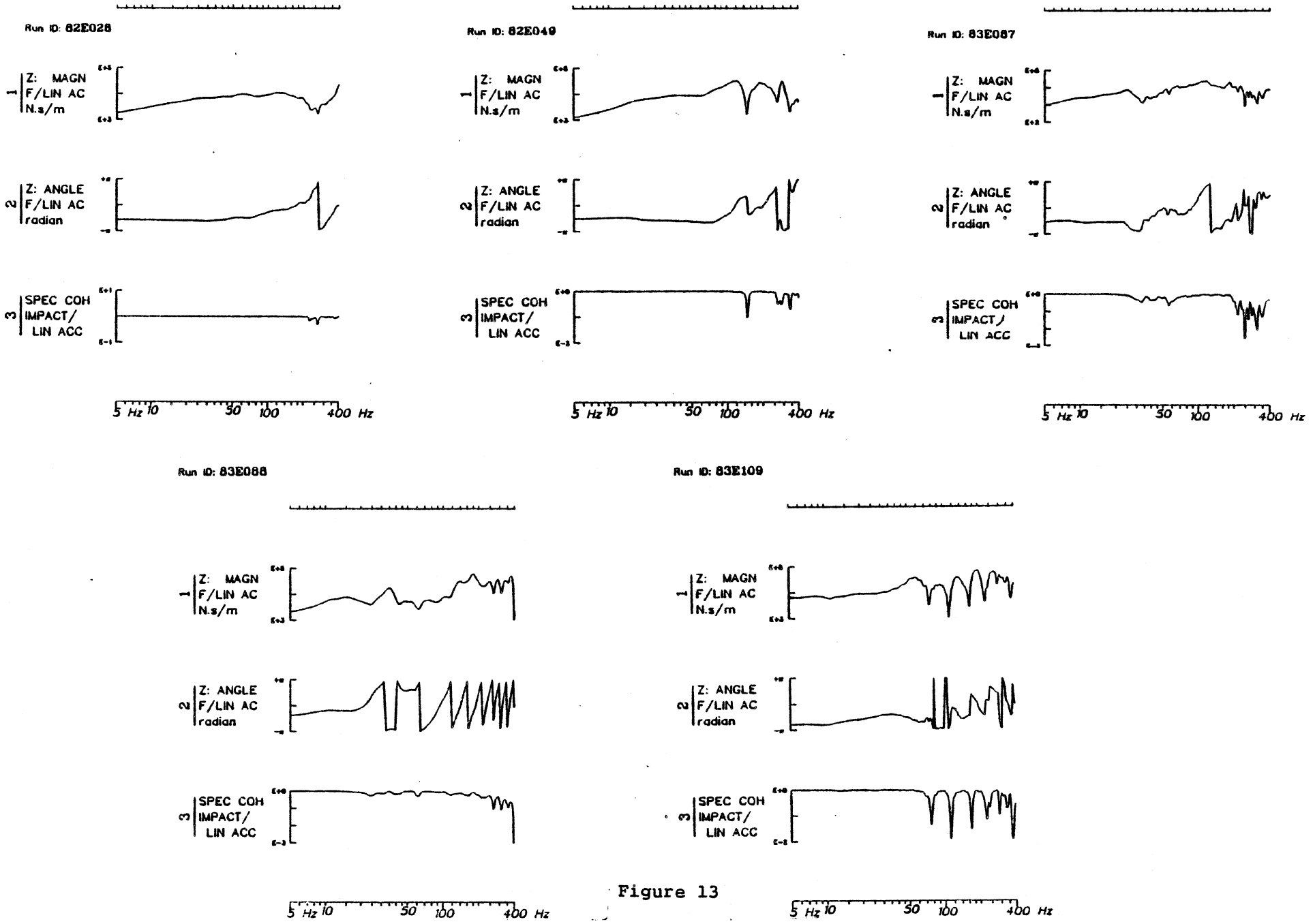

Figure 13
Resultant and Tangential Acceleration

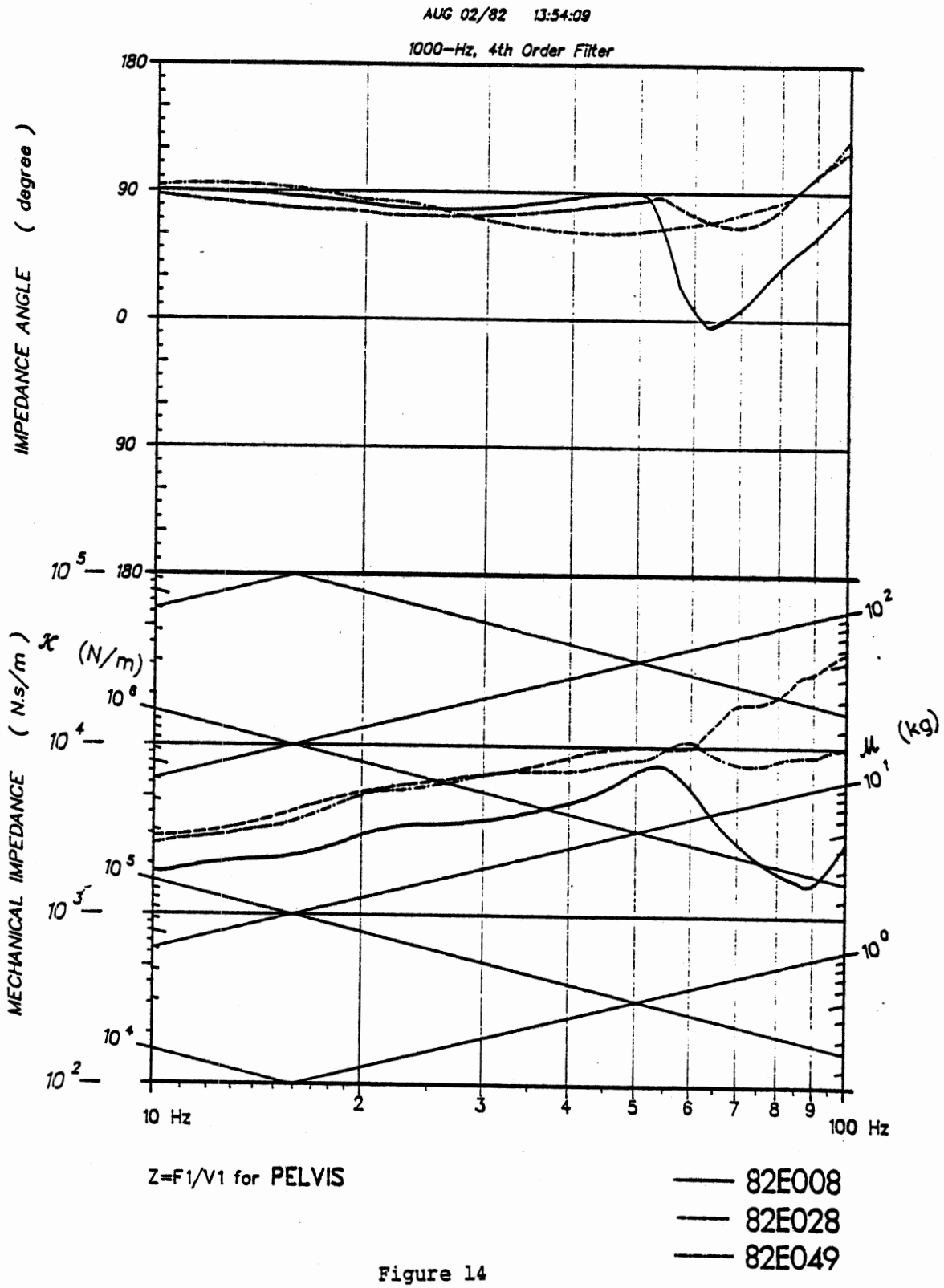

Figure 14

Mechanical Impedance Corridor

The response of the pelvis to impact was complicated not only by dynamic instabilities of the femur-pelvis complex, but also by the variability between subjects. Since load was distributed to the pelvis through both soft tissue and the femur, variations in these physical aspects between subjects can lead to varied stress levels on the acetabulum for a given impact force. For the subjects with large amounts of soft tissue, a longer E1 to E2 interval was observed.

Because of the complex nature of the response of the pelvis to lateral impacts, it becomes difficult to generate a transfer function for these experiments. A transfer function was generated from the tangential acceleration for those tests in which the nine-accelerometer plate was used (Figure 2). The transfer function shows that in these tests for low frequencies (from 10 to 40 Hz) the pelvis behaves as a mass of about 25 kg indicating that the gross overall motion of the pelvis may be simply modeled.

7.3 Damage -- The pelvic bone damages observed in these tests are similar to those observed in the automotive environment as reported in [16-17,20,30,32]; however, no bilateral fractures occurred. The complex nature of the response of the pelvis to lateral loads may preclude the determination of a single tolerance criterion. In this regard, peak force does not relate to the damage produced. This is believed to be a result of the interactions of the padding, impactor surface shape, and/or the soft tissue between the impactor and the pelvis. With additional padding and soft tissue the load can be distributed over a larger area of the pelvis, and therefore less of the available impact energy would be concentrated on the acetabulum. The maximum force tolerable appears

to increase with an increase in load-distributing padding for a similar amount of available impact energy.

Based on differences in the initial conditions of the tests performed at UMTRI [23] and by Cesari, et al. [7], it is not readily verifiable that peak force and impulse are accurate pelvis injury criteria. The test methods used by Cesari, et al. [7] employed a subject seated in an upright position and impacted by an unpadded 17.3 kg impactor with a hemispherical surface. It was revealed in a series of tests performed at UMTRI (which employed an unrestrained subject and an impactor with a flat surface) that variations in impactor padding, mass, and load path may result in large differences in the peak force and impulse of the impact, which did not necessarily predict a certain type of injury [23]. Additional test parameters, such as subject configuration, may also have affected comparisons between test series results in an unknown manner. For example, in one research program the subject was seated in a fixed position which may have caused subject-seat interactions, thus producing different injuries for an otherwise similar impact.

The issues of lateral pelvic impact tolerance are complex in their technical details, but they nonetheless focus on a reasonably simple central problem: understanding the factors necessary to cause injury to the pelvis and understanding the mechanism of injury. A number of procedures and techniques have been utilized to understand natural phenomena in the scientific arena. Two of the most commonly used are the direct and indirect methods. The direct approach usually starts with first principles and then attempts to derive the basic laws governing the phenomena of interest. One direct approach is to assume

that the phenomena under study (in this case, the pelvis) can be characterized by minimizing the Lagrange density L which is a function of the independent variables (coordinates, velocities, potentials, gradients, field amplitudes, etc.) of the system and the derivatives of these variables with respect to the integration that is to be minimized.

$$\mathcal{L} = \int_{a_1}^{b_1} \cdots \int_{a_m}^{b_m} L\left(\psi, \frac{\partial \psi}{\partial X}, x\right) dx_1 \cdots dx_m \tag{1}$$

One such direct method characterization would be the equation for governing the behavior of an elastic medium under its own restoring force.

$$\begin{aligned} &\text{div grad } \Psi = p(x,y,z)\ k(x,y,z)\,dd\ \Psi/dtdt, \\ &k(x,y,z) = 1/(y(x,y,z)+2*u(x,y,z)) \end{aligned} \tag{2}$$

Where u is the shear modulus of the medium and y+2/3u is its compressive modulus. An example of this direct approach would be to compute the velocity and displacement of the medias under impact given the density p(x,y,z) and the elastic modulus k(x,y,z).

In contrast, it may be possible indirectly through the use of strain gauges and accelerometers to measure the velocity, displacement, and acceleration when the elastic modulus is the unknown. Indeed, in the case of the pelvis, which is inhomogeneous, the elastic modulus varies from point to point. A more realistic problem then is determining k(x,y,z) from the displacement field which is is an example

of an inverse problem using the indirect method. Utilizing measurable quantities obtained in laboratory experiments employs the indirect method. One parameter in impact biomechanics commonly addressed through the indirect method is the tolerance level or failure criteria. Impact experiments such as the ones presented here, measure the force time-history and then attempt to determine tolerance in terms of this variable. However, the indirect method requires a considerable amount of time and effort in the laboratory. Procedures may vary from laboratory to laboratory and for complex phenomena, such as pelvic impact response, assumptions have to be made to simplify the problem.

To determine the failure criteria of the pelvis for lateral impacts, a considerable number of variables need to be addressed. The anatomical structures are inhomogeneous with complex geometry, and other structures, such as the femur and soft tissues, intervene between the impactor and the acetabulum. The pelvis is a deformable object that rarely makes direct contact with the impacting surface. In most lateral impact environments there are two basic load paths into the pelvis, one through the iliac wing and another through the acetabulum via the femur.

Although other quantities such as maximum strain, maximum strain energy, and maximum distortion are used to specify the failure criteria of solid materials, a maximum stress value is popularly used. A first approximation to finding maximum stress is to utilize maximum impact force as a failure criterion for a one-dimensional case, assuming that failure occurs near maximum force.

$$\sigma = f/a \tag{3}$$

Where f is the force and a is the effective contact area of the femur with the pelvis. Then, for a given impact, the failure criteria can be defined in terms of maximum force. If the contact surface is such that it is a weak function of initial condition and force time-history, e.g., the effective contact area has reached a maximum, the soft tissue is not an effective energy absorber, and the force is transmitted directly to the pelvis, then maximum force is directly related to maximum stress and might be used as a failure criterion. Cesari and Ramet [6] have proposed that a 10 kN (3 ms clip) peak force for males and a 4 kN (3 ms clip) peak force for females would be a reasonable fracture tolerance level for lateral impacts in the pelvis without loading the wing of the illium. However, they have pointed out the efficacy of using a different stress-related variable instead of raw force for a specific type of fracture. They hypothesized that many lateral pelvic fractures were the result of excess bending stress in the pubic rami. They computed moments of inertia and used the formula:

$$\sigma = f*d/(I/y) \tag{4}$$

Where d is the characteristic moment and I/y is the area moment of inertia divided by the offset from the neutral axis. They were able to correlate fracture force and moments of inertia. This then improved

their correlation coefficient between calculated stress and fracture. Additional efforts have been made to base a fracture criterion on an acceleration. Toward this end Haffner (1985) based on the work of Nusholtz et al. [23] constructed a one-dimensional linear lumped-parameter model as shown in Figure 15. Mass 1 is associated with the structure side upper mass, and Mass 2 is associated with the pelvic mass upon which the pelvic accelerometer is attached. They cautioned that the model is not to be taken as a literal model but as a useful device for prediction of pelvic stress along the lines of others (Haffner, 1985) and [23]. Although, this seems to be a useful method of producing a fracture tolerance criterion, the limited data preclude determining the method's predictive value over peak force.

The relationship between acceleration and force and, therefore, potentially between stress and acceleration can be envisioned by the assumption that the motion during impact to the pelvic area (to which the accelerometers are attached) is that of a rigid body undergoing one-dimensional motion. It has been pointed out [23] that a complete three-dimensional description, consisting of three linear translations and three angular rotations, is invaluable in determining the response of the pelvis to blunt lateral impact. This is a result of the ball and socket nature of the interface of the acetabulum and the head of the femur, as well as of the difficulty of impacting through the center of the mass of the pelvis-femur complex. This type of geometry will result in asymmetric loading of the pelvis and will produce a wide range of responses for a given impact. Therefore, for small deformations of the pelvis, it is more reasonable to assume that the acceleration motion of

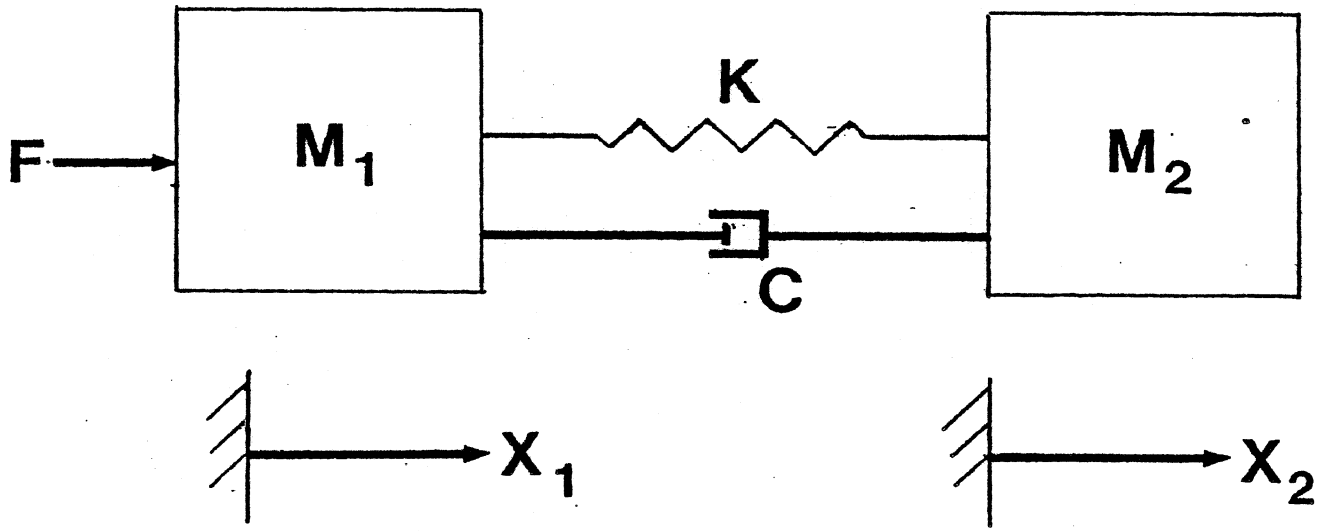

Figure 15

Lumped Parameter Model

any given point on the pelvis sufficiently far from the impact point can be described using the following equation.

$$\vec{X}=\vec{A}+w\hat{}w\hat{}r+(dw/dt)\hat{}\vec{r} \tag{5}$$

Where X is the acceleration of a given point on the pelvis, A is the acceleration of the center of mass, w is the angular velocity of the pelvis, dw/dt is the angular acceleration of the pelvis, and r is the radius vector of the center of mass to the point of interest. A one-dimensional model would give only a rough approximation of the stress produced during impact. A better approximation would have the stress in the pelvis as a function of the forces F(x,y,z) and torques N( ) as well as the point of interest X on the pelvis.

$$\sigma=F(F[x,y,z],N[\beta,\theta,\lambda],\vec{X}) \tag{6}$$

In addition to the three-dimensional motion, the pelvis is composed of inhomogeneous materials and is strain rate sensitive as well as non-linear in response. Therefore:

$$E=F(\sigma,\vec{X},t) \tag{7}$$

Where E is the strain of any given point on the pelvis. The motion of any point on the pelvis would then be:

$$Xi+Ai=w\hat{}w\hat{}r+(dw/dt)\hat{}\,r+dd\vec{R}(E)/dt^2 \tag{8}$$

Where R(E) is the displacement vector of the point of interest from its equilibrium position. From the above discussion, it would seem that the application of the indirect method to determining fracture tolerances or maximum stress needs to address to some degree: the number of initial positions that can occur between the pelvis and the femur, the three-dimensional motion of the pelvis and the femur, and the response rate-sensitivity of the pelvic structures.

This would, in part, then explain the differences seen in the results of others [6-8,22]. Nusholtz et al. [23] observed for an impact experiment using a flat rigid striking surface which loaded the acetabulum through the femur that the fracture level was approximately 7 kN. Since the number of parameters that need to be controlled in lateral impact are numerous, small differences in experimental technique can lead to significant differences in results. The possible reasons for the differences between these two laboratories are:

1. The impactor used by Nusholtz et al. [23] was 56 kg instead of the 17 kg used by Cesari and Ramet [6], and Cesari et al. [7-

8]. If strain-rate is a factor in impact response, then the experiments performed by Nusholtz et al., [23] would have had a higher frequency contact, and, therefore, a higher strain-rate effect. This may, in part, explain why Nusholtz et al. [23] obtained a greater number of acetabular fractures.

2. Striking the femur with a hemispherical impactor permitted it to slide under the impactor, allowing greater loads to be transmitted directly to the pelvis.
3. Nusholtz' [23] test subjects were suspended in the air and struck during free fall. Cesari's were seated. The per se effect of seating on the response is undetermined. However, it seems reasonable to assume that for a short-duration (high frequency) force time-history, this would not have an effect.

If the above discussion is accurate in its characterization of the pelvis, then it would seem desirable to design an experiment that would increase the necessary load to fracture by:

1) Increasing the loading area.
2) Decreasing the strain-rate by decreasing the high-frequency components of the force time-history.
3) Reducing the angular acceleration.

The special padding used in these experiments enabled the femur to be trapped and reduced the angular motion associated with the femur-pelvic instability of the femur-pelvis, eliminated any concentrated loading by utilizing the entire surface of the impactor as a load path, reduced the rate of onset of the force time-history, and, thus, reduced the high frequency components of the force time-history. Because of the effects of the padding, large forces were generated without fracture. This

supports the earlier research results [22-23] in which the importance of protective padding was emphasized.

This has been a limited preliminary study of some important kinematic factors and damage modes associated with indirect loading of the pelvis through the femur. Due to the complex nature of the pelvis-femur interaction during an impact event, more work is necessary before these kinematic factors can be generalized to describe the response of the pelvis. However, the following conclusions can be drawn:

1) The complete description of three-dimensional motion is invaluable to the understanding of pelvic response.

2) The complex nature of the response of the femur/pelvis/soft tissue system, between-subjects variability, and damage patterns produced may preclude the determination of a single tolerance criterion such as maximum force or peak acceleration response.

3) Energy-absorbing and load-distributing materials are effective methods of transmitting greater amounts of energy to the pelvis without damage being produced in lateral impacts.

4) In comparison to the results of others [6-8,23], the pertinent observations of the experiments being reported in this report are that relatively large forces can be generated without fracture (26 kN) and that when the fractures do occur, they are associated with a force of 45 kN. In addition, the damage pattern changed from near (and including) the acetabulum to near (and including) the pubic area.

8.0 UNANSWERED QUESTIONS:

1) Can a well-padded pubic area sufficiently dissipate energy so that force input from a lateral impact to the acetabulum will not cause fracture?
2) Osteoporosis in the elderly population makes them particularly at risk to pelvic fracture. Can padding thickness be determined for an elderly (over 55 years) population?
3) Male and female pelvises are significantly different. Can tolerances for these populations be determined?

9.0 RECOMMENDED RESEARCH

It would seem worthwhile to investigate the effects of different types of paddings in similar indirect lateral pelvic impacts. Investigation of the orientation of the leg in such impacts may also provide valuable information. Also, work examining the effect of different impact contact points may provide information that ultimately might be useful in the assessment of the friendly automotive interior.

ACKNOWLEDGEMENTS

The three test series in the Experimental Data for Development of Finite Element Models: Head/Thoraco-Abdomen/Pelvis research program were funded by the United States Department of Transportation, National Highway Traffic Safety Administration, Contract No. DOT-HS-7-01636. The authors wish to acknowledge the technical assistance of Donald F. Huelke, Nabih Alem, John Melvin, Bryan Suggitt, Gail Muscott, Paula Lux, Marvin Dunlap, Don Erb, and Jean Brindamour. The authors also acknowledge the contributions of Jeff Pinsky, Allen C. Bosio, Zheng Lou, Valerie Moses, Wendy Gould, Steven Richter, Peter Schuetz, Shawn Cowper, Tim Jordan, Patrice Muscott, and Reza Salehi. A special thank you goes to Jeff Marcus.

10.0 REFERENCES

1 Alem, N. et al. 1978. Whole-body Human Surrogate Response to Three-point Harness Restraint. 22nd Stapp Car Crash Conference Proceedings.

2 Ashton, S.J. 1981. Factors Associated with Pelvic and Knee Injuries in Pedestrians Struck by the Fronts of Cars. 25th Stapp Car Crash Conference Proceedings, pp. 863-900.

3 Bartz, J. and Butler, F. 1972. Passenger Compartment with Six Degrees of Freedom. In: Auxilliary Programs to Three Dimensional Computer Simulation of a Motor Vehicle Crash Victim, DOT Contract No. FH-11-7592.

4 Brun-Cassan, F., et al. 1982. Determination of Knee-Femur-Pelvis Tolerance from the Simulation of Car Frontal Impacts. Proceedings 7th International IRCOBI Conference on the Biomechanics of Impacts, pp. 101-115.

5 Calderale, P.M., Garro, A. and Lorenzi, G.L. 1979. Car Accident Mathematical Model: Femur and Pelvis Stress Analysis. Proceedings 4th International IRCOBI Conference on the Biomechanics of Trauma, pp. 305-315.

6 Cesari, D. and Ramet, M. 1982. Pelvic Tolerance and Protection Criteria in Side Impact. 26th Stapp Car Crash Conference Proceedings, pp. 145-154.

7 Cesari, D., Ramet, M. and Clair, P. 1980. Evaluation of Pelvic Fracture tolerance in Side Impact. 24th Stapp Car Crash Conference Proceedings, pp. 145-154.

8 Cesari, D., Ramet, M. and Henry-Martin, D. 1978. Injury Mechanisms in Side Impact. 22nd Stapp Car Crash Conference Proceedings, pp. 429-447.

9 Donati, P.M. and Bonthoux, C. 1983. Biodynamic Response of the Human Body in the Sitting Position When Subjected to Vertical Vibration. Journal of Sound and Vibration 90(3):423-442. Oct.

10 Donishi, H., et al. 1983. Mechanical Analysis of the Human Pelvis and Its Application to the Artificial Hip Joint - By Means of the Three-Dimensional Finite Element Method. Journal of Biomechanics 16(6):427-444.

11 Evans, F. and Lissner, H. 1955. Studies on Pelvic Deformations and Fractures. Anatomical Record 121(2). Feb.

12 Evans, F.G. 1970. Impact Tolerance of Human Pelvic and Long Bones. In: Gurdijian, E.S., et al., eds., Impact Injury and Crash Protection, Charles C. Thomas Publisher, pp. 402-420.

13 Fanyon, A., et al. 1977. Contribution to Defining the Human Tolerance to Perpendicular Side Impact. Proceedings 3rd International Conference on Impact Trauma, pp. 297-309.

14 Haffner, M. 1985. Synthesis of Pelvic Fracture Criteria for Lateral Impact Loading. 10th International Conference on Experimental Safety Vehicles, Oxford, England, July 1-4.

15 Hixson, E. 1976. Mechanical Impedance. In: Harris, C.M. and Crede, C.E., eds., Shock and Vibration Handbook, NY: McGraw-Hill Book Co.

16 Huelke, D. and Lawson, T. 1976. Lower Torso Injuries and Automobile Seatbelts. SAE Paper No. 760370.

17 Huelke, D., et al. 1980. Lower Extremity Injuries in Automobile Crashes. UM-HSRI-80-10. National Highway Traffic Safety Administration. Highway Safety Research Institute, Ann Arbor, MI.

18 Khalil, T., Viano, D. and Taber, L. 1980. Vibrational Characteristics of the Embalmed Human Femur. General Motors Research Laboratories, Publication GMR-3270. 29 April.

19 King, A.I. 1973. Biomechanics of the Spine and Pelvis. In: Biomechanics and Its Application to Automotive Design, NY: Society of Automotive Engineers.

20 Knudsen, P.J.T. 1981. Fracture of the Pelvis in Side Impact Accidents - Fractures of the Pelvis in Four Out of Six Persons in One Car. [in Danish] Ugeskrift for Laeger 143(13):1014-1017.

21 Melvin, J., et al. 1975. Impact Response and Tolerance of the Lower Extremities. 19th Stapp Car Crash Conference Proceedings.

22 Melvin, J.W. and Nusholtz, G.S. 1980. Tolerance and Response of the Knee-Femur-Pelvis Complext to Axial Impacts - Impact Sled Tests. UM-HSRI-80-27. Highway Safety Research Institute, Ann Arbor, MI.

23 Nusholtz, G.S., Alem, N.M. and Melvin, J.W. 1982. Impact Response and Injury of the Pelvis. 26th Stapp Car Crash Conference Proceedings, pp. 103-144.

24 Nusholtz, G.S., et al. 1984. Head Impact Response--Skull Deformation and Angular Accelerations. 28th Stapp Car Crash Conference Proceedings, pp.41-74.

25 Nyquist, G.W. and Murton, C.J. 1975. Static Bending Response of the Human Lower Torso. 19th Stapp Car Crash Conference Proceedings, pp. 513-541.

26 Patrick, L., Kroell, C. and Mertz, H. 1965. Forces on the Human Body in Simulated Crashes. 9th Stapp Car Crash Conference Proceedings.

27 Pope, M.H., et al. 1977. Radiographic and Biomechanical Studies of the Human Spine. AFOSR-TR-78-0063. Vermont University, Burlington.

28 Ramet, M. and Cesari, D. 1979. Experimental Study of Pelvis Tolerance in Lateral Impact. Proceedings 4th International IRCOBI Conference on the Biomechanics of Trauma, pp. 243-249.

29 Reynolds, H.M., Freeman, J.R. and Bender, M. 1978. A Foundation for Systems Anthropometry. UM-HSRI-78-11. Highway Safety Research Institute, Ann Arbor, MI.

30 Ryan, F. 1971. Traffic Injuries of the Pelvis at St. Vincent's Hospital, Melbourne. Medical Journal of Australia 1(27). Feb.

31 Snow, C.C. and Reynolds, H.M. 1976. Anthropometric Data for Pelvic Geometry Definition. 4th Annual Committee Reports and Technical Discussions International Workshop on Human Subjects for Biomechanical Research, pp. 13-25.

32 States, J. and States, D. 1968. The Pathology and Pathogenesis of Injuries Caused by Lateral Impact Accidents. 12th Stapp Car Crash Conference Proceedings.

33 Tarriere, C. et al. 1979. Synthesis of Human Tolerances Obtained from Lateral Impact Simulations. 7th Report International Technical Conference on Experimental Safety Vehicles, pp. 359-373.

11.0 APPENDIX B
TEST PROTOCOL

DEPARTMENT OF TRANSPORTATION

MULTIPLE IMPACT TESTS

_____ Through _____

as performed by

the Biomechanics Department of

the Highway Safety Research Institute

Ann Arbor, Michigan

1982-1983 E Series

This protocol for the use of cadavers in this test series was approved by the Committee to Review Grants for Clinical Research of the University of Michigan Medical Center and follows guidelines established by the U.S. Public Health Service and those recommended by the National Academy of Sciences, National Research Council.

TABLE OF CONTENTS

TEST DESCRIPTION

Cadaver No._____ Sex:_____ Height:_____ Weight:_____

Test No._____ (Head, Shoulder, Pelvis)

Test description: Head impact, subject in a normal seated position, neck angle approx. 10° forward, impact to forehead, angle of head determined by tangent forehead plane.

Type of Impactor: PENDULUM

Type of Bumper: WHITE VIBRATHANE

Type of Striker: 25 Kg PISTON, 15cm DIA.

Impactor Angle: 50°(5.0m/s)

Padding:_____

Pre-Impact Travel: 14cm

Post-Impact Travel: 16cm

35mm stills:

___ Black and White

___ Color

CAMERAS		POSITION
Photosonics 1:	1000	P-A, S-I
Photosonics 2:	_____	_____
HyCam:	3000	P-A, S-I

INSTRUMENTATION

ACCELEROMETERS		TARGETS		TRANSDUCERS	
Head (9 AX)	X	Head	X	Trachea	___
Up. Sternum (3-AX)	___	Acromion	X	Ascending Aorta	___
Lwr. Sternum (1)	___	Sternum (2)	___	Internal Carotid	X
Spine (2 triax)	X	Spine	___		
Pelvis (9 AX)	___	Pelvis	___	Subdural 1:	X
Lwr. Rib R8 (2)	___			2:	X
Up. Rib R4 (2 triax)	___			3:	X
				4:	?

TEST DESCRIPTION

Cadaver No._____ Sex:_____ Height:_____ Weight:_____

Test No._____ (Head, Shoulder, Pelvis)

Test description:_____
Head impact, same as previous.

Type of Impactor: PENDULUM

Type of Bumper: WHITE VIBRATHANE

Type of Striker: 25 Kg PISTON, 15cm DIA.

Impactor Angle: 50°(5.0m/s)

Padding:_____

Pre-Impact Travel: 14cm

Post-Impact Travel: 16cm

35mm stills:

___ Black and White

___ Color

CAMERAS		POSITION
Photosonics 1:	1000	P-A, S-I
Photosonics 2:		
HyCam:	3000	P-A, S-I

INSTRUMENTATION

ACCELEROMETERS		TARGETS		TRANSDUCERS	
Head (9 AX)	X	Head	X	Trachea	___
Up. Sternum (3-AX)	___	Acromion	X	Ascending Aorta	___
Lwr. Sternum (1)	___	Sternum (2)	___	Internal Carotid	X
Spine (2 triax)	X	Spine	___		
Pelvis (9 AX)	___	Pelvis	___	Subdural 1:	X
Lwr. Rib R8 (2)	___			2:	X
Up. Rib R4 (2 triax)	___			3:	X
				4:	?

COMMENTS:

TEST DESCRIPTION

Cadaver No._____ Sex:_____ Height:_____ Weight:_____

Test No._____ (Head, Shoulder, Pelvis)

Test description: Front tap, mid-sternum, angle of thorax determined by sternum tangent plane, top of impact 54 cm from seat pan.

Type of Impactor: PENDULUM

Type of Bumper: WHITE VIBRATHANE

Type of Striker: 25 Kg PISTON, 21cm. sq.

Impactor Angle: 17°(2m/s)

Padding: .5cm ensolite

Pre-Impact Travel: 8cm

Post-Impact Travel: 22cm

35mm stills:

___ Black and White

___ Color

CAMERAS		POSITION
Photosonics 1:	1000	P-A, S-I
Photosonics 2:		
HyCam:	3000	P-A, S-I

INSTRUMENTATION

ACCELEROMETERS		TARGETS		TRANSDUCERS	
Head (9-AX)	X	Head	X	Trachea	X
Up. Sternum (3-AX)	X	Acromion	X	Ascending Aorta	X
Lwr. Sternum (1)	X	Sternum (2)	X	Internal Carotid	___
Spine (2 triax)	X	Spine	___		
Pelvis (9-AX)	___	Pelvis	___	Subdural 1:	___
Lwr. Rib R8 (2)	X			2:	___
Up. Rib R4 (2 triax)	X			3:	___
				4:	___

COMMENTS:

TEST DESCRIPTION

Cadaver No._____ Sex:_____ Height:_____ Weight:_____

Test No._____ (Head, Shoulder, Pelvis)

Test description: Left side tap, 45°P-A into R-L, normal seated posture, move arm if necessary, top of impact 54 cm above seat pan.

Type of Impactor: PENDULUM

Type of Bumper: WHITE VIBRATHANE

Type of Striker: 25 Kg PISTON, 21cm. sq.

Impactor Angle: 17°(2m/s)

Padding: .5cm ensolite

Pre-Impact Travel: 8cm

Post-Impact Travel: 22cm

35mm stills:

___ Black and White

___ Color

CAMERAS		POSITION
Photosonics 1:	1000	45° P-A into R-L, S-I
Photosonics 2:	_____	_____
HyCam:	3000	45° P-A into R-L, S-I

INSTRUMENTATION

ACCELEROMETERS		TARGETS		TRANSDUCERS	
Head (9-AX)	X	Head	X	Trachea	X
Up. Sternum (3-AX)	X	Acromion	X	Ascending Aorta	X
Lwr. Sternum (1)	X	Sternum (2)	X	Internal Carotid	___
Spine (2 triax)	X	Spine	___		
Pelvis (9-AX)	___	Pelvis	___	Subdural 1:	___
Lwr. Rib R8 (2)	X			2:	___
Up. Rib R4 (2 triax)	X			3:	___
				4:	___

COMMENTS:

TEST DESCRIPTION

Cadaver No._____ Sex:_____ Height:_____ Weight:_____

Test No._____ (Head, Shoulder, Pelvis)

Test description: Left side tap arms up, position arms to minimize interference from scapula as well as centering piston in the R-L/I-S plane, normal seated posture. Top of impact 54 cm above seat pan. (This test may be dropped.)

Type of Impactor: PENDULUM

Type of Bumper: WHITE VIBRATHANE

Type of Striker: 25 Kg PISTON, 21cm sq.

Impactor Angle: 17°(2m/s)

Padding: .5cm ensolite

Pre-Impact Travel: 8cm

Post-Impact Travel: 22cm

35mm stills:

___ Black and White

___ Color

CAMERAS		POSITION
Photosonics 1:	1000	R-L, S-I
Photosonics 2:		
HyCam:	3000	R-L, S-I

INSTRUMENTATION

ACCELEROMETERS		TARGETS		TRANSDUCERS	
Head (9-AX)	X	Head	X	Trachea	X
Up. Sternum (3-AX)	X	Acromion	X	Ascending Aorta	X
Lwr. Sternum (1)	X	Sternum (2)	X	Internal Carotid	___
Spine (2 triax)	X	Spine	___		
Pelvis (9-AX)	___	Pelvis	___	Subdural 1:	___
Lwr. Rib R8 (2)	X			2:	___
Up. Rib R4 (2 triax)	X			3:	___
				4:	___

COMMENTS:

TEST DESCRIPTION

Cadaver No._____ Sex:_____ Height:_____ Weight:_____

Test No._____ (Head, Shoulder, Pelvis)

Test description: Left side tap arms down, normal seated posture, in the R-L/I-S plane, top of impact 54 cm above seat pan.

Type of Impactor: PENDULUM

Type of Bumper: WHITE VIBRATHANE

Type of Striker: 25 Kg PISTON, 21cm sq.

Impactor Angle: 17°(2m/s)

Padding: .5cm ensolite

Pre-Impact Travel: 8cm

Post-Impact Travel: 22cm

35mm stills:

___ Black and White

___ Color

CAMERAS		POSITION
Photosonics 1:	1000	R-L, S-I
Photosonics 2:		
HyCam:	3000	R-L, S-I

INSTRUMENTATION

ACCELEROMETERS		TARGETS		TRANSDUCERS	
Head (9-AX)	X	Head	X	Trachea	X
Up. Sternum (3-AX)	X	Acromion	X	Ascending Aorta	X
Lwr. Sternum (1)	X	Sternum (2)	X	Internal Carotid	___
Spine (2 triax)	X	Spine	___		
Pelvis (9-AX)	___	Pelvis	___	Subdural 1:	___
Lwr. Rib R8 (2)	X			2:	___
Up. Rib R4 (2 triax)	X			3:	___
				4:	___

COMMENTS:

TEST DESCRIPTION

Cadaver No._____ Sex:_____ Height:_____ Weight:_____

Test No._____ (Head, Shoulder, Pelvis)

Test description: Left side impact, same as left side arms down tap.

Type of Impactor: PENDULUM

Type of Bumper: WHITE VIBRATHANE

Type of Striker: 25 Kg PISTON, 21cm sq.

Impactor Angle: 100°(8.8m/s)

Padding: 15cm APR pads

Pre-Impact Travel: 9cm

Post-Impact Travel: 21cm

35mm stills:

___ Black and White

___ Color

CAMERAS		POSITION
Photosonics 1:	1000	R-L,S-I
Photosonics 2:	_____	_____
HyCam:	3000	R-L, S-I

INSTRUMENTATION

ACCELEROMETERS		TARGETS		TRANSDUCERS	
Head (9-AX)	X	Head	X	Trachea	X
Up. Sternum (3-AX)	X	Acromion	X	Ascending Aorta	X
Lwr. Sternum (1)	X	Sternum (2)	X	Internal Carotid	___
Spine (2 triax)	X	Spine	___		
Pelvis (9-AX)	___	Pelvis	___	Subdural 1:	___
Lwr. Rib R8 (2)	X			2:	___
Up. Rib R4 (2 triax)	X			3:	___
				4:	___

COMMENTS:

TEST DESCRIPTION

Cadaver No._____ Sex:_____ Height:_____ Weight:_____

Test No._____ (Head, Shoulder, Pelvis)

Test Description: Pelvic impact, right side, 8cm anterior to trochanterion, centered on femur.

Type of Impactor: PENDULUM

Type of Bumper: WHITE VIBRATHANE

Type of Striker: 25 Kg PISTON, 15cm DIA.

Impactor Angle: 100°(8.8m/s)

Padding: .5cm ensolite

Pre-Impact Travel: 12cm

Post-Impact Travel: 18cm

35mm stills:

___ Black and White

___ Color

CAMERAS		POSITION
Photosonics 1:	1000	R-L, S-I
Photosonics 2:		
HyCam:	3000	R-L, S-I

INSTRUMENTATION

ACCELEROMETERS		TARGETS		TRANSDUCERS	
Head (9-AX)	___	Head	___	Trachea	___
Up. Sternum (3-AX)	___	Acromion	___	Ascending Aorta	___
Lwr. Sternum (1)	___	Sternum (2)	___	Internal Carotid	___
Spine (2 triax)	X	Spine	X		
Pelvis (9-AX)	X	Pelvis	X	Subdural 1:	___
Lwr. Rib R8 (2)	___			2:	___
Up. Rib R4 (2 triax)	___			3:	___
				4:	___

COMMENTS:

TEST DESCRIPTION

Cadaver No._____ Sex:_____ Height:_____ Weight:_____

Test No._____ (Head, Shoulder, Pelvis)

Test description:_____

_____

_____

_____

_____

Type of Impactor:_____

Type of Bumper:_____

Type of Striker:_____

Impactor Angle:_____

Padding:_____

Pre-Impact Travel:_____

Post-Impact Travel:_____

35mm stills:

___ Black and White

___ Color

CAMERAS	POSITION
Photosonics 1: _____	_____
Photosonics 2: _____	_____
HyCam: _____	_____

INSTRUMENTATION

ACCELEROMETERS		TARGETS		TRANSDUCERS	
Head (9-AX)	___	Head	___	Trachea	___
Up. Sternum (3-AX)	___	Acromion	___	Ascending Aorta	___
Lwr. Sternum (1)	___	Sternum (2)	___	Internal Carotid	___
Spine (2 triax)	___	Spine	___		
Pelvis (9-AX)	___	Pelvis	___	Subdural 1:	___
Lwr. Rib R8 (2)	___			2:	___
Up. Rib R4 (2 triax)	___			3:	___
				4:	___

COMMENTS:

TEST DESCRIPTION

Cadaver No._____ Sex:_____ Height:_____ Weight:_____

Test No._____ (Head, Shoulder, Pelvis)

Test description:_____

_____

_____

_____

_____

Type of Impactor:_____

Type of Bumper:_____

Type of Striker:_____

Impactor Angle:_____

Padding:_____

Pre-Impact Travel:_____

Post-Impact Travel:_____

35mm stills:

___ Black and White

___ Color

CAMERAS	POSITION
Photosonics 1: _____	_____
Photosonics 2: _____	_____
HyCam: _____	_____

INSTRUMENTATION

ACCELEROMETERS		TARGETS		TRANSDUCERS	
Head (9-AX)	___	Head	___	Trachea	___
Up. Sternum (3-AX)	___	Acromion	___	Ascending Aorta	___
Lwr. Sternum (1)	___	Sternum (2)	___	Internal Carotid	___
Spine (2 triax)	___	Spine	___		
Pelvis (9-AX)	___	Pelvis	___	Subdural 1:	___
Lwr. Rib R8 (2)	___			2:	___
Up. Rib R4 (2 triax)	___			3:	___
				4:	___

COMMENTS:

TEST DESCRIPTION

Cadaver No._____ Sex:_____ Height:_____ Weight:_____

Test No._____ (Head, Shoulder, Pelvis)

Test description:_____

_____

_____

_____

_____

Type of Impactor:_____

Type of Bumper:_____

Type of Striker:_____

Impactor Angle:_____

Padding:_____

Pre-Impact Travel:_____

Post-Impact Travel:_____

35mm stills:

___ Black and White

___ Color

CAMERAS	POSITION
Photosonics 1: _____	_____
Photosonics 2: _____	_____
HyCam: _____	_____

INSTRUMENTATION

ACCELEROMETERS		TARGETS		TRANSDUCERS	
Head (9-AX)	___	Head	___	Trachea	___
Up. Sternum (3-AX)	___	Acromion	___	Ascending Aorta	___
Lwr. Sternum (1)	___	Sternum (2)	___	Internal Carotid	___
Spine (2 triax)	___	Spine	___		
Pelvis (9-AX)	___	Pelvis	___	Subdural 1:	___
Lwr. Rib R8 (2)	___			2:	___
Up. Rib R4 (2 triax)	___			3:	___
				4:	___

COMMENTS:

PRE-SURGERY

TASK	TIME	COMMENTS
Pick up cadaver from U of M Anatomy Dept. and transport to HSRI Biomedical lab.		
Weigh cadaver and log cadaver information.		
Store cadaver if necessary.		
Sanitary preparation.		
Pretest X-rays: (KV/MA/T) head A-P (100/10/1) ___/___/___ thorax A-P (90/10/1) ___/___/___ thorax A-P(2) (90/10/1) ___/___/___ pelvis (105/10/1) ___/___/___ femur (80/10/1) ___/___/___		
Anthropometry.		

ANTHROPOMETRY

Height:_____

Weight:_____

Sex:_____

Age:_____

Stature: left:_____ right:_____

Suprasternale height:_____

Substernale height:_____

Substernale depth:_____

Substernale breadth:_____

Substernale circumference:_____

Vertex to 12th rib:_____

Head to C7:_____

Mastoid to vertex: left:_____ right:_____

Tragon to vertex: left:_____ right:_____

Menton to vertex:_____

Bitragon diameter:_____

Acromion height: left:_____ right:_____

Acromion to tip of finger:_____

Biacromion:_____

Axillary breadth:_____

Axillary depth:_____

Axillary circumference:_____

Head breadth (R-L):_____

Head depth (A-P):_____

Head circumference:_____

Neck circumference:_____

Bitrochanteric breadth:_____

Symphysion depth:_____

Vertex to Symphysion:_____

Bispinous (ASIS) diameter:_____

Biiliocristale breadth:_____

ASIS to Symphysion:_____

Anatomical Anomalies / Clinical Observations

1. Head: a. Brain b. Skull

2. Neck:

3. Thorax: a. Ribs b. Heart c. Lungs d. Diaphragm

4. Pelvis:

5. Femur

6. Abdomen

RIB AND STERNUM MOUNTS

TASK	TIME	COMMENTS
Locate right and left R4 by palpation.		
Make incisions over ribs near flat region. Surface must be normal to the R-L vector.		
Loop two pieces of wire (1/2" apart) around each rib.		
Locate R8 by counting down from R4 and up from R12.		
Make incision over rib near flat region. Surface must be normal to the R-L vector.		
Make incisions over suprasternale and substernale.		
Secure mounts to rib by anchoring with pins and wire.		
Screw lag bolt into each acromion.		

PRESSURIZATION

TASK	TIME	COMMENTS
Locate right carotid and cut lengthwise.		
Locate right vertebral artery and ligate.		
Loop six pieces of string around carotid artery.		
Insert fabricated Foley catheter (#18 or #20) into descending aorta.		
Insert Kulite shield into ascending aorta.		
Insert Kulite shield into carotid artery.		
Insert arterial pressurization catheters into carotid artery.		
Using syringe, squirt acrylic into artery. Tie and sew.		
Locate left carotid, cut, loop strings.		
Locate left vertebral artery and ligate.		

PRESSURIZATION (CONT'D)

TASK	TIME	COMMENTS
Insert arterial pressurization catheters (#10, #12, or #14) into carotid artery.		
Acrylic, tie and sew.		
Locate trachea and cut lengthwise.		
Loop two Tie Wraps around trachea.		
Insert polyethelyne tube snugly, tie and sew.		
Calibrate lungs.		
Pulmonary pressure relief valve calibration.		
Vascular flow check.		
Sternal geometry if necessary.		

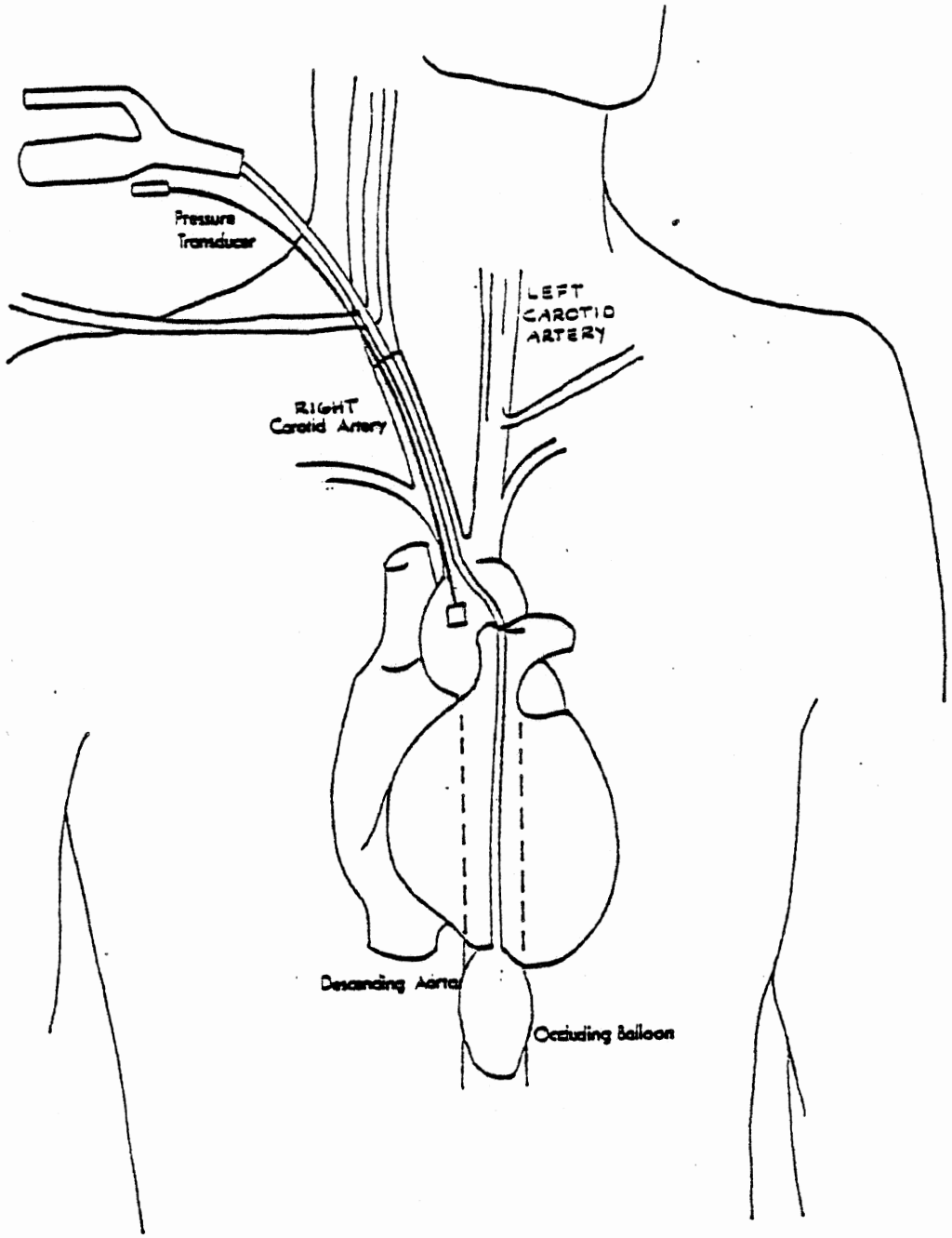
Pressure
Transducer
LEFT
CAROTID
ARTERY
RIGHT
Carotid Artery
Occluding balloon

Mounts - 30

HEAD 9-AX MOUNT

TASK	TIME	COMMENTS
With cadaver facing down, remove a 2x2" area of scalp spanning the right parietal and occipital bones.		
Drill three holes in a triangular pattern, approximately the size of the 9-ax plate.		
Insert three screws.		
Attach four feet to the 9-ax plate such that three of the feet can be positioned near the screws on the exposed forehead.		
Place acrylic around screws.		
Place plate on top of acrylic base, making sure the acrylic goes through the center holes in the plate.		
Insert a strain relief bolt in the acrylic base of the head platform. Make sure bolt does not contact plate.		

HEAD TRANSDUCERS

TASK	TIME	COMMENTS
Holes for transducers go on frontal,parietal, and occipital bones. Make sure no Xducers will contact the impacting surface. Also, the holes should not be drilled into suture.		
To drill holes, remove a 1/4" dia. circle of scalp.		
Drill through skull with a #7 drill. Be sure not to drill through the dura.		
Perforate the dura without cutting brain.		
Tap hole with a No.7 tap.		
Pinhead screws are attached 2cm from each transducer. Acrylic is applied to each area, carefully molding around the transducers.		
Note positions of head transducers on the figure.		

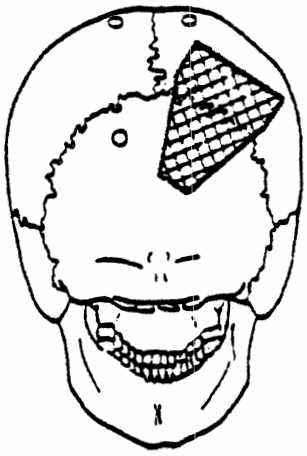

Posterior View

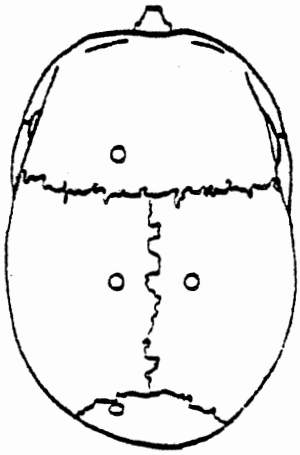

Superior View

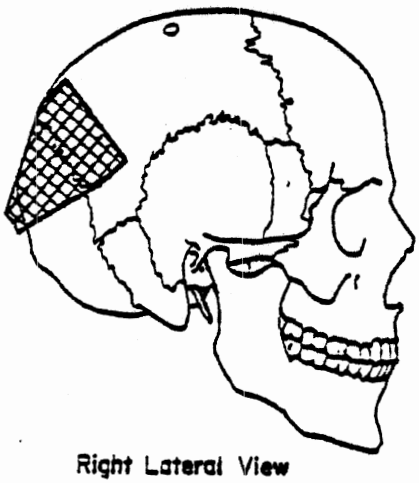

Right Lateral View

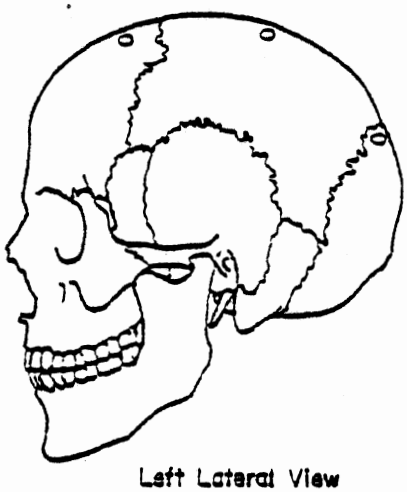

Left Lateral View

PELVIS MOUNT

TASK	TIME	COMMENTS
Locate the posterior-superior iliac spines.		
Screw two lag bolts into each spine such that the large 9-ax plate spans the bolts.		
Attach four feet to the plate such that the feet are near the lag bolts.		
Place acrylic around screws and feet.		
Imbed feet and posterior surface into acrylic.		
Test plate to see that it is secure.		

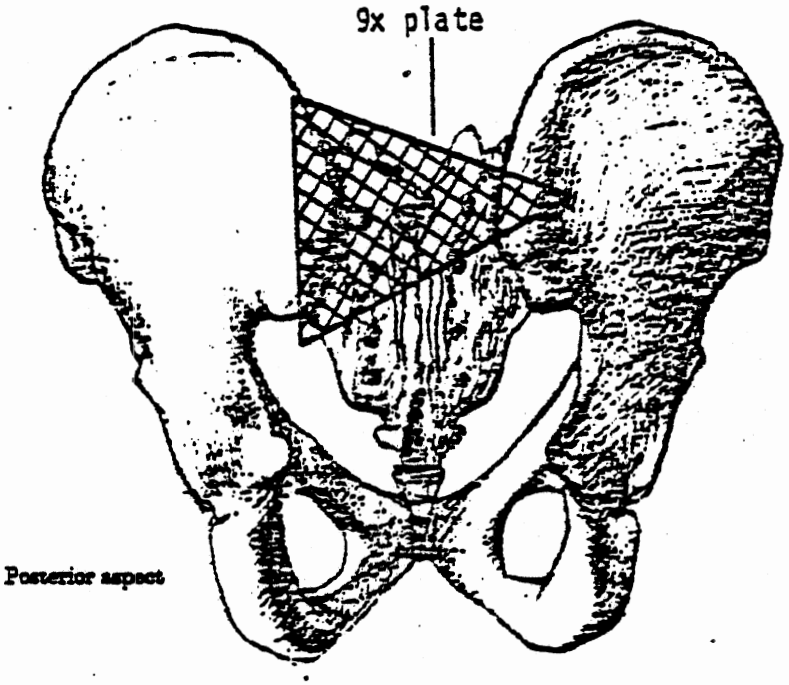
9x plate
Posterior aspect

SPINAL MOUNTS

TASK	TIME	COMMENTS
Spinal mounts go on T1 and T12.		
Make incisions over T1 and T12. Clear muscle and tissue away from process, but do not cut between processes.		
Drill a small hole 1/4" deep in each process.		
Screw mounts on with wood screws (be sure screws are in process).		
Place stabilizing and mooring probic devices on each side of the laminae. Secure with Tie Wraps.		
Mold acrylic around (and under) mounts and mooring devices and allow to dry.		
Make sure accelerom-eters are anatomically oriented.		
Spinal geometry if necessary.		

CEREBROSPINAL PRESSURIZATION

TASK	TIME	COMMENTS
Locate L2 by palpation and counting from T12.		
Core a small hole in the lamina.		
Insert Foley catheter (#14 or #16) such that balloon is in mid-thorax.		
Insert small screws in lamina and process.		
Seal off hole with acrylic.		
Check for structural integrity of vertebra.		
Cerebral-spinal flow check.		
Check pressurization.		

PREPARATION

TASK	TIME	COMMENTS
Dress cadaver.		
Place head and body harnesses on cadaver.		
Store cadaver if necessary.		
Transport cadaver to sled lab, being careful not to damage mounts.		
Place head, sternum, and rib transducers on cadaver. Stuff and sew.		
Set up pressurization equipment (pulmonary, cerebro-spinal, vascular head and vascular thorax).		

ELECTRONICS CHECK AND PRETEST TRIAL RUN

Electronics Check

___ check accelerometers (excitation and zero)
___ check wiring and cables
___ mount accelerometers in triax clusters
___ check amplifiers
___ calibrate tape with impedance-matching amp
___ recorder
___ complete wiring
___ check pendulum accelerometer
___ check velocity, strobe, gate, timer, rope cutters
___ run trial test
___ load cell mounted on pendulum day before test
___ load Photosonics and HyCam cameras with Kodak 16mm 7242-#FB-430 color film

Pretest Trial Run

1. ___ Suspend rubber tube five inches from pendulum with fiber tape.
2. ___ Tape all accelerometers to seat with paper tape.
3. ___ Attach the contact switches to the load cell and shock absorber with paper tape.
4. ___ Run trial test.
5. ___ Record all signals, gate, and strobe.
6. ___ Put a one-volt signal on a junk tape and check to see if one volt is played back. Use signal generator or impedance-matching amp with the scope to calibrate output.

HEAD IMPACT 1

Test No._____

TASK	TIME	COMMENTS
Head impact 1.		
Attach ball targets and phototargets.		
Change padding on impactor head surface.		
Set up head catch and spinal backup.		
Final positioning (see figure).		
Measure and record head and neck angles		
Setup photos.		
Final checklist.		
Start pressurization of vascular and cerebrospinal systems.		
Finish pressurizatons.		
Run test.		

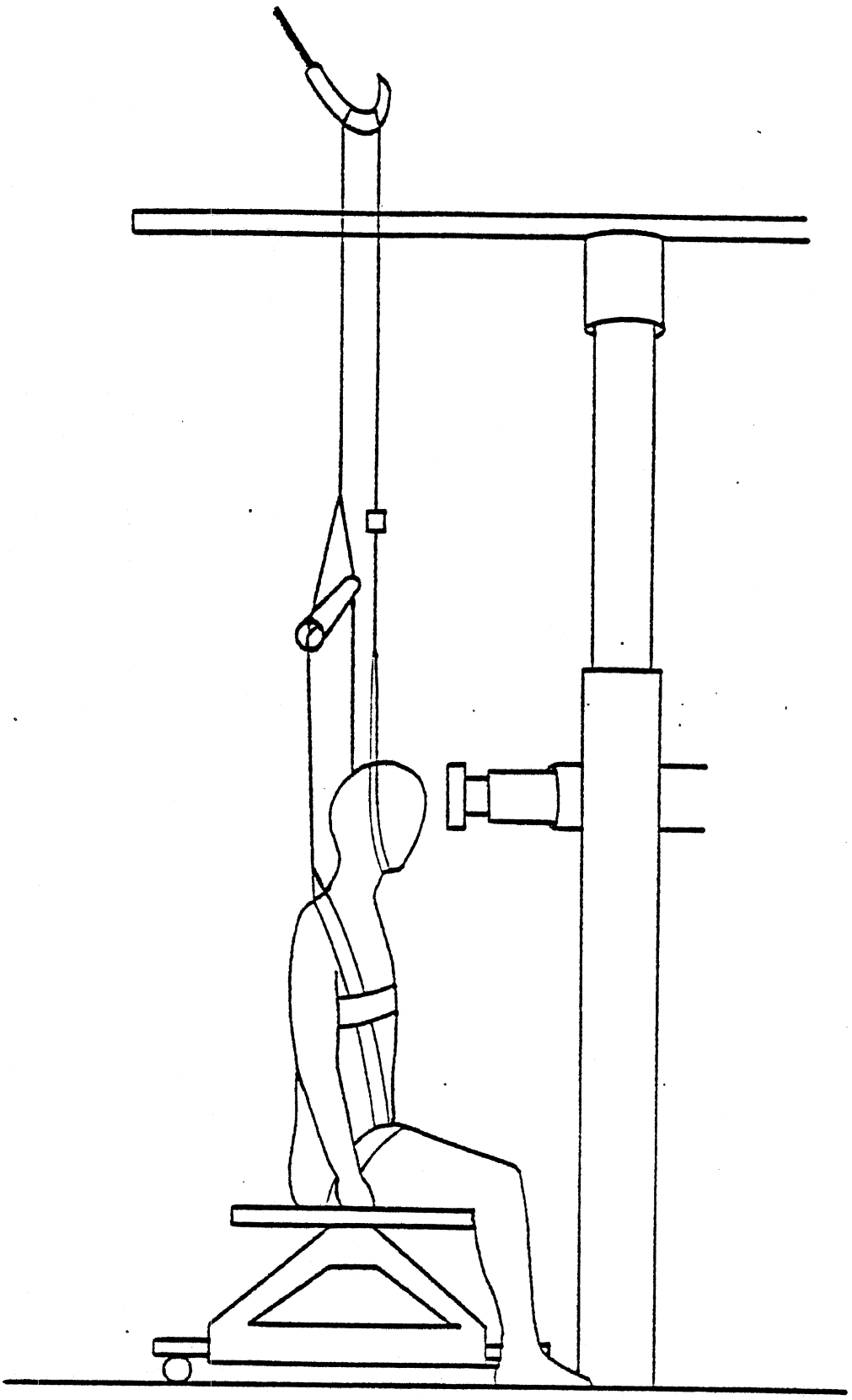

HEAD IMPACT 1

Timer Box Setup

EQUIPMENT	TIMER VALUES		
_____ Impact	Delay		Run
Gate (from strobe 1)	0011	1	0170
Lights (start)	0001	2	2600
HyCam (start)	1200	3	1600
Pendulum rope cutter(start)	1390	4	0050
Photosonics (start)	1000	5	1600
		6	
Head, pelvis, rope cutter (from velocity probe)	0001	7	0050
Piston Acceleration Corridor	0009	8	0050

FINAL CHECKLIST

____ check transducers

____ tape positioned

____ slots for velocity probe lined up

____ both strobes charged

____ timer box values correct

____ all timer box switches to 'off'

____ rope cutter threaded and ready

____ nylon (rope cutter) string unfrayed

____ rope cutter cable free

____ cameras set

____ Newtonian reference

____ calibration target

____ targets in view of cameras

____ padding

____ correct timers charged

____ gate trigger established

____ timing lights on

____ doors locked

____ final positioning

____ correct pressure system used

____ pendulum raised

____ power on

____ all pressure connections secured

____ zero piston accelerometer

____ head and neck angles

HEAD IMPACT 2

Test No._____

TASK	TIME	COMMENTS
Reposition as for tap.		
Check spinal brace and head catch.		
Final positioning		
Measure and record head and neck angles		
Setup photos.		
Start pressurization of vascular and cerebrospinal systems.		
Final checklist.		
Finish pressurization.		
Run test.		

HEAD IMPACT 2

Timer Box Setup

EQUIPMENT _____ Impact	TIMER VALUES Delay		Run
Gate (from strobe 1)	0008	1	0170
Lights (start)	0001	2	2600
HyCam (start)	1200	3	1600
Pendulum rope cutter(start)	1290	4	0050
Photosonics (start)	1000	5	1600
		6	
Head, pelvis, rope cutter (from velocity probe)	0001	7	0050
Piston Acceleration Corridor	0009	8	0050

FINAL CHECKLIST

____ check transducers

____ tape positioned

____ slots for velocity probe lined up

____ both strobes charged

____ timer box values correct

____ all timer box switches to 'off'

____ rope cutter threaded and ready

____ nylon (rope cutter) string unfrayed

____ rope cutter cable free

____ cameras set

____ Newtonian reference

____ calibration target

____ targets in view of cameras

____ padding

____ correct timers charged

____ gate trigger established

____ timing lights on

____ doors locked

____ final positioning

____ correct pressure system used

____ pendulum raised

____ power on

____ all pressure connections secured

____ zero piston accelerometer

____ head and neck angles

THORAX FRONT TAP

Test No._____

TASK	TIME	COMMENTS
Place seat in position and square on pendulum.		
String up rope cutters.		
Position subject as per figure with body and head harnesses. Protect any mounts that may be hit with gauze and padding.		
Subject should be in normal sitting position with back inclined approx. 10° forwards.		
Attach ball targets and phototargets.		
Place one of the pressure transducers that was in the head in the trachea, and place the Kulite in the descending aorta.		
Final positioning and setup photos (see fig)		
Final checklist.		
Start pressurization of vascular and respiratory systems.		
Finish pressurization.		
Run test.		

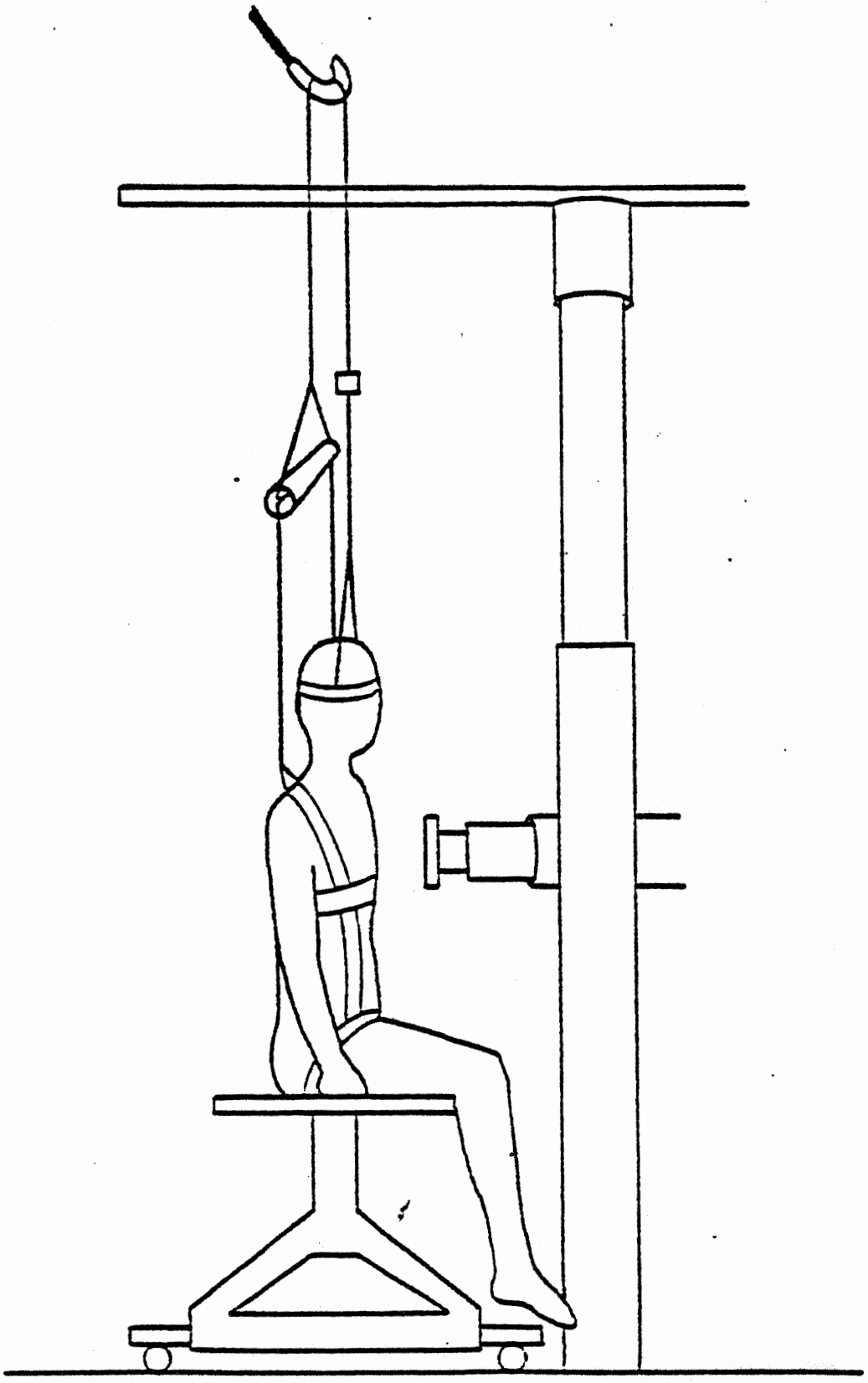

THORAX FRONT TAP

Timer Box Setup

EQUIPMENT	TIMER VALUES		
_____ Impact	Delay		Run
Gate (from strobe 1)	0021	1	0170
Lights (start)	0001	2	2600
HyCam (start)	1200	3	1600
Pendulum rope cutter(start)	1400	4	0050
Photosonics (start)	1000	5	1600
		6	
Head, pelvis, rope cutter (from velocity probe)	0001	7	0050
Piston Acceleration Corridor	0012	8	0150

FINAL CHECKLIST

____ check transducers

____ tape positioned

____ slots for velocity probe lined up

____ both strobes charged

____ timer box values correct

____ all timer box switches to 'off'

____ rope cutter threaded and ready

____ nylon (rope cutter) string unfrayed

____ rope cutter cable free

____ cameras set

____ Newtonian reference

____ calibration target

____ targets in view of cameras

____ padding

____ correct timers charged

____ gate trigger established

____ timing lights on

____ doors locked

____ final positioning

____ correct pressure system used

____ pendulum raised

____ power on

____ all pressure connections secured

____ zero piston accelerometer

____ head and neck angles

45° THORAX TAP

Test No._____

TASK	TIME	COMMENTS
Place seat in position.		
String up rope cutters.		
Position subject as per figure with body and head harnesses. Protect any mounts that may be hit with gauze and padding.		
Subject should be in normal sitting position with back inclined approx. 10° forwards.		
Attach ball targets and phototargets.		
Final positioning and setup photos (see fig)		
Final checklist.		
Start pressurization of vascular and respiratory systems.		
Finish pressurization.		
Run test.		

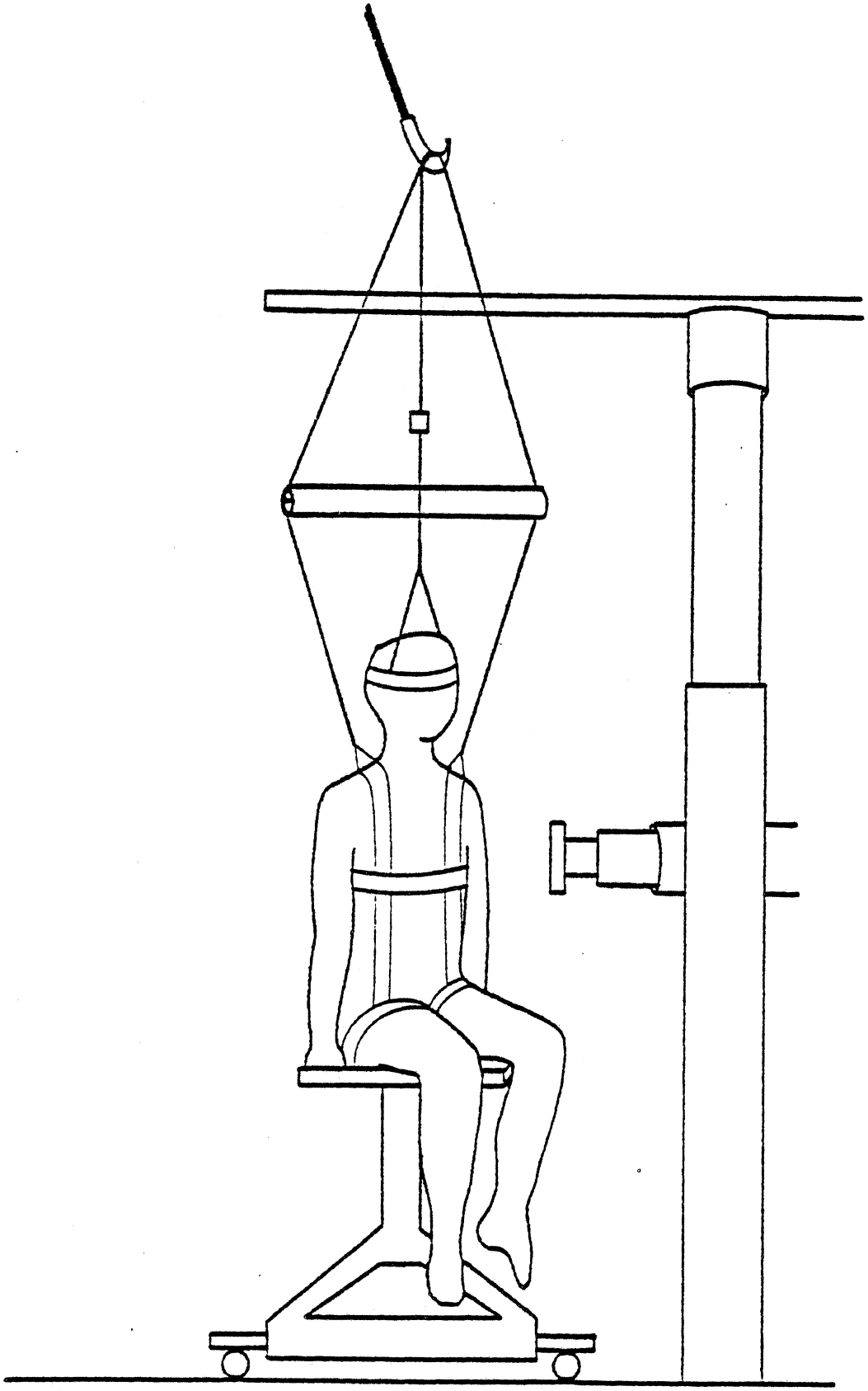

45° THORAX TAP

Timer Box Setup

EQUIPMENT _____ Impact	TIMER VALUES Delay		 Run
Gate (from strobe 1)	0021	1	0170
Lights (start)	0001	2	2600
HyCam (start)	1200	3	1600
Pendulum rope cutter(start)	1400	4	0050
Photosonics (start)	1000	5	1600
		6	
Head, pelvis, rope cutter (from velocity probe)	0001	7	0050
Piston Acceleration Corridor	0012	8	0150

FINAL CHECKLIST

____ check transducers

____ tape positioned

____ slots for velocity probe lined up

____ both strobes charged

____ timer box values correct

____ all timer box switches to 'off'

____ rope cutter threaded and ready

____ nylon (rope cutter) string unfrayed

____ rope cutter cable free

____ cameras set

____ Newtonian reference

____ calibration target

____ targets in view of cameras

____ padding

____ correct timers charged

____ gate trigger established

____ timing lights on

____ doors locked

____ final positioning

____ correct pressure system used

____ pendulum raised

____ power on

____ all pressure connections secured

____ zero piston accelerometer

____ head and neck angles

OPTIONAL ARMS-UP THORAX TAP

Test No._____

TASK	TIME	COMMENTS
Place seat in position.		
String up rope cutters.		
Position subject as per figure with body and head harnesses. Protect any mounts that may be hit with gauze and padding.		
Subject should be in normal sitting position with back inclined approx. 10° forwards.		
Attach ball targets and phototargets.		
Final positioning and setup photos see drawings and figures by ***PAULA LUX***		
Final checklist.		
Start pressurization of vascular and respiratory systems.		
Finish pressurization.		
Run test.		

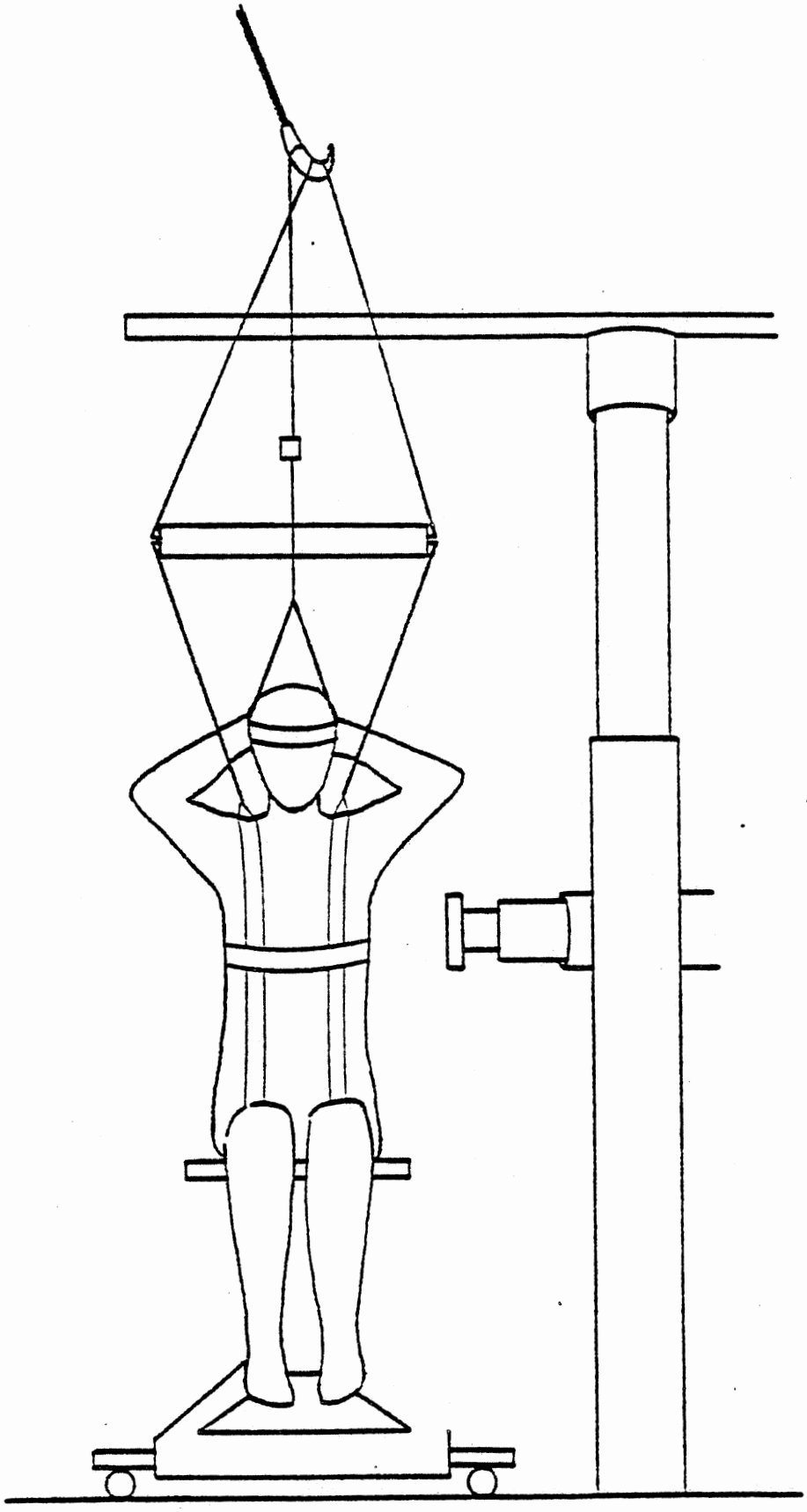

B60

OPTIONAL ARMS-UP THORAX TAP

Timer Box Setup

EQUIPMENT	TIMER VALUES		
_____ Impact	Delay		Run
Gate (from strobe 1)	0021	1	0170
Lights (start)	0001	2	2600
HyCam (start)	1200	3	1600
Pendulum rope cutter(start)	1400	4	0050
Photosonics (start)	1000	5	1600
		6	
Head, pelvis, rope cutter (from velocity probe)	0001	7	0050
Piston Acceleration Corridor	0012	8	0150

FINAL CHECKLIST

____ check transducers

____ tape positioned

____ slots for velocity probe lined up

____ both strobes charged

____ timer box values correct

____ all timer box switches to 'off'

____ rope cutter threaded and ready

____ nylon (rope cutter) string unfrayed

____ rope cutter cable free

____ cameras set

____ Newtonian reference

____ calibration target

____ targets in view of cameras

____ padding

____ correct timers charged

____ gate trigger established

____ timing lights on

____ doors locked

____ final positioning

____ correct pressure system used

____ pendulum raised

____ power on

____ all pressure connections secured

____ zero piston accelerometer

____ head and neck angles

ARMS-DOWN THORAX TAP

Test No._____

TASK	TIME	COMMENTS
Place seat in position.		
String up rope cutters.		
Position subject as per figure with body and head harnesses. Protect any mounts that may be hit with gauze and padding.		
Subject should be in normal sitting position with back inclined approx. 10° forwards.		
Attach ball targets and phototargets.		
Final positioning and setup photos (see fig)		
Final checklist.		
Start pressurization of vascular and respiratory systems.		
Finish pressurization.		
Run test.		

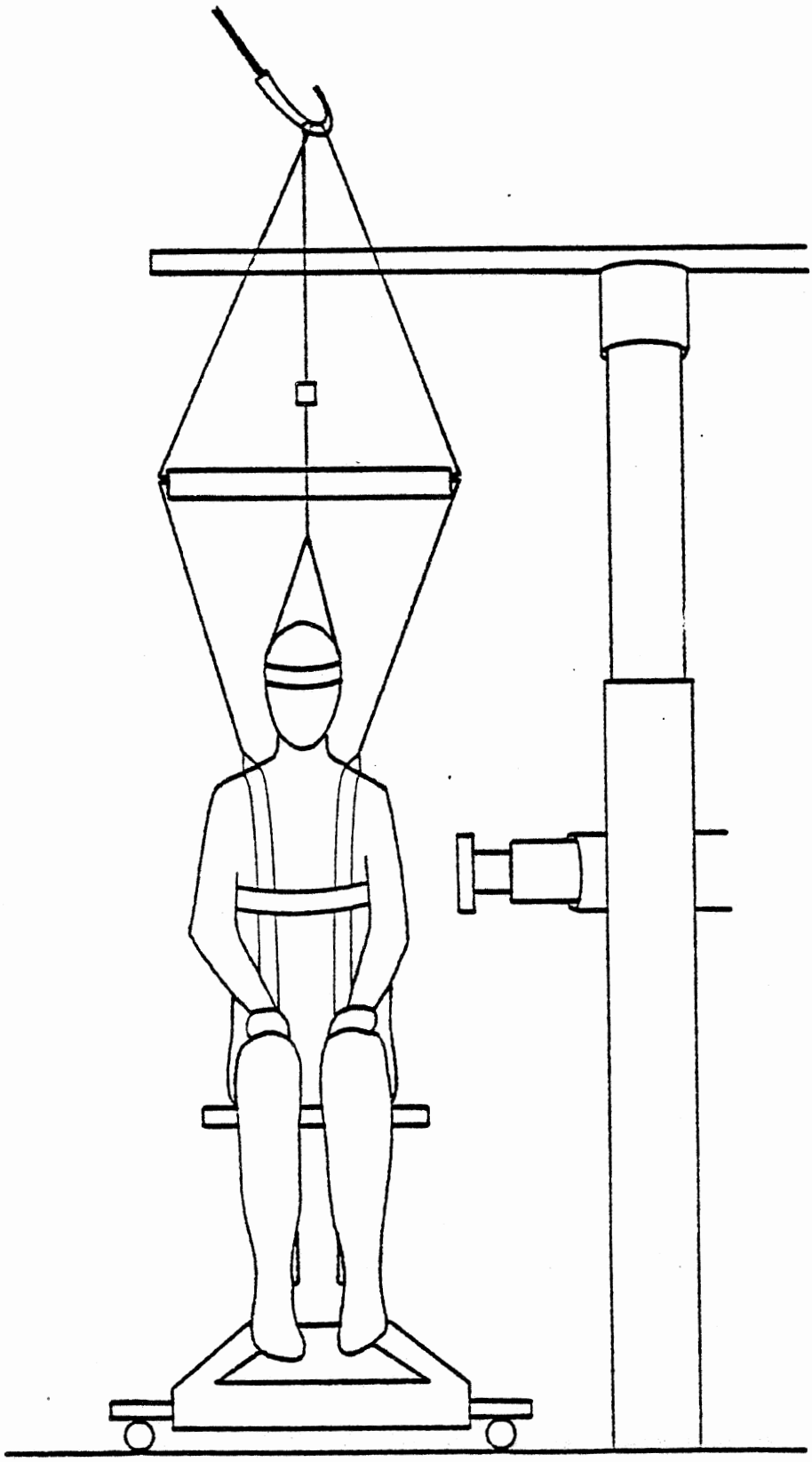

ARMS-DOWN THORAX TAP

Timer Box Setup

EQUIPMENT	TIMER VALUES		
_____ Impact	Delay		Run
Gate (from strobe 1)	0021	1	0170
Lights (start)	0001	2	2600
HyCam (start)	1200	3	1600
Pendulum rope cutter(start)	1400	4	0050
Photosonics (start)	1000	5	1600
		6	
Head, pelvis, rope cutter (from velocity probe)	0001	7	0050
Piston Acceleration Corridor	0012	8	0150

FINAL CHECKLIST

____ check transducers

____ tape positioned

____ slots for velocity probe lined up

____ both strobes charged

____ timer box values correct

____ all timer box switches to 'off'

____ rope cutter threaded and ready

____ nylon (rope cutter) string unfrayed

____ rope cutter cable free

____ cameras set

____ Newtonian reference

____ calibration target

____ targets in view of cameras

____ padding

____ correct timers charged

____ gate trigger established

____ timing lights on

____ doors locked

____ final positioning

____ correct pressure system used

____ pendulum raised

____ power on

____ all pressure connections secured

____ zero piston accelerometer

____ head and neck angles

THORAX IMPACT

Test No._____

TASK	TIME	COMMENTS
Reposition for shoulder (arms down) impact.		
Set up catch net.		
Slacken body harness.		
Start pressurization of vascular and respiratory systems.		
Final checklist.		
Finish pressurization.		
Run test		

ARMS-DOWN THORAX IMPACT

Timer Box Setup

EQUIPMENT _____ Impact	TIMER VALUES Delay		Run
Gate (from strobe 1)	0006	1	0170
Lights (start)	0001	2	2600
HyCam (start)	1200	3	1600
Pendulum rope cutter(start)	1220	4	0050
Photosonics (start)	1000	5	1600
		6	
Head, pelvis, rope cutter (from velocity probe)	0002	7	0050
Piston Acceleration Corridor	0006	8	0050

FINAL CHECKLIST

____ check transducers

____ tape positioned

____ slots for velocity probe lined up

____ both strobes charged

____ timer box values correct

____ all timer box switches to 'off'

____ rope cutter threaded and ready

____ nylon (rope cutter) string unfrayed

____ rope cutter cable free

____ cameras set

____ Newtonian reference

____ calibration target

____ targets in view of cameras

____ padding

____ correct timers charged

____ gate trigger established

____ timing lights on

____ doors locked

____ final positioning

____ correct pressure system used

____ pendulum raised

____ power on

____ all pressure connections secured

____ zero piston accelerometer

____ head and neck angles

PELVIS IMPACT

Test No._____

TASK	TIME	COMMENTS
Install pelvic and spinal accelerometers. Stuff and sew. Pad pelvic plate.		
Attach ball targets and phototargets.		
Change padding on impact head surface.		
Final positioning, setup photos (see fig)		
Final checklist.		
Run test.		

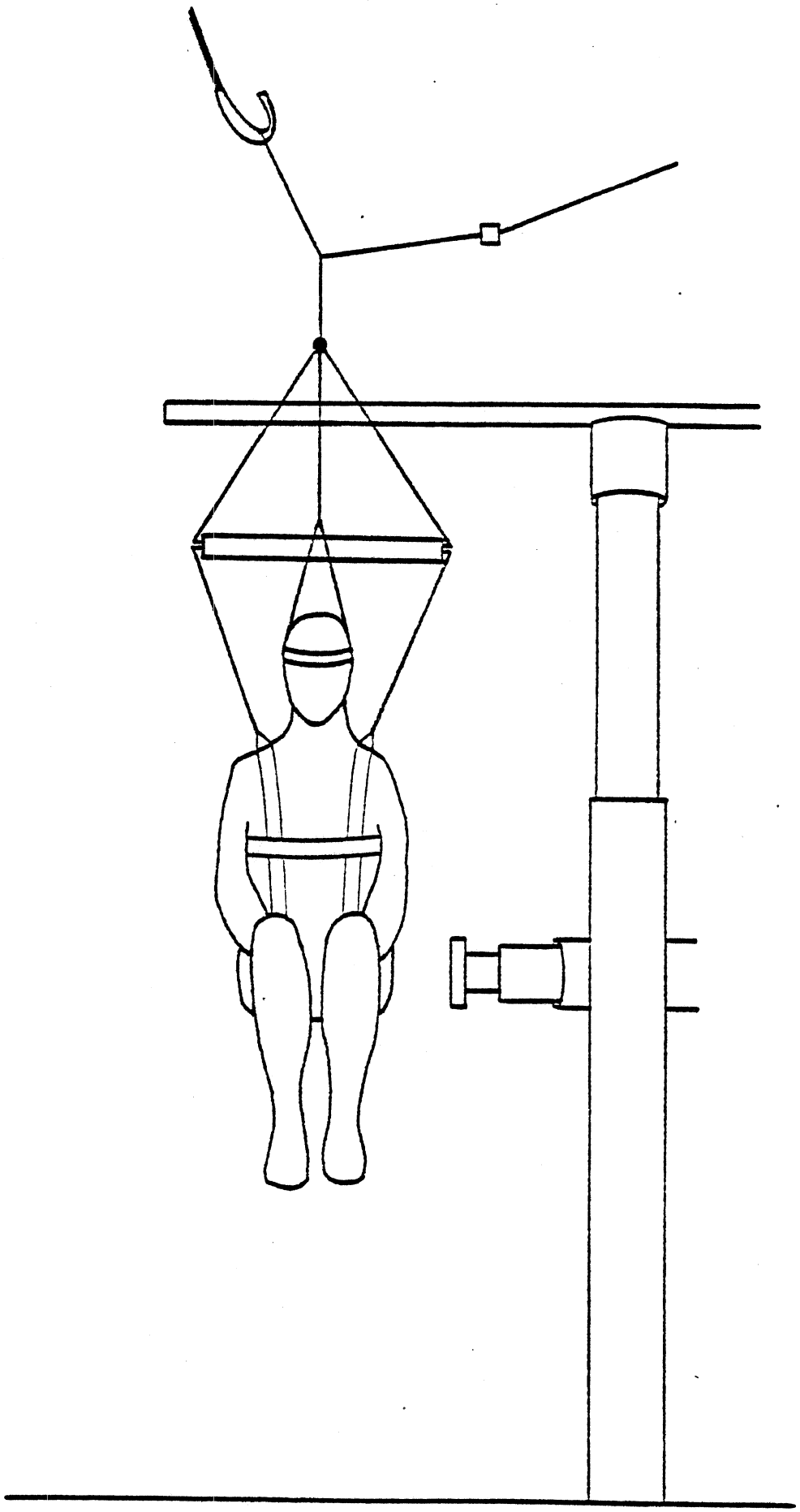

PELVIS IMPACT

Timer Box Setup

EQUIPMENT _____ Impact	TIMER VALUES Delay		 Run
Gate (from strobe 1)	0006	1	0170
Lights (start)	0001	2	2600
HyCam (start)	1200	3	1600
Pendulum rope cutter(start)	1220	4	0050
Photosonics (start)	1000	5	1600
		6	
Head, pelvis, rope cutter (from velocity probe)	0002	7	0050
Piston Acceleration Corridor	0006	8	0050

FINAL CHECKLIST

____ check transducers

____ tape positioned

____ slots for velocity probe lined up

____ both strobes charged

____ timer box values correct

____ all timer box switches to 'off'

____ rope cutter threaded and ready

____ nylon (rope cutter) string unfrayed

____ rope cutter cable free

____ cameras set

____ Newtonian reference

____ calibration target

____ targets in view of cameras

____ padding

____ correct timers charged

____ gate trigger established

____ timing lights on

____ doors locked

____ final positioning

____ correct pressure system used

____ pendulum raised

____ power on

____ all pressure connections secured

____ zero piston accelerometer

____ head and neck angles

POST TEST PROCEDURE

TASK	TIME	COMMENTS
Remove all targets and triax clusters.		
Store cadaver if necessary.		
Transport cadaver to anatomy lab.		
Remove all instrumentation, except for 9AX head plate.		
Remove head and transport it to X-Ray Room for post test radiographs.		

Z-X
(Profile)

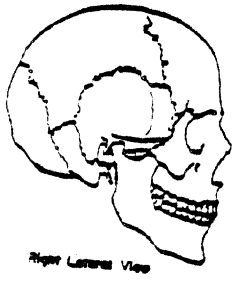

Z-Y
(Frontal)

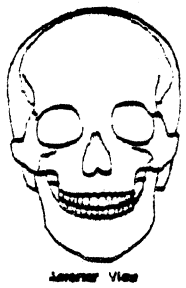

X-RAYS (X-RAY ROOM)

Reference Point	Z-X Distance from Table	Z-Y Distance from Table
R. Eye		
L. Eye		
R. Ear		
L. Ear		
Q1		
Q2		
Q3		
CG		

KVP MA SEC LABEL

Z-X ____/____/____/_____ (100/10/1)

Z-Y ____/____/____/_____ (100/10/1)

AUTOPSY

TASK	TIME	COMMENTS
After completion of radiographs, transport head to Anatomy Room for commencement of Autopsy.		
Autopsy		
SAVE RIBS RIGHT SIDE 4, 5, 6		

Observed Injuries

1. Head: a. Brain b. Kull

2. Neck:

3. Thorax: a. Ribs b. Heart c. Lungs d. Diaphragm

4. Pelvis:

5. Femur

6. Abdomen

COMMENTS:

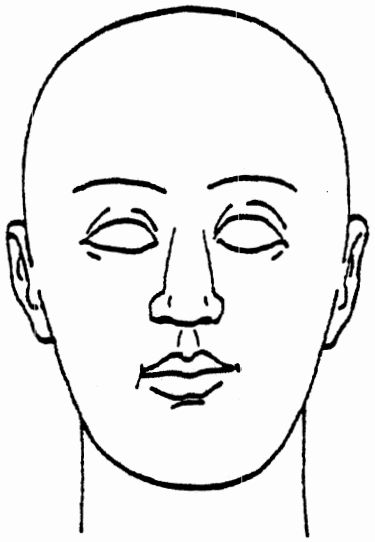

Anterior View

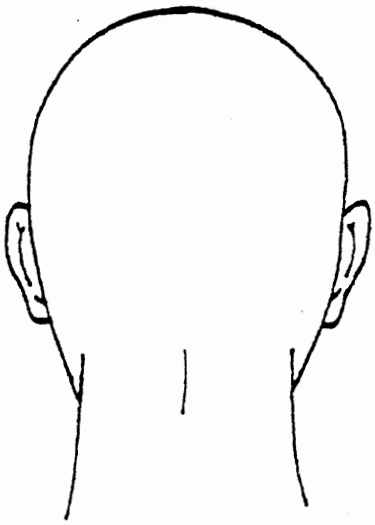

Posterior View

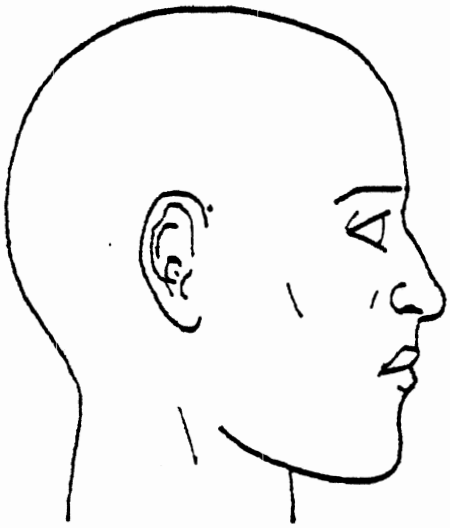

Right Lateral View

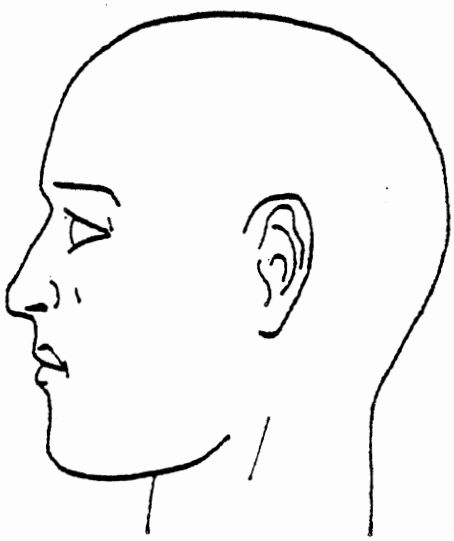

Left Lateral View

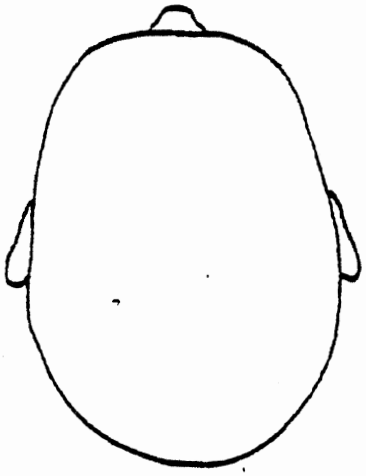

Superior View

TEST NO. _____

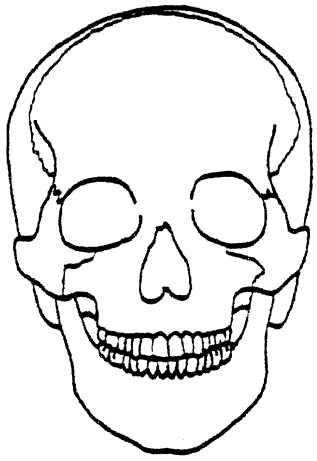

Anterior View

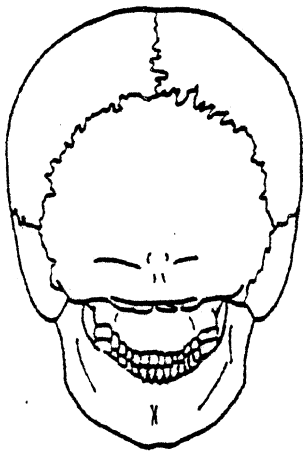

Posterior View

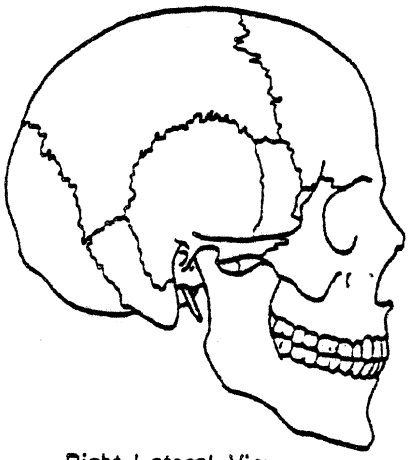

Right Lateral View

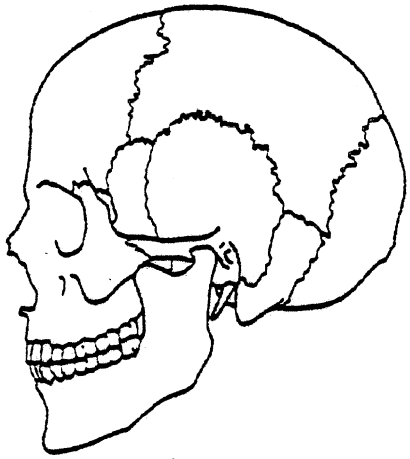

Left Lateral View

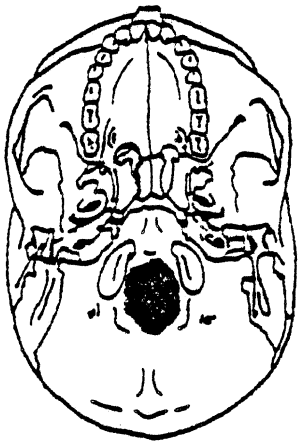

Inferior View

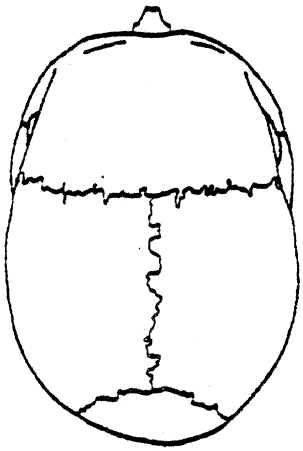

Superior View

TEST NO. _____

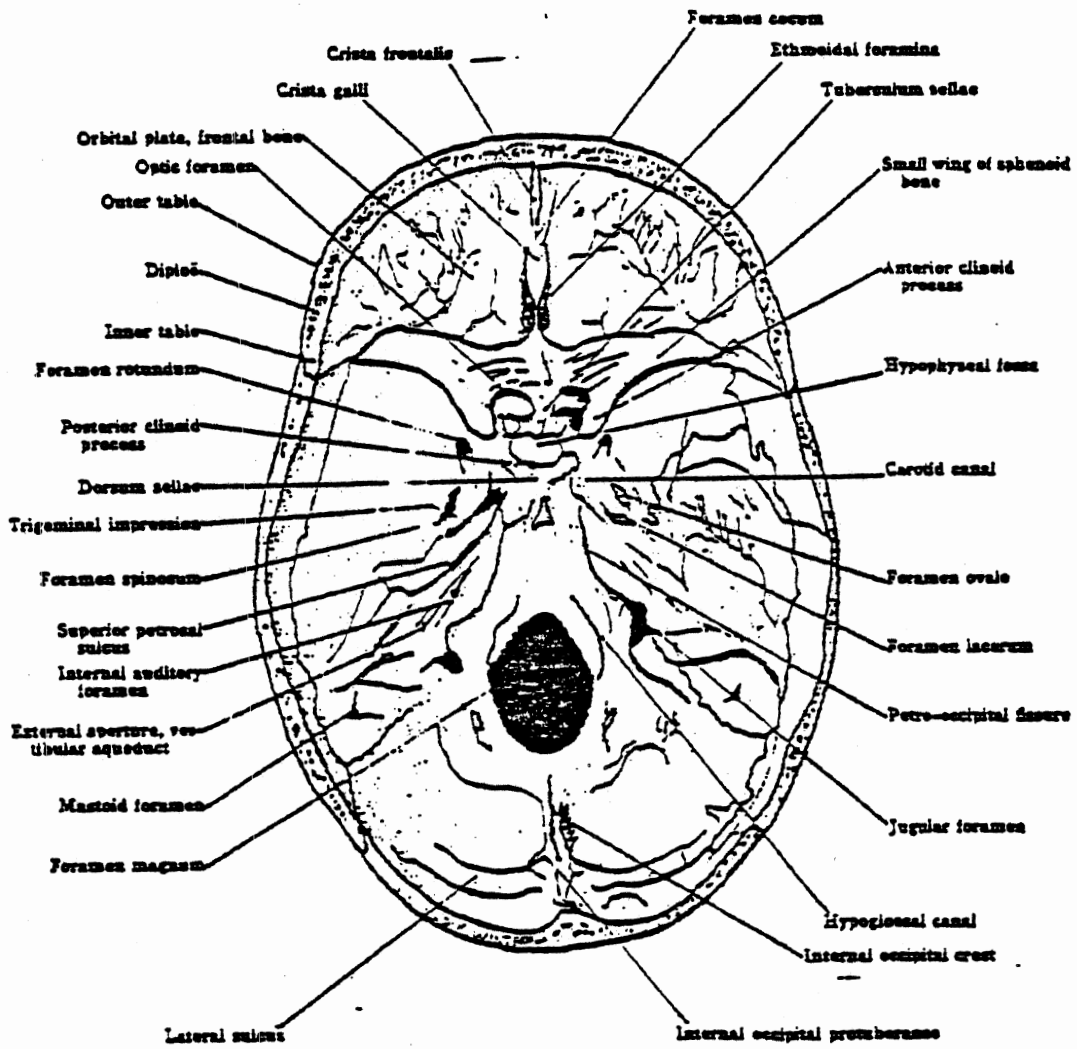

FIG. 109.—THE SKULL, INTERNAL ASPECT OF THE BASE.

TEST NO ____ _____

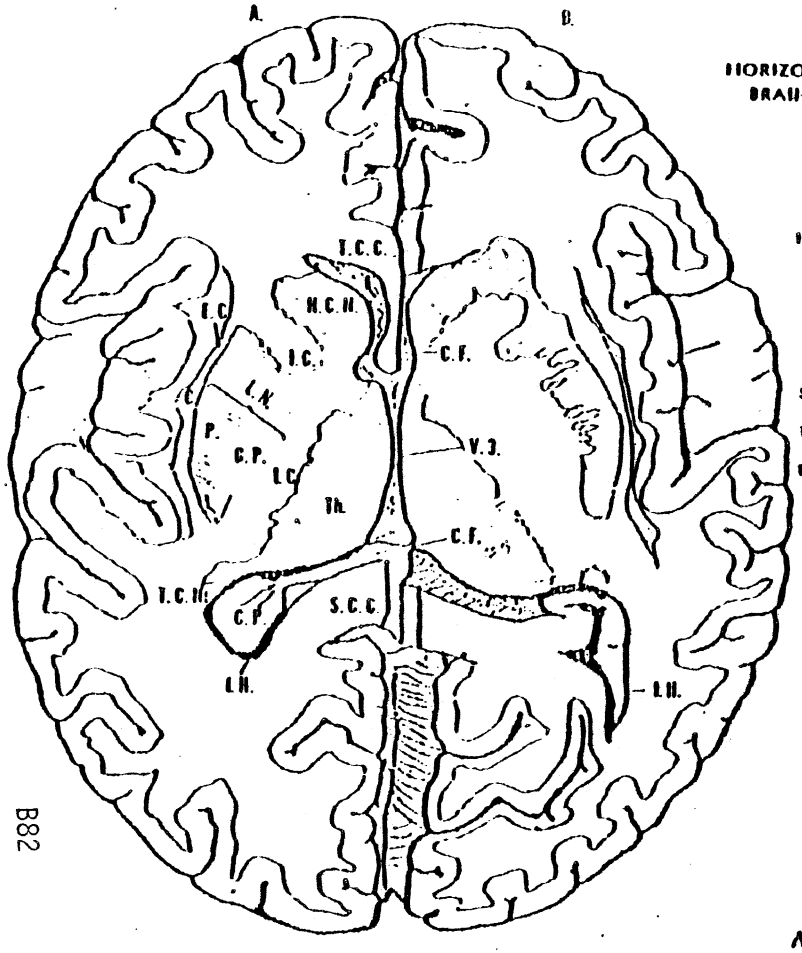

HORIZONTAL SECTIONS OF BRAIN AT TWO LEVELS

C. — Claustrum
C.F. — Crus of Fornix
C.P. — Choroid Plexus
E.C. — External Capsule
G.P. — Globus Pallidus
H.C.N. — Head of Caudate Nucleus
I.C. — Internal Capsule
I.H. — Inferior Horn of Lateral Ventricle
L.N. — Lenticular Nucleus
P. — Putamen
S.C.C. — Splenium of Corpus Callosum
T.C.C. — Trunk of Corpus Callosum
T.C.N. — Tail of Caudate Nucleus
Th. — Thalamus
V.3. — 3rd Ventricle

B82

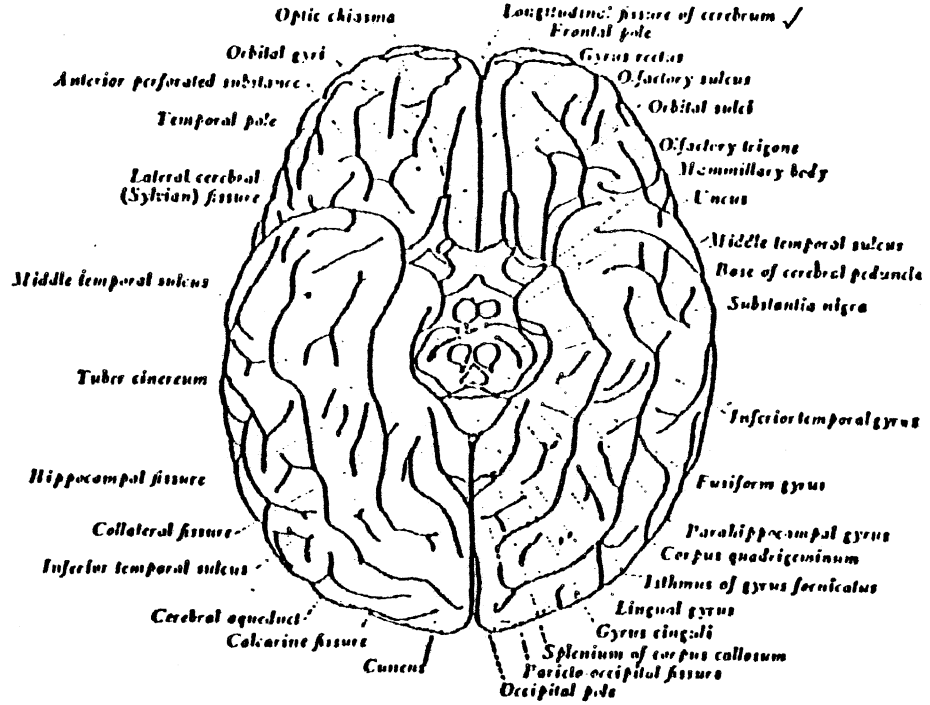

Basal aspect of the human cerebral hemisphere. (Sobotta-McMurrich.)

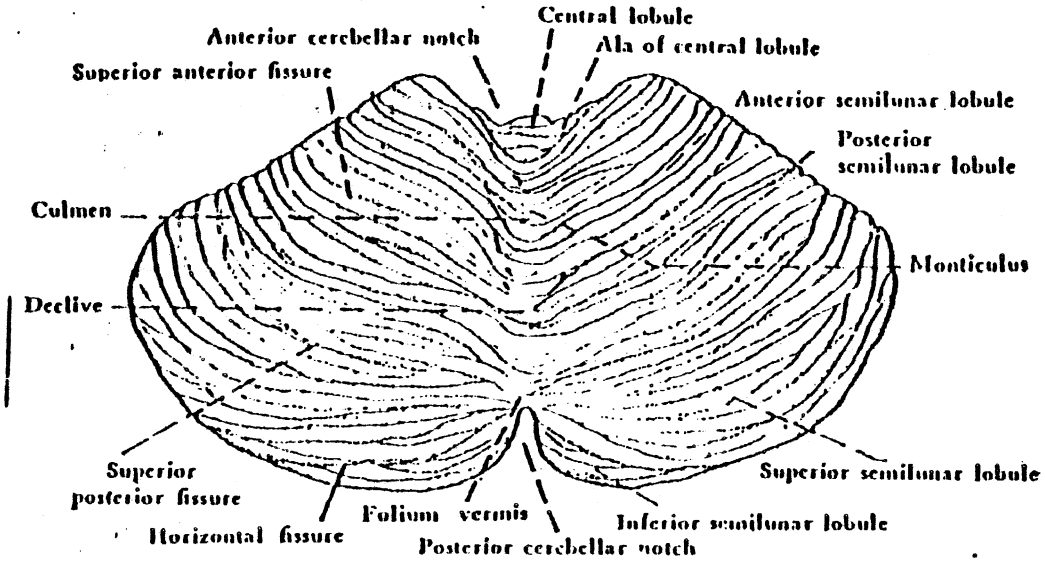

TEST NO. _____

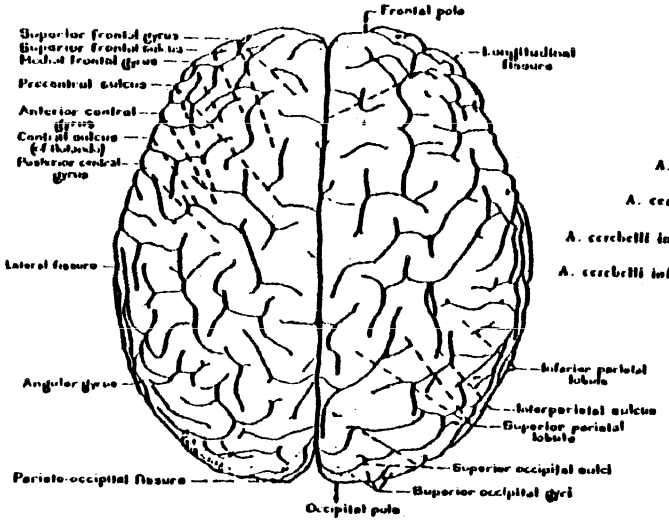

— Cerebral Hemispheres Viewed from Above.

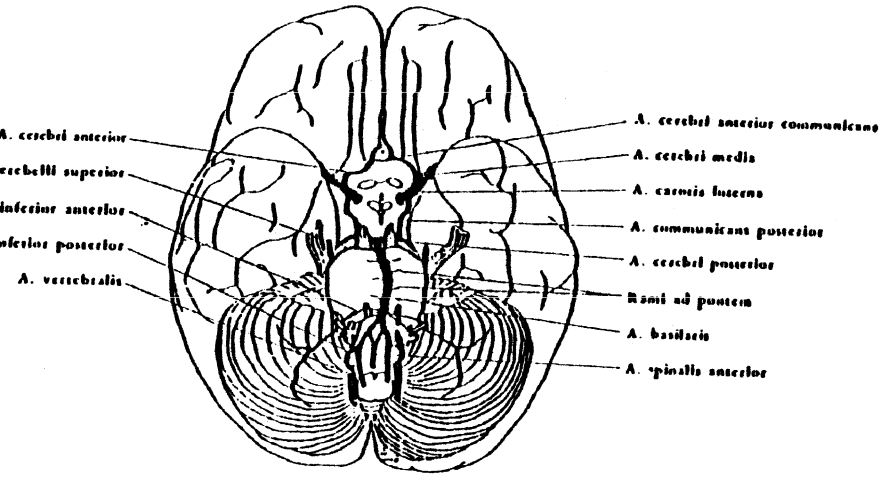

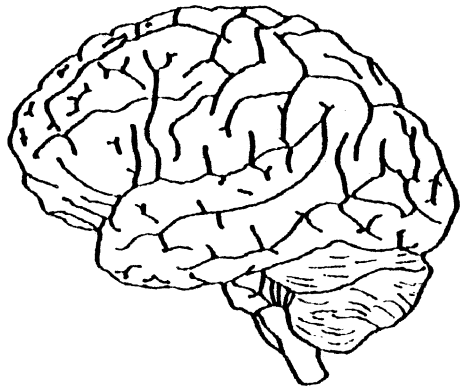

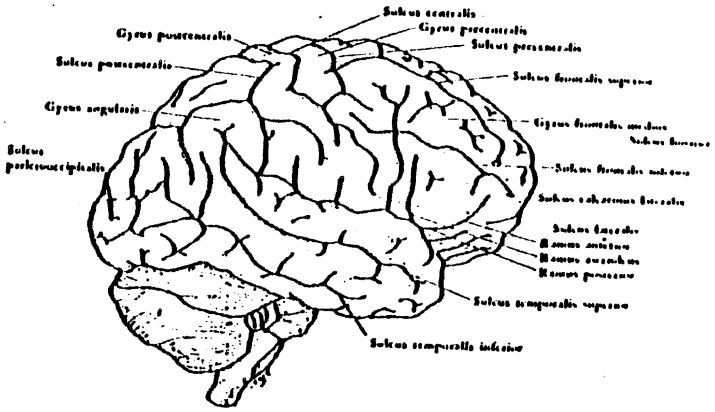

B83

TEST NO. _____

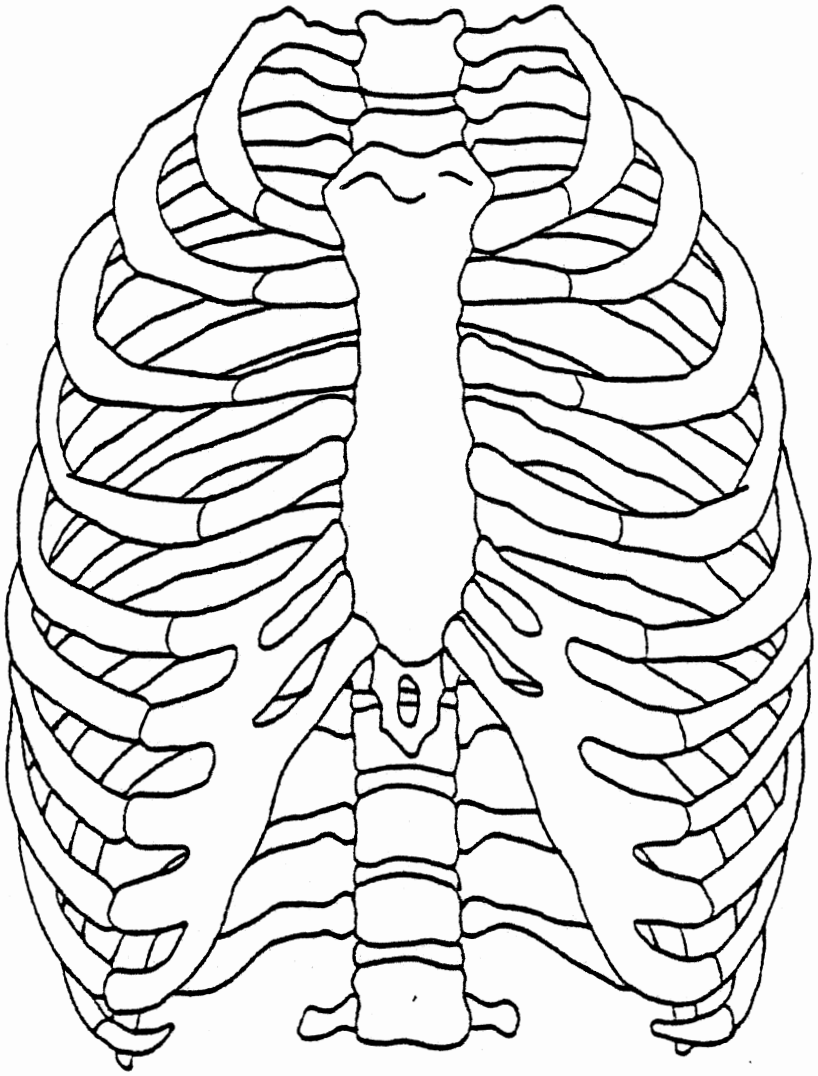

ANTERIOR THORAX

Test No._____

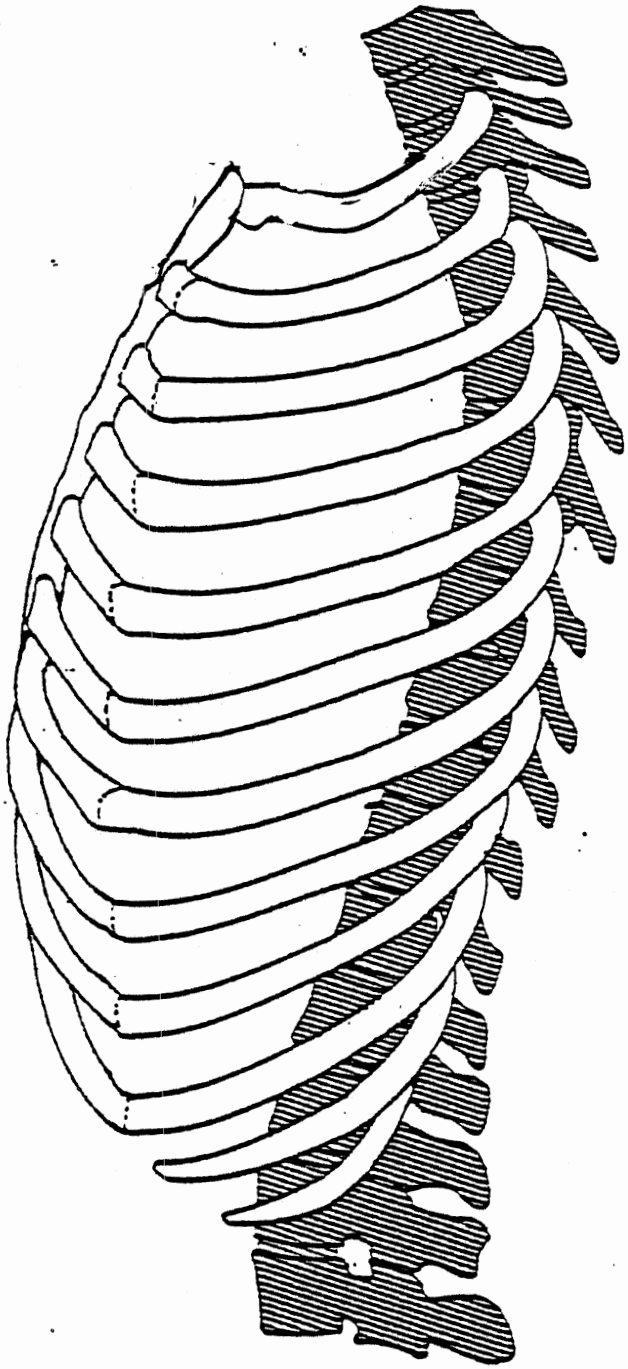

Test No._____

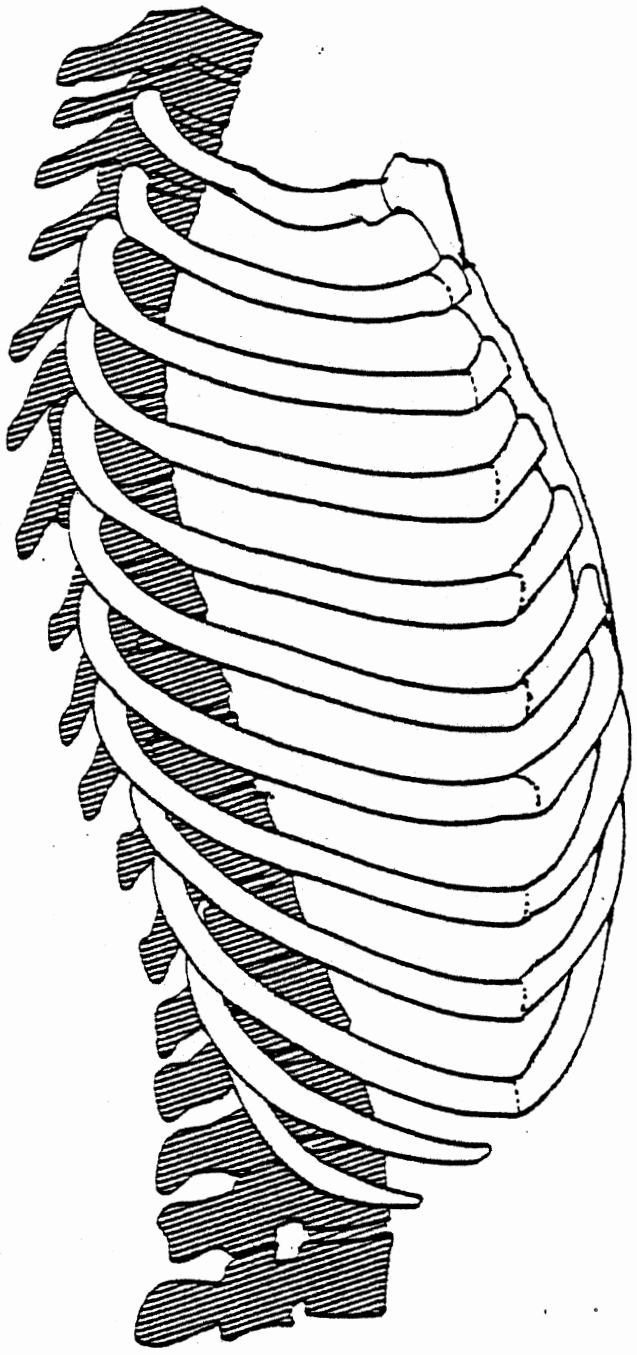

TEST NO. _____

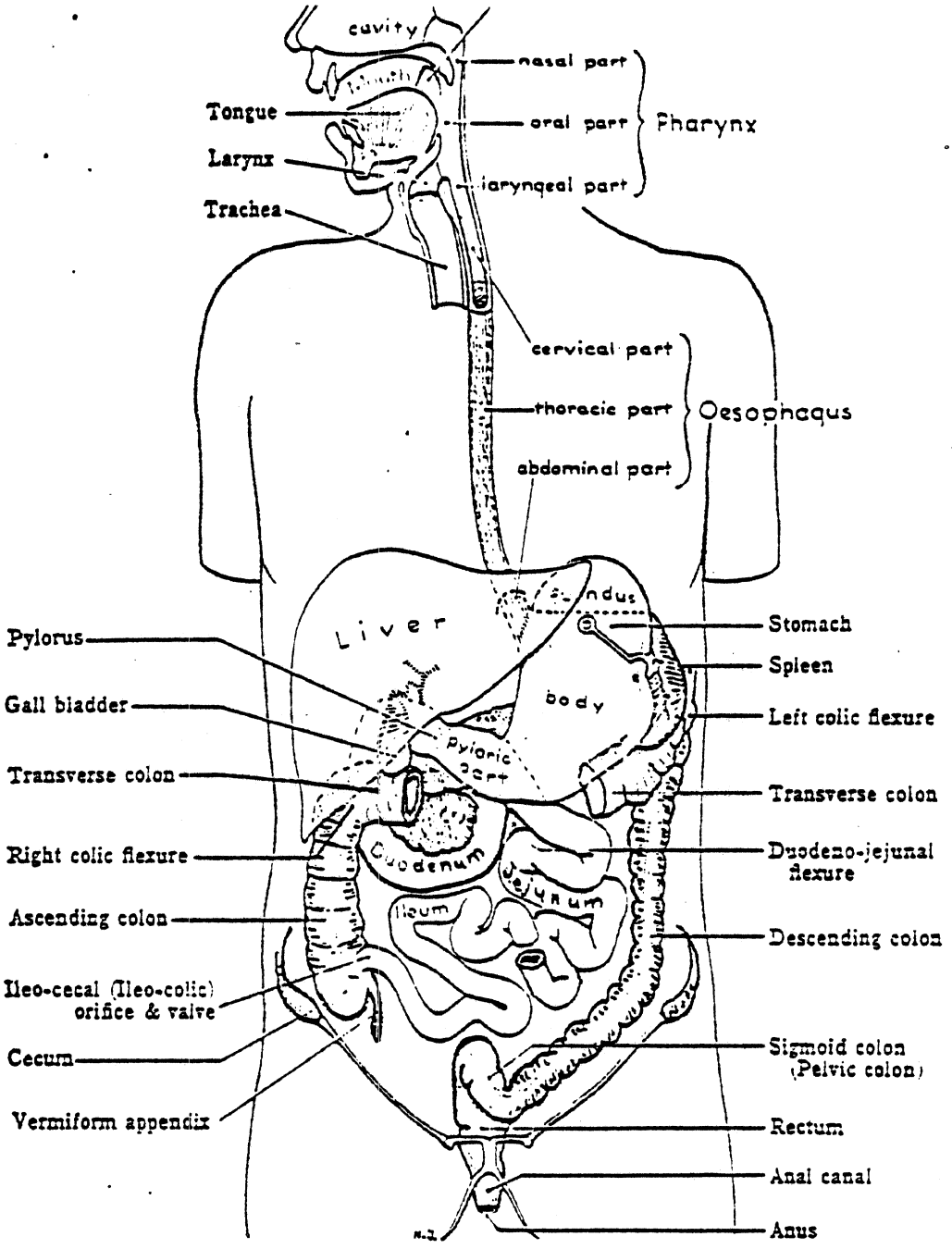
cavity
nasal part
Tongue
oral part
Pharynx
Larynx
laryngeal part
Trachea
cervical part
thoracic part
Oesophagus
abdominal part
Liver
Fundus
Stomach
Pylorus
Spleen
body
Gall bladder
Left colic flexure
Pyloric part
Transverse colon
Transverse colon
Duodenum
Right colic flexure
Duodeno-jejunal flexure
Jejunum
Ileum
Ascending colon
Descending colon
Ileo-cecal (Ileo-colic) orifice & valve
Sigmoid colon (Pelvic colon)
Cecum
Vermiform appendix
Rectum
Anal canal
Anus

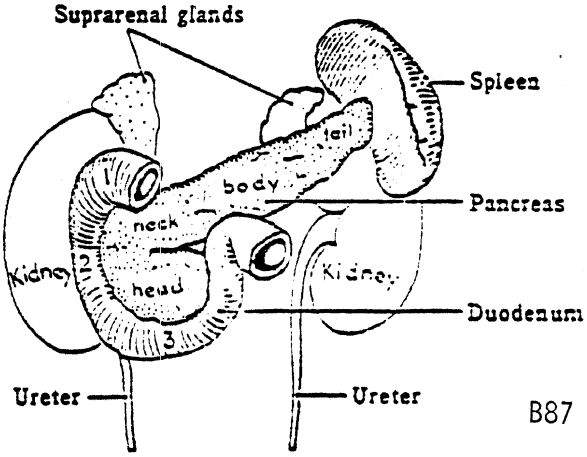
Suprarenal glands
Spleen
tail
body
Pancreas
neck
Kidney
Kidney
head
Duodenum
Ureter
Ureter

B87

Test No._____

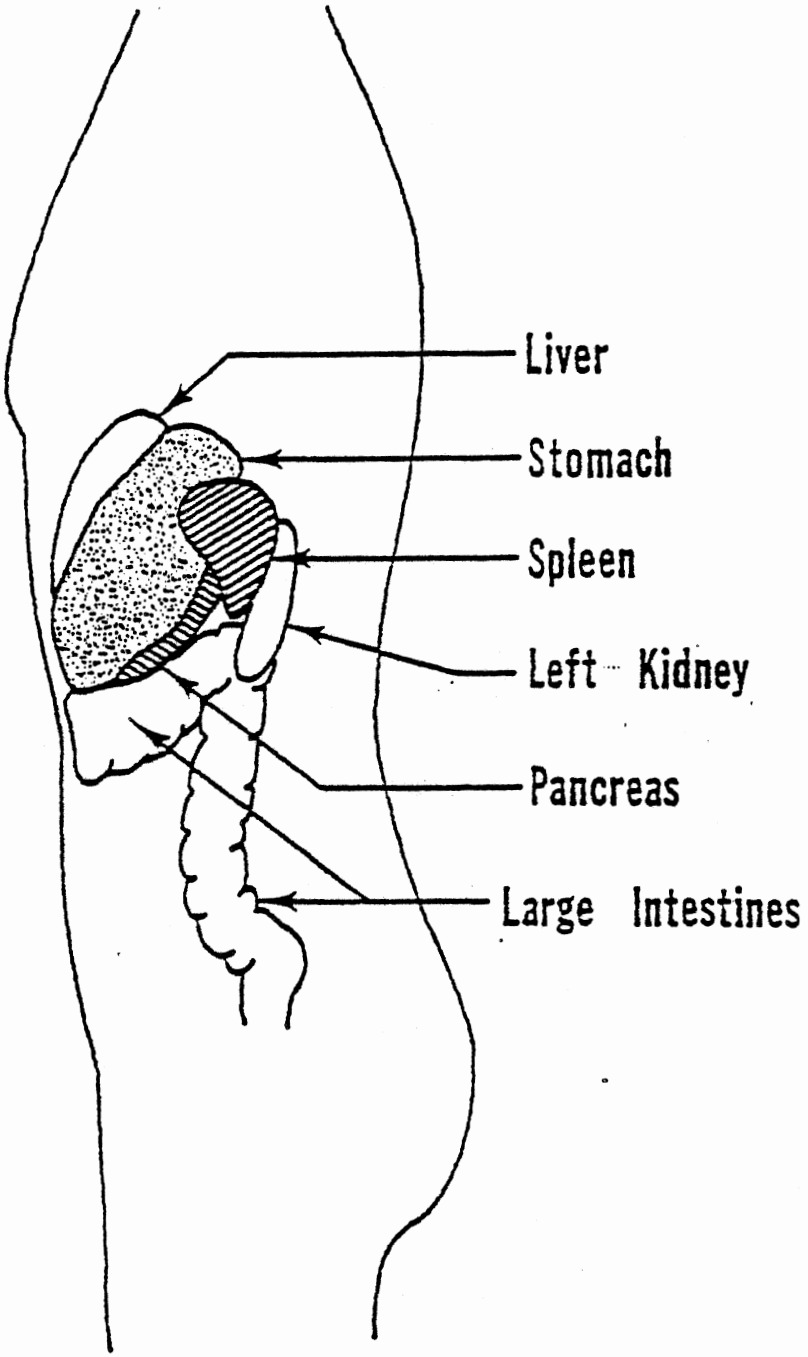

LEFT SIDE

TEST NO. _____

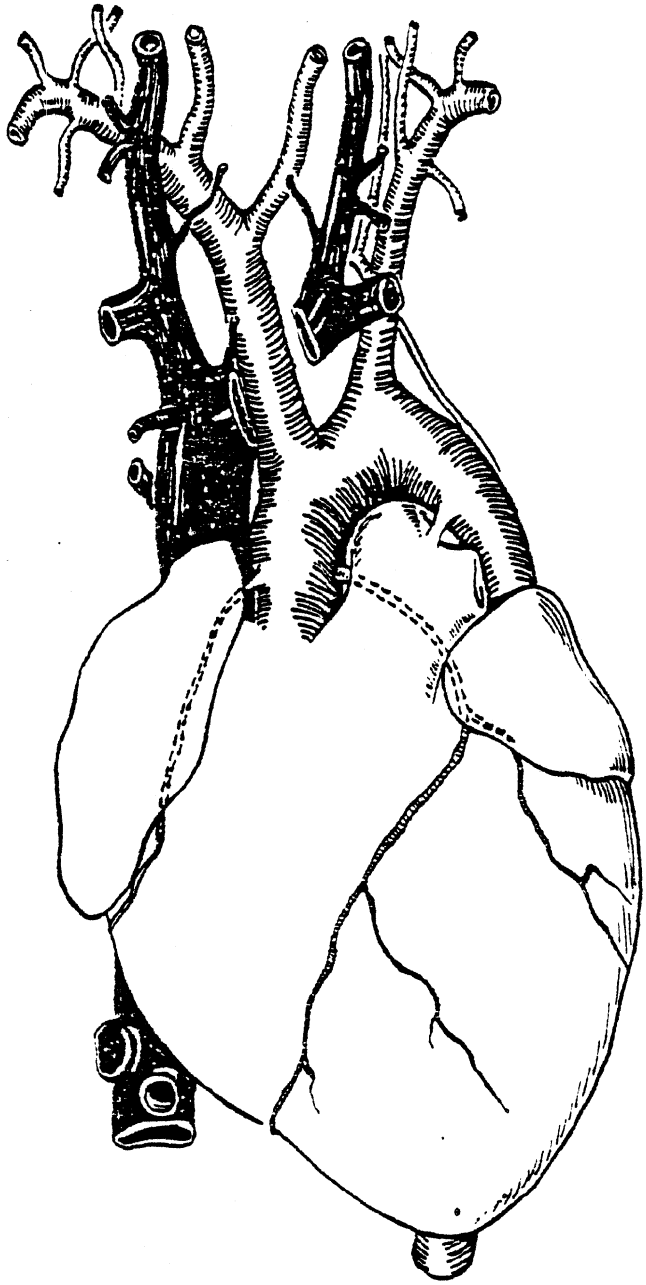

TEST NO. _____

Left Side View of Pericardium and Diaphragm

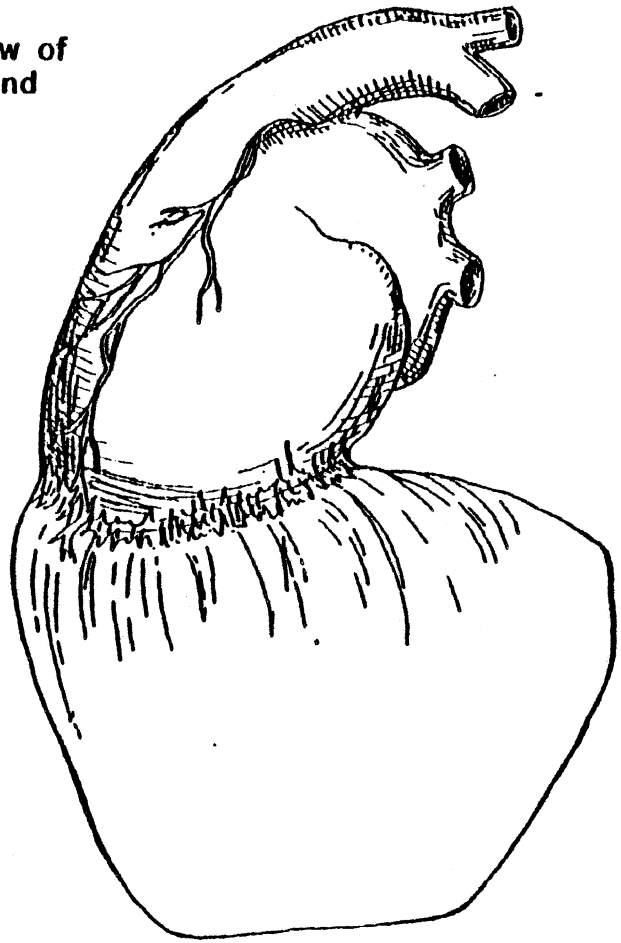

Diaphragmatic View of Heart

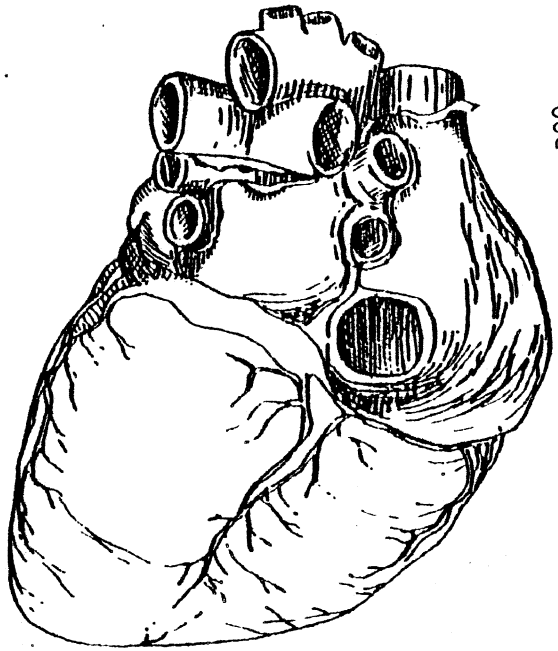

B90

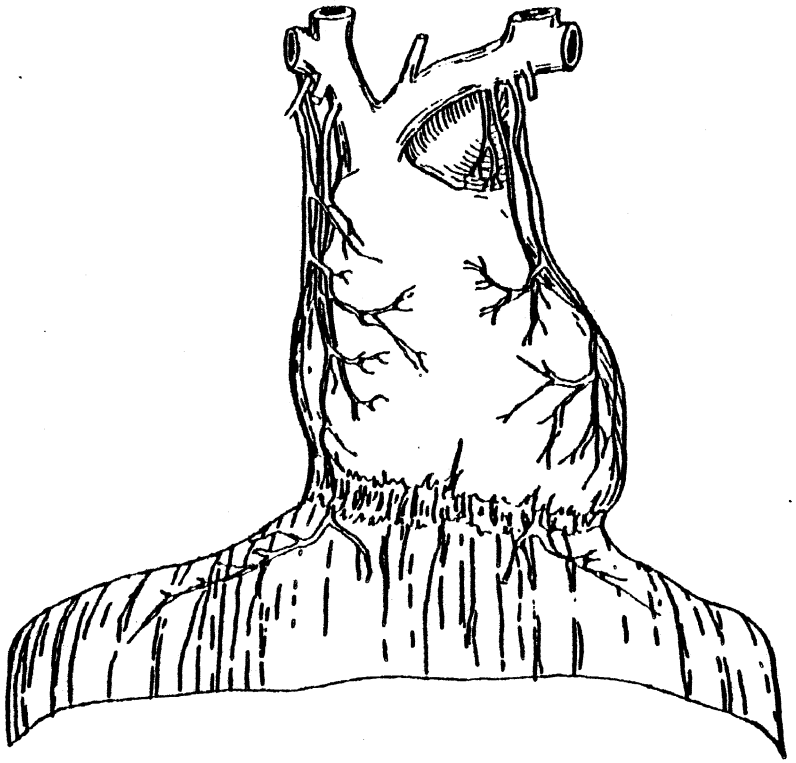

Anterior View of Pericardium and Diaphragm

ST NO. _____

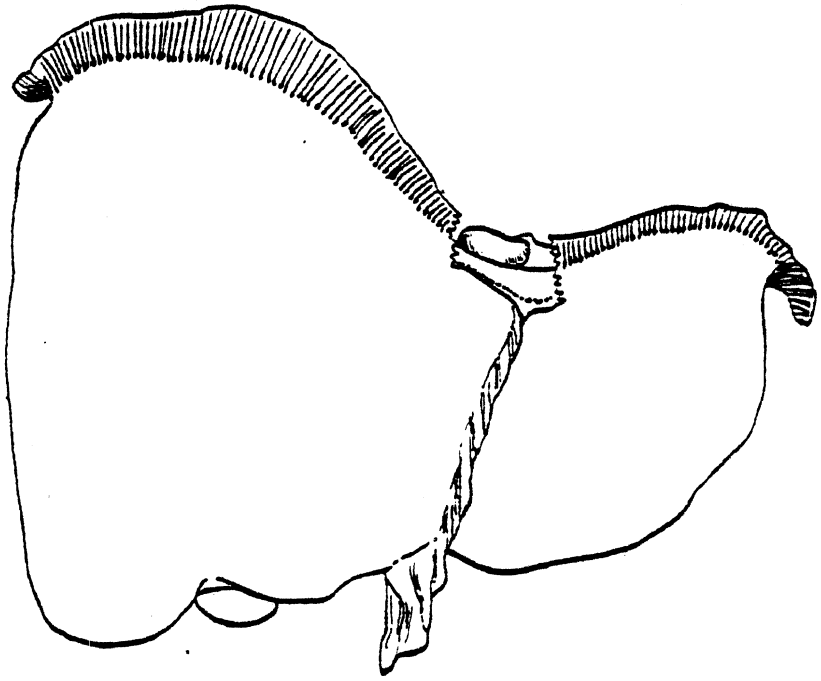

SUPERIOR SURFACE OF THE LIVER

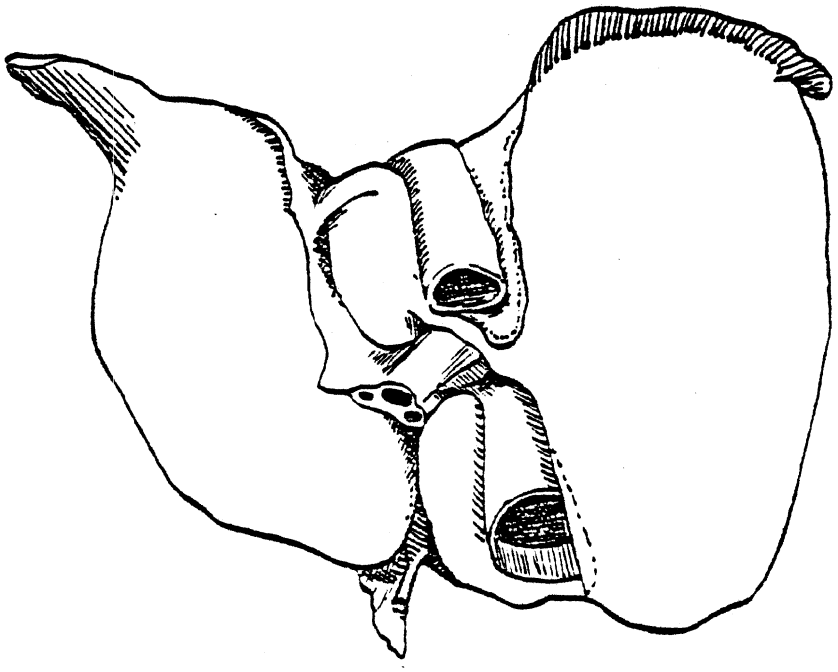

VISCERAL SURFACE OF THE LIVER

TEST NO. _____

DATE _____

PATELLA

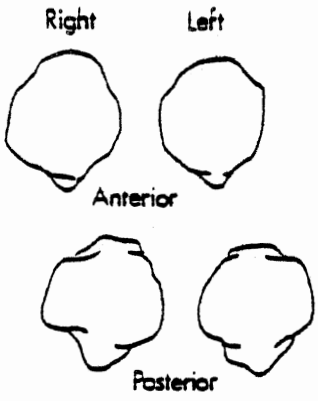

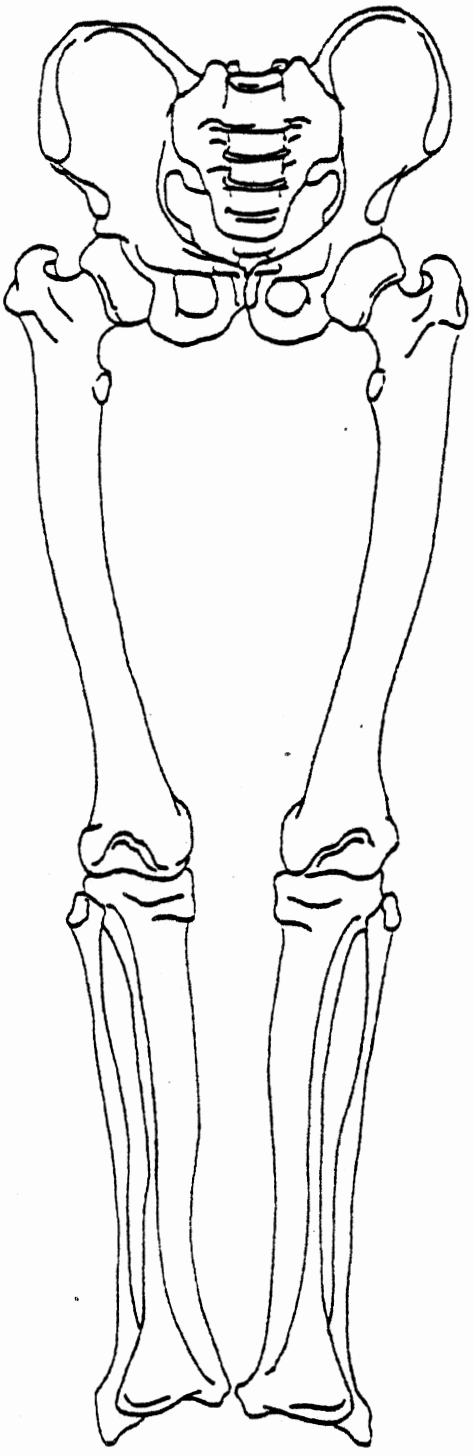

Anterior

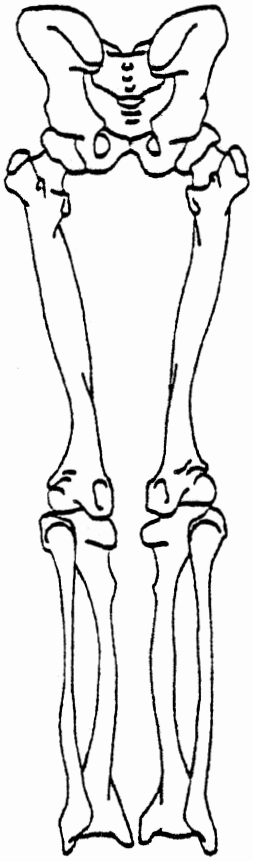

Posterior

LOWER EXTREMITIES

TEST NO. _____

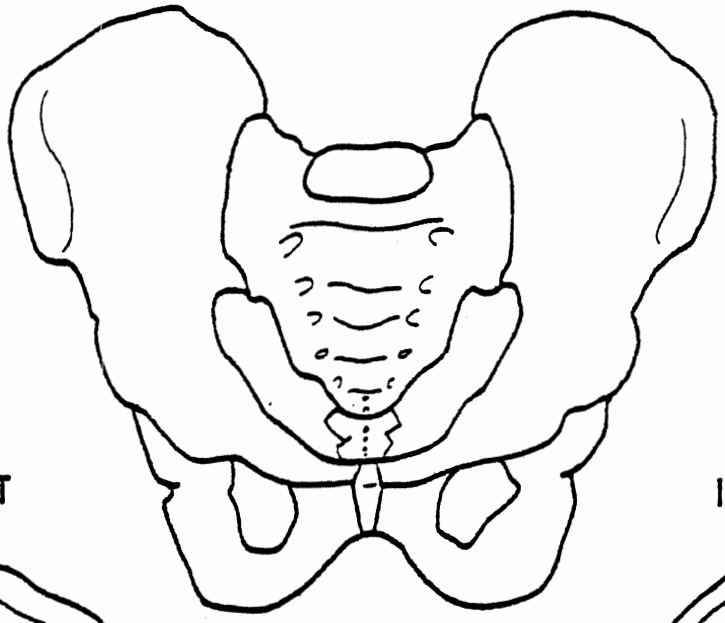

OUTER ASPECT

INNER ASPECT

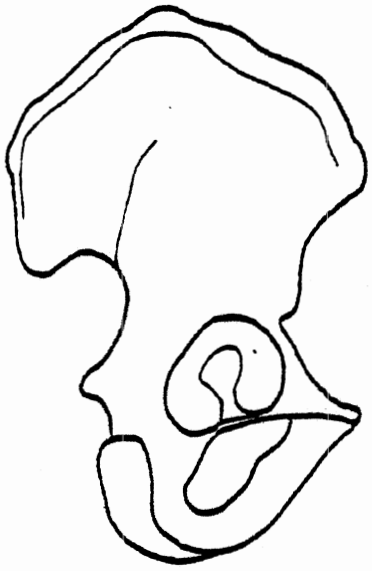

RIGHT ILIUM

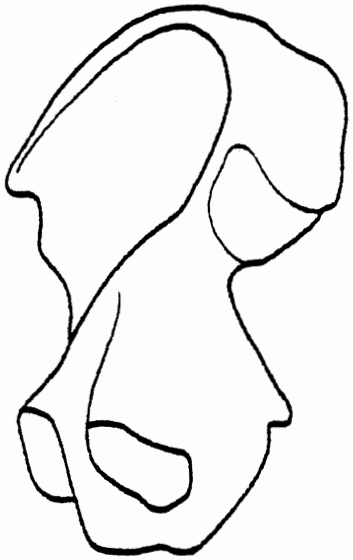

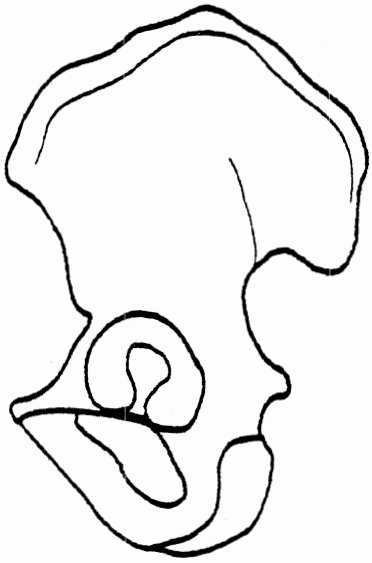

LEFT ILIUM

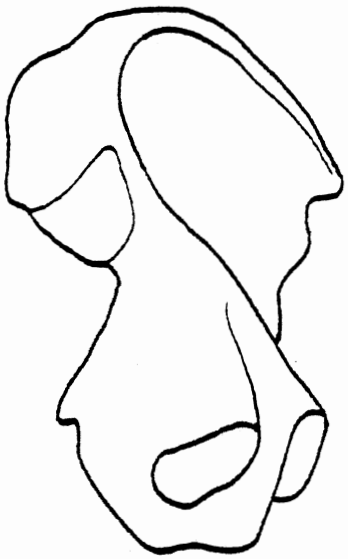

TEST NO. _____

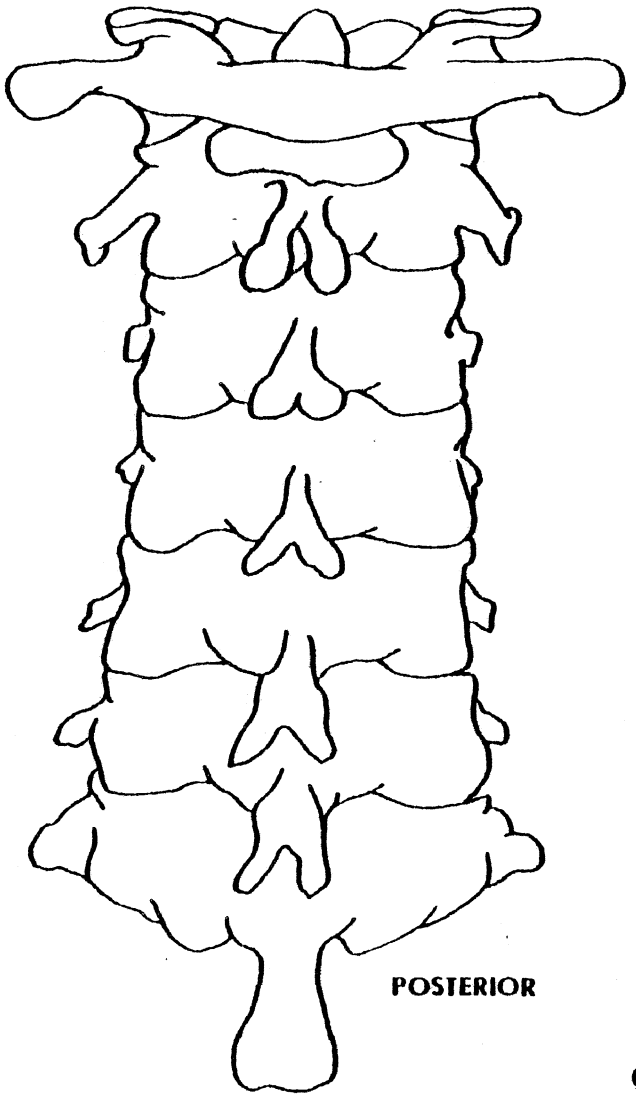

POSTERIOR

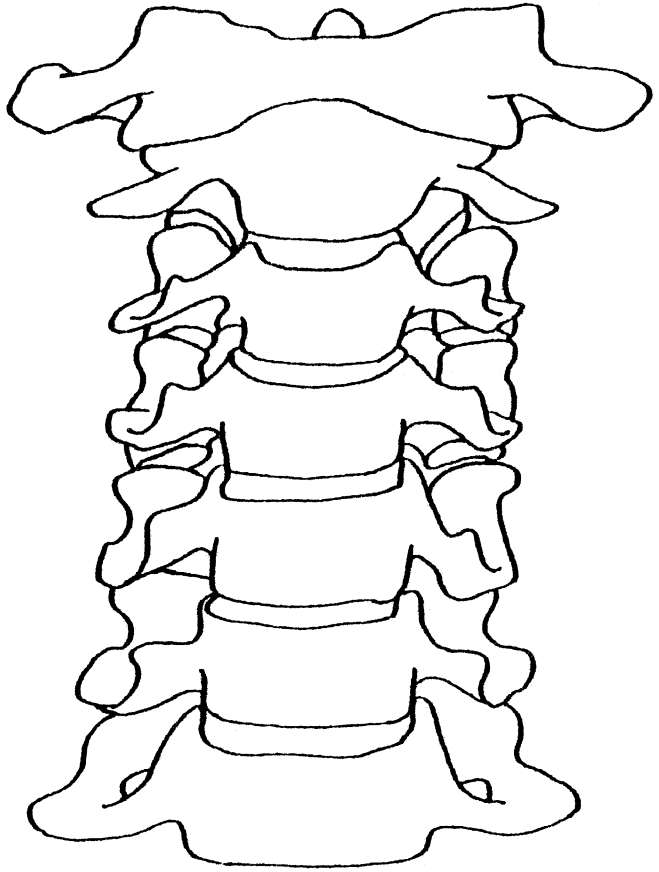

ANTERIOR

B94

CERVICAL VERTEBRAE

TEST NO. _____

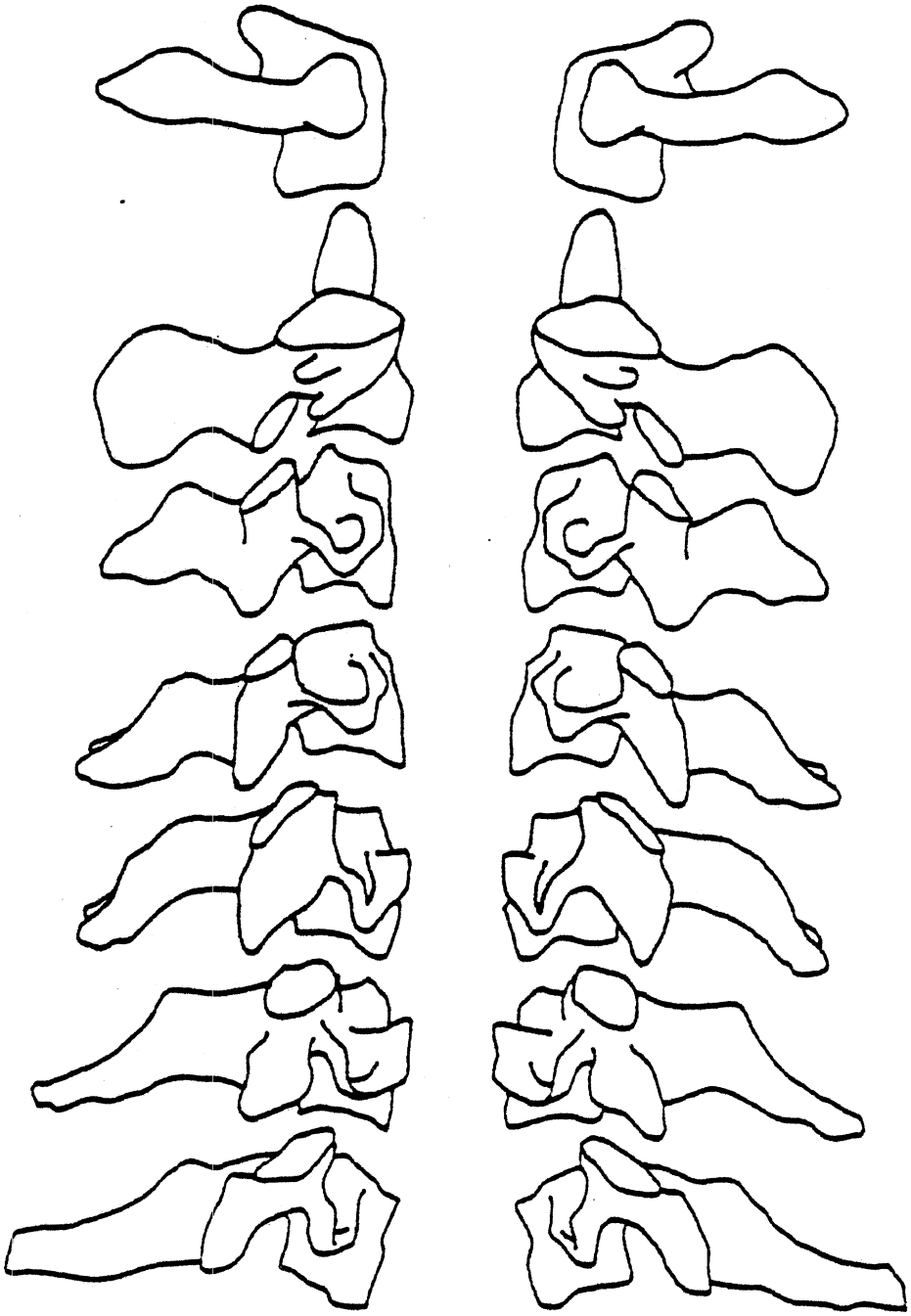

Right Profile

Left Profile

TEST NO. _____

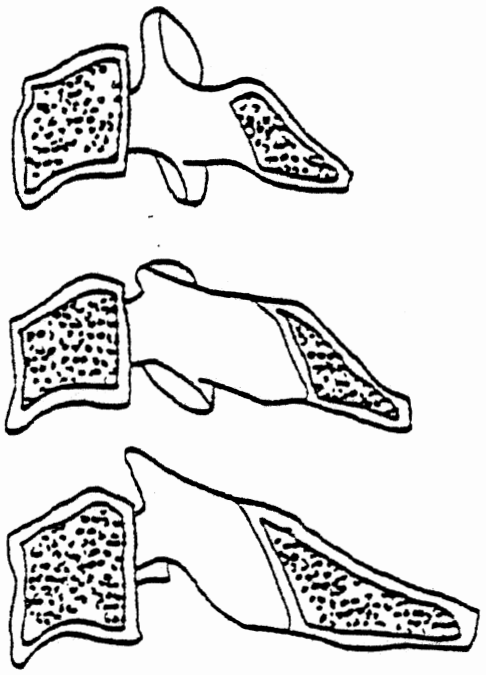

Cross Section

TEST NO. _____

THORACIC VERTEBRAE (T1 - T4)

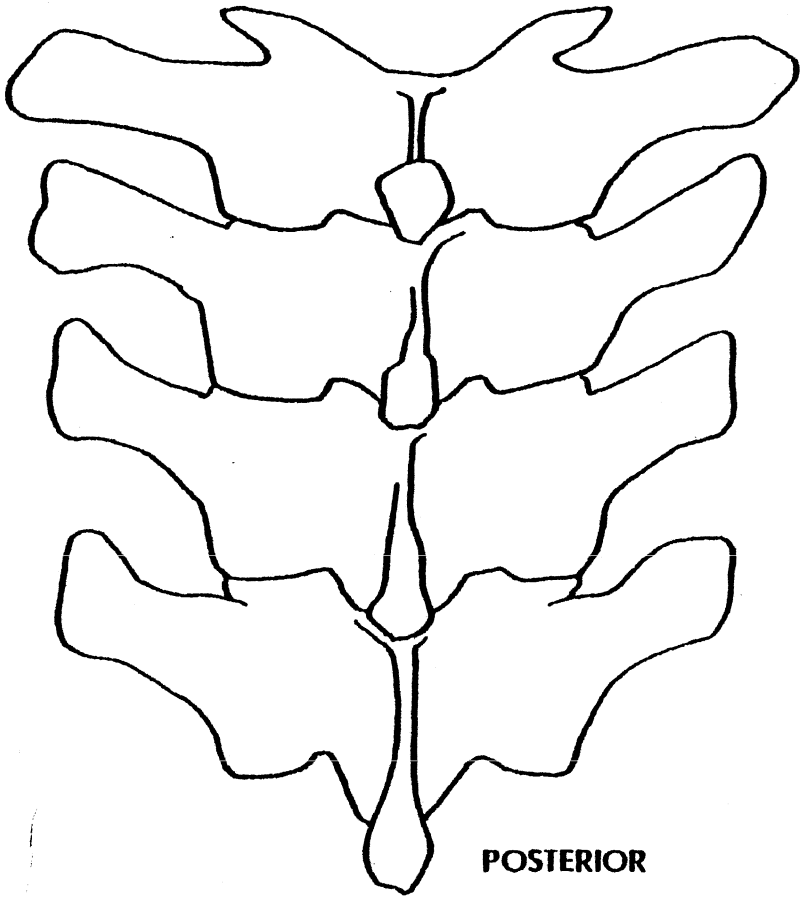

POSTERIOR

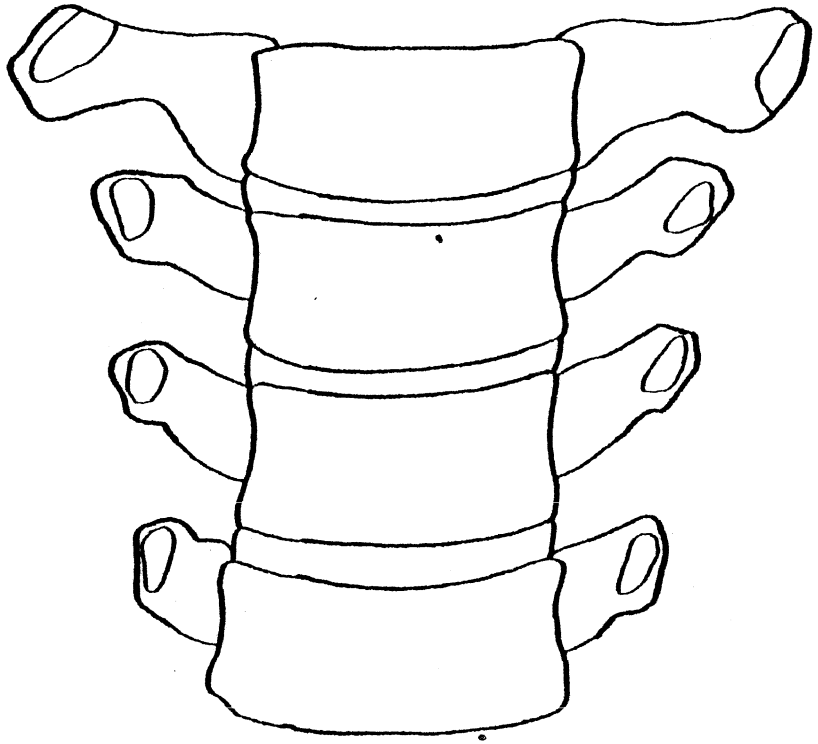

ANTERIOR

B97

TEST NO. _____

THORACIC VERTEBRAE (T1-T4)

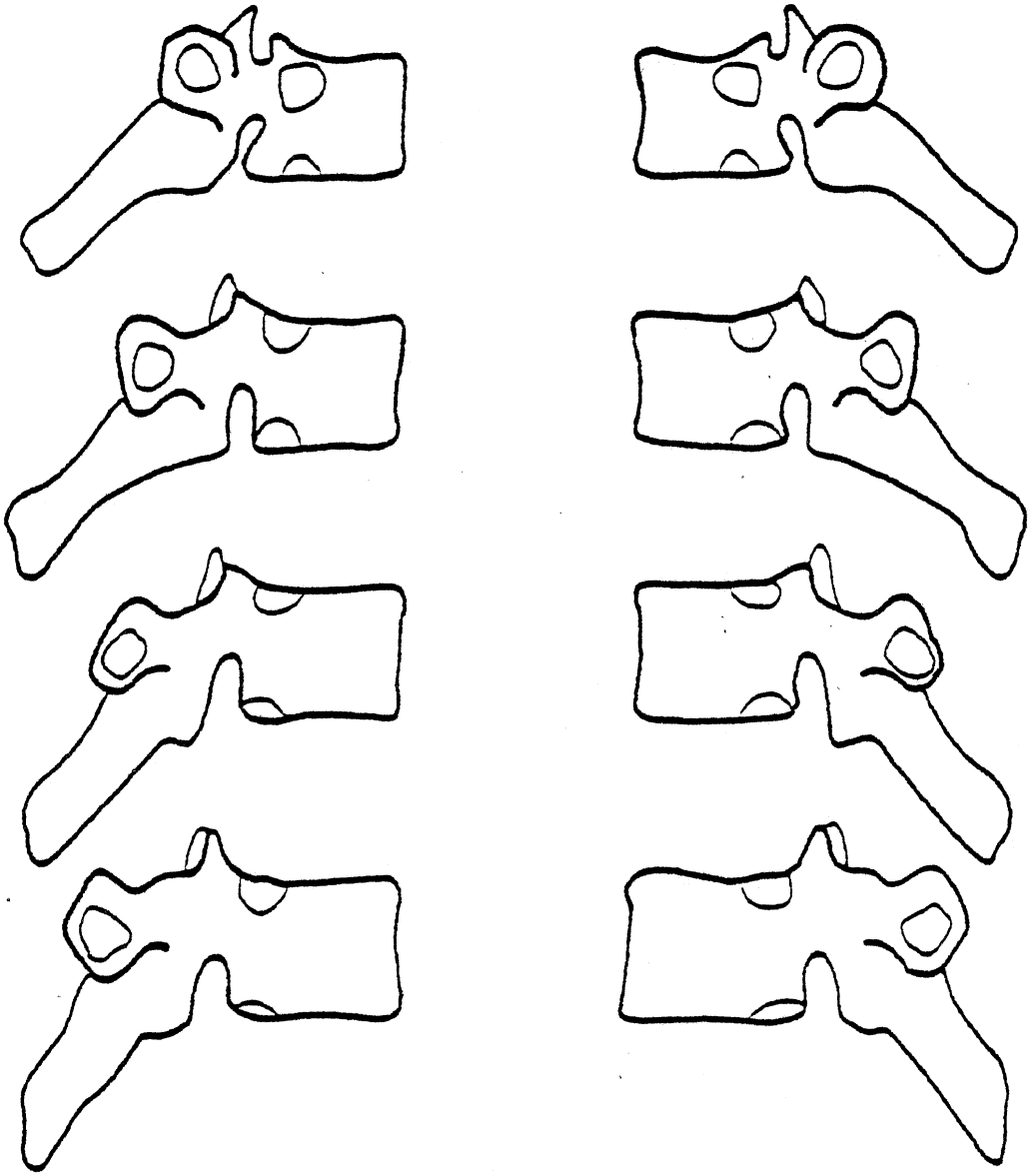

RIGHT PROFILE

LEFT PROFILE

APPENDICES

Anatomy Room Setup
Sled Lab Setup
Cart Setup
Autopsy Setup
Timer Box Setup
Pendulum Wierdness

MEASUREMENT

___ Anthropometer

___ Metric measuring tape

PAPER AND PLASTICS

___ Visqueen on autopsy table

___ Blue pads on table

___ Gauze

TAPES AND STRINGS

___ Silver tape

___ Masking tape

___ Adhesive tape

___ Fiber tape

___ Flat waxed string

SCALPELS

___ 2 large (#8) handles

___ 2 medium (#4) handles

___ 2 small (#3) handles

___ 2 #60 blades

___ 5 #22 blades

___ 5 #15 blades

___ 2 #12 blades

FORCEPS

___ 2 hooked

___ 2 large plain

___ 2 small plain

HEMOSTATS

___ needle

___ small straight

___ small curved

___ large straight

___ large curved

SCISSORS

___ 2 small

___ 2 medium

___ 2 large

SPREADERS

___ 2 large

___ 2 medium

NEEDLES

___ 2 double curved

___ 8 Trocar with stainless steel lockwire

___ 2 5cc sringes

CLOTHING

___ Tampons

___ Thermoknit longjohns and top

___ Cotton socks

___ Blue vinyl pants and top

___ Head and body harnesses

PRESSURIZATION

___ Modified Foley (#18 or #20) balloon catheters

___ Kulite shield

___ Tracheal tube

___ Right and left carotid pressurization catheters (Foley #10-14)

___ Cerebral spinal catheter (Foley #14-16)

___ Respiratory pressure tank

___ Manometer

___ Fluid pressure tank

___ 7% saline solution with India ink

BOLTS AND SCREWS

___ 6 self-tapping lag bolts

___ 3 lengths of wood screws

___ 1-72 screws

___ 10-32 tap

___ Strain relief bolt

___ Wood and metal self-tapping screw boxes

MOUNTS

___ Spine(2)

___ Rib (2, triax)

___ Rib (2, uniax, R-L)

___ Nine-accelerometer plates (large, small, and 8 feet)

___ Sternum

___ Substernale

___ Suprasternale (triax)

___ Dental acrylic

___ Bone wax

. TOOLS

___ Electric hair clippers

___ Electric drill

___ Drill bits (No. 7, approx. 1/16", etc.)

___ large and small screwdrivers

___ nut driver (for lag bolts)

___ wire twisters

___ bone shears

___ Executive Slinky object space calibrated and nearly functional

MATERIALS

___ balsa wood

___ rags

___ foam (at least 2 sheets of 3x4 ft 6")

___ Ensolite

___ Styrofoam

___ Dow Ethafoam

___ Overhead support bar

ROPE CUTTERS

___ head, 1/8"

___ pendulum (with spring, 3/16")

___ nylon strings (10 24" 3/16"; 10 18" 1/8")

___ shock absorber and styrofoam bumper

WEIGHTS

___ steel blocks on pendulum

MISCELLANEOUS

___ calculator

___ bone wax

___ Pressurization equipment (pulmonary, thoracic arterial, head arterial, cerebral spinal)

___ Timer box

___ Strobes

___ Head impact back brace and foam padding

TAPES

___ adhesive

___ fiber

___ silver

___ masking

___ black

___ double stick

PAPER AND PLASTIC

___ blue pads

___ gauze

___ gloves

___ plastic garbage bags

SCALPELS

___ 1 medium (#4) handle

___ 1 small (#3) handle

___ 2 #22 blades

___ 2 #15 blades

___ 1 #12 blade

SURGICAL TOOLS

___ 2 forceps

___ 2 hemostats

___ large scissors

___ 2 double curved needles

STRING

___ flat waxed string

___ black thread

TOOLS

___ small (1-72) screwdriver

___ large screwdriver

___ nut driver

___ ball driver (6-32, 0-80)

___ 1-72 screws

___ 2-56 screws

___ 0-80 screws

___ wiretwisters

MISCELLANEOUS

___ ball targets

___ paper targets

___ bone wax

___ vaseline

___ Q-tips

___ tubing connectors

___ tie wraps

___ lockwire

___ 50cc syringe

___ pulmonary pressurization relief valves

AUTOPSY SETUP

PAPER AND PLASTICS

___ Visqueen on autopsy table

___ blue pads

___ gauze

TAPE

___ silver tape

___ masking tape

___ fiber tape

SCALPELS

___ 2 large (#8) handles

___ 2 medium (#4) handles

___ 2 small (#3) handles

___ 2 #60 blades

___ 5 #22 blades

___ 5 #15 blades

___ 2 #12 blades

FORCEPS

___ 2 hooked

___ 2 large plain

___ 2 small plain

HEMOSTATS

___ needle

___ small straight

___ small curved

___ large straight

___ large curved

SCISSORS

___ 2 small

___ 2 medium

___ 2 large

SPREADERS

___ 3 medium

___ 3 large

MISCELLANEOUS

___ Stryker saw and blade

___ bone shears

___ wedge

___ rib cutters

TIMER BOX SETUP

EQUIPMENT _____ Impact	TIMER VALUES Delay		Run
Gate (from strobe 1)	0012-y	1	0150
Lights (start)	0001	2	2600
HyCam (start)	1200	3	1600
Pendulum rope cutter(start)	2200-x*	4	0050
Photosonics (start)	1000	5	1600
		6	
Head, pelvis, rope cutter (from velocity probe)	0001	7	0050
Piston Acceleration Corridor	1 + Z	8	0050-0150

* x obtained from elliptic integral of the first kind. For 100° .87 sec, 20 ° .70 sec. y=angle/20 Z=210/angle

PENDULUM WEIRDNESS

Average	60.84	61.00	61.26	61.56
Standard Deviation	±.28	±.37	±.05	±.23
Period	3.042	3.050	3.063	3.078
(MGL/I)‡2	2.065	2.060	2.051	2.041
t/2pi	.484	.485	.487	.489

12.0 APPENDIX D: ANTHROPOMETRY

HUMAN SUBJECT INFORMATION

CADAVER NO.: 000 DURATION OF BED CONFINEMENT Unknown

AGE: 60 SEX: M CAUSE OF DEATH: Unknown

PHYSICAL APPEARANCE: Caucasian DATE OF DEATH: 3/21/82

ANOMALY: None

ANTHROPOMETRY

0 - Weight*	52 kg	
1 - Stature**	184 cm	
2 - Shoulder (acromial) Height	159.4 cm	62.8 in
3 - Vertex to Symphysion Length	91.2 cm	35.9 in
4 - Waist Height	109.8 cm	43.2 in
5 - Shoulder Breadth (Biacromial Breadth)	31.8 cm	12.5 in
6 - Chest Breadth	27.9 cm	11 in
7 - Waist Breadth	29.2 cm	11.5 in
8 - Hip Breadth	25 cm	9.8 in
9 - Shoulder to Elbow Length (Acromion-radiale Length)	999	999
10 - Forearm-hand Length (elbow-middle finger)	999	999
11 - Tibiale Height	999	999
12 - Ankle Height (outside) (lateral malleous)	999	999
13 - Foot Breadth	999	999
14 - Foot Length	999	999

Note: * weight in kilograms

** lengths in centimeters

*** measures 16 and 17 must be made in case where the subject will be used in the seated position during the tests. In all other cases enter 9999 when under these measures.

LABORATORY UMTRI D2 TEST NO. 82E001-3 82E004-7 82E008

15 - Top of Head to Trochanterion Length.....	88.5 cm	34.8 in
16 - Seated Height***.....	999	999
17 - Knee Height (seated)***.....	999	999
18 - Head Length.....	19.7 cm	7.8 in
19 - Head Breadth.....	15.7 cm	6.2 in
20 - Head to Chin Height (Vertex to Mentum).....	22.8 cm	9 in
21 - Biceps Circumference.....	999	999
22 - Elbow Circumference.....	999	999
23 - Forearm Circumference.....	999	999
24 - Wrist Circumference.....	999	999
25 - Thigh Circumference.....	999	999
26 - Lower Thigh Circumference.....	999	999
27 - Knee Circumference.....	999	999
28 - Calf Circumference.....	999	999
29 - Ankle Circumference.....	999	999
30 - Neck Circumference.....	32.3cm	12.7 in
31 - Scye (armpit-shoulder) Circumference.....	999	999
32 - Chest Circumference.....	79.3 cm	31.2 in
33 - Waist Circumference.....	999	999
34 - Buttock Circumference.....	999	999
35 - Chest Depth.....	15.8 cm	6.2 in
36 - Waist Depth.....	999	999
37 - Buttock Depth.....	999	999
38 - Interscye.....	999	999

LABORATORY UMTRI TEST NO. 82E001-3 82E004-7 82E008

HUMAN SUBJECT INFORMATION

CADAVER NO.: 020 DURATION OF BED CONFINEMENT Unknown

AGE: 67 SEX: M CAUSE OF DEATH: Unknown

PHYSICAL APPEARANCE: Caucasian DATE OF DEATH: 3/23/82

ANOMALY: Excessive fat increased time required for spinal mounts

ANTHROPOMETRY

0 - Weight*	77 kg	
1 - Stature**	179.8 cm	
2 - Shoulder (acromial) Height	156 cm	61.4 in
3 - Vertex to Symphysion Length	88.5 cm	34.8 in
4 - Waist Height	107.3 cm	42.2 in
5 - Shoulder Breadth (Biacromial Breadth)	33.2 cm	13.1 in
6 - Chest Breadth	32.7 cm	12.9 in
7 - Waist Breadth	24 cm	9.4 in
8 - Hip Breadth	36 cm	14.2 in
9 - Shoulder to Elbow Length (Acromion-radiale .. Length)	999	999
10 - Forearm-hand Length (elbow-middle finger)	999	999
11 - Tibiale Height	999	999
12 - Ankle Height (outside) (lateral malleous)	999	999
13 - Foot Breadth	999	999
14 - Foot Length	999	999

Note: * weight in kilograms

** lengths in centimeters

*** measures 16 and 17 must be made in case where the subject will be used in the seated position during the tests. In all other cases enter 9999 when under these measures.

LABORATORY UMTRI D4 TEST NO. 82E021-22 82E023-27 82E028

15 - Top of Head to Trochanterion Length.....	999	999
16 - Seated Height***.....	999	999
17 - Knee Height (seated)***.....	999	999
18 - Head Length.....	21 cm	8.2 in
19 - Head Breadth.....	15.8 cm	6.2 in
20 - Head to Chin Height (Vertex to Mentum).....	24.9 cm	9.8 in
21 - Biceps Circumference.....	999	999
22 - Elbow Circumference.....	999	999
23 - Forearm Circumference.....	999	999
24 - Wrist Circumference.....	999	999
25 - Thigh Circumference.....	999	999
26 - Lower Thigh Circumference.....	999	999
27 - Knee Circumference.....	999	999
28 - Calf Circumference.....	999	999
29 - Ankle Circumference.....	999	999
30 - Neck Circumference.....	42 cm	16.5 in
31 - Scye (armpit-shoulder) Circumference.....	999	999
32 - Chest Circumference.....	99 cm	39 in
33 - Waist Circumference.....	999	999
34 - Buttock Circumference.....	999	999
35 - Chest Depth.....	22.2 cm.	8.7 in
36 - Waist Depth.....	999	999
37 - Buttock Depth.....	999	999
38 - Interscye.....	999	999

LABORATORY UMTRI TEST NO. 82E021-22 82E023-27 82E028

HUMAN SUBJECT INFORMATION

CADAVER NO.: 040 DURATION OF BED CONFINEMENT Unknown

AGE: 65 SEX: M CAUSE OF DEATH: Myocardial infarction

PHYSICAL APPEARANCE: Caucasian DATE OF DEATH: 3/27/82

ANOMALY: Upper ribs very close together and embedded in deep fat.

ANTHROPOMETRY

0 - Weight*	87 kg	
1 - Stature**	169.2 cm	
2 - Shoulder (acromial) Height	146.7 cm	57.8 in
3 - Vertex to Symphysion Length	81.8 cm	32.2 in
4 - Waist Height	102 cm	40.2 in
5 - Shoulder Breadth (Biacromial Breadth)	35.4 cm	13.9 in
6 - Chest Breadth	32.7 cm	12.9 in
7 - Waist Breadth	32 cm	12.6 in
8 - Hip Breadth	33.5 cm	13.2 in
9 - Shoulder to Elbow Length (Acromion-radiale Length)	999	999
10 - Forearm-hand Length (elbow-middle finger)	999	999
11 - Tibiale Height	999	999
12 - Ankle Height (outside) (lateral malleous)	999	999
13 - Foot Breadth	999	999
14 - Foot Length	999	999

Note: * weight in kilograms

** lengths in centimeters

*** measures 16 and 17 must be made in case where the subject will be used in the seated position during the tests. In all other cases enter 9999 when under these measures.

LABORATORY UMTRI D6 TEST NO. 82E041-42 82E043-48 82E049

15 - Top of Head to Trochanterion Length.....	999	999
16 - Seated Height***.....	999	999
17 - Knee Height (seated)***.....	999	999
18 - Head Length.....	20 cm	7.9 in
19 - Head Breadth.....	16.5 cm	6.5 in
20 - Head to Chin Height (Vertex to Mentum).....	21.4 cm	8.4 in
21 - Biceps Circumference.....	999	999
22 - Elbow Circumference.....	999	999
23 - Forearm Circumference.....	999	999
24 - Wrist Circumference.....	999	999
25 - Thigh Circumference.....	999	999
26 - Lower Thigh Circumference.....	999	999
27 - Knee Circumference.....	999	999
28 - Calf Circumference.....	999	999
29 - Ankle Circumference.....	999	999
30 - Neck Circumference.....	50.4 cm	19.8 in
31 - Scye (armpit-shoulder) Circumference.....	999	999
32 - Chest Circumference.....	104.5 cm	41.1 in
33 - Waist Circumference.....	999	999
34 - Buttock Circumference.....	999	999
35 - Chest Depth.....	23.8 cm	9.4 in
36 - Waist Depth.....	999	999
37 - Buttock Depth.....	999	999
38 - Interscye.....	999	999

LABORATORY UMTRI TEST NO. 82E041-42 82E043-48 82E049

HUMAN SUBJECT INFORMATION

CADAVER NO.: 050 DURATION OF BED CONFINEMENT Unknown

AGE: 60 SEX: M CAUSE OF DEATH: Coronary thrombosis

PHYSICAL APPEARANCE: Caucasian DATE OF DEATH: 6/7/82

ANOMALY: Right and left ribs R4-R5 broken, probably from CPR.

ANTHROPOMETRY

0 - Weight*.....	67 kg	
1 - Stature**.....	180.2 cm	
2 - Shoulder (acromial) Height.....	155.7 cm	61.8 in
3 - Vertex to Symphysion Length.....	999	999
4 - Waist Height.....	999	999
5 - Shoulder Breadth (Biacromial Breadth).....	37.5 cm	14.8 in
6 - Chest Breadth.....	999	999
7 - Waist Breadth.....	999	999
8 - Hip Breadth.....	999	999
9 - Shoulder to Elbow Length (Acromion-radiale .. Length)	999	999
10 - Forearm-hand Length (elbow-middle finger)....	999	999
11 - Tibiale Height.....	999	999
12 - Ankle Height (outside) (lateral malleous)....	999	999
13 - Foot Breadth.....	999	999
14 - Foot Length.....	999	999

Note: * weight in kilograms

** lengths in centimeters

*** measures 16 and 17 must be made in case where the subject will be used in the seated position during the tests. In all other cases enter 9999 when under these measures.

LABORATORY UMTRI D8 TEST NO. 82E051-53

15 - Top of Head to Trochanterion Length.....	999	999
16 - Seated Height***.....	999	999
17 - Knee Height (seated)***.....	999	999
18 - Head Length.....	20 cm	7.9 in
19 - Head Breadth.....	16.2 cm	6.4 in
20 - Head to Chin Height (Vertex to Mentum).....	999	999
21 - Biceps Circumference.....	999	999
22 - Elbow Circumference.....	999	999
23 - Forearm Circumference.....	999	999
24 - Wrist Circumference.....	999	999
25 - Thigh Circumference.....	999	999
26 - Lower Thigh Circumference.....	999	999
27 - Knee Circumference.....	999	999
28 - Calf Circumference.....	999	999
29 - Ankle Circumference.....	999	999
30 - Neck Circumference.....	40.5 cm	15.9 in
31 - Scye (armpit-shoulder) Circumference.....	999	999
32 - Chest Circumference.....	999	999
33 - Waist Circumference.....	999	999
34 - Buttock Circumference.....	999	999
35 - Chest Depth.....	999	999
36 - Waist Depth.....	999	999
37 - Buttock Depth.....	999	999
38 - Interscye.....	999	999

LABORATORY UMTRI TEST NO. 82F051-53

HUMAN SUBJECT INFORMATION

CADAVER NO.: 060 DURATION OF BED CONFINEMENT Unknown

AGE: 60 SEX: M CAUSE OF DEATH: Unknown

PHYSICAL APPEARANCE: Caucasian DATE OF DEATH: 6/1/82

ANOMALY: None

ANTHROPOMETRY

0 - Weight*.....	67 kg	
1 - Stature**.....	169.8 cm	
2 - Shoulder (acromial) Height.....	148.4 cm	58.4 in
3 - Vertex to Symphysion Length.....	86.1 cm	33.9 in
4 - Waist Height.....	99.8 cm	39.3 in
5 - Shoulder Breadth (Biacromial Breadth).....	34.7 cm	13.7 in
6 - Chest Breadth.....	29.1 cm	11.5 in
7 - Waist Breadth.....	23 cm	9.1 in
8 - Hip Breadth.....	28.6 cm	11.3 in
9 - Shoulder to Elbow Length (Acromion-radiale .. Length)	999	999
10 - Forearm-hand Length (elbow-middle finger)....	999	999
11 - Tibiale Height.....	999	999
12 - Ankle Height (outside) (lateral malleous)....	999	999
13 - Foot Breadth.....	999	999
14 - Foot Length.....	999	999

Note: * weight in kilograms

** lengths in centimeters

*** measures 16 and 17 must be made in case where the subject will be used in the seated position during the tests. In all other cases enter 9999 when under these measures.

LABORATORY UMTRI D10 TEST NO. 82E061-62 82E063-66 82E067

15 - Top of Head to Trochanterion Length.....	999	999
16 - Seated Height***.....	999	999
17 - Knee Height (seated)***.....	999	999
18 - Head Length.....	19.2 cm	7.6 in
19 - Head Breadth.....	15.5 cm	6.1 in
20 - Head to Chin Height (Vertex to Mentum).....	22.1 cm	8.7 in
21 - Biceps Circumference.....	999	999
22 - Elbow Circumference.....	999	999
23 - Forearm Circumference.....	999	999
24 - Wrist Circumference.....	999	999
25 - Thigh Circumference.....	999	999
26 - Lower Thigh Circumference.....	999	999
27 - Knee Circumference.....	999	999
28 - Calf Circumference.....	999	999
29 - Ankle Circumference.....	999	999
30 - Neck Circumference.....	44.6 cm	17.6 in
31 - Scye (armpit-shoulder) Circumference.....	999	999
32 - Chest Circumference.....	90.2 cm	35.5 in
33 - Waist Circumference.....	999	999
34 - Buttock Circumference.....	999	999
35 - Chest Depth.....	21.6 cm	8.5 in
36 - Waist Depth.....	999	999
37 - Buttock Depth.....	999	999
38 - Interscye.....	999	999

LABORATORY UMTRI TEST NO. 82E061-62 82E063-66 82E067

HUMAN SUBJECT INFORMATION

CADAVER NO.: 070 DURATION OF BED CONFINEMENT unknown

AGE: 61 SEX: M CAUSE OF DEATH: unknown

PHYSICAL APPEARANCE: Causian DATE OF DEATH: 9/9/82

ANOMALY: Ribs broken during CPR attached to sternum with wire.

ANTHROPOMETRY

0 - Weight*	55 kg	
1 - Stature**	181 cm	
2 - Shoulder (acromial) Height	156 cm	61.4 in
3 - Vertex to Symphysion Length	999	999
4 - Waist Height	999	999
5 - Shoulder Breadth (Biacromial Breadth)	36.2 cm	14.3 in
6 - Chest Breadth	999	999
7 - Waist Breadth	999	999
8 - Hip Breadth	999	999
9 - Shoulder to Elbow Length (Acromion-radiale Length)	999	999
10 - Forearm-hand Length (elbow-middle finger)	999	999
11 - Tibiale Height	999	999
12 - Ankle Height (outside) (lateral malleous)	999	999
13 - Foot Breadth	999	999
14 - Foot Length	999	999

Note: * weight in kilograms

** lengths in centimeters

*** measures 16 and 17 must be made in case where the subject will be used in the seated position during the tests. In all other cases enter 9999 when under these measures.

LABORATORY UMTRI D12 TEST NO. 82E071

15 - Top of Head to Trochanterion Length.....	999	999
16 - Seated Height***.....	999	999
17 - Knee Height (seated)***.....	999	999
18 - Head Length.....	20.6 cm	8.1 in
19 - Head Breadth.....	15.3 cm	6 in
20 - Head to Chin Height (Vertex to Mentum).....	999	999
21 - Biceps Circumference.....	999	999
22 - Elbow Circumference.....	999	999
23 - Forearm Circumference.....	999	999
24 - Wrist Circumference.....	999	999
25 - Thigh Circumference.....	999	999
26 - Lower Thigh Circumference.....	999	999
27 - Knee Circumference.....	999	999
28 - Calf Circumference.....	999	999
29 - Ankle Circumference.....	999	999
30 - Neck Circumference.....	32 cm	12.6 in
31 - Scye (armpit-shoulder) Circumference.....	999	999
32 - Chest Circumference.....	999	999
33 - Waist Circumference.....	999	999
34 - Buttock Circumference.....	999	999
35 - Chest Depth.....	999	999
36 - Waist Depth.....	999	999
37 - Buttock Depth.....	999	999
38 - Interscye.....	999	999

LABORATORY UMTRI TEST NO. 82E071

HUMAN SUBJECT INFORMATION

CADAVER NO.: 079 DURATION OF BED CONFINEMENT Unknown

AGE: 51 SEX: M CAUSE OF DEATH: Myocardial infarction

PHYSICAL APPEARANCE: Caucasian DATE OF DEATH: 2/26/83

ANOMALY: Structures weakened from CPR.

ANTHROPOMETRY

0 - Weight*	83 kg	
1 - Stature**	169 cm	
2 - Shoulder (acromial) Height	146.5 cm	57.7 in
3 - Vertex to Symphysion Length	999	999
4 - Waist Height	999	999
5 - Shoulder Breadth (Biacromial Breadth)	30.4 cm	12 in
6 - Chest Breadth	34.2 cm	13.5 in
7 - Waist Breadth	999	999
8 - Hip Breadth	31 cm	12.2 in
9 - Shoulder to Elbow Length (Acromion-radiale Length)	999	999
10 - Forearm-hand Length (elbow-middle finger)	999	999
11 - Tibiale Height	999	999
12 - Ankle Height (outside) (lateral malleous)	999	999
13 - Foot Breadth	999	999
14 - Foot Length	999	999

Note: * weight in kilograms

** lengths in centimeters

*** measures 16 and 17 must be made in case where the subject will be used in the seated position during the tests. In all other cases enter 9999 when under these measures.

LABORATORY UMTRI TEST NO. 83E076

15 - Top of Head to Trochanterion Length.....	999	999
16 - Seated Height***.....	999	999
17 - Knee Height (seated)***.....	999	999
18 - Head Length.....	20 cm	7.8 in
19 - Head Breadth.....	16 cm	6.3 in
20 - Head to Chin Height (Vertex to Mentum).....	999	999
21 - Biceps Circumference.....	999	999
22 - Elbow Circumference.....	999	999
23 - Forearm Circumference.....	999	999
24 - Wrist Circumference.....	999	999
25 - Thigh Circumference.....	999	999
26 - Lower Thigh Circumference.....	999	999
27 - Knee Circumference.....	999	999
28 - Calf Circumference.....	999	999
29 - Ankle Circumference.....	999	999
30 - Neck Circumference.....	36 cm	14.2 in
31 - Scye (armpit-shoulder) Circumference.....	999	999
32 - Chest Circumference.....	999	999
33 - Waist Circumference.....	999	999
34 - Buttock Circumference.....	999	999
35 - Chest Depth.....	999	999
36 - Waist Depth.....	999	999
37 - Buttock Depth.....	999	999
38 - Interscye.....	999	999

LABORATORY UMTRI TEST NO. 83E076

HUMAN SUBJECT INFORMATION

CADAVER NO.: 080 DURATION OF BED CONFINEMENT Unknown

AGE: 44 SEX: M CAUSE OF DEATH: Pulmonary edema

PHYSICAL APPEARANCE: Caucasian DATE OF DEATH: 3/6/83

ANOMALY: Left rib R4 weakened. Sternum weakened.

ANTHROPOMETRY

0 - Weight*	72 kg	
1 - Stature**	171 cm	
2 - Shoulder (acromial) Height	147.4 cm	58 in
3 - Vertex to Symphysion Length	88 cm	34.6 in
4 - Waist Height	89.5 cm	35.2 in
5 - Shoulder Breadth (Biacromial Breadth)	32.5 cm	12.8 in
6 - Chest Breadth	33.8 cm	13.3 in
7 - Waist Breadth	25 cm	9.8 in
8 - Hip Breadth	31.4 cm	12.4 in
9 - Shoulder to Elbow Length (Acromion-radiale Length)	999	999
10 - Forearm-hand Length (elbow-middle finger)	999	999
11 - Tibiale Height	999	999
12 - Ankle Height (outside) (lateral malleous)	999	999
13 - Foot Breadth	999	999
14 - Foot Length	999	999

Note: * weight in kilograms

** lengths in centimeters

*** measures 16 and 17 must be made in case where the subject will be used in the seated position during the tests. In all other cases enter 9999 when under these measures.

LABORATORY UMTRI TEST NO. 83E081-82 83E083-86 83E087-88

15 - Top of Head to Trochanterion Length.....	999	999
16 - Seated Height***.....	999	999
17 - Knee Height (seated)***.....	999	999
18 - Head Length.....	19.8 cm	7.8 in
19 - Head Breadth.....	15.5 cm	6.1 in
20 - Head to Chin Height (Vertex to Mentum).....	23 cm	9.1 in
21 - Biceps Circumference.....	999	999
22 - Elbow Circumference.....	999	999
23 - Forearm Circumference.....	999	999
24 - Wrist Circumference.....	999	999
25 - Thigh Circumference.....	999	999
26 - Lower Thigh Circumference.....	999	999
27 - Knee Circumference.....	999	999
28 - Calf Circumference.....	999	999
29 - Ankle Circumference.....	999	999
30 - Neck Circumference.....	57 cm	22.4 in
31 - Scye (armpit-shoulder) Circumference.....	999	999
32 - Chest Circumference.....	100 cm	39.4 in
33 - Waist Circumference.....	999	999
34 - Buttock Circumference.....	999	999
35 - Chest Depth.....	15.3 cm	6 in
36 - Waist Depth.....	999	999
37 - Buttock Depth.....	999	999
38 - Interscye.....	999	999

LABORATORY UMTRI TEST NO. 83E081-82 83E083-86 83E087-88

HUMAN SUBJECT INFORMATION

CADAVER NO.: 089 DURATION OF BED CONFINEMENT Unknown

AGE: 62 SEX: M CAUSE OF DEATH: Myocardial infarction

PHYSICAL APPEARANCE: Caucasian DATE OF DEATH: 1/26/83

ANOMALY: None

ANTHROPOMETRY

0 - Weight*	76 kg	
1 - Stature**	175.8 cm	
2 - Shoulder (acromial) Height	152 cm	59.8 in
3 - Vertex to Symphysion Length	84.5 cm	33.3 in
4 - Waist Height	999	999
5 - Shoulder Breadth (Biacromial Breadth)	34.7 cm	13.7 in
6 - Chest Breadth	34 cm	13.4 in
7 - Waist Breadth	999	999
8 - Hip Breadth	31.5 cm	12.4 in
9 - Shoulder to Elbow Length (Acromion-radiale Length)	999	999
10 - Forearm-hand Length (elbow-middle finger)	999	999
11 - Tibiale Height	999	999
12 - Ankle Height (outside) (lateral malleous)	999	999
13 - Foot Breadth	999	999
14 - Foot Length	999	999

Note: * weight in kilograms

** lengths in centimeters

*** measures 16 and 17 must be made in case where the subject will be used in the seated position during the tests. In all other cases enter 9999 when under these measures.

LABORATORY UMTRI D18 TEST NO. 83E071-75 83E091

15 - Top of Head to Trochanterion Length.....	999	999
16 - Seated Height***.....	999	999
17 - Knee Height (seated)***.....	999	999
18 - Head Length.....	19.0 cm	7.5 in
19 - Head Breadth.....	15.3 cm	6 in
20 - Head to Chin Height (Vertex to Mentum).....	999	999
21 - Biceps Circumference.....	999	999
22 - Elbow Circumference.....	999	999
23 - Forearm Circumference.....	999	999
24 - Wrist Circumference.....	999	999
25 - Thigh Circumference.....	999	999
26 - Lower Thigh Circumference.....	999	999
27 - Knee Circumference.....	999	999
28 - Calf Circumference.....	999	999
29 - Ankle Circumference.....	999	999
30 - Neck Circumference.....	37 cm	14.6 in.
31 - Scye (armpit-shoulder) Circumference.....	999	999
32 - Chest Circumference.....	999	999
33 - Waist Circumference.....	999	999
34 - Buttock Circumference.....	999	999
35 - Chest Depth.....	999	999
36 - Waist Depth.....	999	999
37 - Buttock Depth.....	999	999
38 - Interscye.....	999	999

LABORATORY UMTRI TEST NO. 83E071-75 83E091

HUMAN SUBJECT INFORMATION

CADAVER NO.: 090 DURATION OF BED CONFINEMENT Unknown

AGE: 51 SEX: M CAUSE OF DEATH: Cerebral Contusion

PHYSICAL APPEARANCE: Caucasian DATE OF DEATH:

ANOMALY: None

ANTHROPOMETRY

0 - Weight*	68 kg	
1 - Stature**	180 cm	
2 - Shoulder (acromial) Height	155.4 cm	61.2 in
3 - Vertex to Symphysion Length	999	999
4 - Waist Height	999	999
5 - Shoulder Breadth (Biacromial Breadth)	33.3 cm	13.1 in
6 - Chest Breadth	31.9 cm	12.6 in
7 - Waist Breadth	999	999
8 - Hip Breadth	30 cm	11.8 in
9 - Shoulder to Elbow Length (Acromion-radiale Length)	999	999
10 - Forearm-hand Length (elbow-middle finger)	999	999
11 - Tibiale Height	999	999
12 - Ankle Height (outside) (lateral malleous)	999	999
13 - Foot Breadth	999	999
14 - Foot Length	999	999

Note: * weight in kilograms

** lengths in centimeters

*** measures 16 and 17 must be made in case where the subject will be used in the seated position during the tests. In all other cases enter 9999 when under these measures.

LABORATORY UMTRI D20 TEST NO. 83E092 83E093

15 - Top of Head to Trochanterion Length.....	999	999
16 - Seated Height***.....	999	999
17 - Knee Height (seated)***.....	999	999
18 - Head Length.....	19.4 cm	7.6 in
19 - Head Breadth.....	15.5 cm	6.1 in
20 - Head to Chin Height (Vertex to Mentum).....	999	999
21 - Biceps Circumference.....	999	999
22 - Elbow Circumference.....	999	999
23 - Forearm Circumference.....	999	999
24 - Wrist Circumference.....	999	999
25 - Thigh Circumference.....	999	999
26 - Lower Thigh Circumference.....	999	999
27 - Knee Circumference.....	999	999
28 - Calf Circumference.....	999	999
29 - Ankle Circumference.....	999	999
30 - Neck Circumference.....	37 cm	14.6 in
31 - Scye (armpit-shoulder) Circumference.....	999	999
32 - Chest Circumference.....	999	999
33 - Waist Circumference.....	999	999
34 - Buttock Circumference.....	999	999
35 - Chest Depth.....	999	999
36 - Waist Depth.....	999	999
37 - Buttock Depth.....	999	999
38 - Interscye.....	999	999

LABORATORY UMTRI TEST NO. 83E092 83E093

HUMAN SUBJECT INFORMATION

CADAVER NO.: 100 DURATION OF BED CONFINEMENT Unknown

AGE: 60 SEX: M CAUSE OF DEATH: Cardiac arrest - Carcinoma of Pancrea

PHYSICAL APPEARANCE: Caucasian DATE OF DEATH: 5/20/83

ANOMALY: Right rib R7 is abnormal.

ANTHROPOMETRY

0 - Weight*	76.5 kg	
1 - Stature**	182.3 cm	
2 - Shoulder (acromial) Height	158.5 cm	62.4 in
3 - Vertex to Symphysion Length	91.7 cm	36.1 in
4 - Waist Height	108.6 cm	42.8 in
5 - Shoulder Breadth (Biacromial Breadth)	31.4 cm	12.4 in
6 - Chest Breadth	27 cm	10.6 in
7 - Waist Breadth	31.3 cm	12.3 in
8 - Hip Breadth	33.9 cm	13.3 in
9 - Shoulder to Elbow Length (Acromion-radiale Length)	999	999
10 - Forearm-hand Length (elbow-middle finger)	999	999
11 - Tibiale Height	999	999
12 - Ankle Height (outside) (lateral malleous)	999	999
13 - Foot Breadth	999	999
14 - Foot Length	999	999

Note: * weight in kilograms

** lengths in centimeters

*** measures 16 and 17 must be made in case where the subject will be used in the seated position during the tests. In all other cases enter 9999 when under these measures.

LABORATORY UMTRI D22 TEST NO. 83E101-103 83E104-108 83E109

15 - Top of Head to Trochanterion Length.....	999	999
16 - Seated Height***.....	999	999
17 - Knee Height (seated)***.....	999	999
18 - Head Length.....	19.3 cm	7.6 in
19 - Head Breadth.....	14.6 cm	5.7 in
20 - Head to Chin Height (Vertex to Mentum).....	21.8 cm	8.6 in
21 - Biceps Circumference.....	999	999
22 - Elbow Circumference.....	999	999
23 - Forearm Circumference.....	999	999
24 - Wrist Circumference.....	999	999
25 - Thigh Circumference.....	999	999
26 - Lower Thigh Circumference.....	999	999
27 - Knee Circumference.....	999	999
28 - Calf Circumference.....	999	999
29 - Ankle Circumference.....	999	999
30 - Neck Circumference.....	38.3 cm	15.1 in
31 - Scye (armpit-shoulder) Circumference.....	999	999
32 - Chest Circumference.....	91.7 cm	36.1 in
33 - Waist Circumference.....	999	999
34 - Buttock Circumference.....	999	999
35 - Chest Depth.....	22.5 cm	8.9 in
36 - Waist Depth.....	999	999
37 - Buttock Depth.....	999	999
38 - Interscye.....	999	999

LABORATORY UMTRI TEST NO. 83E101-103 83E104-108 83E109

HUMAN SUBJECT INFORMATION

CADAVER NO.: 120 DURATION OF BED CONFINEMENT Unknown

AGE: 20 SEX: F CAUSE OF DEATH: Renal failure

PHYSICAL APPEARANCE: Negro DATE OF DEATH: 8/22/83

ANOMALY: Sores on skin probably from needle punctures.

ANTHROPOMETRY

0 - Weight*.....	46 kg	
1 - Stature**.....	162.7 cm	
2 - Shoulder (acromial) Height.....	141.6 cm	55.7 in
3 - Vertex to Symphysion Length.....	76.3 cm	30 in
4 - Waist Height.....	99.2 cm	39.1 in
5 - Shoulder Breadth (Biacromial Breadth).....	31 cm	12.2 in
6 - Chest Breadth.....	25.7 cm	10.1 in
7 - Waist Breadth.....	21.9 cm	8.6 in
8 - Hip Breadth.....	27.2 cm	10.7 in
9 - Shoulder to Elbow Length (Acromion-radiale .. Length)	999	999
10 - Forearm-hand Length (elbow-middle finger)....	999	999
11 - Tibiale Height.....	999	999
12 - Ankle Height (outside) (lateral malleous)....	999	999
13 - Foot Breadth.....	999	999
14 - Foot Length.....	999	999

Note: * weight in kilograms

** lengths in centimeters

*** measures 16 and 17 must be made in case where the subject will be used in the seated position during the tests. In all other cases enter 9999 when under these measures.

LABORATORY UMTRI D24 TEST NO. 83E121A-C

15 - Top of Head to Trochanterion Length.....	72.9 cm	28.7 in
16 - Seated Height***.....	999	999
17 - Knee Height (seated)***.....	999	999
18 - Head Length.....	18.9 cm	7.4 in
19 - Head Breadth.....	14.4 cm	5.7 in
20 - Head to Chin Height (Vertex to Mentum).....	24.5 cm	9.6 in
21 - Biceps Circumference.....	999	999
22 - Elbow Circumference.....	999	999
23 - Forearm Circumference.....	999	999
24 - Wrist Circumference.....	999	999
25 - Thigh Circumference.....	999	999
26 - Lower Thigh Circumference.....	999	999
27 - Knee Circumference.....	999	999
28 - Calf Circumference.....	999	999
29 - Ankle Circumference.....	999	999
30 - Neck Circumference.....	32 cm	12.6 in
31 - Scye (armpit-shoulder) Circumference.....	999	999
32 - Chest Circumference.....	71.4 cm	28.1 in
33 - Waist Circumference.....	999	999
34 - Buttock Circumference.....	999	999
35 - Chest Depth.....	17.6 cm	6.9 in
36 - Waist Depth.....	999	999
37 - Buttock Depth.....	999	999
38 - Interscye.....	999	999

LABORATORY UMTRI TEST NO. 83E121A-C

HUMAN SUBJECT INFORMATION

CADAVER NO.: 130 DURATION OF BED CONFINEMENT Unknown

AGE: 57 SEX: M CAUSE OF DEATH: Acute myocardial infarction

PHYSICAL APPEARANCE: Caucasian DATE OF DEATH: 9/11/83

ANOMALY: Autopsy revealed evidence of previous thoracic surgery. Ribs weakened at cartilaginous junction.

ANTHROPOMETRY

0 - Weight*	72.5 kg	
1 - Stature**	175.3 cm	
2 - Shoulder (acromial) Height	151.4 cm	59.6 in
3 - Vertex to Symphysion Length	87.5 cm	34.4 in
4 - Waist Height	104.8 cm	41.3 in
5 - Shoulder Breadth (Biacromial Breadth)	33.5 cm	13.2 in
6 - Chest Breadth	33.2 cm	13.1 in
7 - Waist Breadth	31.9 cm	12.6 in
8 - Hip Breadth	33.9 cm	13.3 in
9 - Shoulder to Elbow Length (Acromion-radiale Length)	999	999
10 - Forearm-hand Length (elbow-middle finger)	999	999
11 - Tibiale Height	999	999
12 - Ankle Height (outside) (lateral malleous)	999	999
13 - Foot Breadth	999	999
14 - Foot Length	999	999

Note: * weight in kilograms

** lengths in centimeters

*** measures 16 and 17 must be made in case where the subject will be used in the seated position during the tests. In all other cases enter 9999 when under these measures.

LABORATORY UMTRI D26 TEST NO. 83E131A-C

15 - Top of Head to Trochanterion Length.....	999	999
16 - Seated Height***.....	999	999
17 - Knee Height (seated)***.....	999	999
18 - Head Length.....	21.5 cm	8.5 in
19 - Head Breadth.....	15.4 cm	6.1 in
20 - Head to Chin Height (Vertex to Mentum).....	25.9 cm	10.2 in
21 - Biceps Circumference.....	999	999
22 - Elbow Circumference.....	999	999
23 - Forearm Circumference.....	999	999
24 - Wrist Circumference.....	999	999
25 - Thigh Circumference.....	999	999
26 - Lower Thigh Circumference.....	999	999
27 - Knee Circumference.....	999	999
28 - Calf Circumference.....	999	999
29 - Ankle Circumference.....	999	999
30 - Neck Circumference.....	42.2 cm	16.6 in
31 - Scye (armpit-shoulder) Circumference.....	999	999
32 - Chest Circumference.....	99.8 cm	39.3 in
33 - Waist Circumference.....	999	999
34 - Buttock Circumference.....	999	999
35 - Chest Depth.....	23.5 cm	9.3 in
36 - Waist Depth.....	999	999
37 - Buttock Depth.....	999	999
38 - Interscye.....	999	999

LABORATORY UMTRI TEST NO. 83E131A-C

13.0 APPENDIX F

26th STAPP CAR CRASH CONFERENCE PROCEEDINGS ARTICLE

821160

Impact Response and Injury of the Pelvis

Guy S. Nusholtz, Nabih M. Alem,
and John W. Melvin
University of Michigan
Highway Safety Research Institute

ABSTRACT

Multiple axial knee impacts and/or a single lateral pelvis impact were performed on a total of 19 cadavers. The impacting surface was padded with various materials to produce different force-time and load distribution characteristics. Impact load and skeletal acceleration data are presented as functions of both time and frequency in the form of mechanical impedance. Injury descriptions based on gross autopsy are given.

The kinematic response of the pelvis during and after impact is presented to indicate the similarities and differences in response of the pelvis for various load levels. While the impact response data cannot prescribe a specific tolerance level for the pelvis, they do indicate variables which must be considered and some potential problems in developing an accurate injury criterion.

INTRODUCTION

Pelvis injuries of varying type and severity have been found to occur in a significant number of automotive accidents (1-5). Investigations of trauma of the pelvis resulting from impact in an automotive environment have been documented primarily through accident investigation methods. There have only been a limited number of biomechanical studies attempting to research pelvis impact trauma under laboratory conditions. One of the earliest of these studies was conducted by Evans and Lissner in 1955 (6), and consisted of impacts to the denuded pelvis in the inferior-superior direction. Although no fracture tolerance data were obtained, it was concluded from this study that the pelvis exhibited elastic behavior and failed due to tensile stresses in various structural members. Ten years later a study of the behavior of the knee-femur-pelvis complex in an automotive impact environment was reported by Patrick et al. (7) In this series of tests, an impact sled was used to apply femoral-axis impacts to the knee of embalmed cadavers. The lowest applied load found to cause pelvis injury was 7.1 kN, and loads ranging from 8.5 kN to 17 kN were found to cause multiple fractures of the pelvis. It was suggested that a maximum force criterion (of about 6.2 kN) should be the threshold level for injury for the patella/femur/pelvis complex. A similar study using unembalmed cadavers was reported by Melvin and Nusholtz in 1980. A single pelvis fracture was found to occur at an applied load of about 20 kN, however loads up to 26 kN were applied with no resulting pelvis injury.

A recent biomechanical study of pelvis impact in an automotive environment was documented first in 1979 (9) and more completely in 1980 (10) by Cesari and Ramet. The goal of this research was to supply data for design of side door padding by impacting cadavers laterally in the pelvis and recording the force/injury relationships observed. It was suggested from this study that the response to impact is characterized by velocity of impacts, maximum force, and impulse. Admissible force tolerance for females was documented as 5-7 kN (1100-1600 lb) and for males as 7-13 kN (1600-2900 lb). These studies essentially characterize pelvis injury tolerance using maximum force and impulse indicators.

To further investigate the kinematic and injury response of the pelvis in automotive-environment impacts, a series of tests involving indirect impacts to the pelvis have been

conducted by the Biomechanics Deprtment at HSRI. The tests were conducted using unembalmed cadavers and two types of impact facilities: a pendulum impactor and a pneumatic impactor. Indirect loads were delivered to the acetabulum of the pelvis by impacting the femur either axially or laterally. This allowed loads to be delivered to the acetabulum in either anterior-to-posterior or right-to-left directions. The cadavers were instrumented to measure pelvic triaxial accelerations in all tests, while in some tests three-dimensional motion of the pelvis was recorded with nine accelerometers. Additionally, triaxial accelerations of the femur and the thoracic vertebrae (T8) were measured. Photographic targets on the pelvis and femur were used for photokinemetric analysis of motion due to the impact.

ANATOMICAL OVERVIEW

The bony pelvis (Figure 1) consists of two large, flat irregular shaped hip (coxal) bones that join one another at the pubic symphysis on the anterior midline. Posteriorly the wedge shaped sacrum completes the pelvic ring forming a relatively rigid structure.

In the adult, each hip bone is formed by the fusion of three separate bones, the ilium, ischium, and pubis, which join at the acetabulum. The ilium forms the broad upper lateral part of the hip bone and the upper portion of the acetabulum. Its upper curved edge is the iliac crest. The most commonly refered to prominence on this crest is the anterior-superior iliac spine. Posteriorly the crest ends in the posterior iliac spine, adjacent to its articulation with the sacrum, the sacroiliac joint. The ischium forms part of the acetabulum and has a superior ramus that ends below in the ischial tuberosity. From there the inferior ramus ascends to join with the inferior ramus of the pubic bone. Together this bar of bone is frequently referred to as the ischio-pubic ramus or inferior pubic ramus. The body of the pubic bone forms the anterior part of the acetabulum. From here the superior pubic ramus passes to the midline where it joins its fellow of the opposite side through the pubic symphysis. Below the inferior pubic ramus joins the inferior ischial ramus. The posterior-lateral bony pelvis is covered by multiple muscle layers, buttock fat and skin. The iliac crest is relatively free of heavy musculature. The rounded head of the femur articulates wih the acetabulum and is held within the socket by ligaments. Laterally, on the upper femur is a large bony prominence, the greater trochanter, for the attachment of muscles.

METHODOLOGY

SUBJECT PREPARATION

Following transfer to HSRI, the cadaveric subjects were stored at 4° C until subsequent use. The cadavers were sanitarily prepared and were examined radiologically prior to the installation of accelerometer hardware and after the test.

IMPACT TESTING

Impact tests were conducted using HSRI's pendulum and pneumatic impacting devices. A total of 19 cadavers were used in three series of tests. Multiple left knee impacts (described below) and a single lateral impact were performed on a group of eight cadavers, instrumented with triaxial accelerometer clusters on the pelvis and right trochanter of the femur. A second group of eight cadavers was subjected to knee impacts along the direction of the femoral axis of each side. Of these eight subjects, four had triaxial accelerometer clusters on both trochanters, one was instrumented with a nine-accelerometer plate on the pelvis, and three had no instrumentation. Finally, three cadavers were subject to left-side lateral impacts, each instrumented with a pelvic nine-accelerometer plate.

Acceleration Measurement -- Accelerations were measured in three orthogonal directions at two different sites (trochanter and pelvis) with Endevco 2264-2000 piezoresistive accelerometers by securing a triaxial accelerometer cluster to a mounting platform at each site. Three-dimensional motion determination was made possible by affixing three triaxial clusters of accelerometers to a lightweight magnesium plate which was in turn rigidly attached to the pelvis. The location of the center of gravity, the coordinate system of the triaxial clusters, and the nine accelerometer array are shown in Figure 2. The figure is divided into four sections. The top half of the figure shows the location of the instrumentation for those tests in which the response of both trochanters were obtained. The lower left hand corner shows the location of triaxial clusters in those tests in which both trochanter and pelvis response were measured. The lower right hand corner shows the location of the triaxial cluster or nine accelerometer array for those tests in which only pelvis response was measured. The location and mounting of the accelerometer platforms were as follows:

Trochanter: An incision was made below the greater trochanter and several short self-

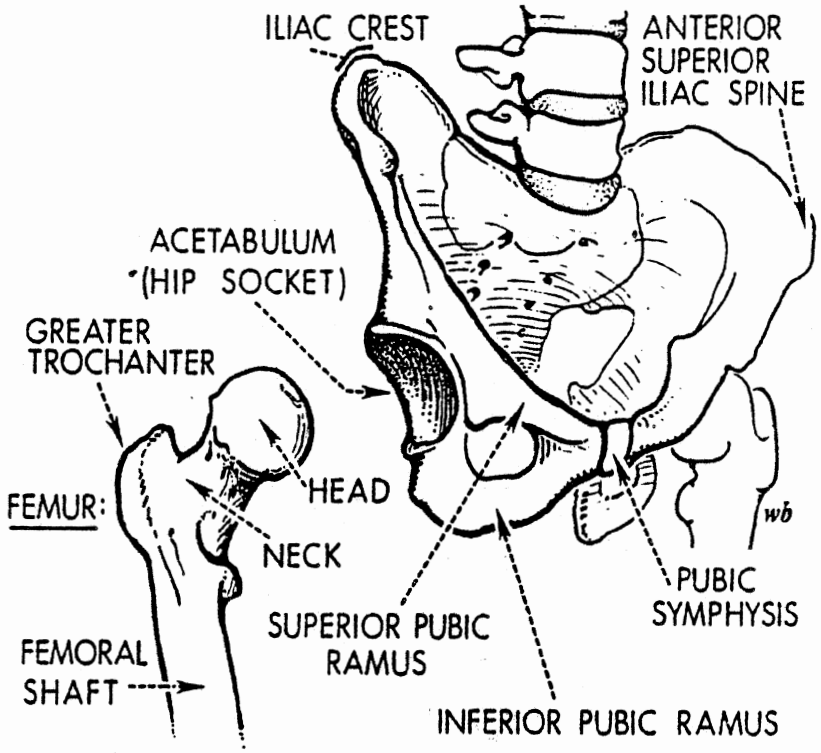

Fig. 1 - Anatomical overview of pelvis (5)

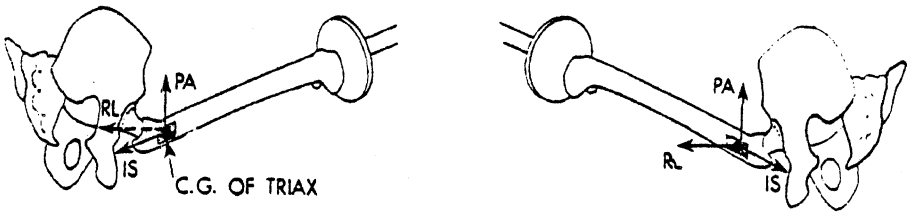

BI-TROCHANTERION RESPONSE

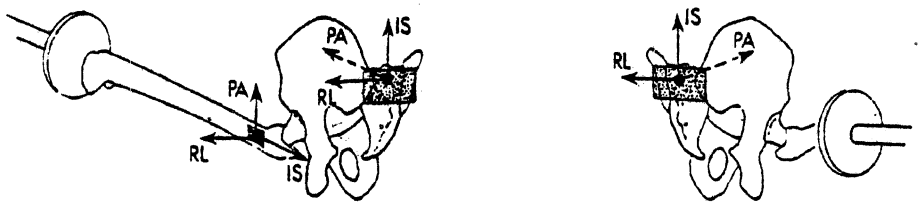

LEFT TROCHANTER AND/OR PELVIC RESPONSE

Fig. 2 - Instrumentation and phototarget location

tapping screws using a multi-point attachment scheme secured the mounting platform to the femur. The platform was then anchored with acrylic to insure rigidity.

Pelvis 9-Accelerometer: Four lag bolts were screwed into the pelvis near the posterior-superior iliac spines. Acrylic was applied, encasing both the bolts and the mounting plate, with the CG of the instrumentation plate midway between the posterior-superior iliac spines.

Pelvis Triax: Two lag bolts with tapped heads were screwed into the posterior-superior iliac spines. A lightweight magnesium plate spanned the bolts and was secured by two screws anchored into the tapped heads of the lag bolts.

Pendulum Impacts -- The pendulum impact device consists of a free-falling pendulum as an energy source which strikes either a 25 kg or a 56 kg impact piston. The impactor, guided by a set of Thompson linear ball bushings, was brought to impact velocity prior to impact and traveled up to 25 cm before being arrested. Axial loads were measured with either a GSE biaxial load cell or a Setra model 111 accelerometer. Shear loads were measured (when relevant) with the GSE biaxial load cell. Impact conditions between tests were controlled by varying impact velocity (up to 8.5 m/s), and the type and depth of padding on the impact piston surface. The piston excursion and the distance the piston traveled from the point of contact to the point of arrest ranged from 3 to 20 cm. The velocity of the piston was measured by timing the pulses from a magnetic probe which sensed the motion of targets on the piston at 0.89 cm intervals. A specially designed timer box was used to control and synchronize the events of a test, such as the release of the pendulum and activation and deactivation of lights and high speed cameras.

For tests conducted with this device, the subject was placed in a restraint harness and suspended in a seated position. Indirect impacts to the acetabulum in the anterior-to-posterior direction were delivered by impacting the knee along the direction of the femoral shaft axis ("axial knee impacts"). Indirect lateral impacts to the acetabulum were delivered by impacting the trochanteric region of the femur, along the axis of the neck of the femur.

Pneumatic Impacts -- The pneumatic impact device consists of an air reservoir which is connected to a honed steel cylinder. A driver piston is propelled down the cylinder by the pressurized air in the reservoir. The driver piston contacts a striker piston which is fitted with a piezoelectric accelerometer (Kistler 904A) and a piezoelectric load washer (Kistler 805A) to allow the determination of acceleration-compensated contact loads applied to the test subject. The mass, velocity, and stroke of the striker piston can be controlled to provide the desired impact conditions for a particular test. The velocity of the impactor is measured by timing the pulses from a magnetic probe which senses the motion of targets on the impactor at 1.3 cm intervals.

For the pneumatic impactor tests, the subject was suspended by a body harness and an overhead pulley system and in addition was seated on a block of balsa wood. Impacts were delivered indirectly to the pelvis through loading of the femur at the knee, as described above.

THREE-DIMENSIONAL MOTION DETERMINATION

The HSRI method used for measuring the three-dimensional motion of the pelvis is based on a technique used to measure the general motion of a vehicle in a simulated crash (11). In the current application, three triaxial clusters of Endevco 2264-2000 accelerometers are affixed to a light-weight magnesium plate which is then rigidly attached to the pelvis. With this method it is possible to take advantage of the physical and geometrical properties of the test subject as well as the site of impact in the design of a system for measurements of 3-D motion.

The nine acceleration signals obtained from the three triaxial clusters are used for the computation of the pelvis motion using a least-squares technique, the details of which are described elsewhere (12,13). The method takes advantage of the redundancy of nine independent acceleration measurements to minimize the effect of experimental error.

PHOTOKINEMETRICS

Each subject underwent two radiologic examinations, one prior to and one following the test. High-speed photographic coverage of the test consisted of two lateral views. A Hycam camera operating at 3000 frames per second provided a close-up view of the pelvis, while a Photosonics 1B camera operating at 1000 frames per second was used to obtain an overall view of the test subject. The motion of the subject was determined from the film by following the motions of five-point phototargets. The targets were affixed to the rigid accelerometer mounts located on the pelvis, trochanter, and spine. Since the resulting film provided a lateral view of the test, the motion observed was two-dimensional and restricted to the plane of the film.

INITIAL CONDITIONS AND POSITIONING

For all tests, the subject was placed in a restraint harness which was in turn suspended from the ceiling. For the axial knee impacts, the subject was positioned as in Figure 3 with the impactor initially 8 to 10 cm from the knee. These tests used as padding either 2.5 cm of Ensolite, 2.5 cm of styrofoam, or a combination of 2.5 cm Ensolite and 2.5 cm styrofoam. The lateral pelvis impacts required that the subject be positioned as in Figure 4, with the impactor initially centered 8 cm anterior to the greater trochanter. For these tests, the impactor was either rigid, padded with 2.5 cm Ensolite, or a combination of 2.5 cm Ensolite and 2.5 cm styrofoam.

PELVIS IMPACT RESPONSE

One method for analyzing the motion of a material body is to analyze the motion of a point on that body. In the case of the tests performed in this study, the point chosen is midway between posterior-superior iliac spines (PSIS). The motion is then analyzed using the concept of a moving frame discussed elsewhere (13) and briefly summarized here.

A vector field is a function which assigns a uniquely defined vector to each point along the path generated by the moving point. Similarly, any collection of three mutually orthogonal unit vectors emanating from each point on the path is a frame field. Thus any vector defined on the path (for example, acceleration) may be resolved into three orthogonal components of any well defined frame field.

In biomechanics research, frame fields which are frequently used are defined based on anatomical reference frames. The anatomical reference frames used here are shown in Figure 2. The frames are based on the anatomical orientation of a standing test subject. Therefore, the I-S direction of the trochanter is roughly equivalent to the minus A-P direction of the pelvis for a seated subject. Other frame fields such as the Principal Direction Triad (14) or Frenet-Serret frame (13), which contain information about the motion embedded in the frame field, have also been used to describe motion resulting from impact.

The Frenet-Serret frame consists of three mutually orthogonal vectors T, N, B. At any point in time a unit vector can be constructed that is co-directional with the velocity vector. This normalized velocity vector defines the tangent direction T. A second unit vector N is constructed by forming a unit vector co-directional with the time derivative of the tangent vector T (the derivative of a unit vector is normal to the vector). To complete the orthogonal frame, a third unit vector B (the unit binormal) can be defined as the cross product T x N. This then defines a frame at each point along the path and resolves the acceleration into two distinct types. The tangent acceleration (Tan(T)) is always the rate of change of speed (absolute velocity) and the normal acceleration (Nor(N)) contains acceleration information about the change in direction of the velocity vector. The binormal direction contains no acceleration.

In the case of a single triaxial accelerometer, the use of the Frenet-Serret frame is impractical but it has been found (14) that in many cases during direct impacts it is possible to find the most significant component of acceleration, therefore the principal direction of motion can be obtained.

One method of determining the principal direction of motion and constructing the Principal Direction Triad is to determine the direction of the acceleration vector in the moving frame of the triaxial accelerometer cluster and then prescribe the transformation necessary to obtain a new moving frame that would have one of its axes in the principal direction. A single point in time at which the acceleration is a maximum was chosen to define the directional cosines for transforming from the triax frame to a new frame in such a way that the resultant acceleration vector (AR) and "principal" unit vector (A1) were co-directional. This then can be used to construct a new frame rigidly fixed to the triax, but differing from the original one by an initial rotation. After completing the necessary transformation, a comparison between the magnitude of the principal direction and the resultant acceleration is performed. In the case of the impacts presented here, there was only a slight difference between the two quantities during the most significant part of the impact. However, for responses occurring after impact this was not always the case.

FORCE-TIME DURATION DETERMINATION

In order to define the pulse duration, a standard procedure was adopted which determines the beginning and end of the pulse. The procedure is to determine first the peak and the time at which it occurs. Next, the left half of the pulse, defined from the point where the pulse starts to rise to the time of the peak, is

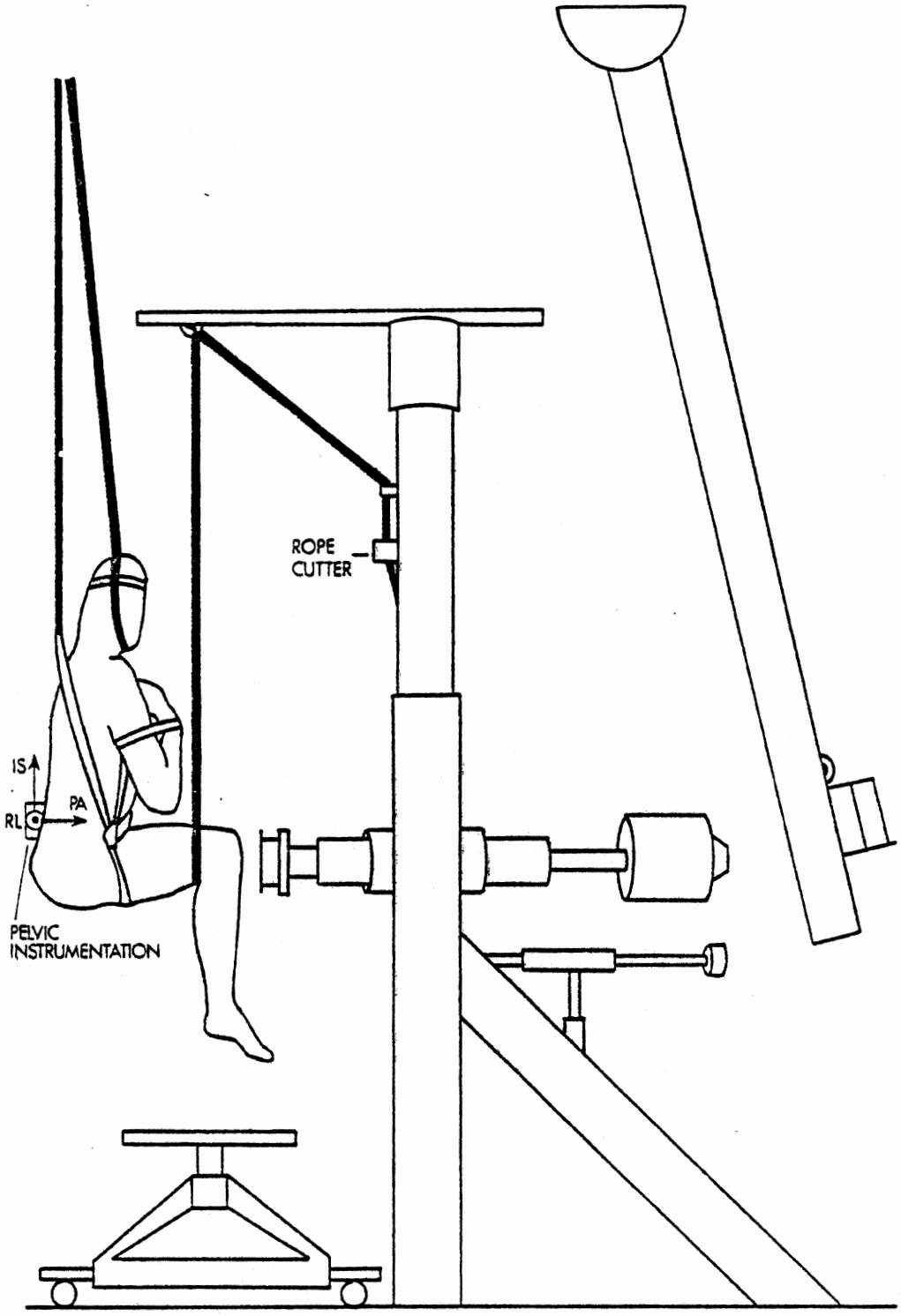

Fig. 3 - Schematic pendulum test setup — right leg impact

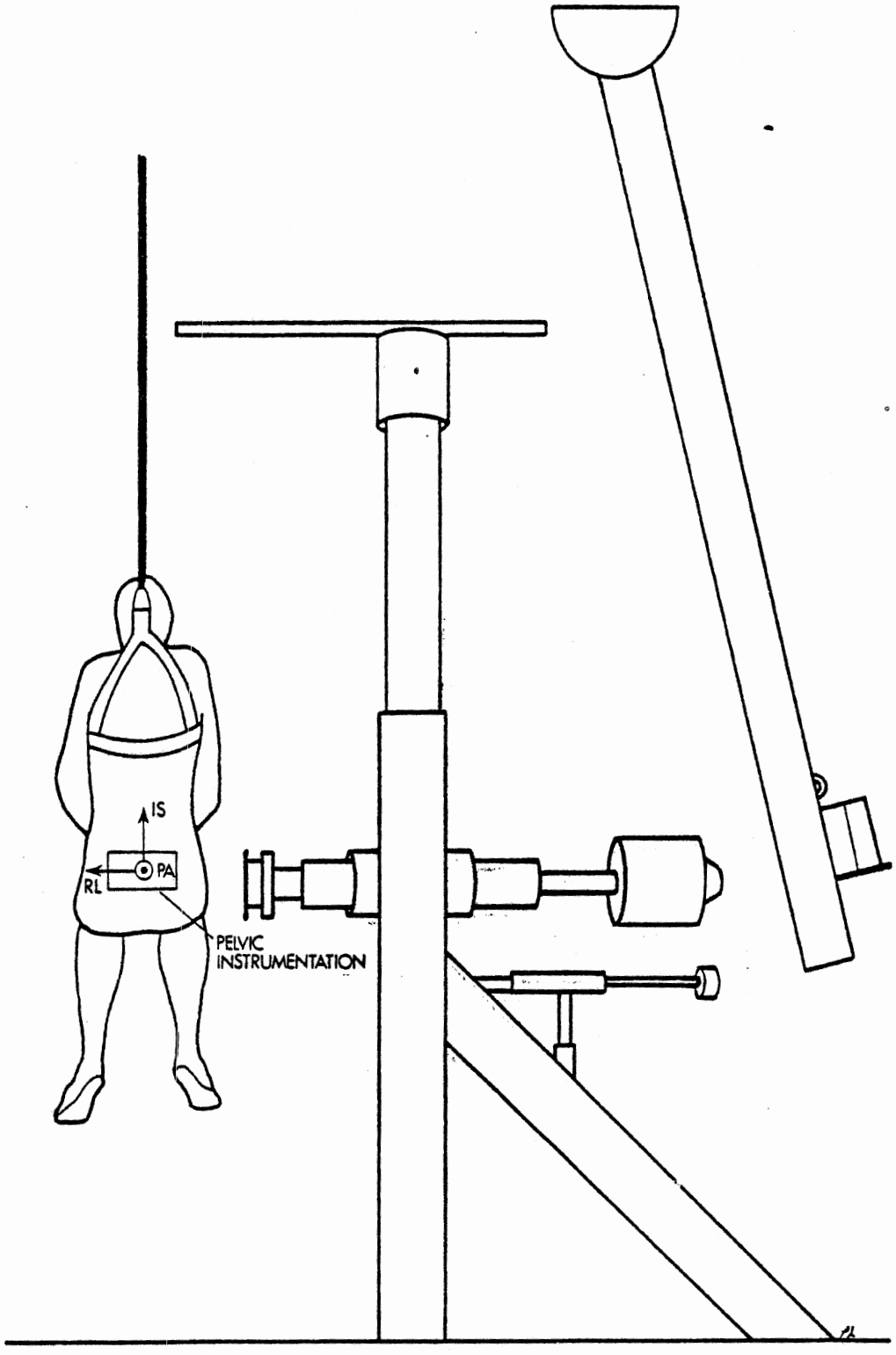

Fig. 4 - Schematic pendulum test setup — pelvis impact

least-squares fitted with a straight line. This rise line intersects the time axis at a point which is taken as the formal beginning of the pulse. For those tests which exhibit multimodal signals, the least-squares line is fitted from where the pulse starts to the time of the first significant peak. A similar procedure is followed for the right half of the pulse, i.e., a least squares line is fitted to the fall section of the pulse which is defined from the peak to the point where the first pulse minimum occurs. The formal end of the pulse is defined then as the point where the fall line intersects the time axis. In many cases, however, the formal end of the pulse (as defined above) is not the end of contact between the impactor and the subject. In these instances, two durations are used; one to indicate the end of the most significant aspect of the force-time history and one to indicate the end of the contact.

IMPACT TRANSFER FUNCTION ANALYSIS

With blunt impacts, the relationship between impact force and the motion resulting at various points of the impacted system can be expressed in the frequency domain through the use of a transfer function. A fast Fourier transformation of simultaneously monitored transducer time histories can be used to obtain the frequency response functions of impact force and accelerations of remote points. Once obtained a transfer function of the form

$$Z(i\omega) = \omega \cdot \frac{\mathbf{F}(F(t))}{\mathbf{F}(A(t))}$$

can be calculated from the transformed quantities where ω is the given frequency, and $\mathbf{F}(F(t))$ and $\mathbf{F}(A(t))$ are the Fourier transforms of the impact forces and accaleration of the point of interest, at the given frequency. This particular transfer function is closely related to mechanial transfer impedance which is defined as the ratio between simple harmonic driving force and corresponding velocity of the point of interest. Mechanical transfer impedance (15) is a complex valued function which for the purpose of presentation will be described by its magnitude and its phase angle.

RESULTS

The tables and graphs presented on the following pages represent the data considered most pertinent in discussing the test results. Table 1 contains biometric data of all test subjects, as well as the test numbers corresponding to each subject (since most subjects received multiple knee impacts as well as a lateral pelvis impact, one subject will have several corresponding test numbers). The initial conditions for all knee impact tests and all lateral impact tests are presented in Tables 2 and 3, respectively.

A summary of gross autopsy results for the lateral impact tests is presented in Table 4. The series of knee impacts produced only one injury. All pelvic injuries were sustained on the impacted side of the pelvis.

Impact test summaries containing force and three-dimensional motion information for axial knee impacts to each cadaver appear in Table 5, and in Table 6 for lateral pelvis impacts. Surmaries for force and triaxial acceleration are presented in Tables 7 and 8 for the axial knee impacts, and in Table 9 for the lateral impacts.

DISCUSSION

The results presented in this paper have been obtained from a series of pelvis injury research programs conducted during the past five years. The data is presented in abbreviated form to represent the trends which are felt to be important factors in pelvis impact response.

PELVIS RESPONSE FROM AXIAL KNEE IMPACTS

The response of the pelvis as characterized by the time history of various accelerations and velocities (both angular and linear) in addition to the force time history, is dependent on the impactor surface padding, mass and initial velocity as well as variations between individual test subjects. This is arrived at from analysis of three dimensional motion obtained from nine accelerometers, triaxial accelerometer clusters (affixed to the pelvis, the impacted femur and the femur opposite the impactor), as well as high speed photokinemetric documentation.

Three-Dimensional Motion -- Tests 79A243-79A248 represent six impacts to a single test subject. The six tests are divided into three groups with similar impacts on each knee. The three groups are: low velocity (3.5 m/s and 2.5 cm Ensolite impactor surface padding), medium velocity (5.0 m/s with 2.5 cm Ensolite impactor surface padding), and high velocity (8.5 m/s with rigid impactor surfaces). The time history of the three dimensional motion of the pelvis obtained from the nine accelerometer array is summarized in Table 5. The maximum impact force ranged from 4kN to 20kN with the duration of impact ranging from 12 ms to 30 ms.

Table 1. Biometrics

Cadaver No.	Height (cm)	Weight (Kg)	Age	Cause of Death
1	173	29.0	64	Differentiated lymphoma
2	160	57.2	73	Pneumonia
3	175	99.5	76	Cardiac arrest
4	178	106	63	Myocardial infarction
5	176	35.3	67	Cardiac resp. arrest intractible congestion
6	169	65.9	89	Cardiac arrest
7	176	68.1	76	Coronary occlusion
8	174	91.7	76	Myocardial infarction
9	179	41.6	66	Amyotrophic lateral sclerosis
10	174	61.9	73	Terminal pneumonia
11	180	91.2	56	Cardiac arrest
12	175	100	62	Cardiac arrest
13	--	88.0	61	Cardiac arrest
14	--	--	52	Cardiac arrest
15	184	52.0	60	Cardiac arrest
16	180	76.9	67	Cardiac arrest
17	169	86.5	65	Myocardial infarction
18	--	--	--	Cardiac arrest
19	174	68.3	40	Cardiac arrest

Table 2: Summary of Initial Conditions for Knee Impacts

Test No.	Cadaver No.	Impactor Velocity (m/s)	Impactor Mass (Kg)	Padding
77A204	18	15.2	10	10 cm Ensolite
77A205	13	12.2	10	10 cm Ensolite
77A206	13	15.2	10	10 cm Ensolite
77A207	12	18.3	10	10 cm Ensolite
77A208	12	21.3	10	10 cm Ensolite
79A243	14	3.4	25	2.5 cm Ensolite
79A244	14	3.4	25	2.5 cm Ensolite
79A245	14	5.0	25	2.5 cm Ensolite
79A246	14	5.0	25	2.5 cm Ensolite
79A247	14	8.6	25	Rigid
79A248	14	8.5	25	Rigid
79L081	1	5.5	56	2.5 cm Ensolite+ 2.5 cm Styrofoam
79L082	1	5.5	56	2.5 cm Ensolite+ 2.5 cm Styrofoam
79L085	2	5.5	56	2.5 cm Ensolite+ 2.5 cm Styrofoam
79L086	2	5.5	56	2.5 cm Ensolite+ 2.5 cm Styrofoam
79L089	3	5.5	56	2.5 cm Ensolite+ 2.5 cm Styrofoam
79L090	3	5.5	56	2.5 cm Ensolite+ 2.5 cm Styrofoam
80L094	4	5.9	56	2.5 cm Ensolite
80L097	5	5.5	56	2.5 cm Ensolite
80L098	5	5.9	56	Rigid

Table 2: Summary of Initial Conditions for Knee Impacts (continued)

Test No.	Cadaver No.	Impactor Velocity (m/s)	Impactor Mass (Kg)	Padding
80L102	6	5.5	56	2.5 cm Ensolite
80L103	6	5.8	56	Rigid
80L109	7	5.5	56	2.5 cm Ensolite
80L110	7	5.9	56	Rigid
80L114	8	5.9	56	2.5 cm Ensolite
80L115	8	5.8	56	Rigid
80L118	9	4.1	56	Rigid
80L119	9	4.2	56	Rigid
80L120	9	5.9	56	Rigid
80L124	10	4.1	56	Rigid
80L125	10	5.9	56	Rigid
80L129	11	4.0	56	Rigid
80L130	11	5.9	56	Rigid
80L135	19	4.0	56	Rigid
80L135	19	6.0	56	Rigid
80L135	19	4.0	56	Rigid
80L136	19	6.0	56	Rigid

Table 3. Summary of Initial Conditions for Lateral Impacts

Test No.	Cadaver No.	Impactor Velocity (m/s)	Impactor Mass (Kg)	Padding
80L095	4	5.1	56	2.5 cm Ensolite
80L099	5	5.7	56	2.5 cm Ensolite
80L104	6	5.8	56	Rigid
80L111	7	5.8	56	Rigid
80L116	8	5.7	56	Rigid
80L121	9	5.9	56	Rigid
80L126	10	5.8	56	Rigid
80L131	11	5.5	56	Rigid
80L137	19	5.9	56	Rigid
82E008	15	8.4	25	2.5 cm Ensolite+ 1.3 cm Styrofoam
82E028	16	8.4	25	0.5 cm Ensolite
82E049	17	8.6	25	2.5 cm Ensolite+ 2.5 cm Styrofoam

Table 4. Summary of Autopsy Results

Test No.	Results
80L095	No observed injuries.
80L099	No observed injuries.
80L104	Vertical separation fracture of superior pubic ramus approximately one inch from pubic symphysis.
80L111	Horizontal separation fracture of ilio-pubic ramus, connected to a horizontal fracture of the acetabulum.
80L116	No observed injuries.
80L121	Vertical stellar fracture on outer aspect of ilium extending from iliac crest to anterior-inferior iliac spine.
80L126	Non-separational fractures of superior and ischio-pubic ramus.
80L131	Horizontal fracture of ilio-pubic ramus.
80L137	No observed injuries.
82E008	No observed injuries.
82E028	Vertical Separation fracture of ischio-pubic ramus. Horizontal fracture of acetabulum extending two inches into superior pubic ramus.
82E049	No observed injuries.

Table 5. 3-D Motion Knee Impact Test Summary

Test No.	Peak Force (N)	Impulse (N.s)	Duration (m/s)	Peak Linear Acceleration (m/s/s)				Peak Angular Acceleration (rad/s/s)			
				P-A	R-L	I-S	TAN	P-A	R-L	I-S	RES
79A243 @ ms=	3750 11	58	30	-95 7	-150 6	70 6	160 6	-150 4	-670 5	1200 5	1180 6
79A244 @ ms=	3750 11	59	30	-90 5	200 5	75 5	250 5	430 3	-380 5	-1130 5	1050 5
79A245 @ ms=	5750 12	80	30	-120 7	+300 7	115 6	320 6	530 4	-800 5	-1750 5	2000 6
9A246 @ ms=	6000 11	75	32	-150 4	-260 4	160	340 8	-600 3	-1440 8	2000 5	2200 4
79A247 @ ms=	20000 3	120	12	-1750 2	-2600 2	100 3	3200 2	-1700 3	-30000 3	20000 2	31000 3
79A248 @ ms=	21000 2	135	12	-1050 2	2750 2	1600 2	3200 2	19000 1	-20000 2	-17500 1	25000 1

Table 6: Padded Knee Impacts

Test No.	Force				Acceleration		Velocity	
	Maximum (N)	Duration (ms)	Impulse (N-s)	Energy (N-M)	Troch. Maximum (m/s)	Opposite Troch. Maximum (m/s)	Troch. Maximum (m/s)	Opposite Troch. Maximum (m/s)
79LO81=	1550	25	22	5	43	16	4.9	2.8
@ ms=	11	(35)			4	35	22	60
79LO82=	1750	26	25	6	34	19	5.0	2.8
@ ms=	13	(31)			12	27	22	56
79LO85=	900	30	10	1	21	8	4.0	2.4
@ ms=					12	25		60
79LO86=	1100	30	12	1	7.5	10	4.3	2.5
@ ms=				+	15	20		65
79LO89=	5200	31	65		48	9	4.5	2.5
@ ms=	17	(43)			13	23	30	65
79LO90=	4600	34	60	32	33	13	4.0	2.2
@ ms=	17	(44)			(13)	27	30	65

Table 7: Knee Impacts

Test No.	Force					Acceleration		Velocity	
	1st Peak (N)	Maximum (N)	Duration (ms)	Impulse (N-s)	Energy (N-m)	Troch. Maximum (g's)	Pelvis Maximum (g's)	Troch. Maximum (m/s)	Pelvis Maximum (m/s)
80L094 @ ms=		5850 8	27 (73)	88	69	80 8	60 12	3.7 22	3.4 15
80L097 @ ms=		3950 9	20 (5)	45	18	115 9	80 8	6.2 16	5.2 1
80L098 @ ms=		2475 2	12 (36)	21	3.9	450 1	250 2	5.5 4	6.2 6
80L102 @ ms=		7000 8	24 (46)	100	88.8	140 7	95 8	4.8 11	4.0 10
80L103 @ ms=		7550 3	15 (40)	56	28.4	400 2	120 4	5.9 3	3.2 5
80L109 @ ms=		8100 9	25 (61)	98	85.2	200 9	70 8	5.3 8	3.4 9
80L110 @ ms=		9500 3	20 (44)	89	0.9	700 2	190 3	5.7 6	3.7 5
80L114 @ ms=		10000 7	35 (55)	107	102	230 6		6.2 7	3.1 28
80L115 @ ms=		12000 2	24 (34)	100	92	675 2		5.9 3	3.4 16
80L118 @ ms=	5200 1	6000 2	12 (66)	36	11.6	220 1	115 1.5	3.9 8	3.2 7
80L119 @ ms=	4500 1	5750 2	13 (70)	45.7	18.7	300 2	155 3	4.2 4	3.2 8
80L120 @ ms=	5250 1	8900 3	15 (55)			500 3	150 (3.5)	4.9 3	4.0 10
80L124 @ ms=	1	7500 2	20 (77)	46.9	19.6	390 2	115 4	4.4 4	3.0 7
80L125 @ ms=	5600 1	9700 3	20 (57)	88	70	400 2	175 4	5.2 3	3.5 6
80L129 @ ms=		8750 3	20 (27)	74.4	49.5	205 1	140 2	4.1 6	3.5 15
80L130 @ ms=	8900 2	9750 3	16 (29)	105	100	650 2	185 2	5.6 6	5.1 14
80L135 @ ms=	5000 2	8700 4	17 (28)	75	51	1750 1	135 2	3.9 7	3.4 10
80L136 @ ms=	9700 6	11800 6	16 (58)	105	101	900 2	240 3	5.4 8	4.1 9

Table 8. Lateral Pelvis Impact

Test Number	Force		Acceleration		Velocity
	Maximum (N)	Duration (ms)	1st Peak	Maximum (g's)	Maximum (m/s)
80L095	10700	44		38	4.4
@ ms=	10			10	44
80L099	3200	42	23	50	4.6
@ ms=			5	11	38
80L104	5900	49		40	4.7
@ ms=	9			11	42
80L111	7600	50		100	4.7
@ ms=				4	40
80L116	7700	51		57	4.3
@ ms=	9			11	48
80L121	3300	30	105	110	4.3
@ ms=	15		2	4	56
80L126	7400	44	50	135	4.3
@ ms=	5		4	11	40
80L131	8500	40	50	135	4.3
@ ms=	7		6	11	52
80L137	9200	22	40	48	4.8
@ ms=	5		3	6	50

Table 9. Lateral Impacts

Test No.	Peak Force (N)	Impulse (N-s)	Duration (ms)	Peak Linear Acceleration (m/s/s)				Peak Angular Acceleration (rad/s/s)			
				P-A	R-L	I-S	Tan	P-A	R-L	I-S	Res
82E008	14000	190	29	300	840	-340	831	-2270	-6910	-4600	6010
@ ms=	13			18	11	14	14	14	14	16	11
82E028	13000	190	21	350	710	550	650	3620	10100	8190	10250
@ ms=	7			6	6	11	6	4	8	5	8
82E049	14000	206	26	127	360	-100	370	2700	-3480	-1990	3750
@ ms=	14			15	14	14	14	13	13	16	16

Several distinct events occurred in all the force time histories and could be used as event markers. They are: the beginning of impact noted as E1, the peak force noted as E2, and the end of impact noted as E3. Both angular and linear accelerations begin at the E1 event and reach maximums at or before the E2 event. Even though there is significant angular acceleration during this interval, the primary acceleration is in the tangent direction (with a smaller component in the normal direction) indicating that the direction of motion changes slowly with time. In addition, the angular acceleration during this interval differs in magnitude and direction for each of the three sets of tests. For tests 79A243 and 79A244 (Figures 5 and 6) the angular acceleration was found to be primarily in the I-S direction (although lesser components occurred in the R-L and P-A directions). In tests 79A245 and 79A246, the magnitude of the angular acceleration is greater and is to a greater degree in the R-L and P-A direction. In tests 79A247 and 79A248 (Figures 7 and 8), the magnitude of the angular acceleration in the R-L and P-A direction is similar in magnitude to that of the I-S direction. Along with the changes in magnitude and direction of the angular acceleration with changing impact velocity, there is an increasing ratio of angular acceleration to peak force as well as a change in the relative phasing of the angular acceleration time history to force time history during the E1-E2 interval. In addition to changes in angular acceleration with increasing impactor velocity, there were also changes in the linear accelerations; its magnitude, direction, and phasing with respect to the E2 events. For tests 79A243 and 79A244, the linear acceleration was primarily in the RL-PA plane during the E1-E2 event interval. As the magnitude of the loading increased (as in tests 79A245 through 79A248), a significant component of linear acceleration in the I-S direction developed.

Physically, this implies that the response of the pelvis can be interpreted as the response of one material body (the pelvis) in contact with other material bodies (the femur, spine, abdominal organs, and soft tissue). The degree to which each of the material bodies interacts with the pelvis is dependent upon the amount of available impactor energy and how it is transmitted to the pelvis.

Triaxial Bitrochanteric Response -- Although the padding on the impactor surface was different, the loading in tests 79L081 through 79L090 (Table 7) is similar to that of the the previous tests. The response is measured with two triaxial accelerometer clusters located near each trochanter. Using the same event markers on the force time history as in the previous tests, some information about the response of the pelvis from the trochanteric response may be obtained. Near the E1 event the acceleration of the trochanter of the impacted side begins, however the accelerometer of the opposite trochanter displays little or no motion until near or after the E2 event. Acceleration of the impacted side peaks before the E2 event, whereas the acceleration response of the other trochanter reaches a maximum near the E3 event. The motion indicated by this type of response is somewhat similar to test 79A243 and 79A244 (for the pelvis) with the greatest rotation in the I-S direction. However, it is clear from the accelerometer data and high-speed movies that although the pelvis seems to behave as it were rotating about a fixed point near the trochanter of the opposite femur during the E1-E2 interval, motion after the E2 event is considerably more complex, with the peak velocity of the opposite femur more than half of that of the impacted femur.

Pelvis and Trochanteric Response -- Tests 80L094 to 80L136 (Table 8) represent similar loading to that of the previously mentioned tests (79A243-248 and 79L081-090). The response is measured by the use of triaxial accelerometers located on the pelvis and trochanter on the side of impact, as well as photokinematic documentation. The peak forces range from 6 to 12 kN.

In some of these tests, the force time history is similar to that of 79L081 through 79L090 with one peak and a well defined beginning and end, however a few of the tests have a more complex force time history. They exhibit several local maxima and/or continuing impactor contact after the initial part of the pulse occurs. Although the response of the trochanter as interpreted by the principal direction acceleration and resulting acceleration time-history waveforms is similar to some of the previous heavily-padded tests, others display damped oscillatory motion (Figure 9). This response is generally observed during the first section of the pulse and unobservable shortly after the E2 event. In addition the peak acceleration generally occurs around the time of the first significant maximum of the force time history. Other researchers using finite element modeling of the femur (16) have shown that various modes of bending and torsion can occur. Potentially both the oscillatory nature of the trochanteric response and the multimodal nature of the force time histories for these tests are a result of the bending of the femur.

Although in these tests only triaxial acceleration is measured and the force time history varies from test to test in a very

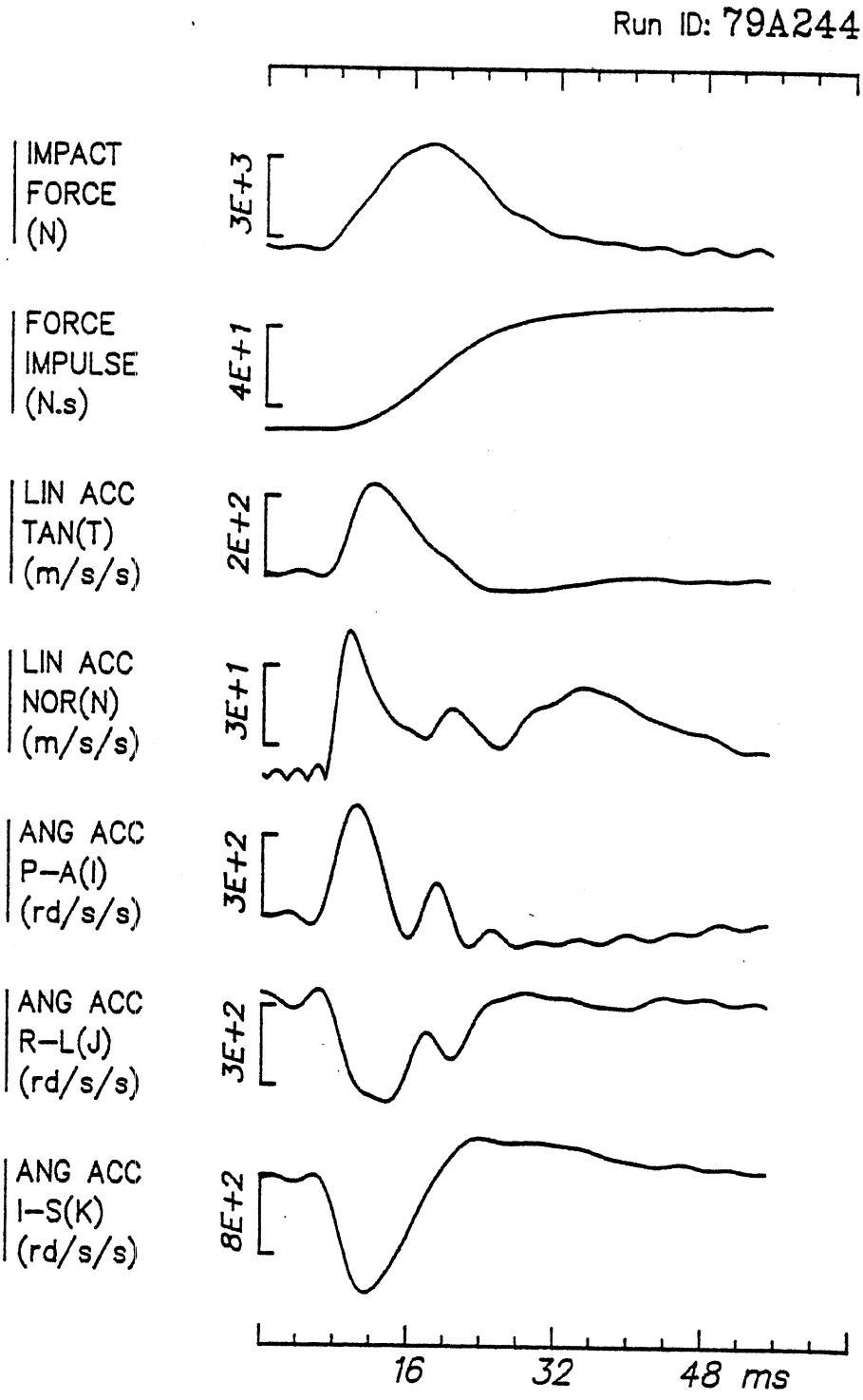

Fig. 5 - Test 79A244

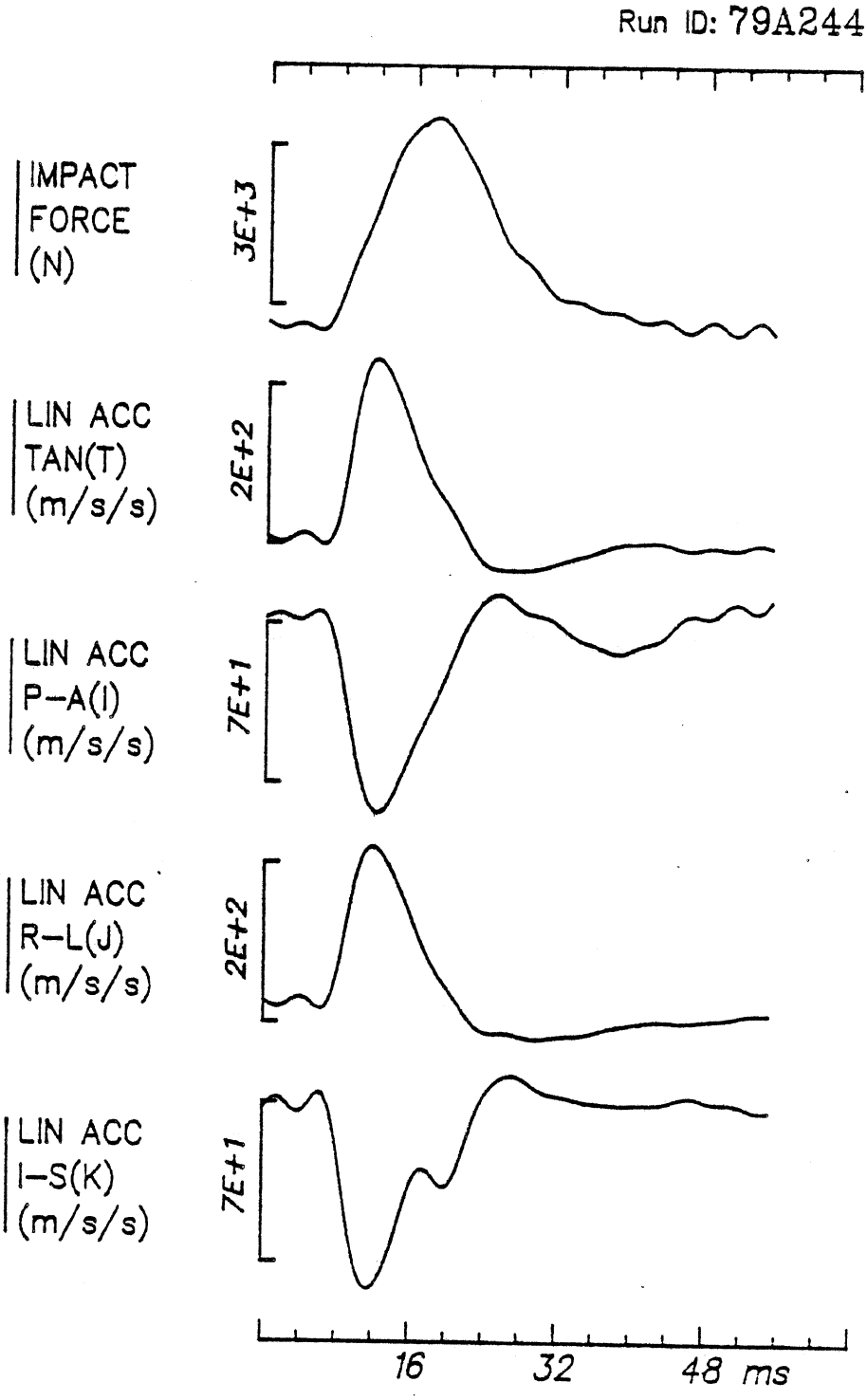

Fig. 6 - Test 79A244

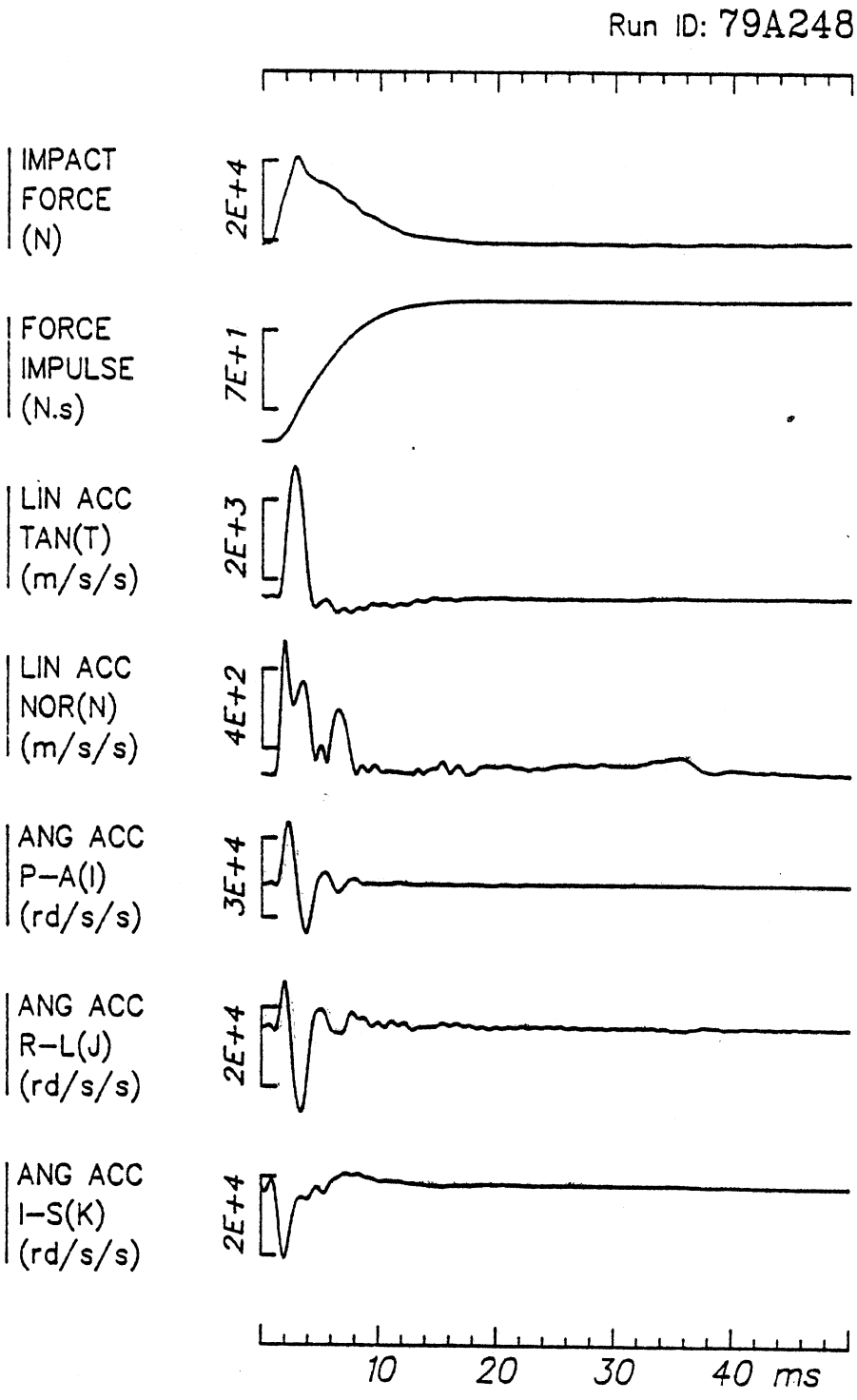

Fig. 7 - Test 79A248

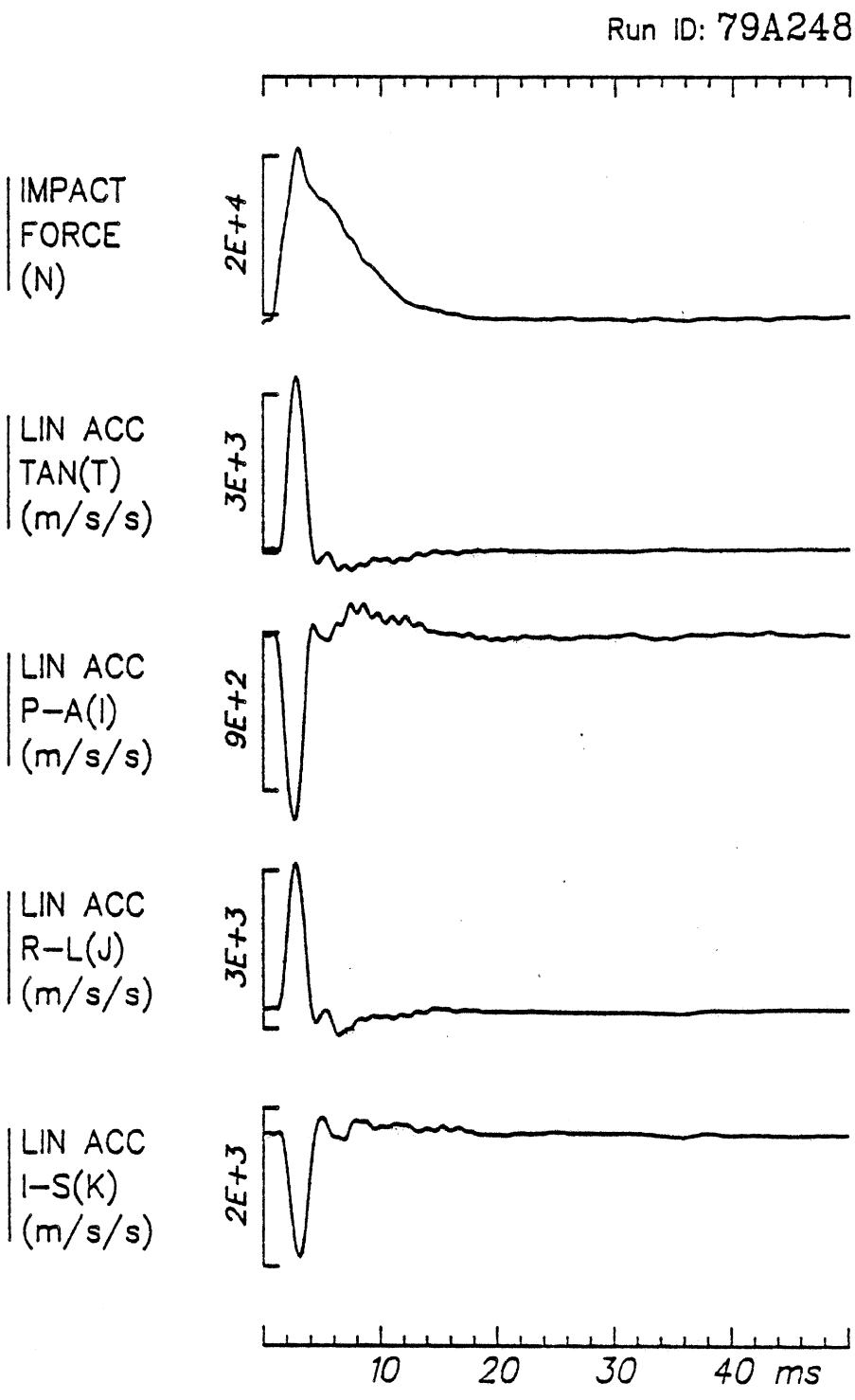

Fig. 8 - Test 79A248

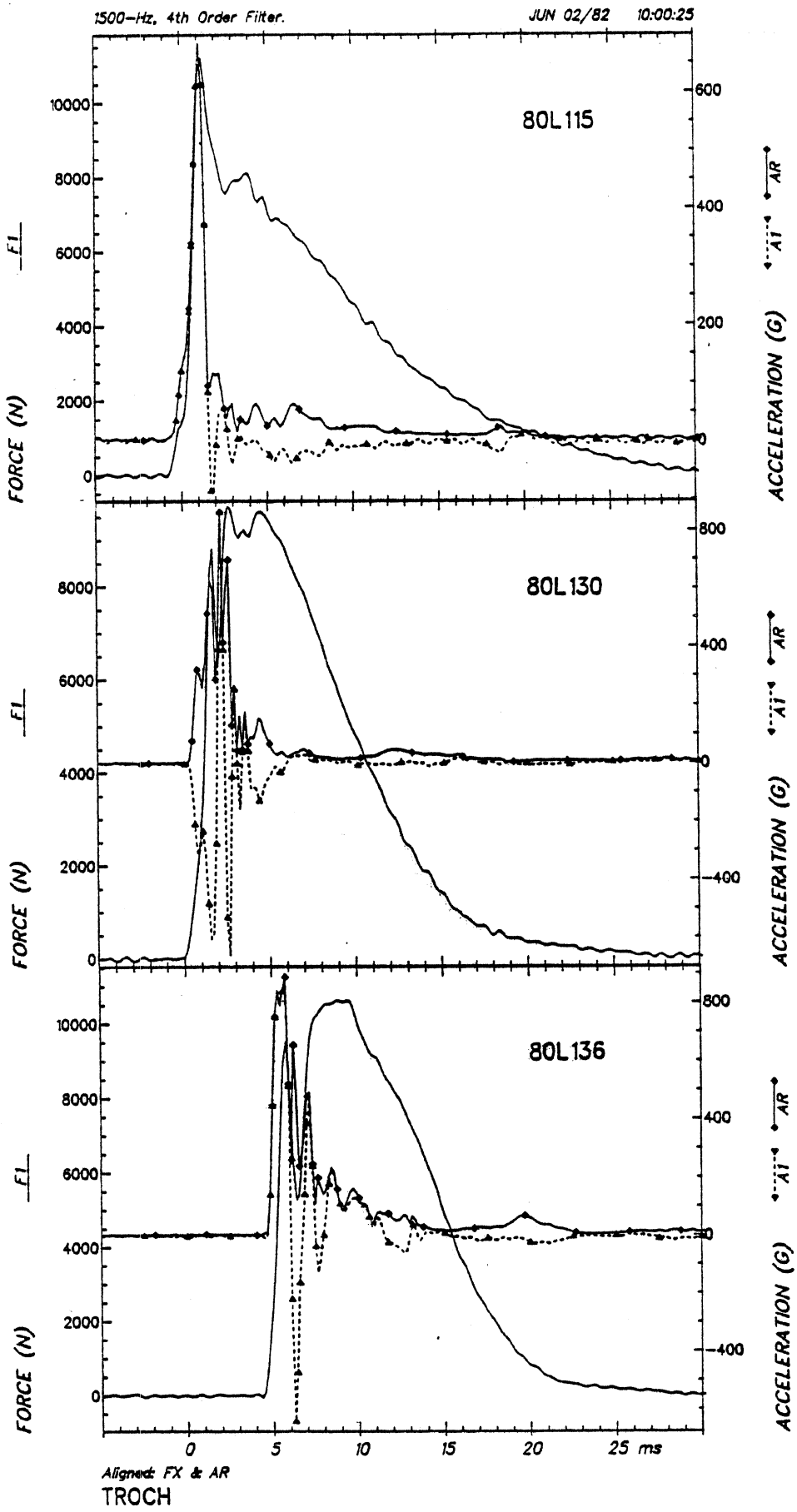

Fig. 9 - Trochanter impact response

general way the response of the pelvis, as interpreted by the principal direction accelerations, is similar in these tests to that of the response interpreted by tangential acceleration in tests 79A247 and 79A248. Table 8 compares the acceleration time history of the pelvis to that of the force time history and acceleration time history of the trochanter. In general, the peak acceleration of the pelvis is less than and lags behind that of peak trochanteric accelerations. In addition, the resultant peak velocity of the trochanter is greater than and precedes the pelvis peak velocity, and is primarily in the I-S direction (of the femur).

Transfer Functions -- The transfer function formed from the impact force and acceleration includes the effects of padding and subject response. A corridor for transfer functions formed from the impact force and tangent acceleration for tests 79A243-79A248 is shown in Figure 10.

For tests 79A243 and 79A244 the transfer function is included in the corridor to 100 Hz. For test 79A245 and 79A246 the transfer function is included to 150 Hz, and for tests 79A247 and 79A248, it is included from 10 to 400 Hz. The corridor representing pelvis response (interpreted by mechanical impedance for force and resulting velocity) shows that all six tests are similar to 100 Hz. Four tests are similar to 150 Hz and two are similar to 400 Hz. This seems to be true despite the different impact conditions (different padding, different initial velocity, opposite side impacts), and different time history responses. This would seem to indicate that the responses for this subject are repeatable, symmetric (same response for opposite sides) and linear to at least 100 Hz.

The mechanical impedance for tests 79A081 - 79A090 (Figure 11) is generated from force and principal direction acceleration, and is considered valid between 10 and 100 Hz. In the frequency range between 10 and 30 Hz it is somewhat similar to the impedance of tests 79A243 through 79A248. Above this range, however, there is a continual decline in the value of the impedance. This is believed to be a result of the styrofoam padding used in these tests.

For pelvis tests 80L094 - 80L136, the mechanical impedance obtained from the principal direction acceleration was significantly less than those calculated from the accelerations in the two directions normal to it above 25 Hz in all tests. For the trochanter, the mechanical impedance was valid for regions below this range however for comparison purposes it is presented down to 25 Hz. The upper limit for the validity of the pelvis impedance was 400 Hz and therefore the trochanteric upper limit is chosen as 400 Hz. To obtain information about the repeatability of the response of different test subjects, multiple impacts (at a subinjurious level) were performed on each subject (Table 8) with each subject in the same initial postural configuration while the impactor surface padding and velocity were varied. The transfer function formed from the principal direction acceleration and force-time history for both the pelvis and trochanter are shown in Figures 12 and 13 for tests 80L114 and 80L115, respectively, and in Figures 14 and 15 for tests 80L135 and 80L136, respectively.

It was observed that the acceleration response of the trochanter is primarily in the same direction as that of the force while the acceleration of the pelvis is not. Despite this and the fact that impact conditions varied between impacts to the same side, observation of these transfer function waveforms (and others not presented) show that the transfer functions for repeated tests on the same side are similar for both the pelvis and trochanter. The transfer function for the pelvis and the trochanter of the same subject are similar in waveform up to 200 Hz, although they differ in magnitude -- values for the mechanical impedance of the pelvis are generally two to four times that of those for the trochanter. The amount of scatter between subjects is addressed in Figures 16 and 17, which represent the corridor for impacts that did not result in injury for both the pelvis and trochanter, respectively. Although the two corridors look similar (differing only in magnitude below 100 Hz), they cover a wide range of possible responses, particularly above 200 Hz. This magnitude indicates that although the response of a single subject is similar for repeated impacts, there is wide scatter between subjects.

In addition to the above observations on the transfer functions, in some of the tests (e.g., 80L135 and 80L136) a resonance was observed between 180 and 280 Hz, which is within the band in which others have observed a resonance (16,17). This resonance (which is observed in both the pelvis and trochanter, although it is more pronounced in the trochanter transfer function) is potentially related to the oscillatory behavior mentioned above and also to the predicted first mode bending (16). Although most of the test subjects did not display this resonance, it does occur in a few of the tests which may help to explain some of the scatter observed.

Damage to the Pelvis and Femur -- Many of the tests involved loads above 10 kN, with only one resulting injury (test 80L103 resulted in a

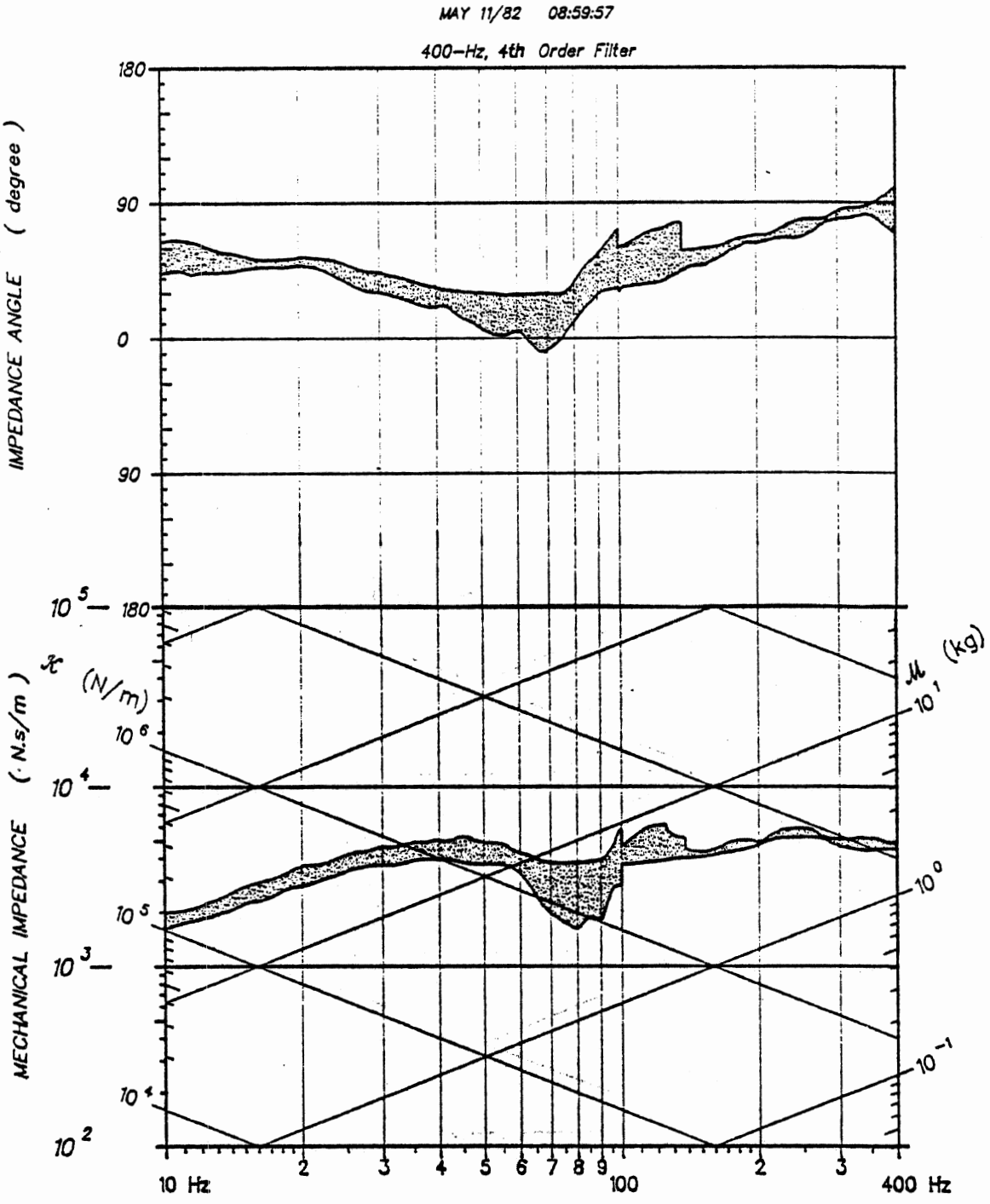

Fig. 10 - Corridor for pelvis impacts, 79A243-79A248

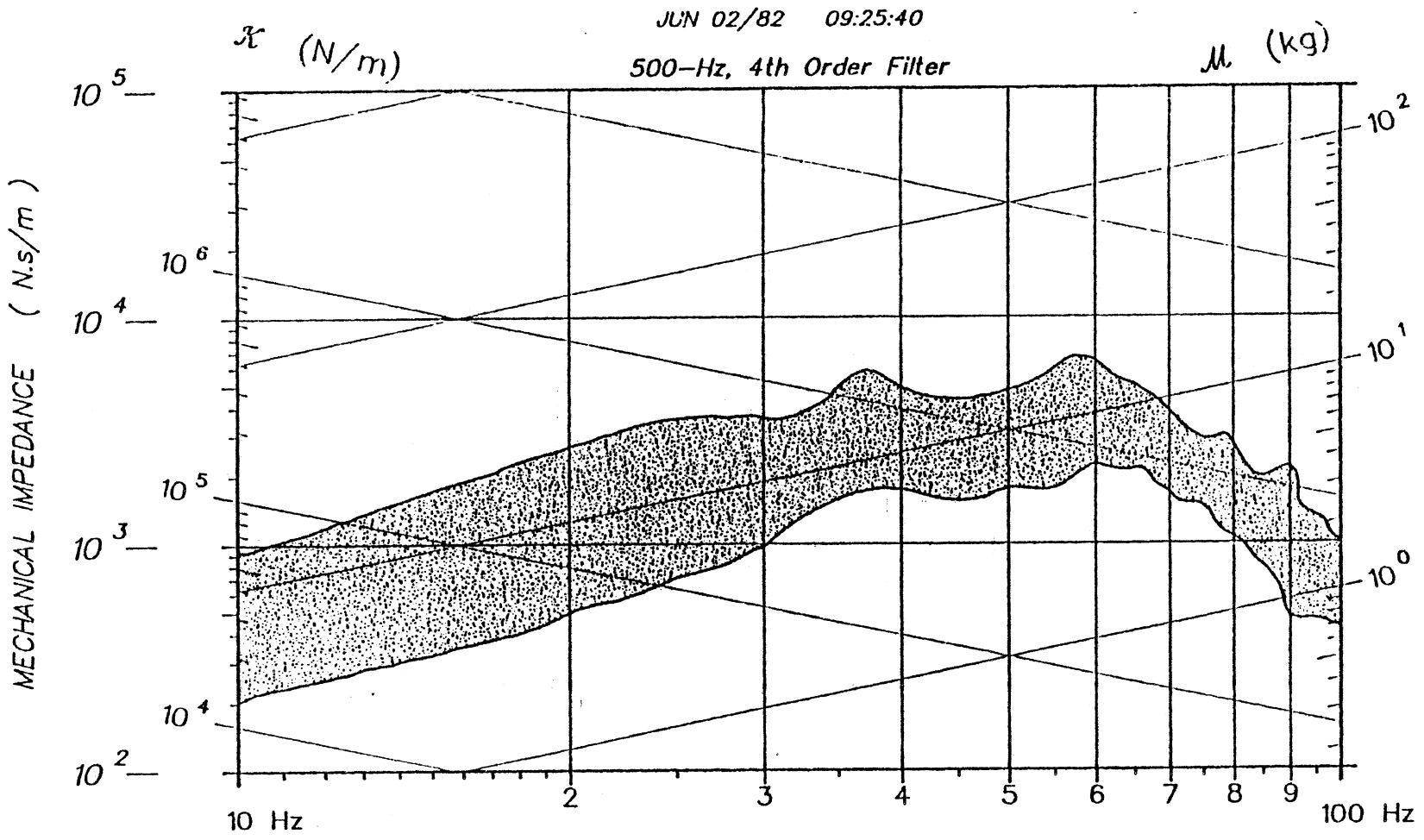

Fig. 11 - Trochanter corridor for axial knee impacts, 79L081-79L092

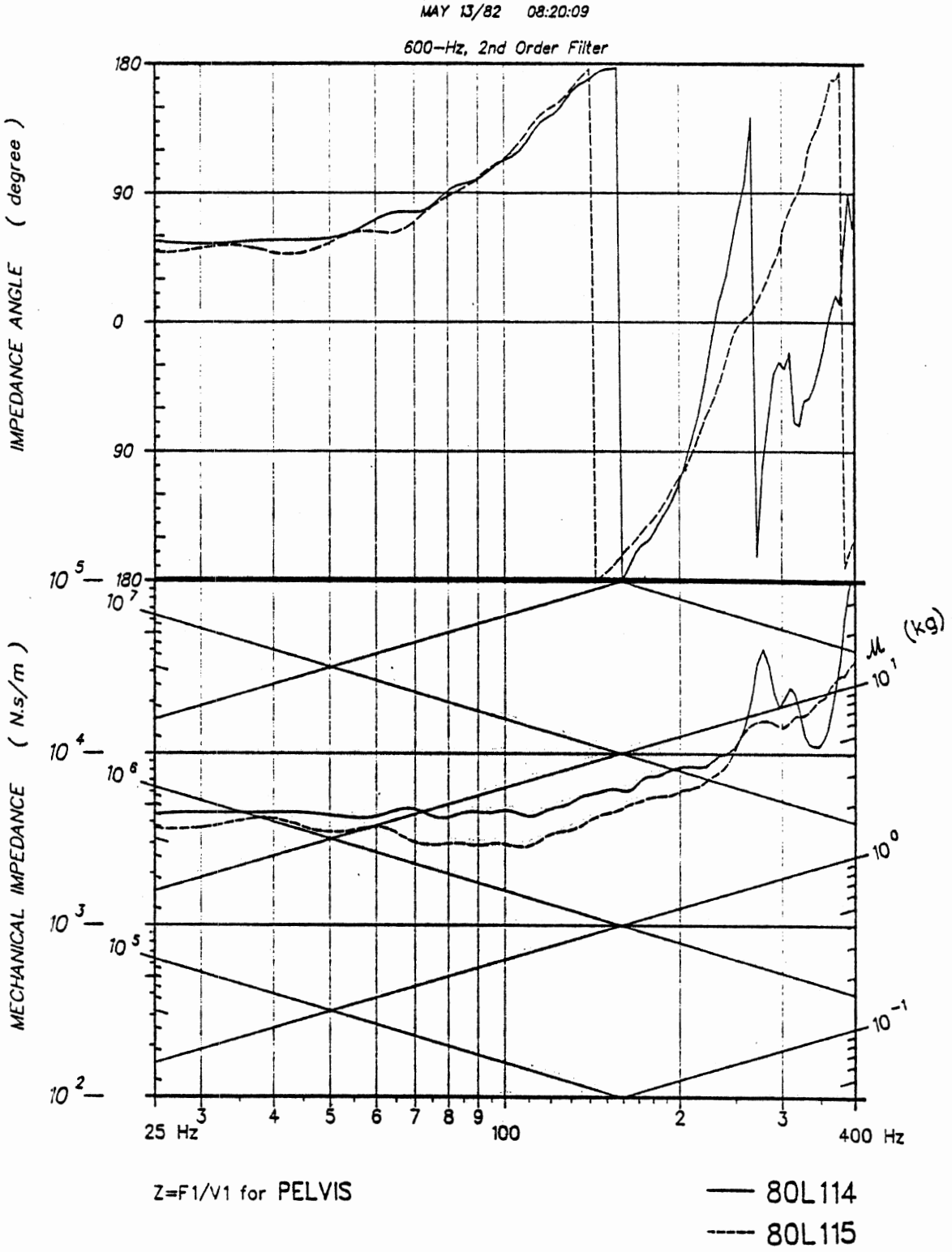
MAY 13/82 08:20:09
600-Hz, 2nd Order Filter
IMPEDANCE ANGLE (degree)
180
90
0
90
180
MECHANICAL IMPEDANCE (N.s/m)
10^5
10^4
10^3
10^2
10^7
10^6
10^5
M (kg)
10^1
10^0
10^-1
25 Hz
3
4
5
6
7
8
9
100
2
3
400 Hz
Z=F1/V1 for PELVIS
80L114
80L115

Fig. 12

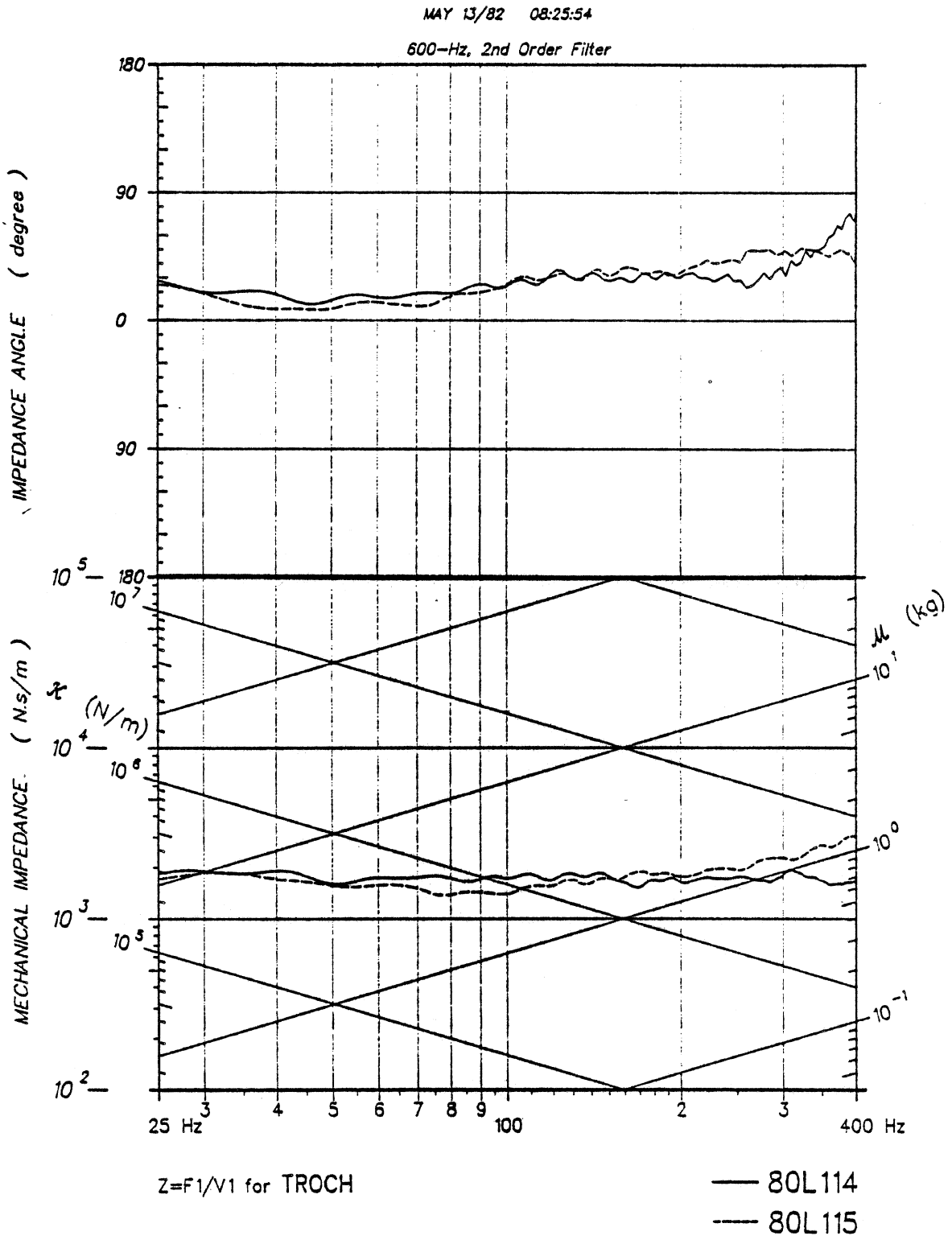
MAY 13/82 08:25:54
600-Hz, 2nd Order Filter
IMPEDANCE ANGLE (degree)
180
90
0
90
180
MECHANICAL IMPEDANCE (N.s/m)
10^5
10^4
10^3
10^2
10^7
10^6
10^5
κ (N/m)
μ (kg)
10^1
10^0
10^-1
25 Hz
3
4
5
6
7
8
9
100
2
3
400 Hz
Z=F1/V1 for TROCH
80L114
80L115

Fig. 13

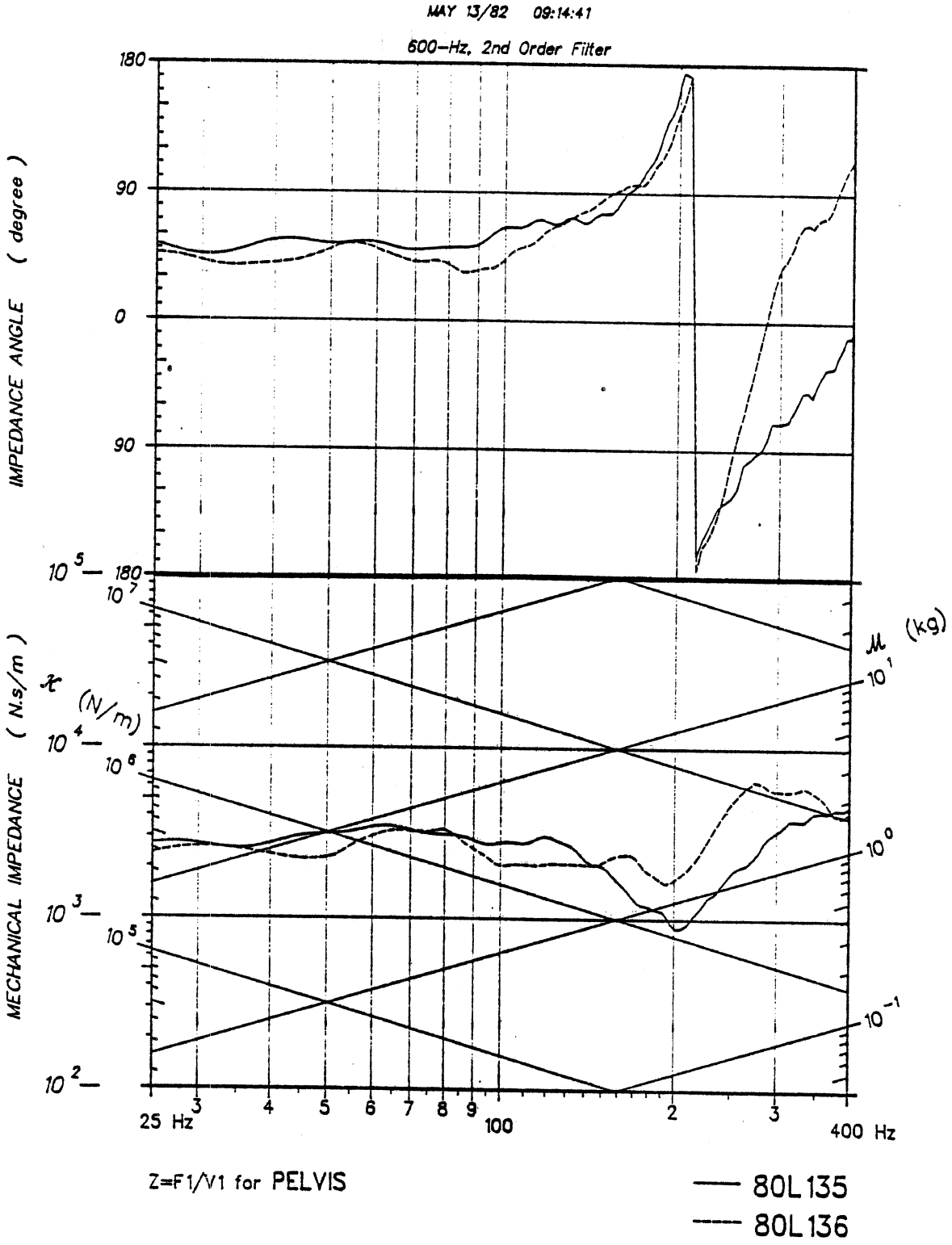
MAY 13/82 09:14:41
600-Hz, 2nd Order Filter
IMPEDANCE ANGLE (degree)
180
90
0
90
180
MECHANICAL IMPEDANCE (N.s/m)
10^5
10^4
10^3
10^2
r (N/m)
10^7
10^6
10^5
M (kg)
10^1
10^0
10^-1
25 Hz
3
4
5
6
7
8
9
100
2
3
400 Hz
Z=F1/V1 for PELVIS
80L135
80L136

Fig. 14

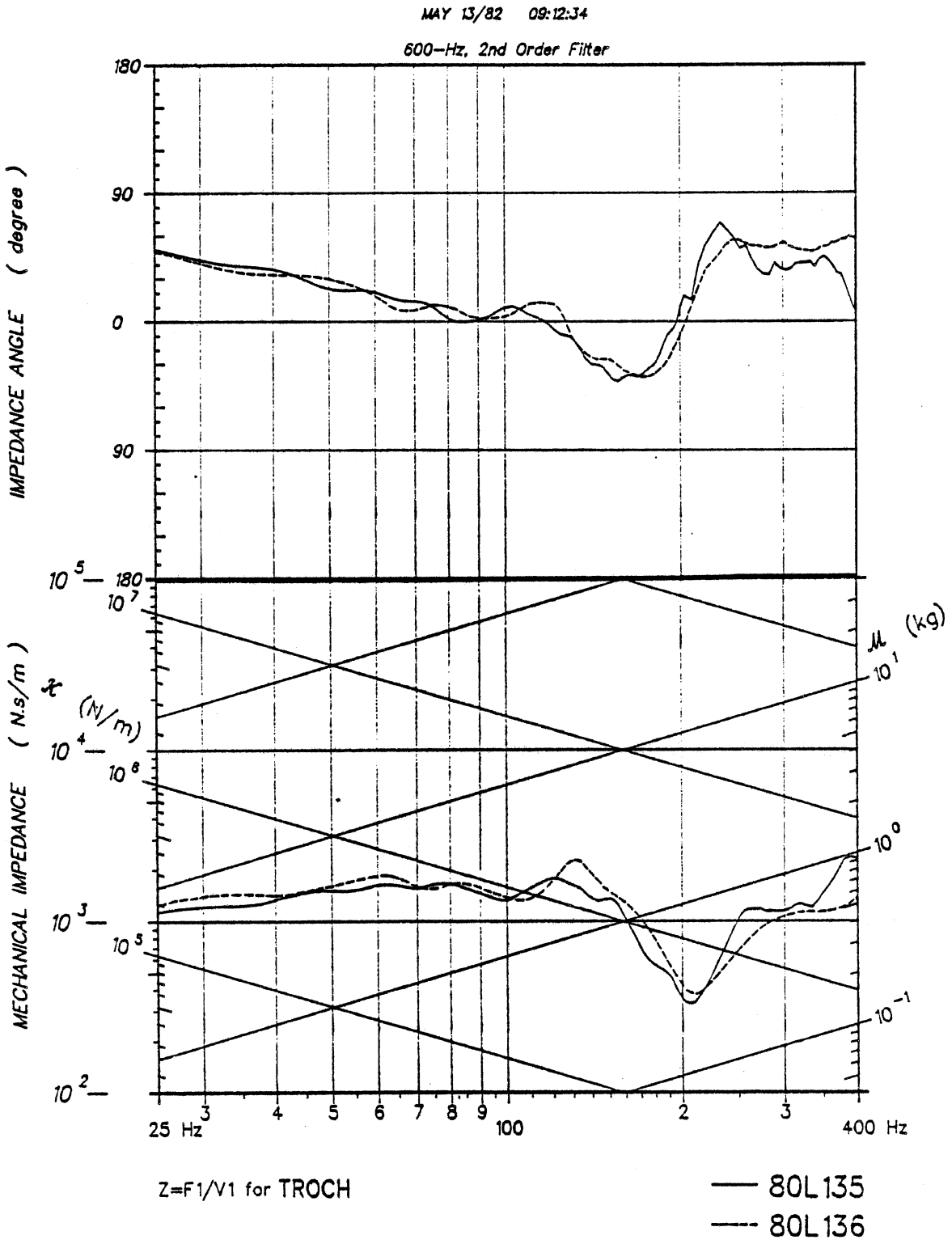
MAY 13/82 09:12:34
600-Hz, 2nd Order Filter
IMPEDANCE ANGLE (degree)
180
90
0
90
180
MECHANICAL IMPEDANCE (N.s/m)
10^5
10^4
10^3
10^2
10^7
10^6
10^5
(N/m)
M (kg)
10^1
10^0
10^-1
25 Hz
3
4
5
6
7
8
9
100
2
3
400 Hz
Z=F1/V1 for TROCH
80L135
80L136

Fig. 15

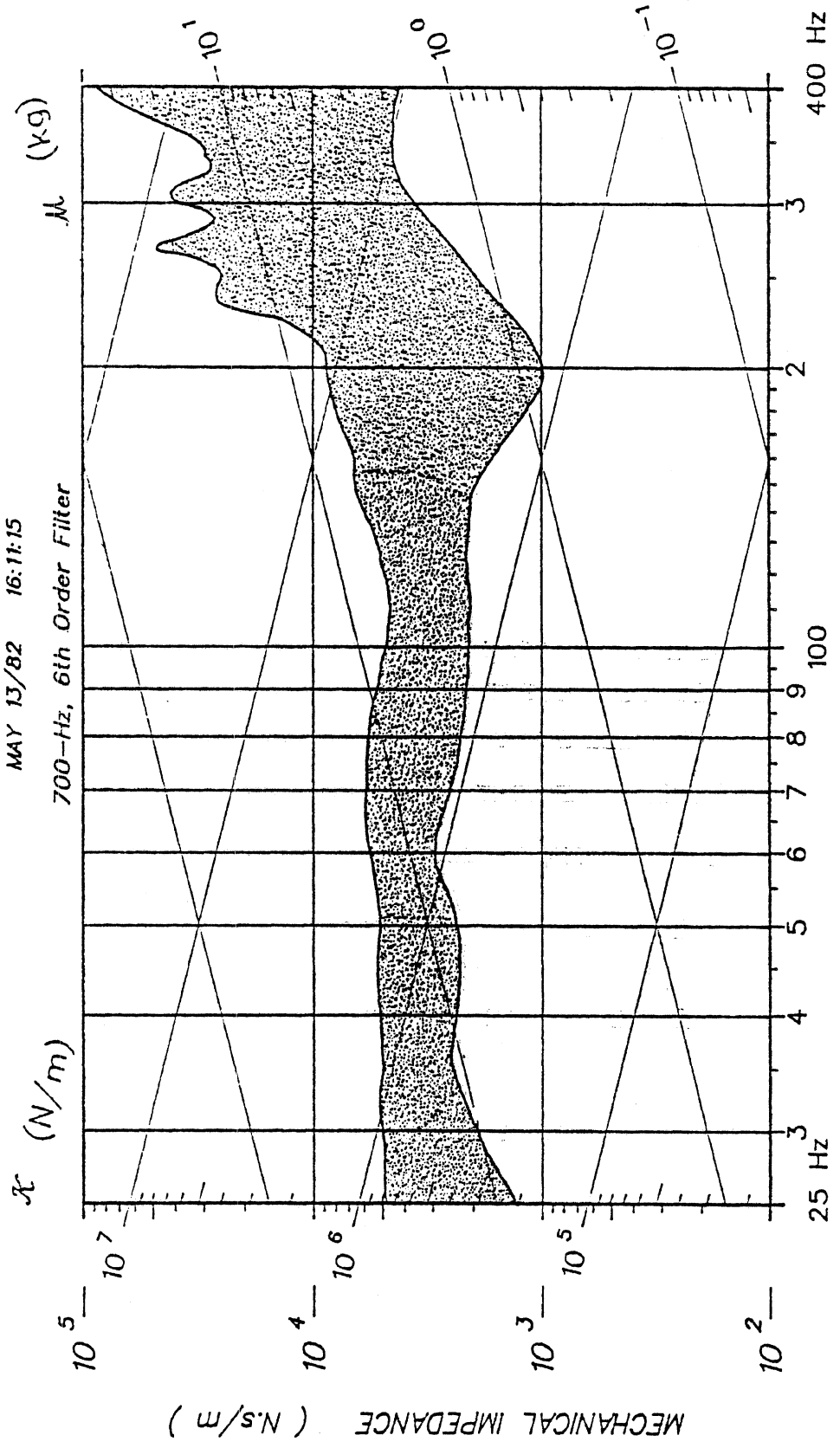

Z=F1/V1 for PELVIS

Fig. 16 - Pelvis corridor

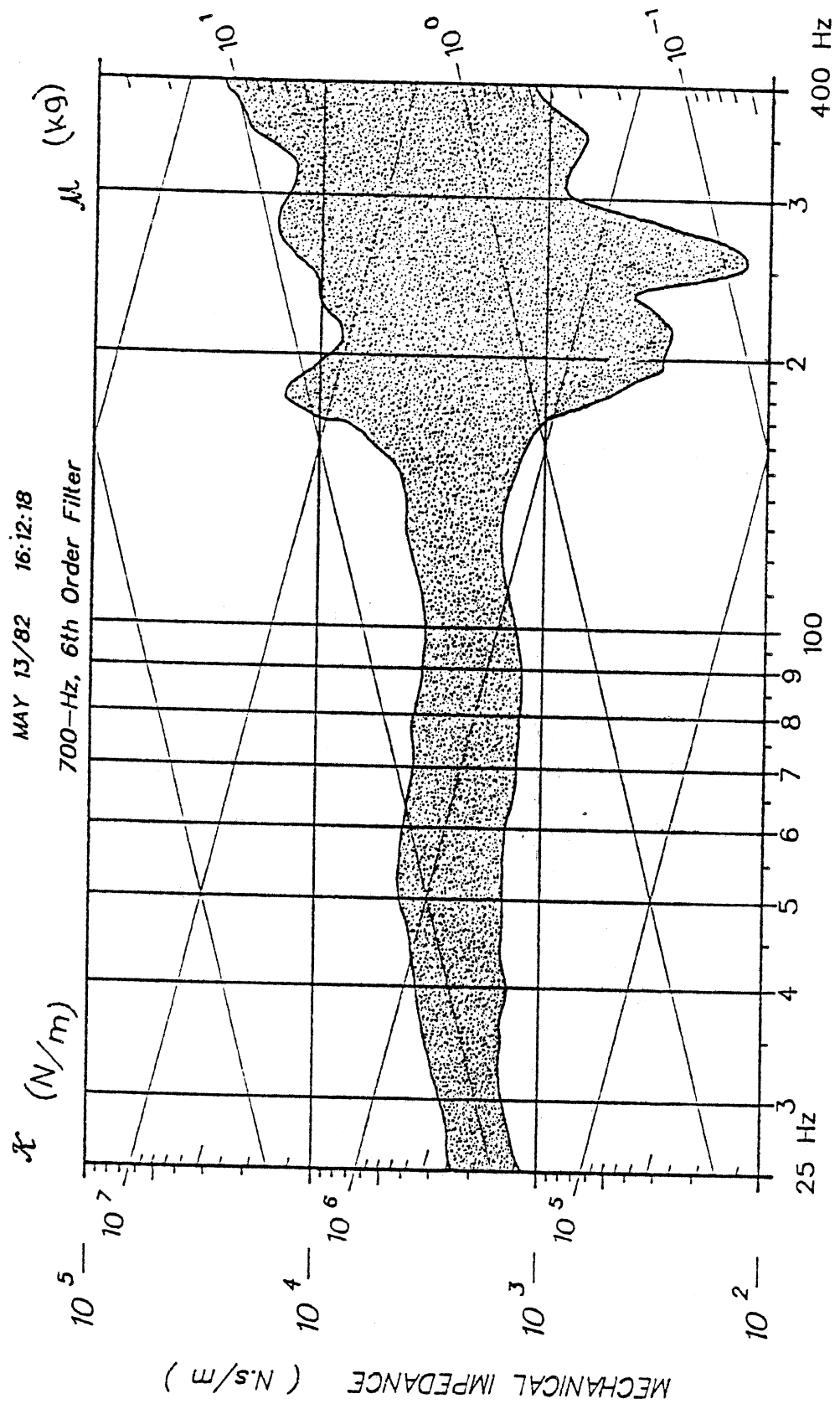

Fig. 17 – Trochanter corridor

commuted fracture of the femoral condyles). In this regard, tests 79A204 to 79A208, with loads from 20 to 37 kN, resulted in no injury to the femur or pelvis. Therefore, with respect to setting tolerance levels, the indication is that either much higher impact velocities (for a given mass) than have been used in these tests must be considered, or else other factors not addressed in this study influence the injury response of the pelvis. In these tests, the subject's initial configuration was held constant and the impactor padding, mass, and initial contact velocity were varied. Possibly, the tolerance level could be influenced by the orientation of the pelvis and/or femur before contact. In addition, no consideration was given to the interaction of the pelvis with a seat, which could be an important factor given the complexity of the pelvis response shown in this study. Therefore, the information generated in these knee impact tests cannot be used to set tolerance levels in and of themselves. The complex nature of the response and the scatter between test subjects emphasize the difficulty of this task.

LATERAL IMPACTS

The response of the pelvis under dynamic lateral loads requires the description of several material bodies: the impactor, the femur, the soft tissue and the pelvis. The ball and socket nature of the interface of the acetabulum and the head of the femur as well as the difficulty of impacting through the effective center of mass of the pelvis-femur complex suggest that in general an instability will result as asymmetric loading of the acetabulum occurs during impact. This type of interaction as well as the effects of damage produced during loading can lead to a wide range of responses. In this regard the accelerometer mounting platform, which is anchored to the pelvis through the use of lag bolts, may add to the lateral stiffness of the pelvis by reducing the differential movement between the two coxal bones during impact, and consequently simplifying the gross whole body motion of the pelvis. However, although the degree to which the accelerometer plate stiffens the pelvis is undetermined. No damage was observed as a result of the lag bolts indicating that the accelerometer platform was not a significant load path. The tests represented in Tables 6 and 9 describe the results of lateral acetabulum loadings through the trochanteric area. Only in test 80L121 was the pelvis loaded directly near the iliac crest. The force time-history from these tests can be described in a manner similar to that of tests 79A243 through 79A248 (Table 5) and 79L081 through 79L090 (Table 7) using the same event markers. The peak forces for the tests ranged from 3 to 19 kN with durations from 30 to 50 ms.

Table 6 summarizes the three-dimensional motion for the pelvis of 82E008, 82E028, and 82E049. In these tests the direction, magnitude, phasing, and waveform of the motion descriptors obtained from the nine accelerometer analysis did not follow a consistent pattern. These differences occur primarily in both angular acceleration and linear accelerations in those directions perpendicular to the impactor motion. Examples are Figures 18 and 19 for 82E049, and Figures 20 and 21 for 82E028. Both the linear and angular variables differ significantly during the E1 to E2 interval even though the gross overall motion as obtained from both the nine accelerometer analysis and the high-speed movies are the same. Variables representing this trend are the relative magnitude and phasing of the resultant and principal direction acceleration for tests 80L095 to 80L137 (depicted in Table 9), with no clear relation between peak force and acceleration as well as when it will occur in the force time history. This is consistent with the results from the acceleration data presented in (10). Figure 22 depicts some of the waveforms observed in these tests.

The response of the pelvis to impact is complicated not only by dynamic instabilities of the femur-pelvis complex, but also by the variability between subjects. Since load is distributed to the pelvis through both soft tissue and the femur, variations in these physical aspects between subjects can lead to varied stress levels on the acetabulum for a given impact force. For those subjects with large amounts of soft tissue, a longer E1 to E2 interval was observed.

Because of the complex nature of the response of the pelvis to lateral impacts, it becomes difficult to generate a transfer function for these experiments. However, for some tests in which a triax was used a transfer function could be obtained that generated mechanical impedance values significantly less than those calculated for the two directions normal to the principal direction above 10 Hz. In addition a transfer function was generated from the tangental acceleration for those tests in which the nine accelerometer plate was used (Figure 23). The transfer function shows that in these tests for low frequencies (from 10 to 40 Hz) the pelvis behaves as a mass of about 25 kg indicating that the gross overall motion of the pelvis may be simply modeled.

Damage -- The pelvic bone damages observed in these tests are similar to those observed in the automotive environment as reported in (1-5);

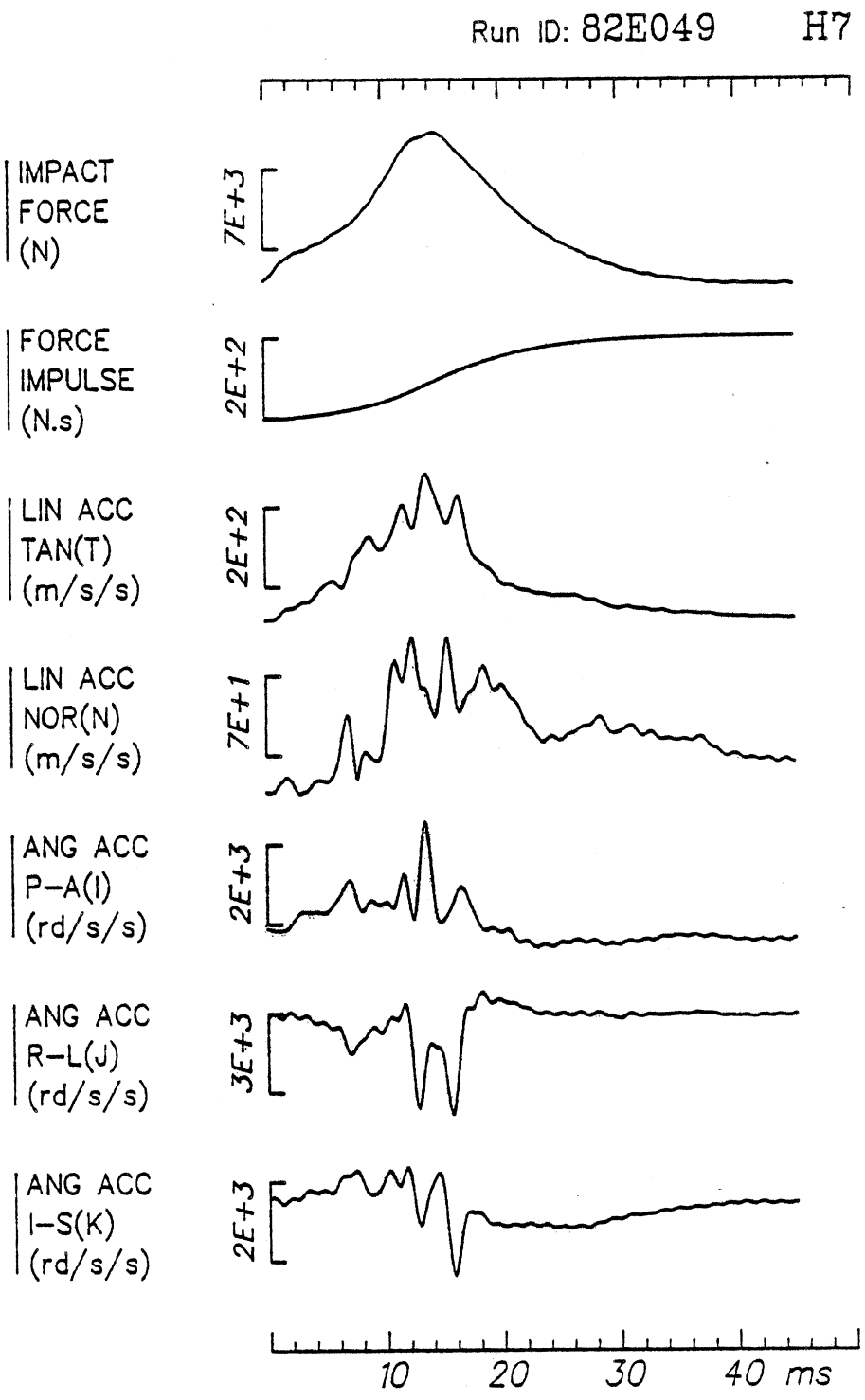

Fig. 18 - Test 82E049

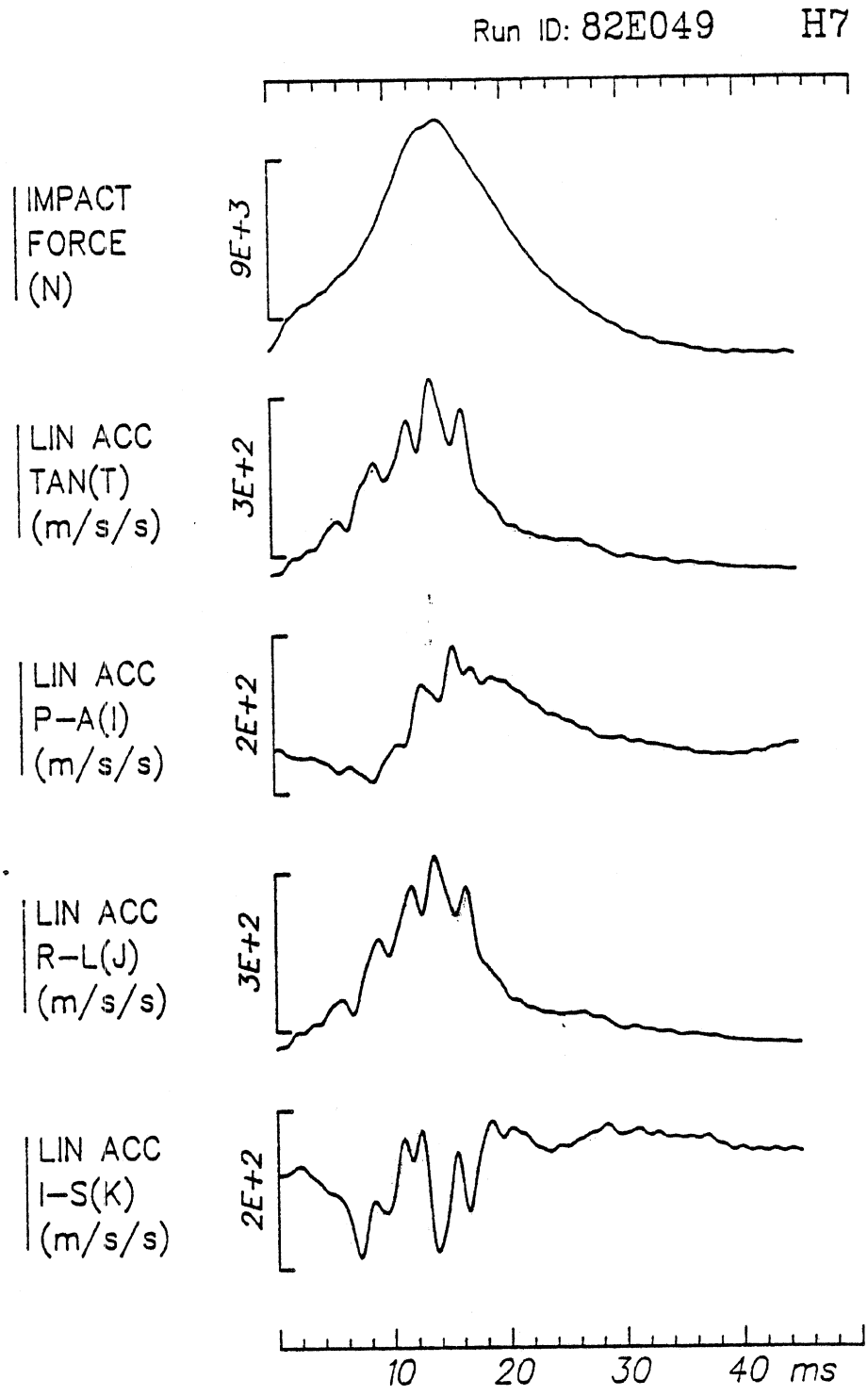

Fig. 19 - Test 82E049

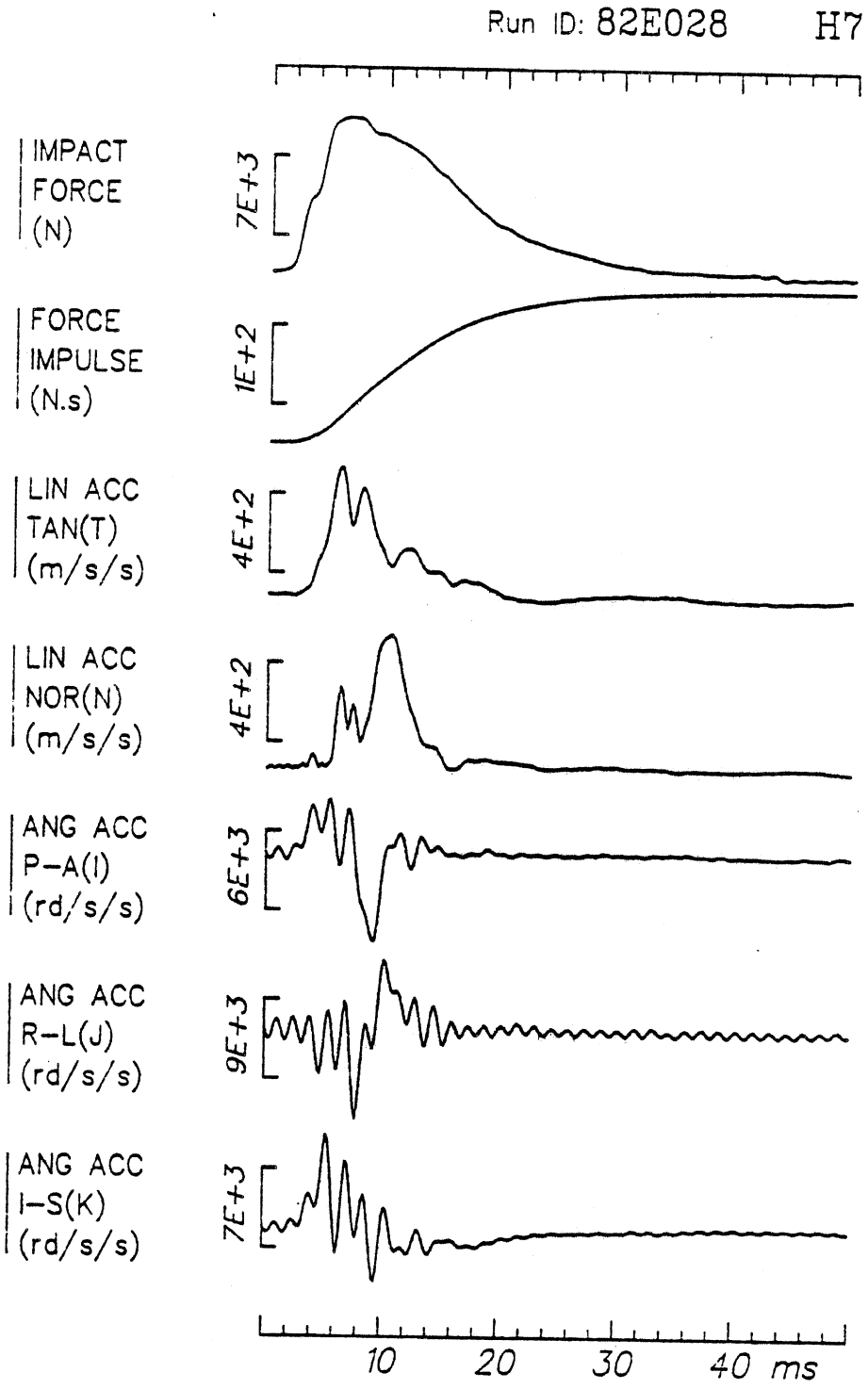

Fig. 20 - Test 82E028

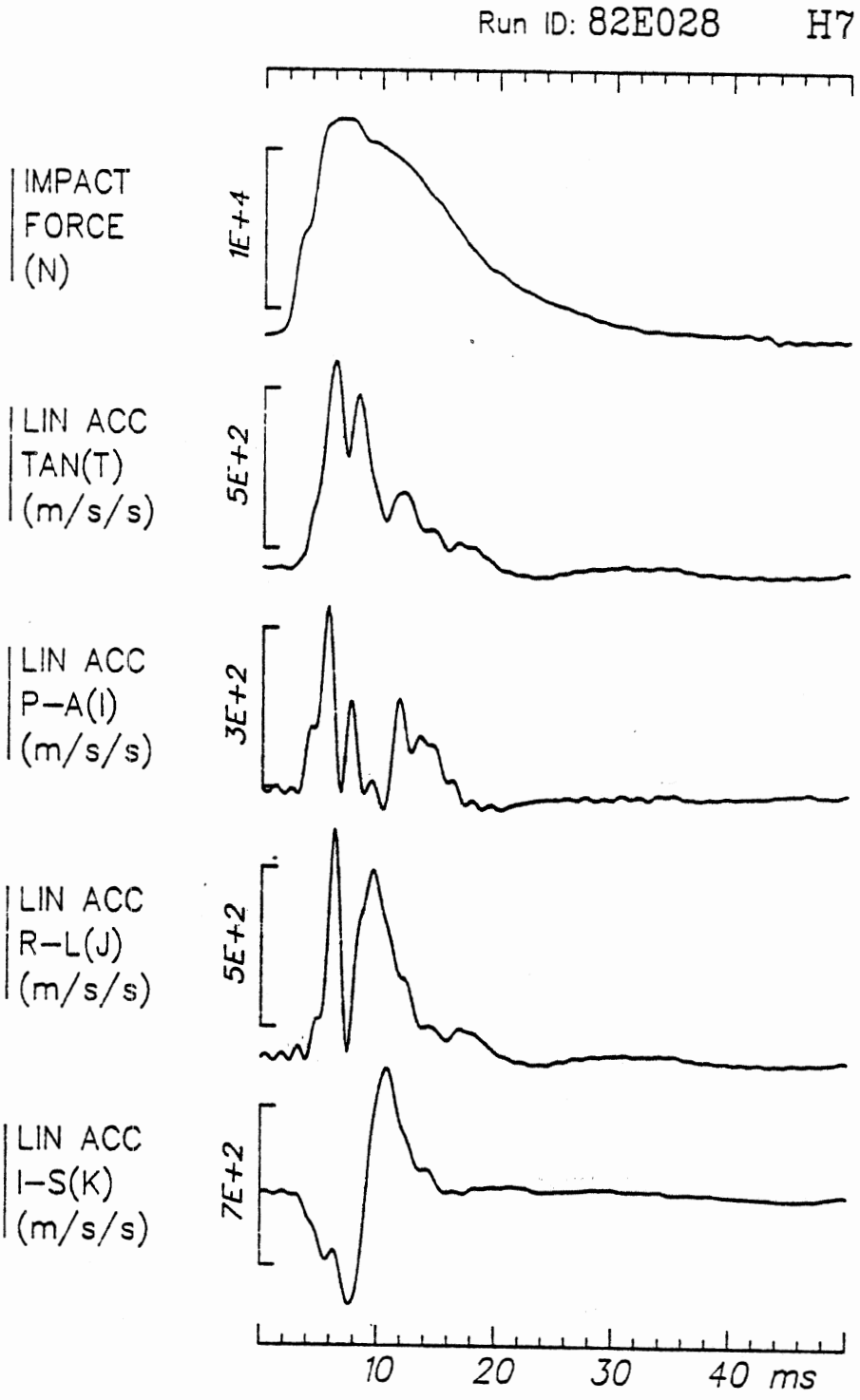

Fig. 21 - Test 82E028

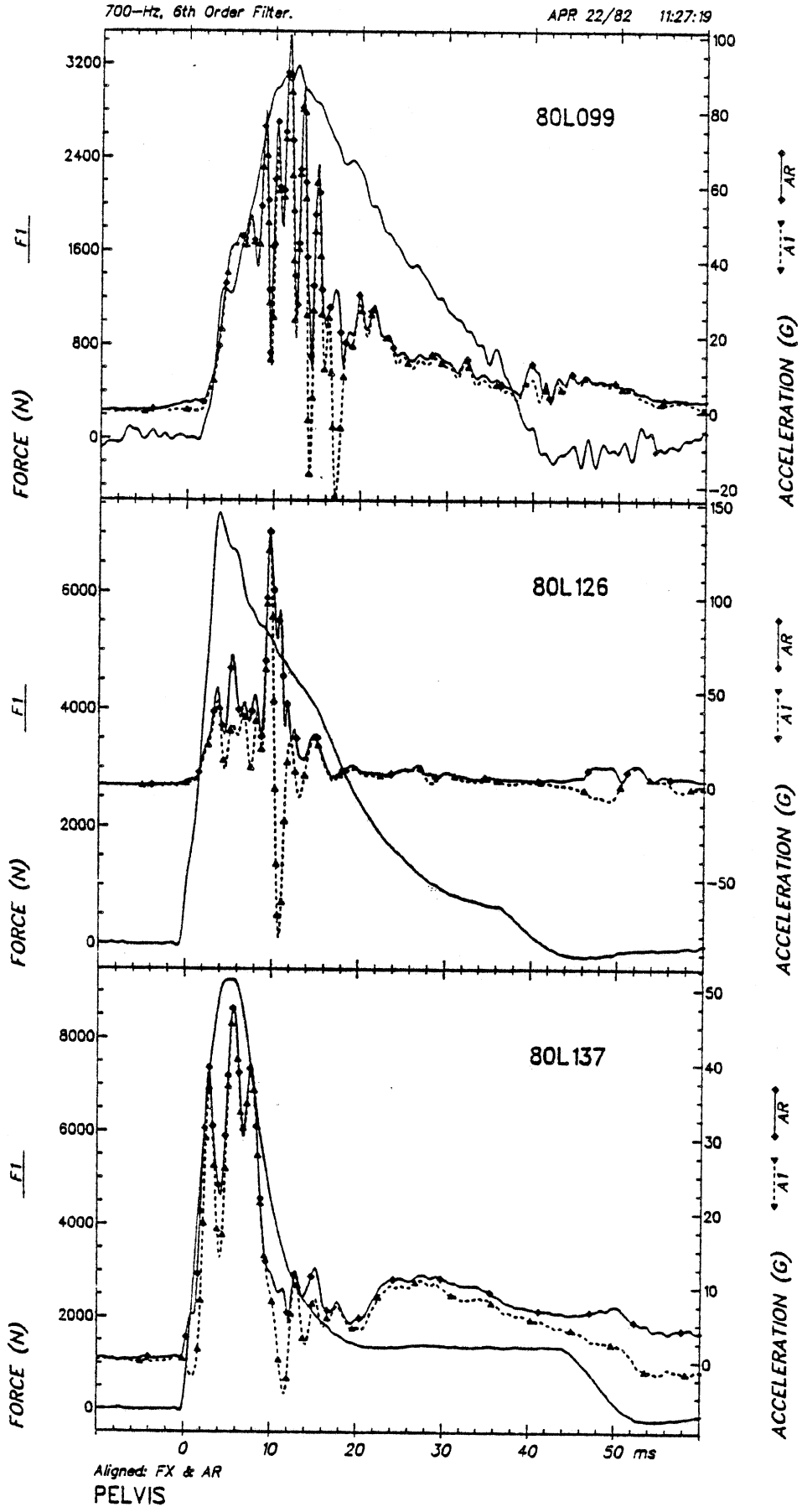

Fig. 22 - Pelvis impact response

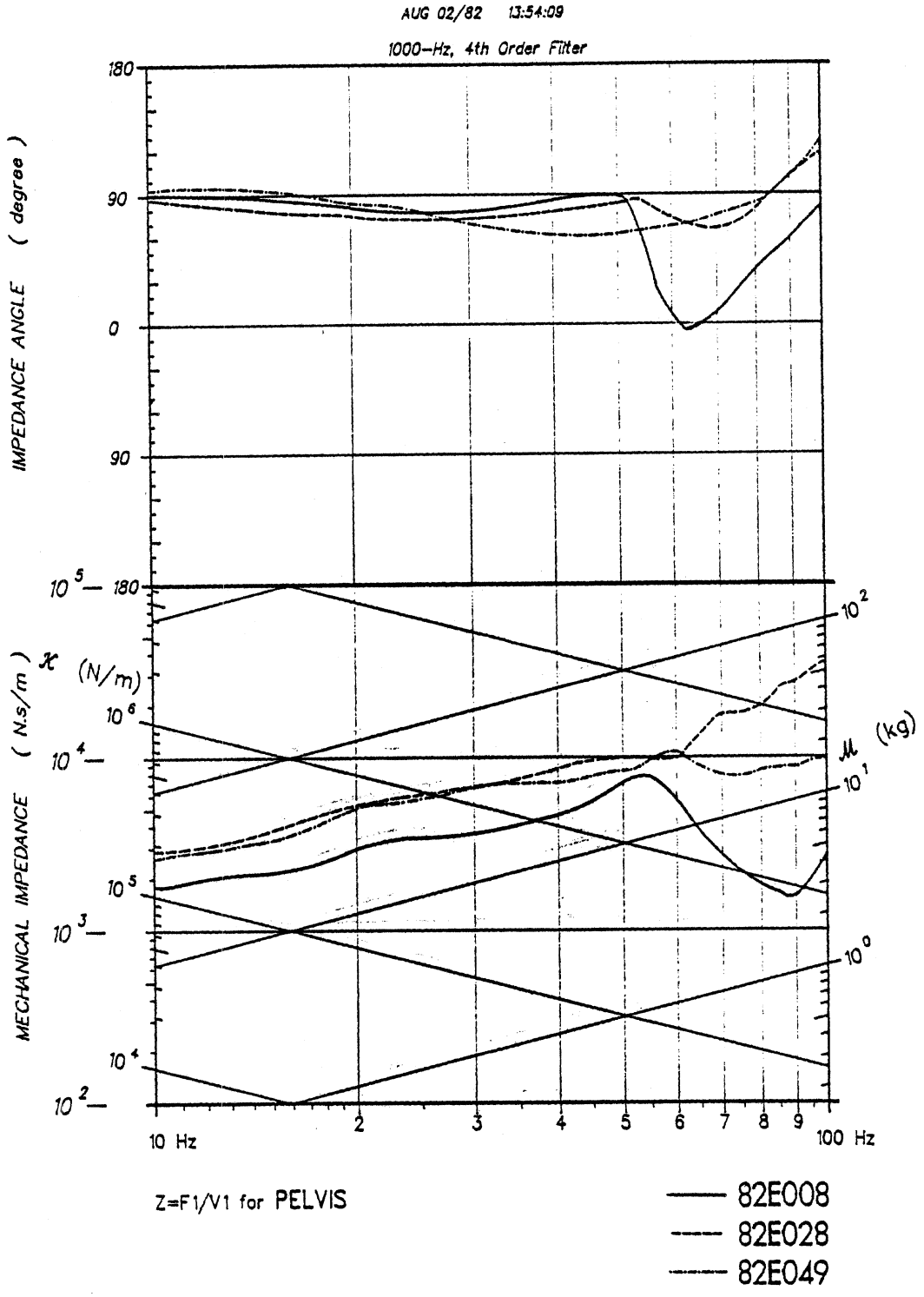
AUG 02/82 13:54:09
1000-Hz, 4th Order Filter
IMPEDANCE ANGLE (degree)
180
90
0
90
180
MECHANICAL IMPEDANCE (N.s/m)
10^5
10^4
10^3
10^2
$\mathcal{K}$ (N/m)
10^6
10^5
10^4
10^2
$\mathcal{M}$ (kg)
10^1
10^0
10 Hz
2
3
4
5
6
7
8
9
100 Hz
Z=F1/V1 for PELVIS
82E008
82E028
82E049

Fig. 23

however, no bilateral fractures occurred. The complex nature of the response of the pelvis to lateral loads may preclude the determination of a single tolerance criterion. This is arrived at by comparing the results in Tables 4 and 9 as well as the above discussion. In this regard, peak force does not relate to the damage produced. This is believed to be a result of the interactions of the padding, impactor surface shape, and/or the soft tissue between the impactor and the pelvis. With additional padding and soft tissue the load can be distributed over a larger area of the pelvis, and therefore less of the available impact energy is concentrated on the acetabulum. The maximum force tolerable seems to increase with an increase in load-distributing padding for similar available impact energy.

Based on differences in the initial conditions of the tests performed at HSRI and those described in (10), it is not readily verifiable that peak force and impulse are accurate pelvis injury criteria. The test methods described in (10) employed a subject seated in an upright position and impacted by an unpadded 17.3 kg impactor with a hemispherical surface. It was found in this series of tests performed at HSRI (which employed an unconstrained subject and flat impactor surface) that variations in impactor padding, mass, and load path may result in large differences in the peak force and impulse of the impact which do not necessarily correspond to the injuries produced. Additional test parameters, such as subject configuration, also affect comparisons between test series results in an unknown manner. For example, the fact that in one research program the subject is seated in a fixed position may result in subject-seat interactions thus producing different injuries for an otherwise similar impact.

CONCLUSIONS

This has been a limited preliminary study of some important kinematic factors and damage modes associated with indirect loading of the pelvis through the femur.

Because of the complex nature of the pelvis-femur interaction during an impact event, more work is necessary before these kinematic factors can be generalized to describe pelvis response. However, the following conclusions can be drawn:

(1) The complete description of three-dimensional motion is invaluable to the understanding of pelvis response.

(2) The response of the pelvis of a single test subject to axial knee impacts as given by mechanical impedance is linear from 10 to 100 Hz, repeatable, and symmetric (the same for each side).

(3) The complex nature of the response of the femur/pelvis/soft tissue system, between-subjects variability, and damage patterns produced may preclude the determination of a single tolerance criterion such as maximum force or peak acceleration response.

(4) Energy-absorbing and load-distributing materials are effective methods of transmitting greater amounts of energy to the pelvis without damage being produced in lateral impacts.

(5) The nature of the impactor/femur/pelvis interaction as well as the biometrics of the population at large are critical factors in understanding the response of the pelvis to impact and subsequent damage patterns.

ACKNOWLEDGEMENTS

The results presented in this paper have been obtained from a series of independently funded research programs conducted during the past five years. The funding agencies were: The Biomedical Science Department of General Motors, the Motor Vehicle Manufacturer's Association, and the United States Department of Transportation, National Highway Traffic Safety Administration.

The authors wish to acknowledge the contributions of Jean Brindamour, Don Huelke, Marv Dunlap, Jodi Blank, Valerie Moses, Paula Lux, Miles Janicki, Jeff Pinsky, and Carol Sobecki in completion of this work.

14.0 APPENDIX G

MANUSCRIPT SUBMITTED TO JOURNAL OF BIOMECHANICS

PELVIC STRESS

G. S. Nusholtz, P. S. Kaiker and B. R. Suggitt
Biomechanics Division, Transportation Research
Institute, University of Michigan, Ann Arbor, MI.

Abstract--A means of channeling energy throughout the pelvic system and dissipating hazardous stress concentrations at the acetabulum is assessed briefly in the context of its relevance and importance in the design of protective devices. Biomechanics testing simulated stress concentrations in the acetabulum resulting from a blow to the right trochanter, as commonly occurs in recreational and passenger contexts. The findings should be pertinent for medical caretakers as well as safety designers.

INTRODUCTION

While walking, climbing, running, jumping or sitting, man is at risk for pelvic fracture. Sports, pedestrian, and passenger victims hazard a mortality rate around 42% (Perry, 1980), ranging between 30% for closed fracture and 60% for open fracture (Niemi and Norton, 1985). Even minor pelvic fracture may have dire consequences: Spencer and Lalanadham reported that minor fractures of the inferior or superior rami frequently were associated with loss of blood and unanticipated death a few days later (Spencer and Lalandham, 1985). Pelvic fractures most commonly occur at the acetabulum, and the pubic rami. The sacro-iliac junction, the wing of the ilium, and the symphysis are also sites of fractures. Lateral impact to the hip can cause injuries to the soft tissues, the hip joint, the pelvis, and the contents of the pelvic cavity--the cecum, sigmoid colon, urinary bladder, uterus or prostate and major blood vessels such as the common, internal or external iliacs.

A limited number of biomechanical studies have attempted to study pelvic impact trauma under laboratory conditions. One of the earliest of these studies (Evans and Lissner, 1955), consisted of impacts to the denuded pelvis in the inferior-superior direction. Although no fracture tolerance data were obtained, it was concluded from this study that the

pelvis exhibited elastic behavior and failed due to tensile stresses in various structural members. Ten years later a study of the behavior of the knee-femur-pelvis complex in an impact environment was reported (Patrick et al., 1965). In this series of tests, an impact sled was used to apply femoral-axis impacts to the knee of embalmed cadavers. The lowest applied load found to cause pelvic injury was 7.1 kN, and loads ranging from 8.5 kN to 17 kN were found to cause multiple fractures of the pelvis. It was suggested that a maximum force criterion (of about 6.2 kN) should be the threshold level for injury of the patella/femur/pelvis complex. A similar study using unembalmed cadavers reported that a single pelvic fracture occurred at an applied load of about 20 kN, however loads up to 26 kN were applied with no resulting pelvis injury (Melvin and Nusholtz, 1980).

The goal of a biomechanical study of pelvic impact in an automotive environment was to supply data for the design of side door padding (Cesari et al., 1978,1980). The pelvis of the cadaver was impacted laterally and the force/injury relationships were observed. It was suggested from this study that pelvic response to impact is characterized by velocity of impact, maximum force, and impulse. Admissible force tolerance for females was documented as 5-7 kN and for males as 10-13 kN. These studies essentially characterized pelvic injury tolerance using maximum force and impulse indicators.

Optimization of a prophylactic for pelvic fracture requires an understanding of the kinematics, stress concentrations and energy paths of the pelvis under blunt impact conditions. Because potential injury types and sites are multiple, it is unlikely that a successful pelvic protection criterion will consist of a single parameter (Haffner, 1985).

It is more likely that multiple parameters can be identified which will be globally predictive of fracture tolerance. Hopefully, such multiple protective parameters would also be protective of the contents of the pelvic cavity (Haffner, 1985). To date, biomechanics research has provided sparse quantification of the stress response of the pelvis to blunt lateral impact (Alem et al. 1978; Ashton, 1981; Brun-Cassan et al., 1982; Calderale et al., 1979; Casari and Ramet, 1982; Casari et al., 1980; Haffner, 1985; Knudsen, 1981; Nusholtz et al., 1982; Ramet and Casari, 1979).

To investigate the kinematic and injury response of the pelvis in impact environments, a series of tests involving indirect impacts to the pelvis have been conducted by the biomechanics unit of the Biosciences Division at the University of Michigan Transportation Research Institute (UMTRI) which are the precursor experiments for the tests being presented in this article, (Nusholtz et al., 1982). The tests were conducted using unembalmed cadavers and two types of impact facilities: a pendulum impactor and a pneumatic impactor. Indirect loads were delivered to the acetabulum of the pelvis by impacting the femur either axially at the knee or laterally above the greater trochanter. This allowed loads to be delivered to the acetabulum in either anterior-to-posterior or right-to-left directions. The cadavers were instrumented to measure pelvic triaxial accelerations in all tests, while in some tests three-dimensional motion of the pelvis was recorded with nine accelerometers. Additionally, triaxial accelerations of the femur and thoracic vertebrae T8 were measured. Photographic targets on the pelvis and femur were used for photokinemetric analysis of motion due to the impact. The conclusions were:

(1) Complete description of three-dimensional motion is invaluable to the understanding of the response of the pelvis.

(2) The nature of the impactor/femur/pelvis interaction, as well as the biometrics of the population at large are critical factors in understanding the response of the pelvis to impact and subsequent damage patterns. A fundamental source of variability in the kinematic response of anatomical structures such as the femur and pelvis during lateral impact appears to originate in the shape of the hip joint, because during impact the rotation of the femoral head in the acetabulum is an unpredictable function of the geometries, the degree of entrapment of the proximal femur by the padded striker, and the population variations in soft tissue thickness and distribution (Haffner, 1985).

(3) The complex nature of the response of the femur/pelvis/soft tissue system, between-subjects variability, and resulting damage patterns may preclude the determination of a single tolerance criterion such as maximum force or peak acceleration response.

(4) In lateral impacts, energy-absorbing and load-distributing materials are effective methods of transmitting greater amounts of energy to the pelvis without damage being produced.

The work being reported in this article continued the UMTRI investigation of the results of indirect impacts to the pelvis by impacting laterally above the trochanter (Nusholtz et al., 1982). The goal of the test series was to investigate the relationship between maximum impact force mediated by padding and resultant skeletal tissue damage caused by lateral blunt impact to the pelvis of the unembalmed

human cadaver*. It was hypothesized that in lateral impacts to the pelvic area, the major loading would be through the femur and careful padding of the impactor surface could profoundly affect the force time-history. The injury response of the pelvis and its relationship to maximum force is presented to indicate the difficulty of determining stress occurring in the pelvis under impact.

ANATOMICAL CONSIDERATIONS

The bony pelvis (Figure 1) consists of two large, flat irregular shaped hip bones that join one another at the pubic symphysis on the anterior midline. Posteriorly, the wedge shaped sacrum completes the pelvic ring forming a relatively rigid structure.

In the adult, each hip bone is formed by the fusion of three separate bones, the ilium, ischium, and pubis, which join at the acetabulum. The ilium forms the broad upper lateral part of the hip bone and the upper portion of the acetabulum. Its upper curved edge is the iliac crest. The ischium forms part of the acetabulum and has a superior ramus that ends below in the ischial tuberosity. From there the inferior ramus ascends to join with the inferior ramus of the pubic bone. Together this bar of bone is frequently referred to as the ischio-pubic ramus or inferior pubic ramus. The pubic bone forms the anterior third of the acetabulum. From here the superior pubic ramus passes to the midline where it joins its fellow of the opposite side through the pubic symphysis. Below, the inferior pubic ramus joins the inferior ischial ramus. The posterior-lateral bony pelvis is covered by

---

* The protocol for the use of cadavers in this study was approved by the University of Michigan Medical Center and followed guidelines established by the U.S. Public Health Service and those recommended by the National Academy of Sciences, National Research Council.

multiple thick muscle layers, buttock fat, and skin. The iliac crest is relatively free of heavy musculature. The rounded head of the femur articulates with the acetabulum and is held within the socket by capsular ligaments. Laterally, on the upper femur, is a large bony prominence, the greater trochanter, for the attachment of muscles.

METHOD

The execution and coordination of the testing sequence was guided by the use of a detailed protocol. The testing sequence is outlined below and additional information about application of specific techniques is available elsewhere (Nusholtz et al., 1982, 1984).

Design - Force was the parameter selected to describe the dynamic kinematics of the impact. The impacting surface was padded with a composite of materials to distribute the load over the impacted side of the pelvis. Pre-test photographs were taken. Injury was assessed by gross autopsy.

Striker padding. The padding for the striker consisted of a composite of materials designed to wrap around the hip and leg during impact. Basically it was a sandwich of 2.5 cm Ensolite, 2.5 cm Styrofoam, and 2.5 Ensolite with wings composed of 2.5 cm Ensolite. See Figure 2 which illustrates the padding in position on the striker and the entrapment of the pelvis-femur during impact.

Subjects - Four unembalmed male cadavers were obtained by UMTRI from the University of Michigan Medical School Department of Anatomy. Following transfer to UMTRI, the cadavers were stored at 4° C until subsequent use. The cadavers were sanitarily prepared and measured (Reynolds et al., 1978, Snow and Reynolds, 1976). The cadaver was also

examined radiologically prior to the installation of accelerometer hardware.

Each subject was suspended by a body harness and an overhead pulley system seated on a block of balsa wood. Lateral pelvic impacts were delivered by a 20 Kg mass ballistic impactor. The target area for the center of the impact for all impacts was 8 cm anterior to trochanterion on the right hip. Three subjects received a single impact while the fourth received triplicate lateral pelvic impacts to the same hip.

Equipment - The basic test equipment includes a timing control device, a signal conditioning unit for the force signal, the cannon, cameras, photographic lights, and a restraint (a hoist system).

Cannon. The pneumatic impact device (Figure 3), consists of an air reservoir which is connected to a honed steel cylinder. A driver piston is propelled down the cylinder by the pressurized air in the reservoir. The driver piston contacts a striker piston which is fitted with a piezoelectric accelerometer and a piezoelectric load washer to allow the determination of acceleration-compensated contact loads applied to the test subject. The mass, velocity, and stroke of the striker piston can be controlled to provide the desired impact conditions for a particular test. For the tests being reported here, a 20 kg mass was selected. The velocity of the impactor is measured by timing the pulses from a magnetic probe which senses the motion of targets on the impactor at 1.3 cm intervals.

Data Handling. All force time-histories were recorded unfiltered on a Honeywell 7600 FM Tape Recorder. The analog data on the FM tapes were played back for digitizing through proper anti-aliasing analog

filters. The analog-to-digital process for all data, results in a digital signal sampled at 6400 Hz equivalent sampling rate.

RESULTS

The table presented below represents the data considered most pertinent in discussing the test results. The issues of lateral pelvic impact tolerance are complex in their technical details, but they nonetheless focus on a reasonably simple central problem: understanding the factors necessary to cause injury to the pelvis and understanding the mechanism of injury. A number of procedures and techniques have been utilized to understand natural phenomena in the scientific arena. Two of the most commonly used are the direct and indirect methods. The direct approach usually starts with first principles and then attempts to derive the basic laws governing the phenomena of interest. One direct approach is to assume that the phenomena under study (in this case, the pelvis) can be characterized by minimizing the Lagrange density L which is a function of the independent variable Ψ (coordinates, velocities, potentials, gradients, field amplitudes, etc.) of the system and the derivatives of these variables with respect to the integration that is to be minimized.

$$\mathcal{L} = \int_{a_1}^{b_1} \cdots \int_{a_m}^{b_m} L\left(\Psi, \frac{\partial \Psi}{\partial x}, x\right) dx_1 \cdots dx_m \qquad (1)$$

One such direct method characterization would be the equation for governing the behavior of an elastic medium under its own restoring force.

TABLE I
PELVIC IMPACT SUMMARY RESPONSE

CADAVER NUMBER	AGE	HEIGHT (cm)	WEIGHT (Kg)	TEST NUMBER	FORCE N	VELOCITY m/s	INJURY
1	60	180.2	67	82E051	2800	20	No injury observed
				82E052	2500	22	No injury observed
				82E053	loss of data	26	No injury observed
2	61	181.0	55	82E071	46000	26	Separational fracture of illo-pubic ramus. Fracture of inferior pubic ramus. Fracture of pubic rami at symphysis pubis.
3	62	175.8	76	83E091	12000	10.2	No injury observed
4	51	180.0	68	83E093	26404	9.2	No injury observed

$$\text{div grad } \Psi = p(x,y,z)\ k(x,y,z)\,dd\ \Psi/dtdt, \qquad (2)$$
$$k(x,y,z) = 1/(y(x,y,z)+2*u(x,y,z))$$

Where u is the shear modulus of the medium and y+2/3u is its compressive modulus. An example of this direct approach would be to compute the velocity and displacement of the medias under impact given the density p(x,y,z) and the elastic modulus k(x,y,z).

In contrast, it may be possible indirectly through the use of strain gauges and accelerometers to measure the velocity, displacement, and acceleration when the elastic modulus is the unknown. Indeed, in the case of the pelvis, which is inhomogeneous, the elastic modulus varies from point to point. A more realistic problem then is determining k(x,y,z) from the displacement field which is is an example of an inverse problem using the indirect method. Utilizing measurable quantities obtained in laboratory experiments employs the indirect method. One parameter in impact biomechanics commonly addressed through the indirect method is the tolerance level or failure criteria. Impact experiments such as the ones presented here, measure the force time-history and then attempt to determine tolerance in terms of this variable. However, the indirect method requires a considerable amount of time and effort in the laboratory. Procedures may vary from laboratory to laboratory and for complex phenomena, such as pelvic impact response, assumptions have to be made to simplify the problem.

To determine the failure criteria of the pelvis for lateral impacts, a considerable number of variables need to be addressed. The anatomical structures are inhomogeneous with complex geometry, and other structures, such as the femur and soft tissues, intervene between the

impactor and the acetabulum. The pelvis is a deformable object that rarely makes direct contact with the impacting surface. In most lateral impact environments there are two basic load paths into the pelvis, one through the iliac wing and another through the acetabulum via the femur.

Although other quantities such as maximum strain, maximum strain energy, and maximum distortion are used to specify the failure criteria of solid materials, a maximum stress value is popularly used. A first approximation to finding maximum stress is to utilize maximum impact force as a failure criterion for a one-dimensional case, assuming that failure occurs near maximum force.

$$\sigma = f/a \tag{3}$$

Where f is the force and a is the effective contact area of the femur with the pelvis. Then, for a given impact, the failure criteria can be defined in terms of maximum force. If the contact surface is such that it is a weak function of initial condition and force time-history, e.g., the effective contact area has reached a maximum, the soft tissue is not an effective energy absorber, and the force is transmitted directly to the pelvis, then maximum force is directly related to maximum stress and might be used as a failure criterion. Cesari and Ramet (1982) have proposed that a 10 kN (3 ms clip) peak force for males and a 4 kN (3 ms clip) peak force for females would be a reasonable fracture tolerance level for lateral impacts in the pelvis without loading the wing of the illium. However, they have pointed out

the efficacy of using a different stress-related variable instead of raw force for a specific type of fracture. They hypothesized that many lateral pelvic fractures were the result of excess bending stress in the pubic rami. They computed moments of inertia and used the formula:

$$\sigma = f * d / (I/y) \qquad (4)$$

Where d is the characteristic moment and I/y is the area moment of inertia divided by the offset from the neutral axis. They were able to correlate fracture force and moments of inertia. This then improved their correlation coefficient between calculated stress and fracture. Additional efforts have been made to base a fracture criterion on an acceleration. Toward this end Haffner (1985) based on the work of Nusholtz et al. (1982) constructed a one-dimensional linear lumped-parameter model as shown in Figure 4. Mass 1 is associated with the structure side upper mass, and Mass 2 is associated with the pelvic mass upon which the pelvic accelerometer is attached. They cautioned that the model is not to be taken as a literal model but as a useful device for prediction of pelvic stress along the lines of others (Haffner, 1985 and Nusholtz et al., 1982). Although, this seems to be a useful method of producing a fracture tolerance criterion, the limited data preclude determining the method's predictive value over peak force.

The relationship between acceleration and force and, therefore, potentially between stress and acceleration can be envisioned by the assumption that the motion during impact to the pelvic area (to which

the accelerometers are attached) is that of a rigid body undergoing one-dimensional motion. It has been pointed out (Nusholtz et al., 1982) that a complete three-dimensional description, consisting of three linear translations and three angular rotations, is invaluable in determining the response of the pelvis to blunt lateral impact. This is a result of the ball and socket nature of the interface of the acetabulum and the head of the femur, as well as of the difficulty of impacting through the center of the mass of the pelvis-femur complex. This type of geometry will result in asymmetric loading of the pelvis and will produce a wide range of responses for a given impact. Therefore, for small deformations of the pelvis, it is more reasonable to assume that the acceleration motion of any given point on the pelvis sufficiently far from the impact point can be described using the following equation.

$$\vec{X}=\vec{A}+w\hat{}w\hat{}r+(dw/dt)\hat{}\vec{r} \qquad (5)$$

Where X is the acceleration of a given point on the pelvis, A is the acceleration of the canter of mass, w is the angular velocity of the pelvis, dw/dt is the angular acceleration of the pelvis, and r is the radius vector of the center of mass to the point of interest. A one-dimensional model would give only a rough approximation of the stress produced during impact. A better approximation would have the stress in the pelvis as a function of the forces F(x,y,z) and torques $N(\beta, \theta, \lambda)$ as well as the point of interest X on the pelvis.

$$\sigma = F(F[x,y,z], N[\beta, \theta, \lambda], \vec{X}) \tag{6}$$

In addition to the three-dimensional motion, the pelvis is composed of inhomogeneous materials and is strain rate sensitive as well as non-linear in response. Therefore:

$$E = F(\sigma, \vec{X}, t) \tag{7}$$

Where E is the strain of any given point on the pelvis. The motion of any point on the pelvis would then be:

$$Xi + Ai = w \hat{} w \hat{} r + (dw/dt) \hat{} r + dd\vec{R}(E)/dt^2 \tag{8}$$

Where R(E) is the displacement vector of the point of interest from its equilibrium position. From the above discussion, it would seem that the application of the indirect method to determining fracture tolerances or maximum stress needs to address to some degree: the number of initial positions that can occur between the pelvis and the femur, the three-dimensional motion of the pelvis and the femur, and the response rate-sensitivity of the pelvic structures.

This would, in part, then explain the differences seen in the results of Nusholtz et al., 1982; Cesari and Ramet, 1982; Cesari et al., 1978 and 1980. Nusholtz et al., (1982) observed for an impact experiment using a flat rigid striking surface which loaded the acetabulum through the femur that the fracture level was approximately 7 kN. Since the number of parameters that need to be controlled in lateral impact are numerous, small differences in experimental technique can lead to significant differences in results. The possible reasons for the differences between these two laboratories are:

1. The impactor used by Nusholtz et al., (1982) was 56 kg instead of the 17 kg used by Cesari and Ramet (1982), and Cesari et al. (1978 and 1980). If strain-rate is a factor in impact response, then the experiments performed by Nusholtz et al., (1982) would have had a higher frequency contact, and, therefore, a higher strain-rate effect. This may, in part, explain why Nusholtz et al., (1982) obtained a greater number of acetabular fractures.
2. Striking the femur with a hemispherical impactor permitted it to slide under the impactor, allowing greater loads to be transmitted directly to the pelvis.
3. Nusholtz' (1982) test subjects were suspended in the air and struck during free fall. Cesari's were seated. The per se effect of seating on the response is undetermined. However, it seems reasonable to assume that for a short-duration (high frequency) force time-history, this would not have an effect.

If the above discussion is accurate in its characterization of the pelvis, then it would seem desirable to design an experiment that would increase the necessary load to fracture by:

1) Increasing the loading area.
2) Decreasing the strain-rate by decreasing the high-frequency components of the force time-history.
3) Reducing the angular acceleration.

The special padding used in these experiments enabled the femur to be trapped and reduced the angular motion associated with the femur-pelvic instability of the femur-pelvis, eliminated any concentrated loading by utilizing the entire surface of the impactor as a load path, reduced the rate of onset of the force time-history, and, thus, reduced the high frequency components of the force time-history. Because of the effects of the padding, large forces were generated without fracture. This supports the results of others (Melvin and Nusholtz, 1980 and Nusholtz et al., 1982) in which the importance of protective padding was emphasized.

CONCLUSIONS

In comparison to the results of others (Nusholtz et al., 1982 and Casari and Ramet, 1982, and Casari et al., 1980, 1978), the pertinent observations of the experiments being reported in this article are that relatively large forces can be generated without fracture (26 kN) and that when the fractures do occur, they are associated with a force of 45 kN. In addition, the damage pattern changed from near (and including) the acetabulum to near (and including) the pubic area.

As is usual in this type of experiment, more questions were generated than answered. Some of these are:

1. What parameter or set of parameters, that can be measured in the laboratory, can be used as a predictive measure of or of pelvic tolerance for a given area of the pelvis?
2. Since large forces can be created without inducing pelvic trauma, what advantage is this for the individual (such as an automobile occupant or sports player) who may be subject to blunt impact?
3. How important is strain-rate to pelvic tolerance, and is this the factor that controls the fracture site on the pelvis when the pelvis is loaded laterally?

Acknowledgement--The results presented in this paper were partially funded by the Department of Transportation, Contract No. DOT-HS-7-01636. The authors also wish to acknowledge the technical assistance of Bryan R. Suggitt, Gail J. Muscott, Valerie A. Moses, Wendy Gould, Shaun Cowper, Steven Richter, Peter Schuetz, Tim Jordan, Patty Muscott, Jean Brindamour, Marvin Dunlap, Don Erb, and Carol Sobecki.

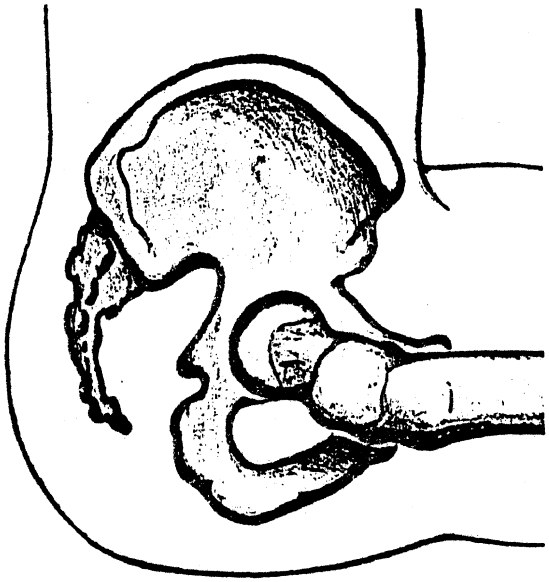

Figure 1

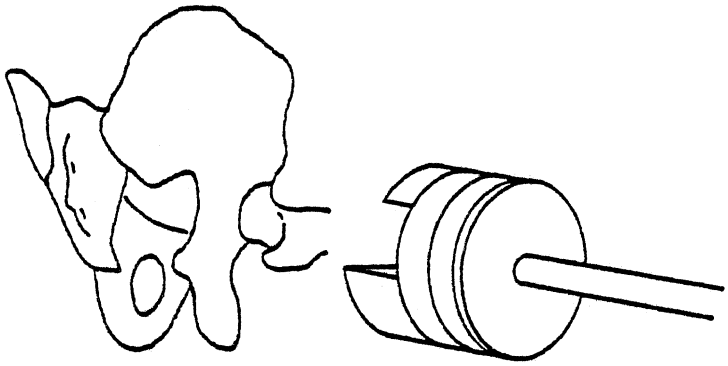

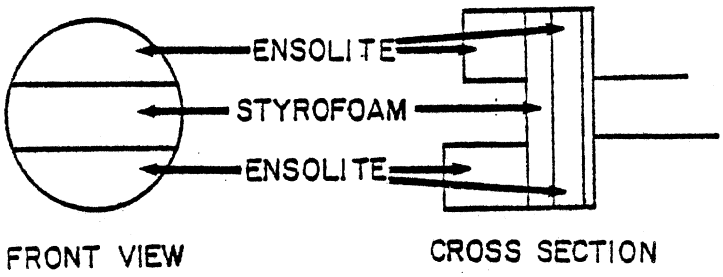

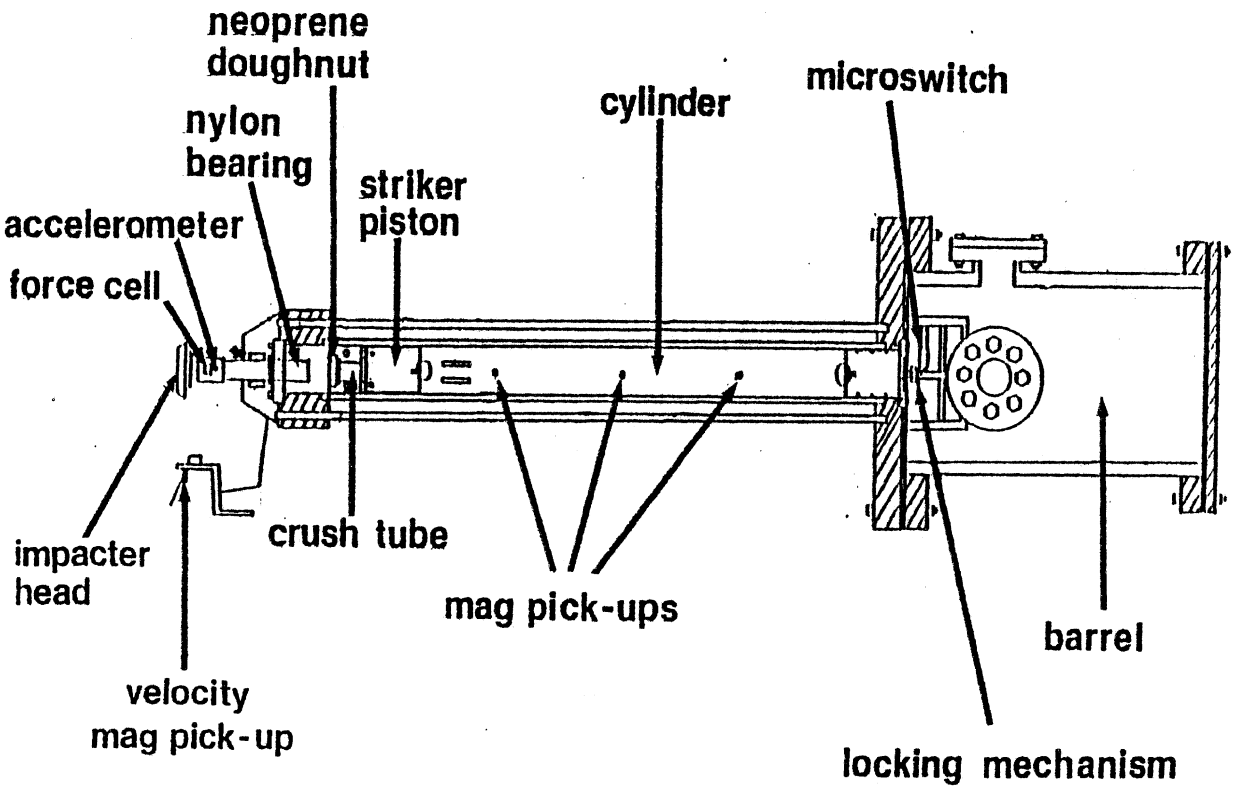

Figures 2 and 3

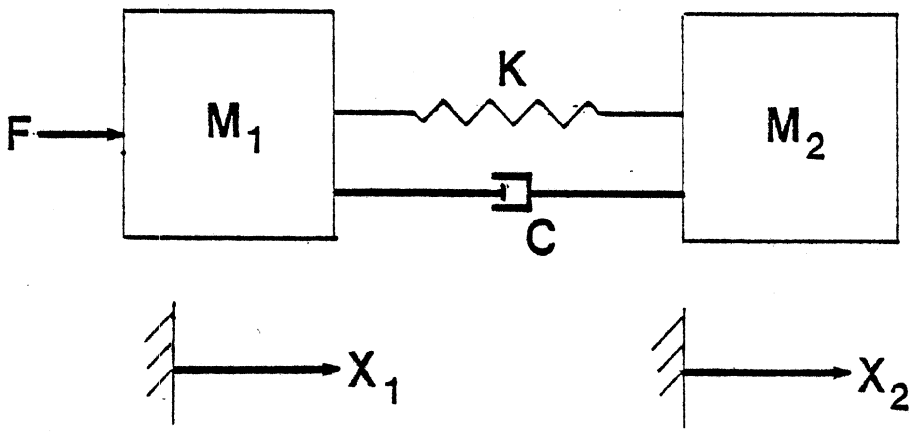

Figure 4

REFERENCES

Alem, N. et al. (1978) Whole-body human surrogate response to three-point harness restraint. Proc. 22nd Stapp Conf.

Ashton, S.J. (1981) Factors associated with pelvic and knee injuries in pedestrians struck by the fronts of cars. Proc. 25th Stapp Conf. 863-900.

Bartz, J. and Butler, F. (1972) Passenger compartment with six degrees of freedom. In: Auxiliary Programs to Three Dimensional Computer Simulation of a Motor Vehicle Crash Victim, DOT Contract No. FH-11-7592.

Brun-Cassan, f., et al. (1982) Determination of knee-femur-pelvis tolerance from the simulation of car frontal impacts. Proceedings 7th International IRCOBI Conference on the Biomechanics of Impacts, 101-115.

Calderale, P.M., Garro, A. and Lorenzi, G.L. (1979) Car accident mathematical model: femur and pelvis stress analysis. Proc 4th Int IRCOBI Conf on the Biomech of Trauma, 302-315.

Cesari, D. and Ramet, M. (1982) Pelvic tolerance and protection criteria in side impact. Proc. 26th Stapp Conf., 145-154.

Cesari, D., Ramet, M. and Clair, P. (1980) Evaluation of pelvic fracture tolerance in side impact. Proc. 24th Stapp Conf. 145-154.;

Cesari, D., Ramet, M. and Henry-Martin, D. (1978) Injury mechanisms in side impact. 22nd Stapp Car Crash Conference Proceedings 429-447.

Donati, P.M. and Bonthoux, C. (1983) Biodynamic response of the human body in the sitting position when subjected to vertical vibration. Journal of Sound and Vibration 90(3) 423-442.

Donishi, H., et al. (1983) Mechanical analysis of the human pelvis and its application to the artificial hip joint - by means of the three-dimensional finite element method. J Biomech 16(6) 427-444.

Evans, F. and Lissner, H. (1955) Studies on pelvic deformations and fractures. Anat Rec 121(2).

Evans, F.G. (1970) Impact tolerance of human pelvic and long bones. In: Gurdjian, E.S., et al., eds., Impact Injury and Crash Protection, Charles C. Thomas Publisher, 402-420.

Fanyon, A., et al. (1977) Contribution to defining the human tolerance to perpendicular side impact. Proc 3rd Int Conf on Impact Trauma 297-309.

Haffner, M. (1985) Synthesis of pelvic fracture criteria for lateral impact loading. 10th Int Conf on Exp Safety Vehicles, Oxford, England, July 1-4.

Hixson, E. (1976) Mechanical Impedance. In: Harris, C.M. and Crede, C.E., eds., Shock and Vibration Handbook, NY: McGraw-Hill Book Co.

Huelke, D. and Lawson, T. (1976) Lower torso injuries and automobile seat belts. SAE Paper No. 760370.

Huelke, D., et al. (1980) Lower extremity injuries in automobile crashes. UM-HSRI-80-10. National Highway Traffic Safety Administration. Highway Safety Research Institute, Ann Arbor, MI.

King, A.I. (1973) Biomechanics of the spine and pelvis. In: Biomechanics and Its Application to Automotive Design, NY: Society of Automotive Engineers.

Knudsen, P.J.T. (1981) Fracture of the pelvis in side impact accidents - fractures of the pelvis in four out of six persons in one car. [in Danish] Ugeskrift for Laeger 143(13) 1014-1017.

London, P.S. (1985) Unsuspected injury of the caecum accompanying fracture of the pelvis. Injury 16, 324-326.

Melvin, J., et al. (1975) Impact response and tolerance of the lower extremities. Proc. 19th Stapp Conf.

Melvin, J.W. and Nusholtz, G.S. (1980) Tolerance and response of the knee-femur-pelvis complex to axial impacts - impact sled tests. UM-HSRI-80-27. Highway Safety Research Institute, Ann Arbor, MI.

Nusholtz, G.S., Alem, N.M. and Melvin, J.W. (1982) Impact response and injury of the pelvis. Proc. 26th Stapp Conf., 103-144.

Nusholtz, G.S., et al. (1984) Head impact response--skull deformation and angular accelerations. Proc. 28th Stapp Conf., 41-74.

Niemi, T.A. and Norton, L.W. (1985) Vaginal injuries in patients with pelvic fractures. J Trauma 25(6) 547-551.

Nyquist, G.W. and Murton, C.J. (1975) Static bending response of the human lower torso. Proc. 19th Stapp Conf., 513-541.

Patrick, L., Kroell, C. and Mertz, H. (1965) Forces on the human body in simulated crashes. Proc. 9th Stapp Conf.

Perry, J.F. (1980) Pelvic open fractures. Clin. Orthop. 151, 41.

Pope, M.H., et al. (1977) Radiographic and biomechanical studies of the human spine. AFOSR-TR-78-0063. Vermont University, Burlington.

Ramet, M. and Cesari, D. (1979) Experimental study of pelvis tolerance in lateral impact. Proc 4th Int IRCOBI Conf on the Biomech of Trauma 243-249.

Reynolds, H.M., Freeman, J.R. and Bender, M. (1978) A foundation for systems anthropometry. UM-HSRI-78-11. Highway Safety Research Institute, Ann Arbor, MI.

Ryan, F. (1971) Traffic injuries of the pelvis at St. Vincent's Hospital, Melbourne. Med J Aust 1(27).

Snow, C.C. and Reynolds, H.M. (1976) Anthropometric data for pelvic geometry definition. 4th Annual Committee Reports and Technical Discussions International Workshop on Human Subjects for Biomechanical Research 13-25.

Spencer, J.D. and Lalanadham, T. (1985). The mortality of patients with minor fractures of the pelvis. Injury (5) 321-323.

States, J. and States, D. (1968) The pathology and pathogenesis of injuries caused by lateral impact accidents. Proc. 12th Stapp Conf.

Tarriere, C. et al. (1979) Synthesis of human tolerances obtained from lateral impact simulations. 7th Report Int Technical Conf on Exp Safety Vehicles, 359-373.

Figure Captions

1. Skeletal Structure of Pelvis and Femur in Initial Test Position
2. Initial Conditioning and Padding
3. Pneumatic Impact Device
4. Acceleration Fracture Criterion Model

15.0 APPENDIX H

DATA

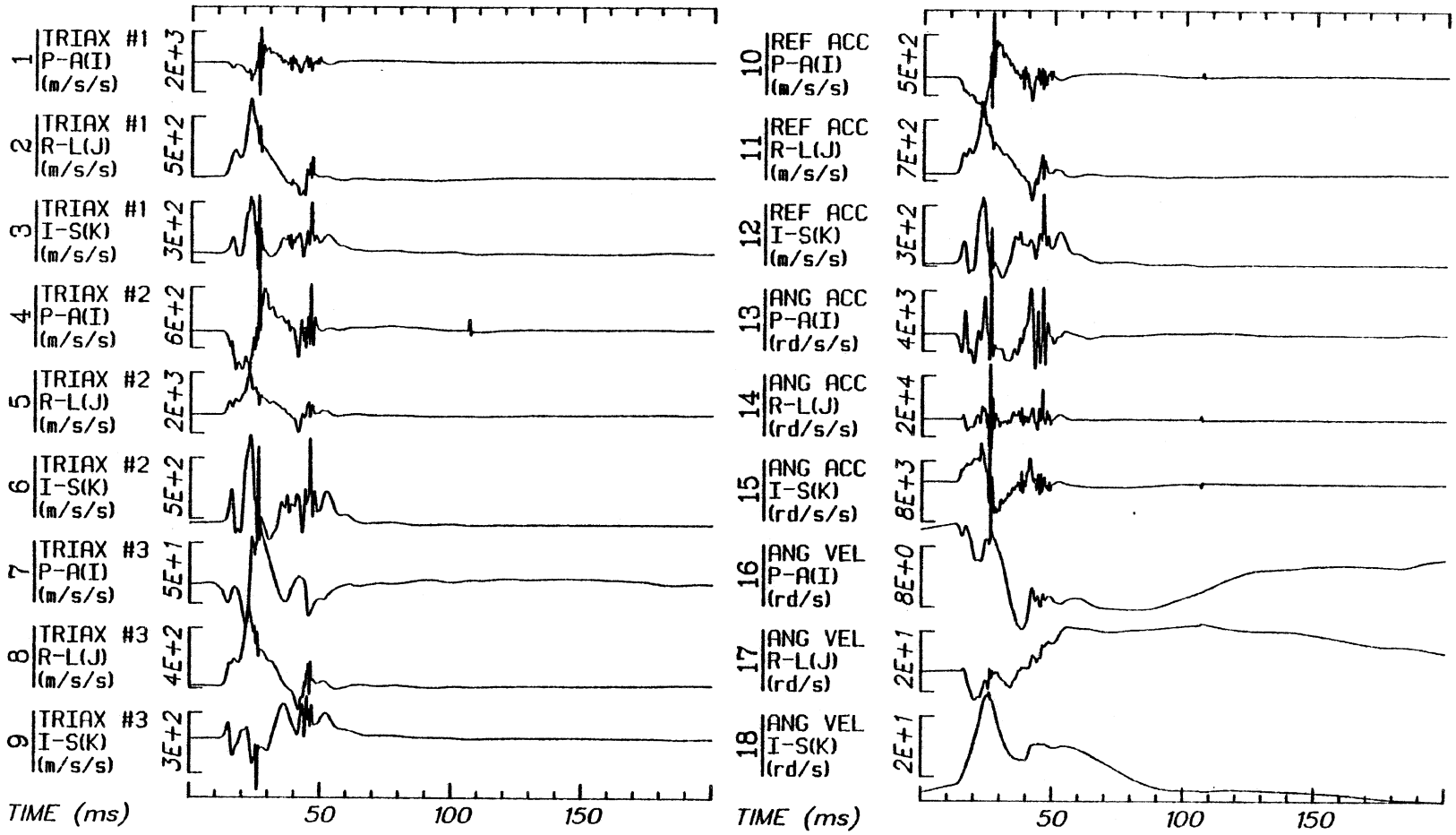

Run ID: 82E008 Disk: 82E008.3 File: 1 Date: MAY 11, 1985 Sheet: 1

Filter:1600*4C

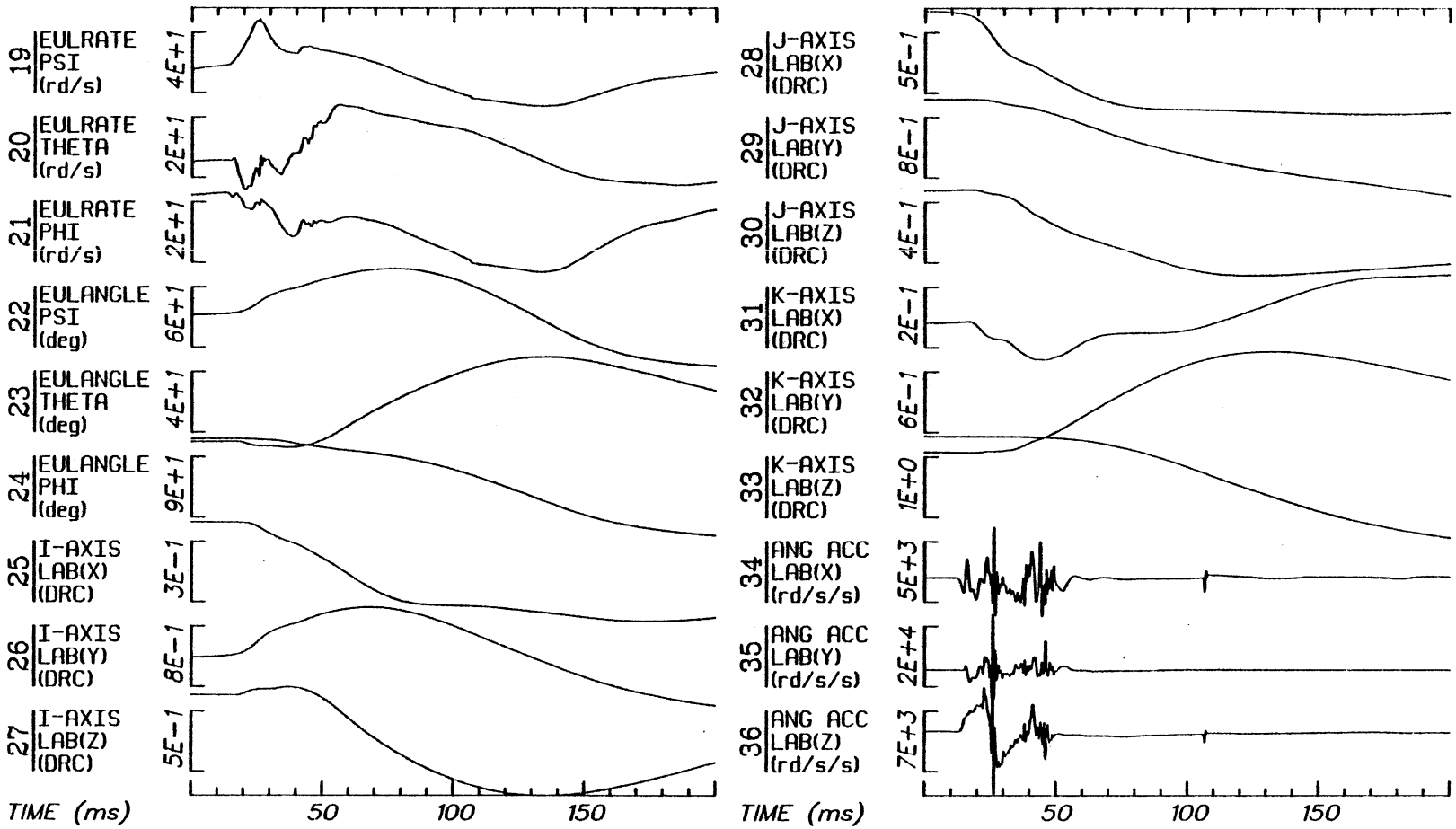

Run ID: 82E008 Disk: 82E008.3 File: 1 Date: MAY 11, 1985 Sheet: 2

Filter:1600*4C

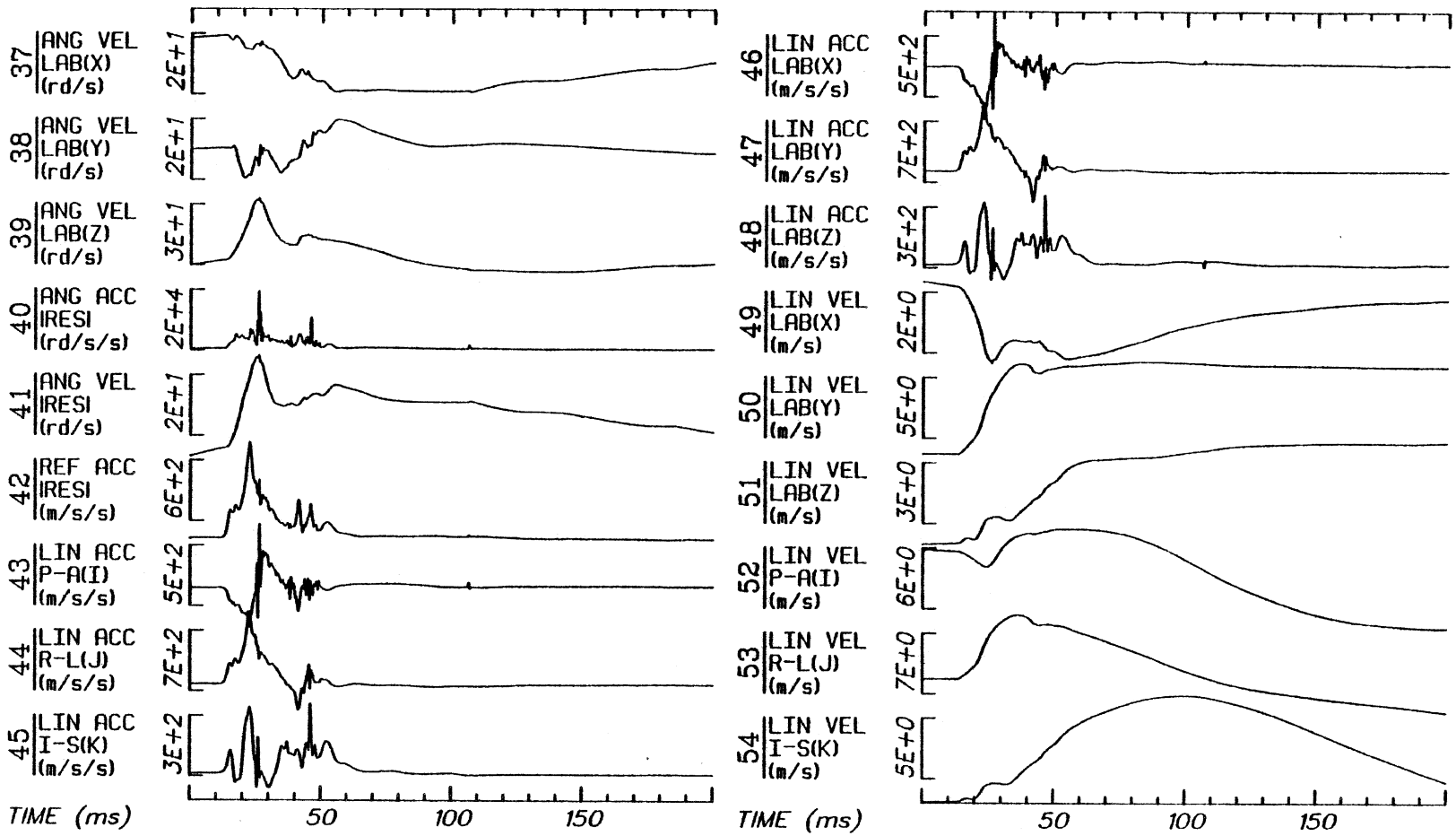

Run ID: 82E008 Disk: 82E008.3 File: 1 Date: MAY 11, 1985 Sheet: 3

Filter:1600*4C

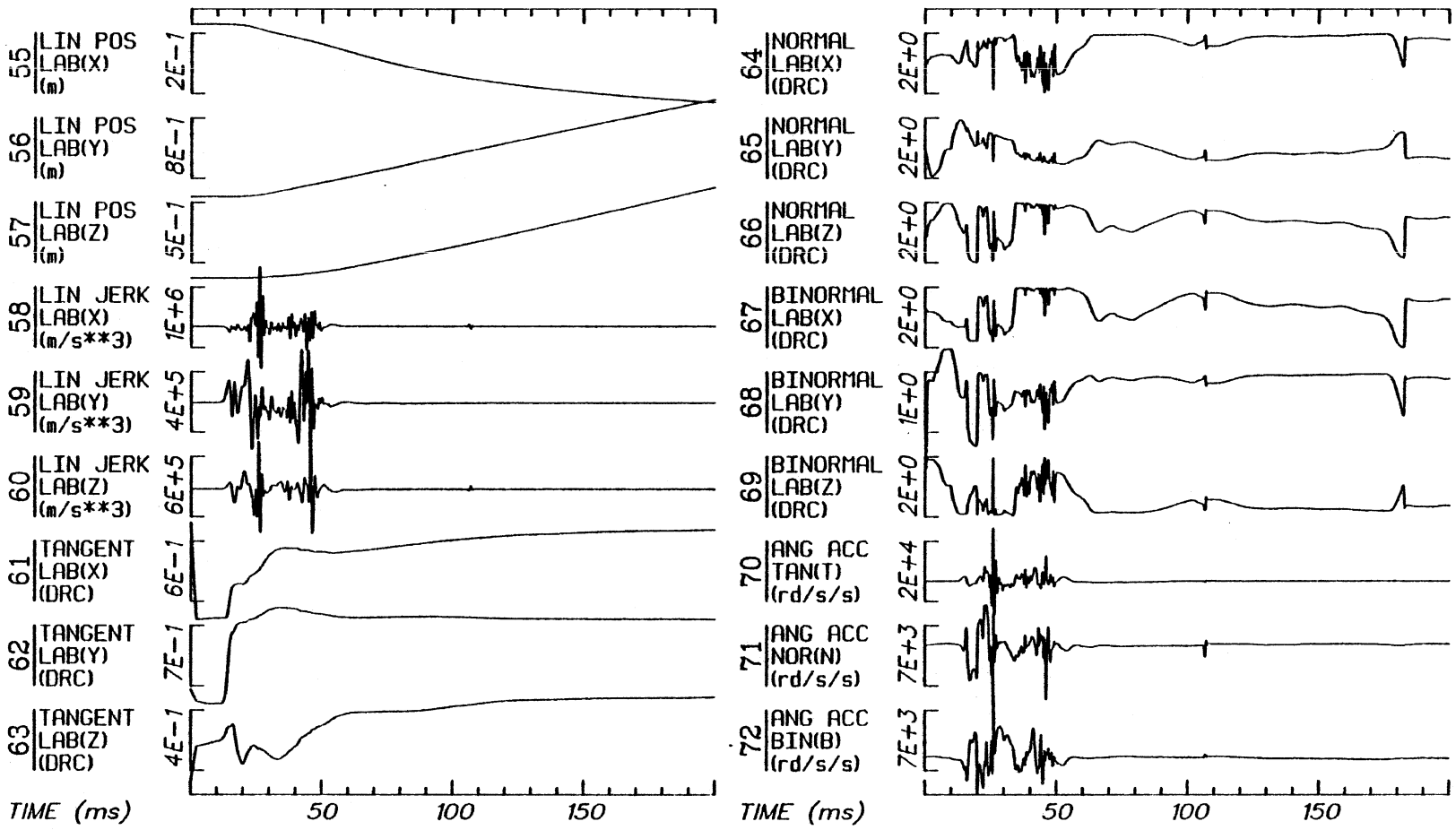

Run ID: 82E008 Disk: 82E008.3 File: 1 Date: MAY 11, 1985 Sheet: 4

Filter:1600*4C

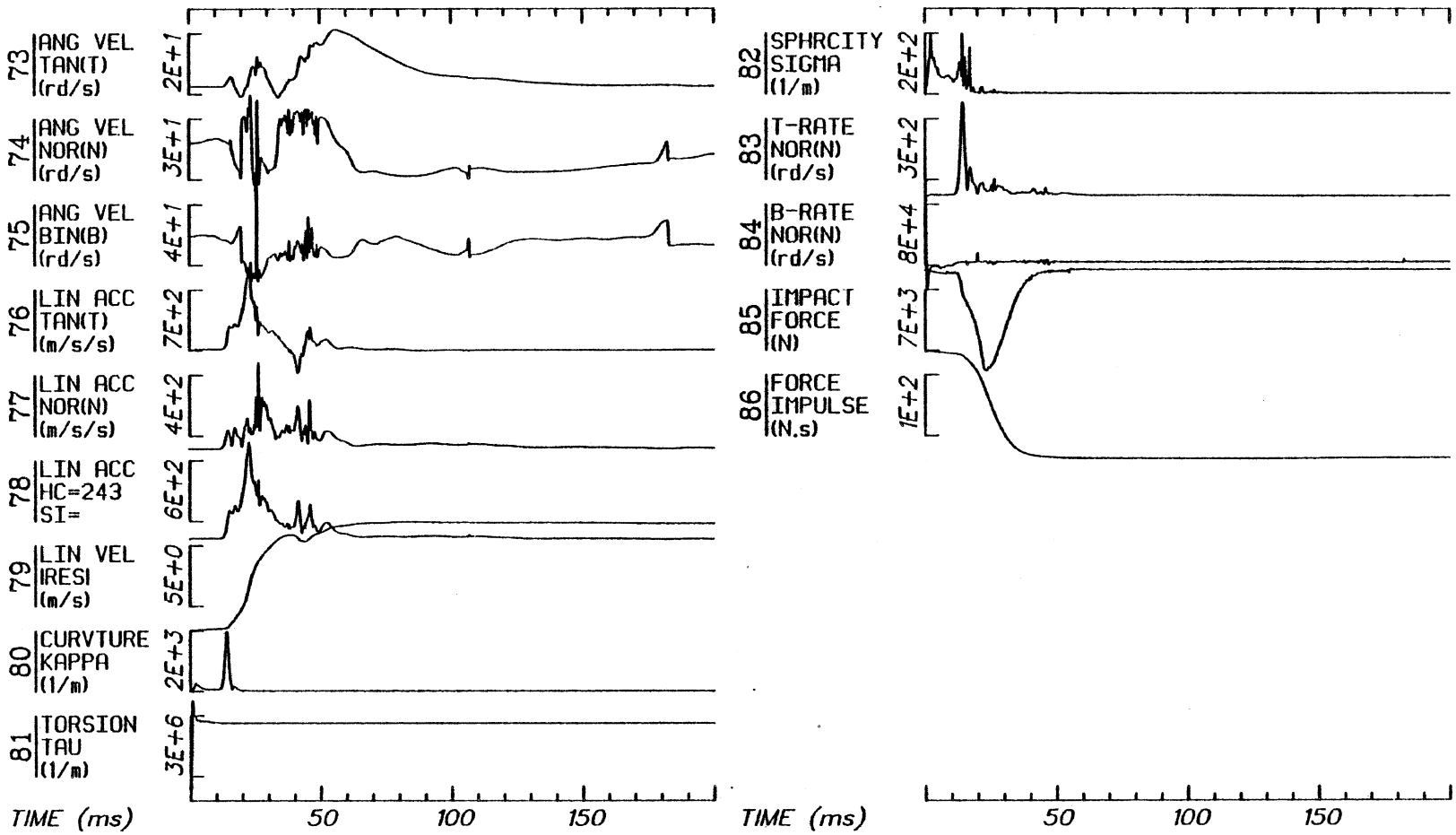

Run ID: 82E008 Disk: 82E008.3 File: 1 Date: MAY 11, 1985 Sheet: 5

Filter:1600*4C

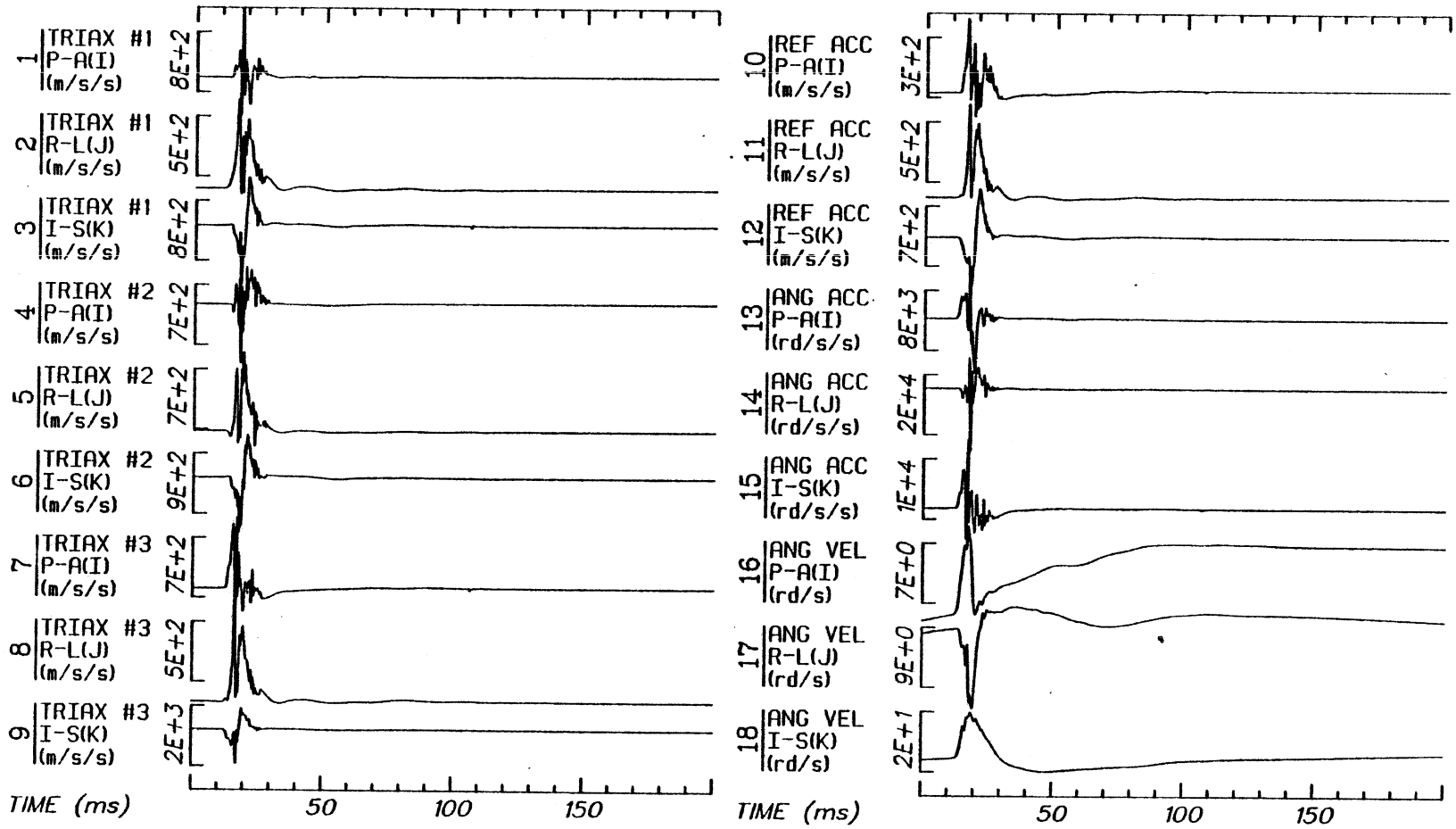

Run ID: 82E028 Disk: 82E028.3 File: 1 Date: MAY 12, 1985 Sheet: 1

Filter:1600*4C

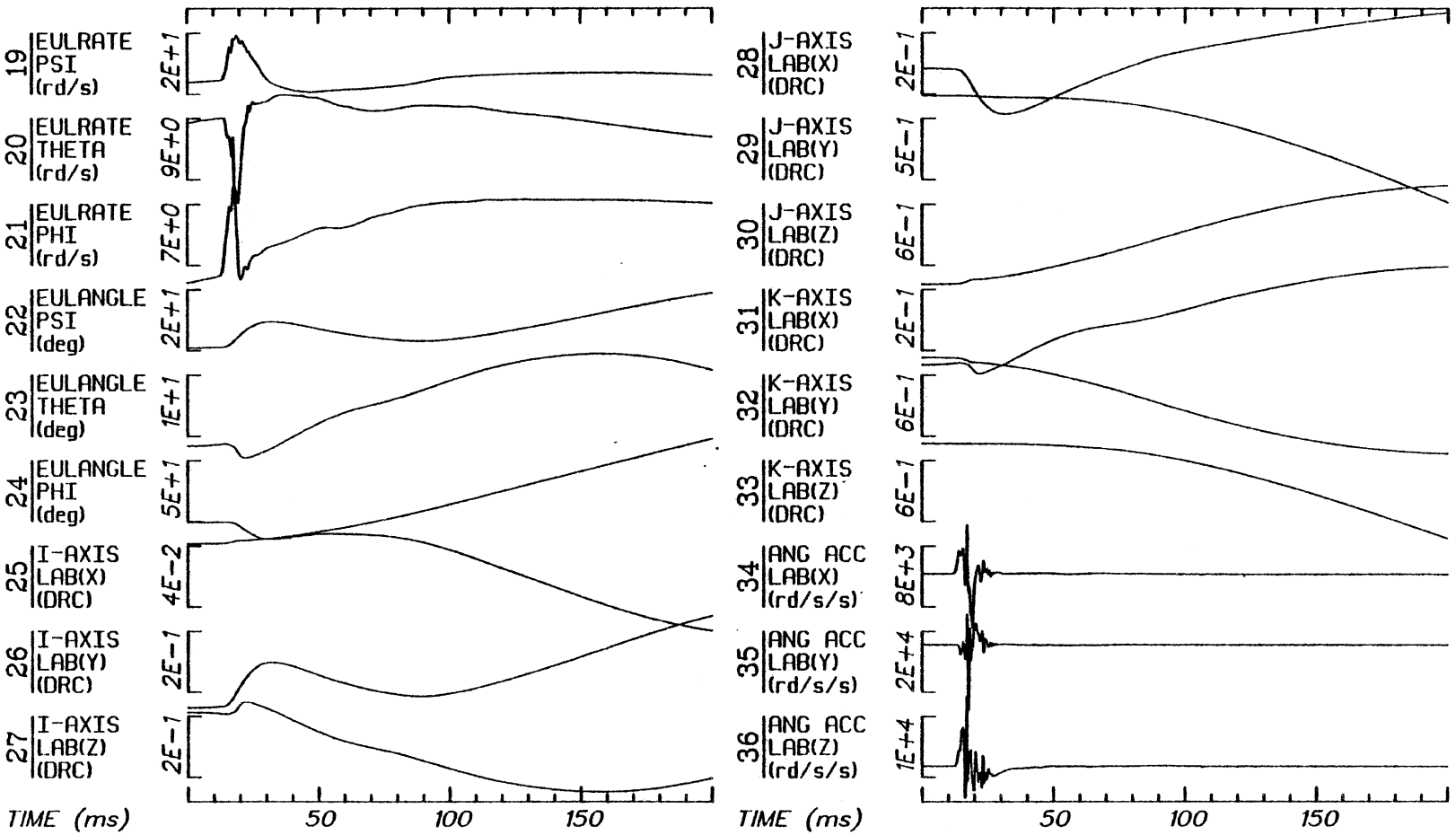

Run ID: 82E028 Disk: 82E028.3 File: 1 Date: MAY 12, 1985 Sheet: 2

Filter:1600*4C

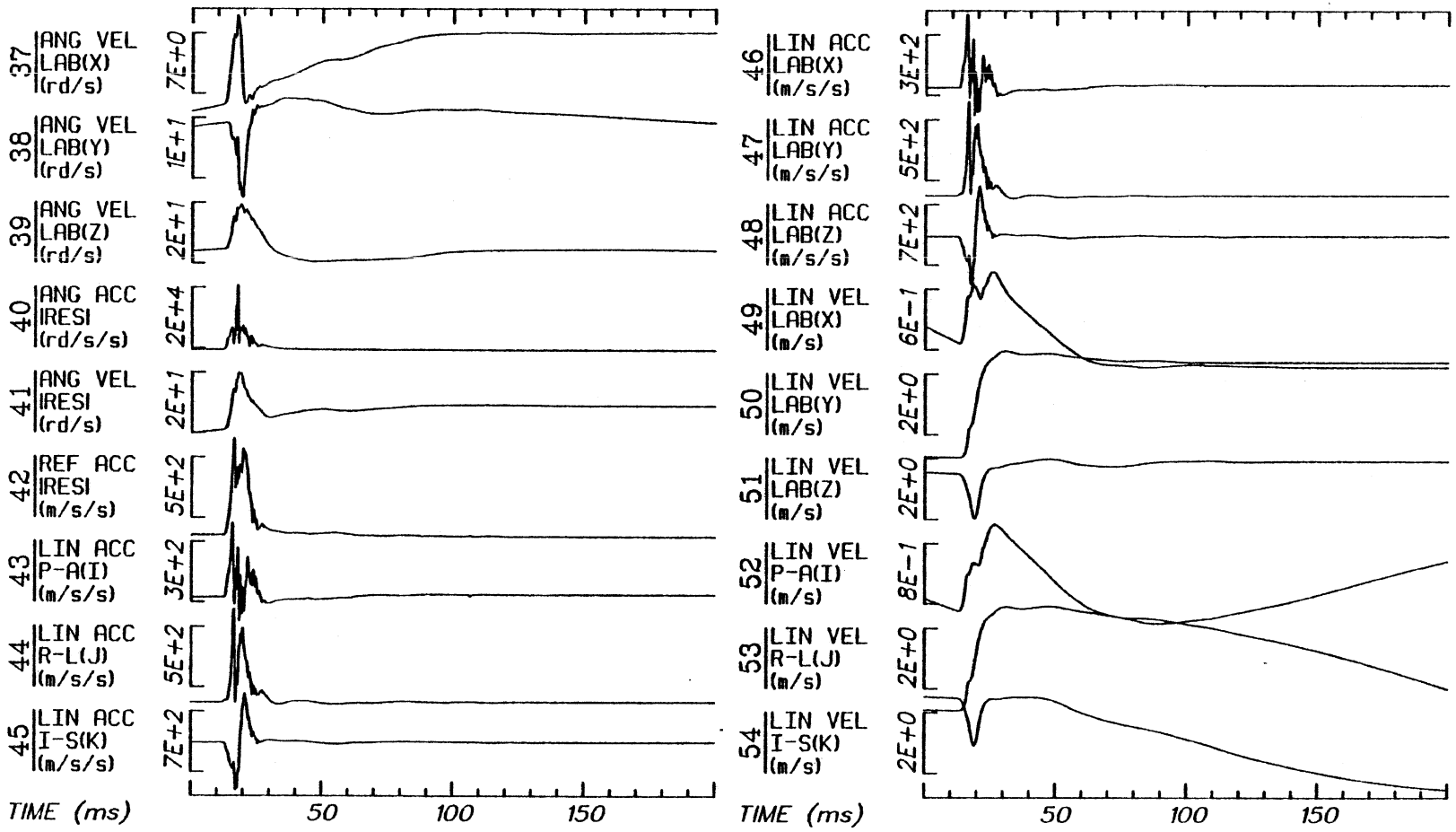

Run ID: 82E028 Disk: 82E028.3 File: 1 Date: MAY 12, 1985 Sheet: 3

Filter:1600*4C

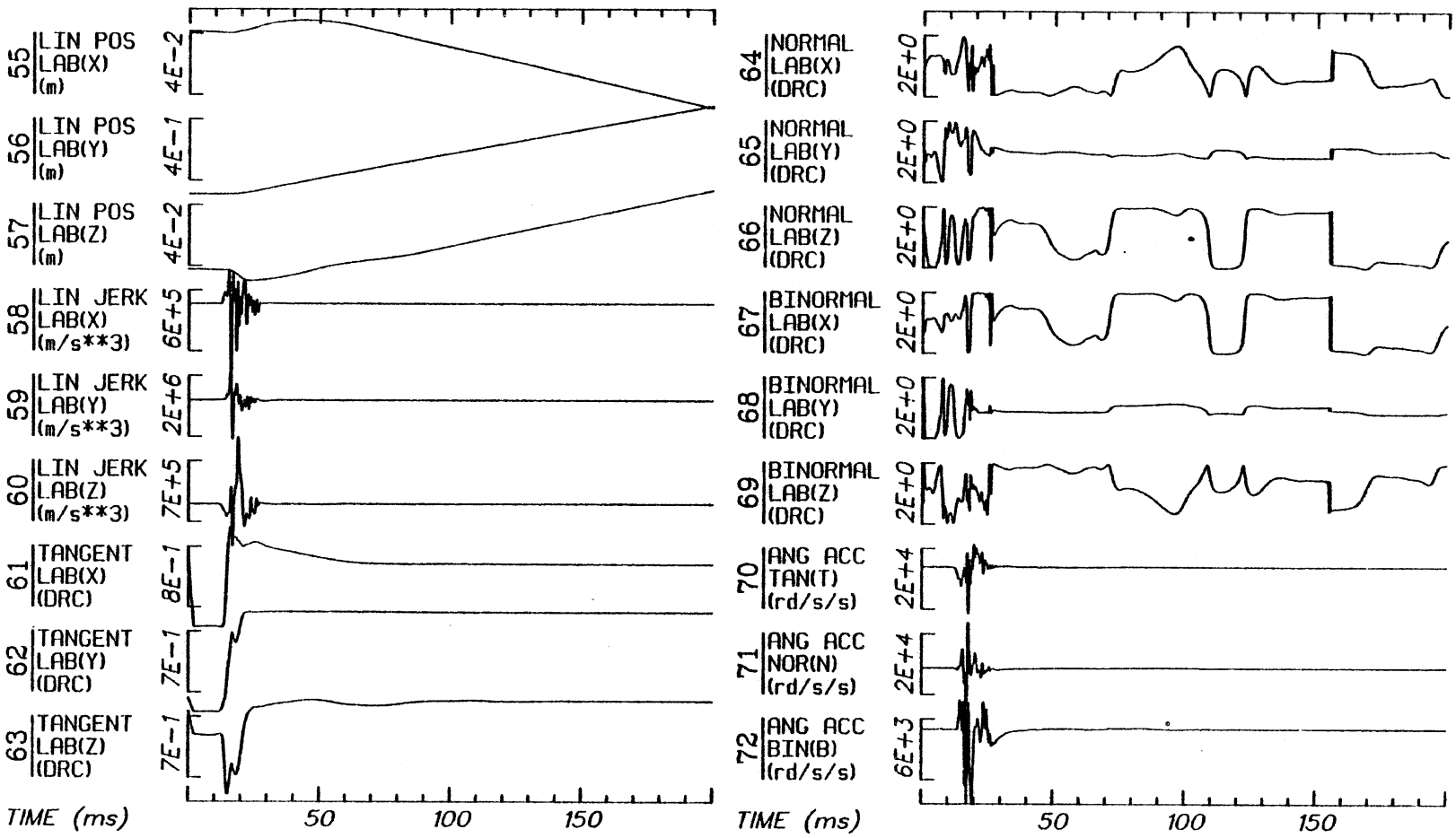

Run ID: 82E028 Disk: 82E028.3 File: 1 Date: MAY 12, 1985 Sheet: 4

*Filter:1600*4C*

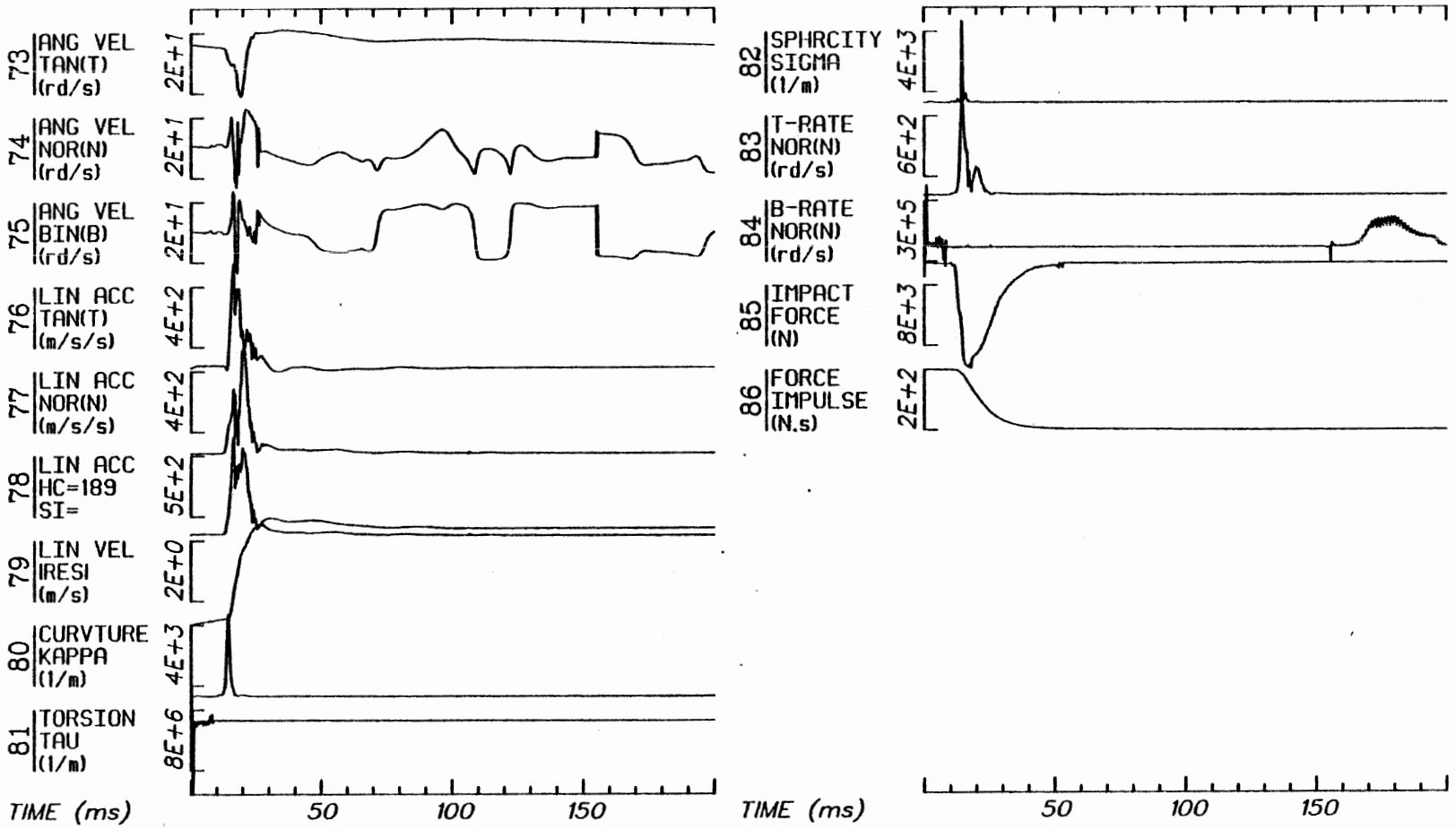

Run ID: 82E028 Disk: 82E028.3 File: 1 Date: MAY 12, 1985 Sheet: 5

Filter:1600*4C

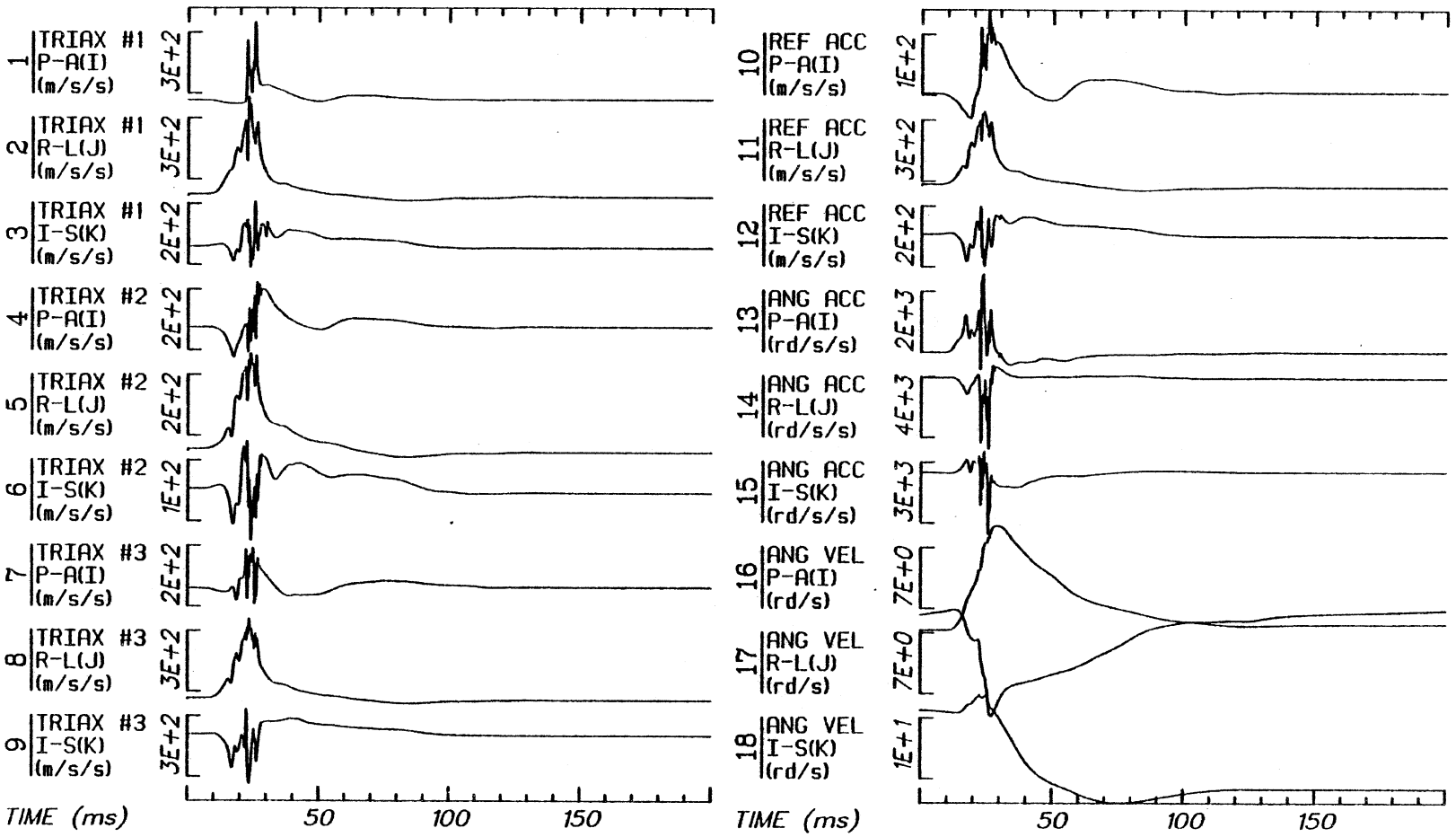

Run ID: 82E049 Disk: 82E049.3 File: 1 Date: MAY 11, 1985 Sheet: 1

Filter:1600*4C

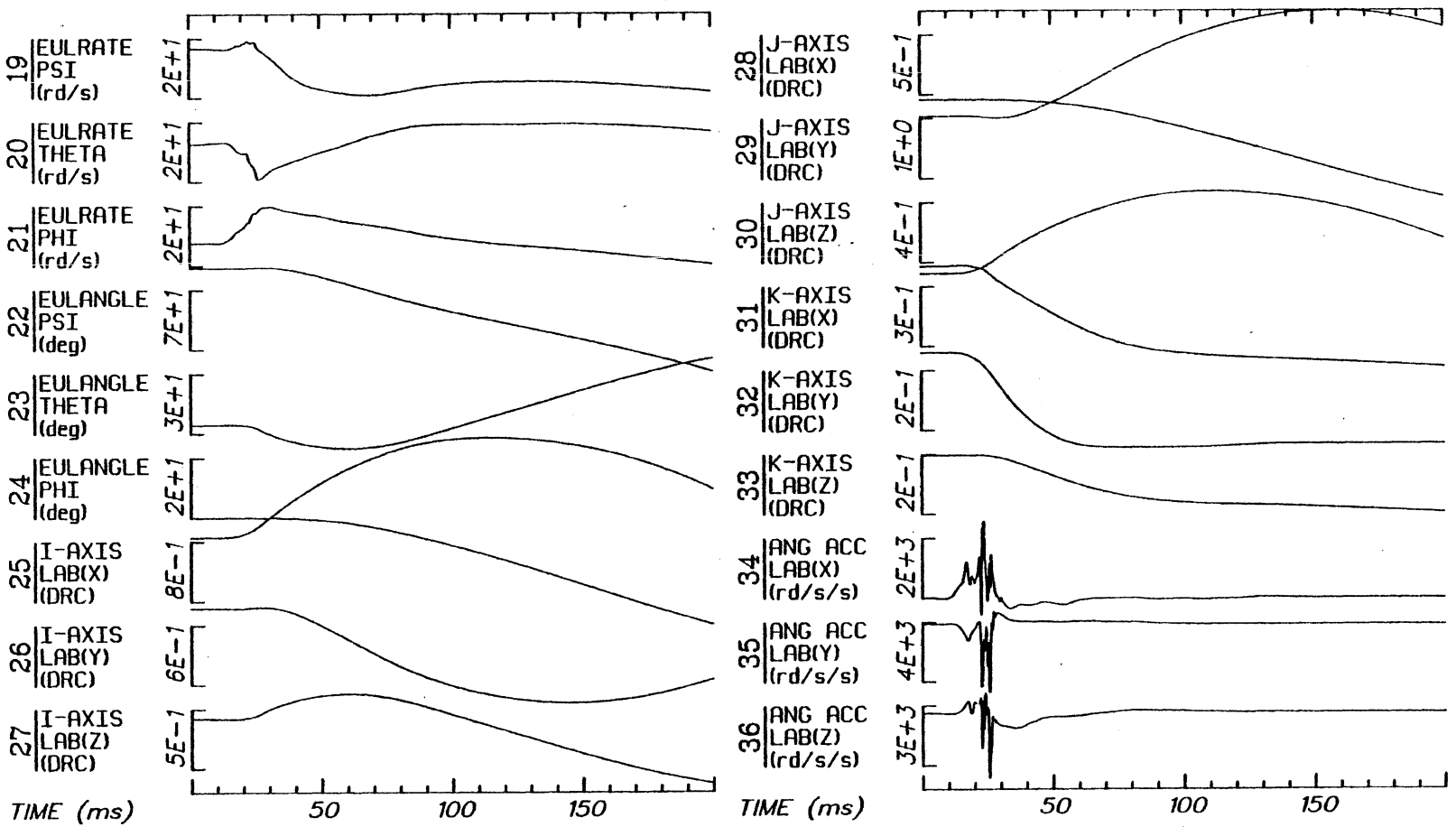

Run ID: 82E049 Disk: 82E049.3 File: 1 Date: MAY 11, 1985 Sheet: 2

*Filter:1600*4C*

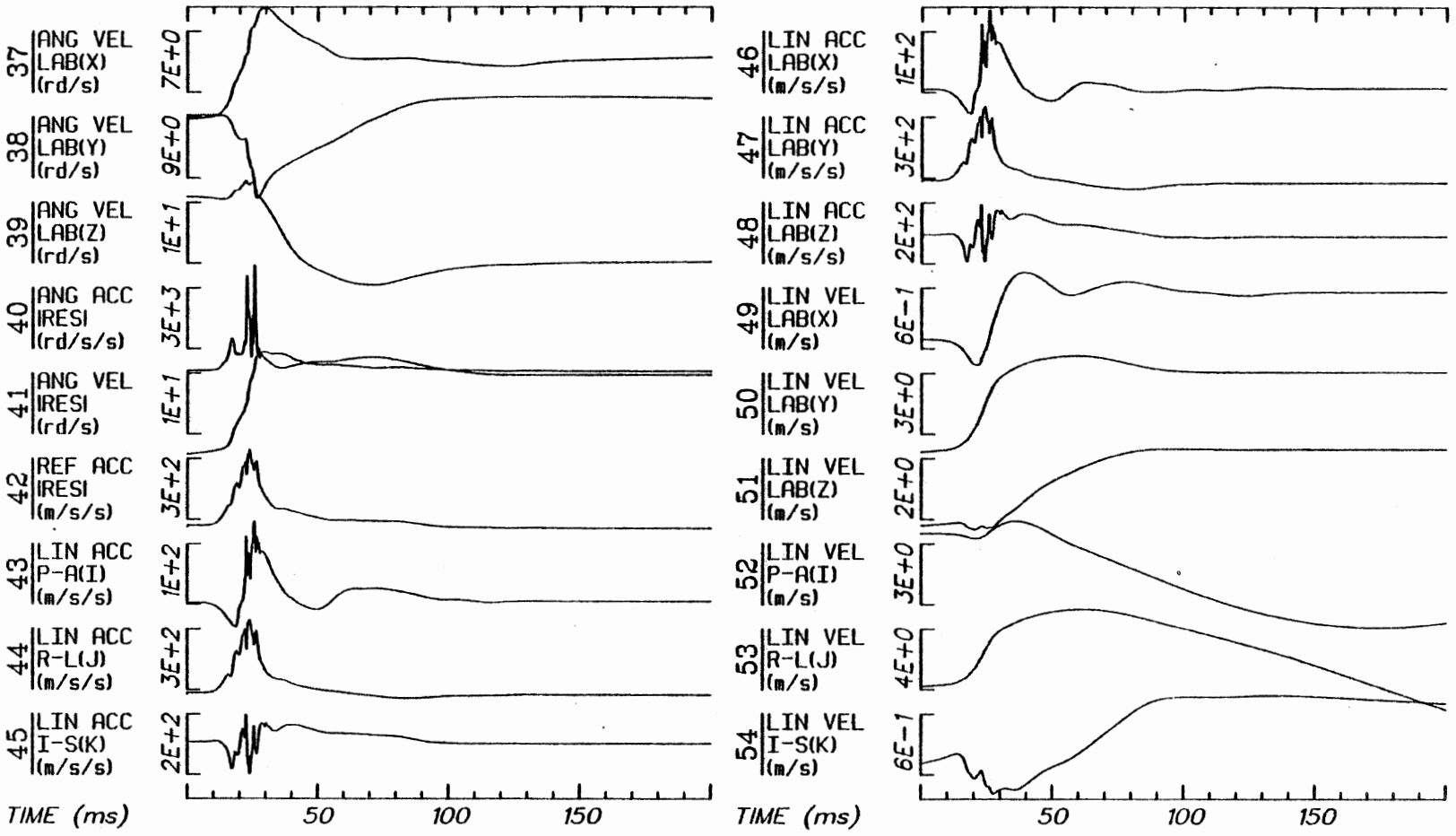

Run ID: 82E049 Disk: 82E049.3 File: 1 Date: MAY 11, 1985 Sheet: 3

Filter:1600*4C

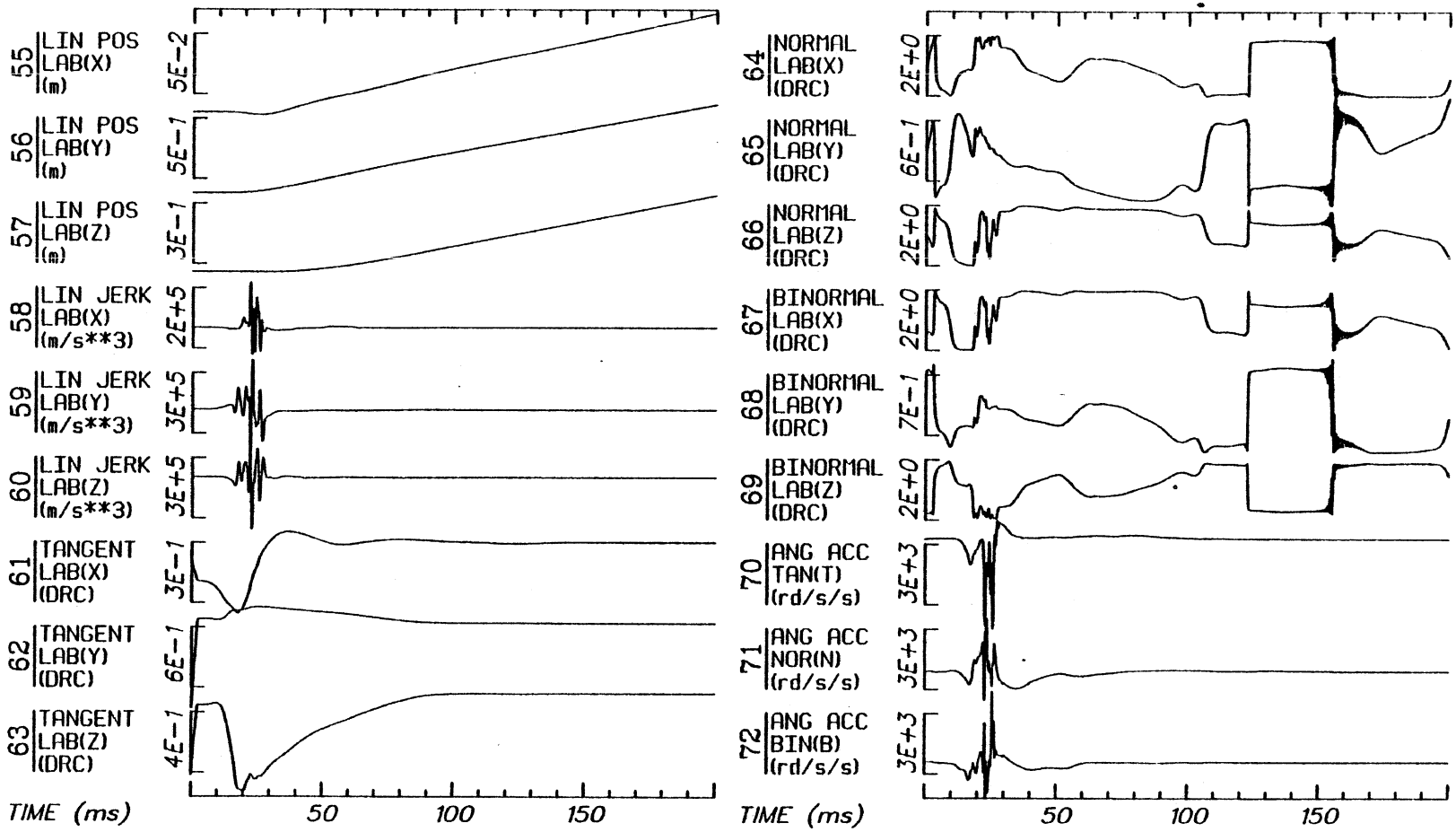

Run ID: 82E049 Disk: 82E049.3 File: 1 Date: MAY 11, 1985 Sheet: 4

Filter:1600*4C

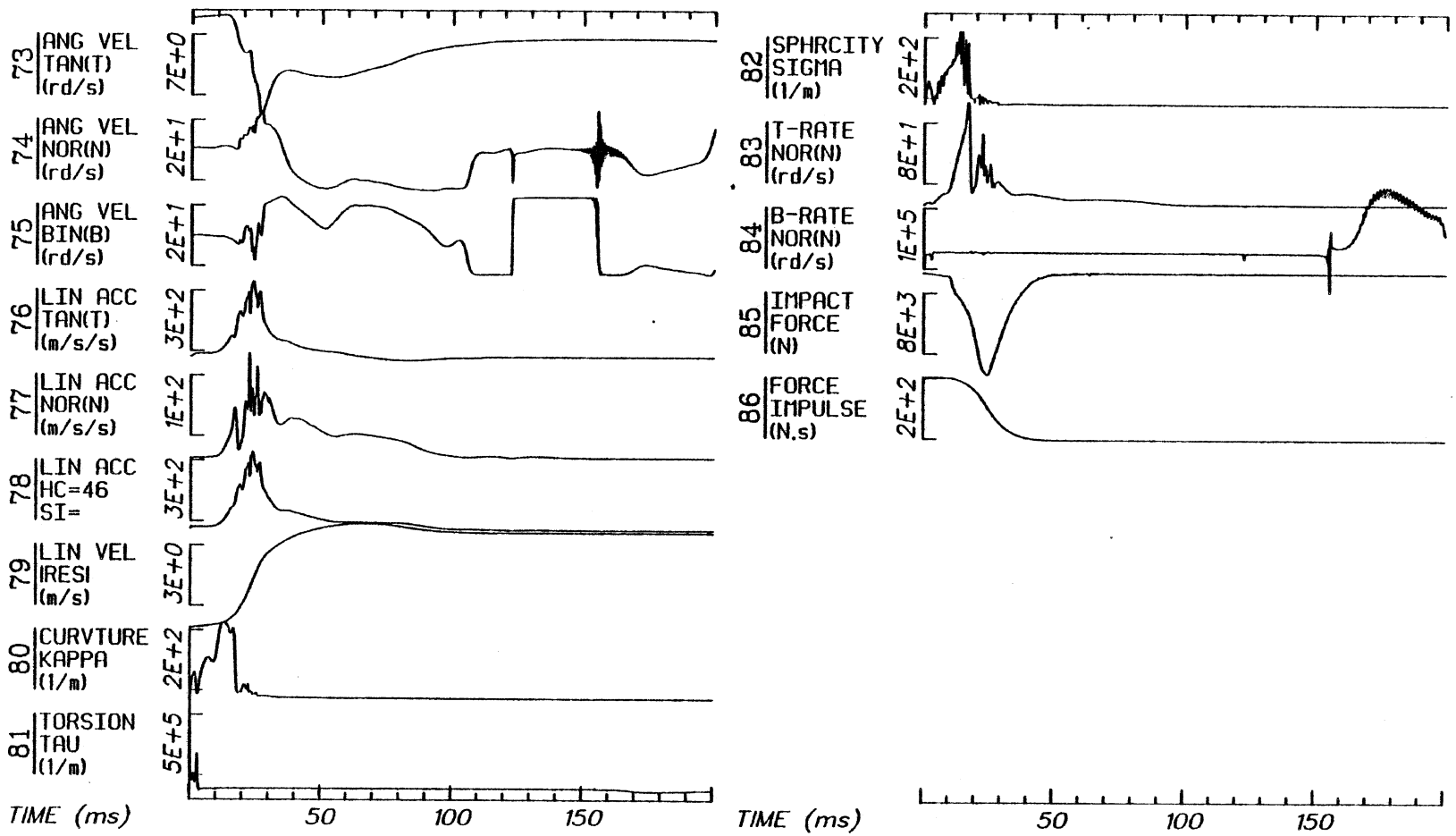

Run ID: 82E049 Disk: 82E049.3 File: 1 Date: MAY 11, 1985 Sheet: 5

Filter:1600*4C

Run ID: 82E051 *Filter:1600*4C Smooth: 3SD*

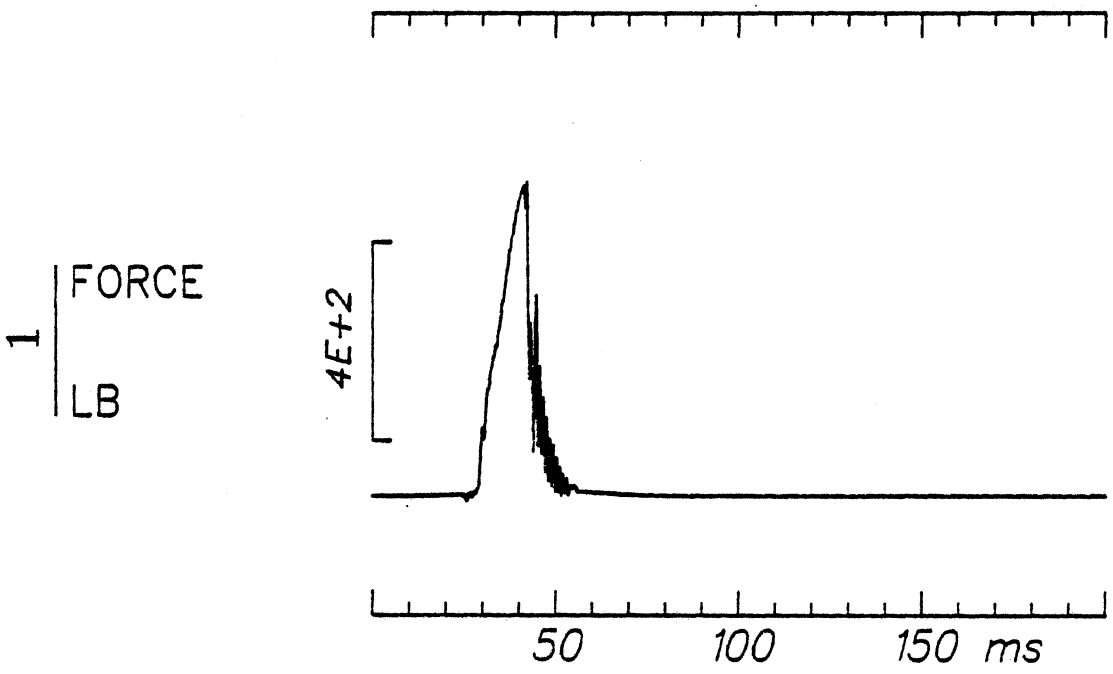

Run ID: 82E052 *Filter:1600*4C Smooth: 3SD*

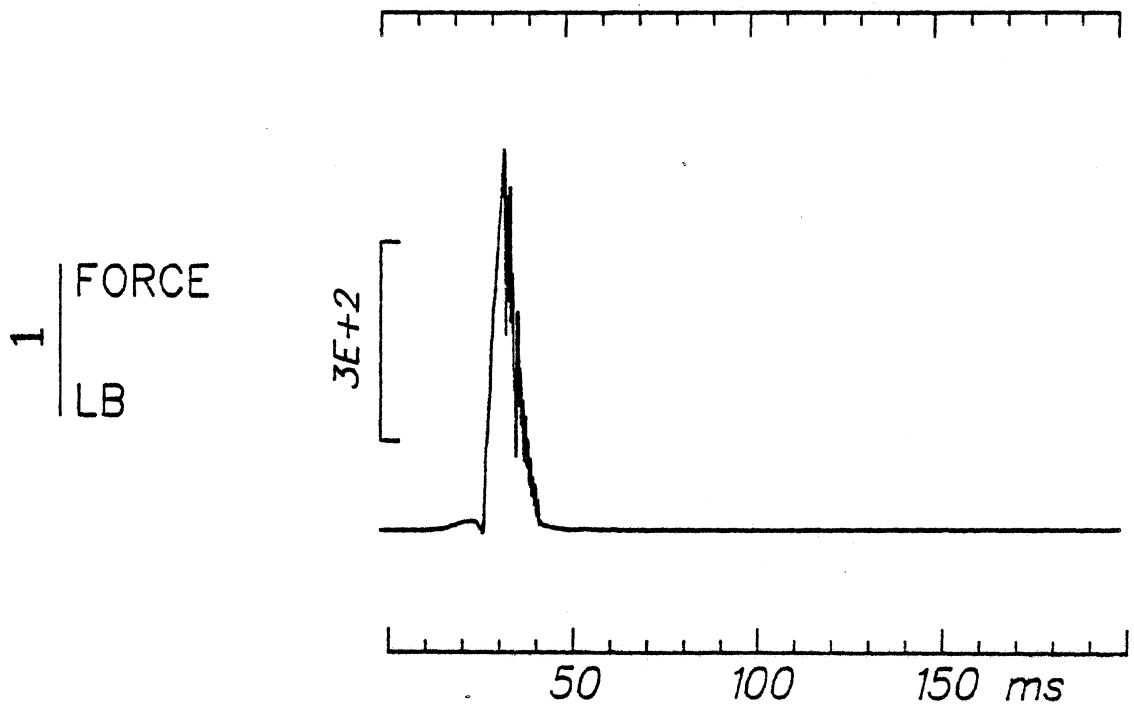

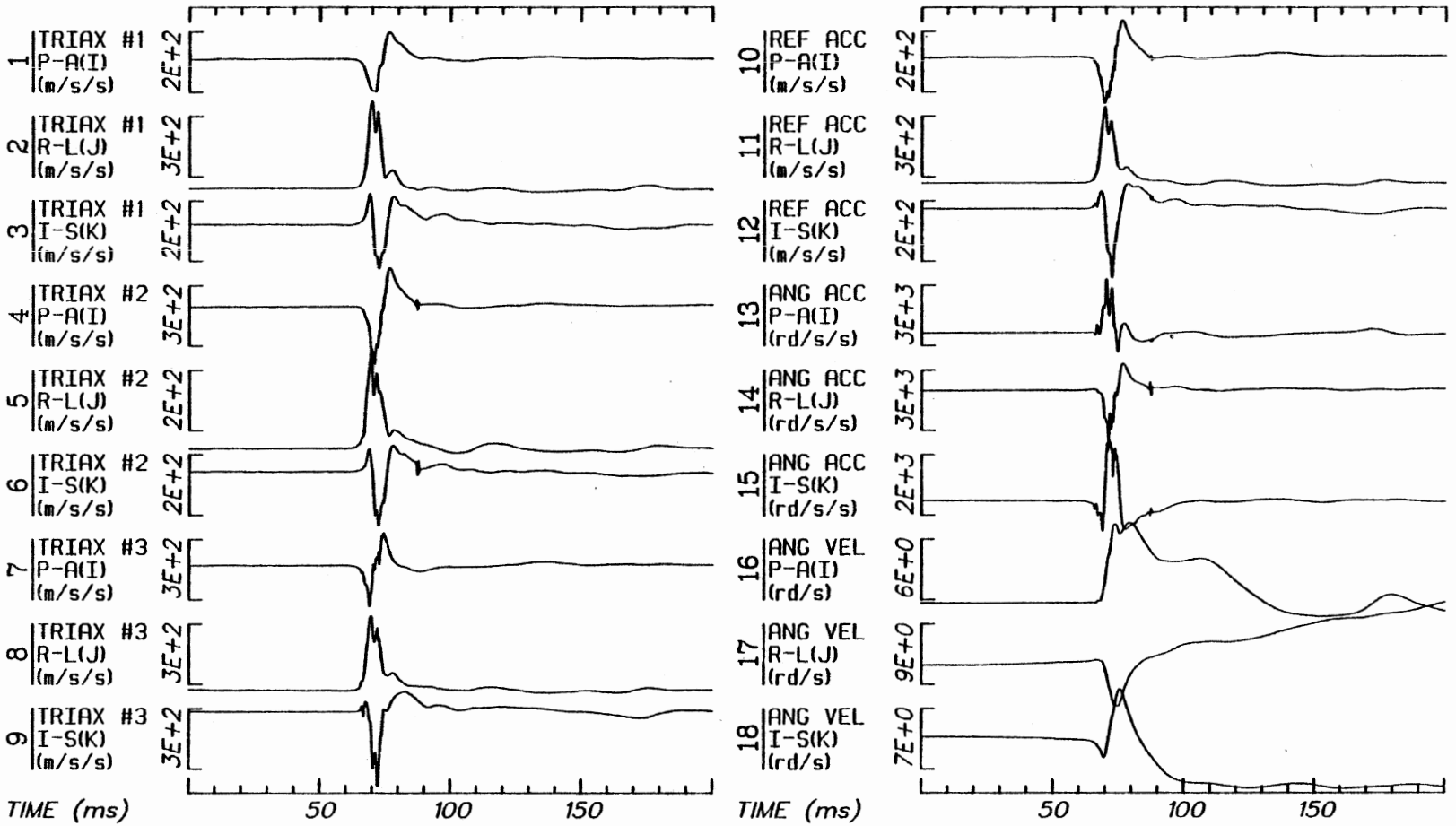

Run ID: 82E067 Disk: 82E067.3 File: 1 Date: MAY 12, 1985 Sheet: 1

Filter:1600*4C

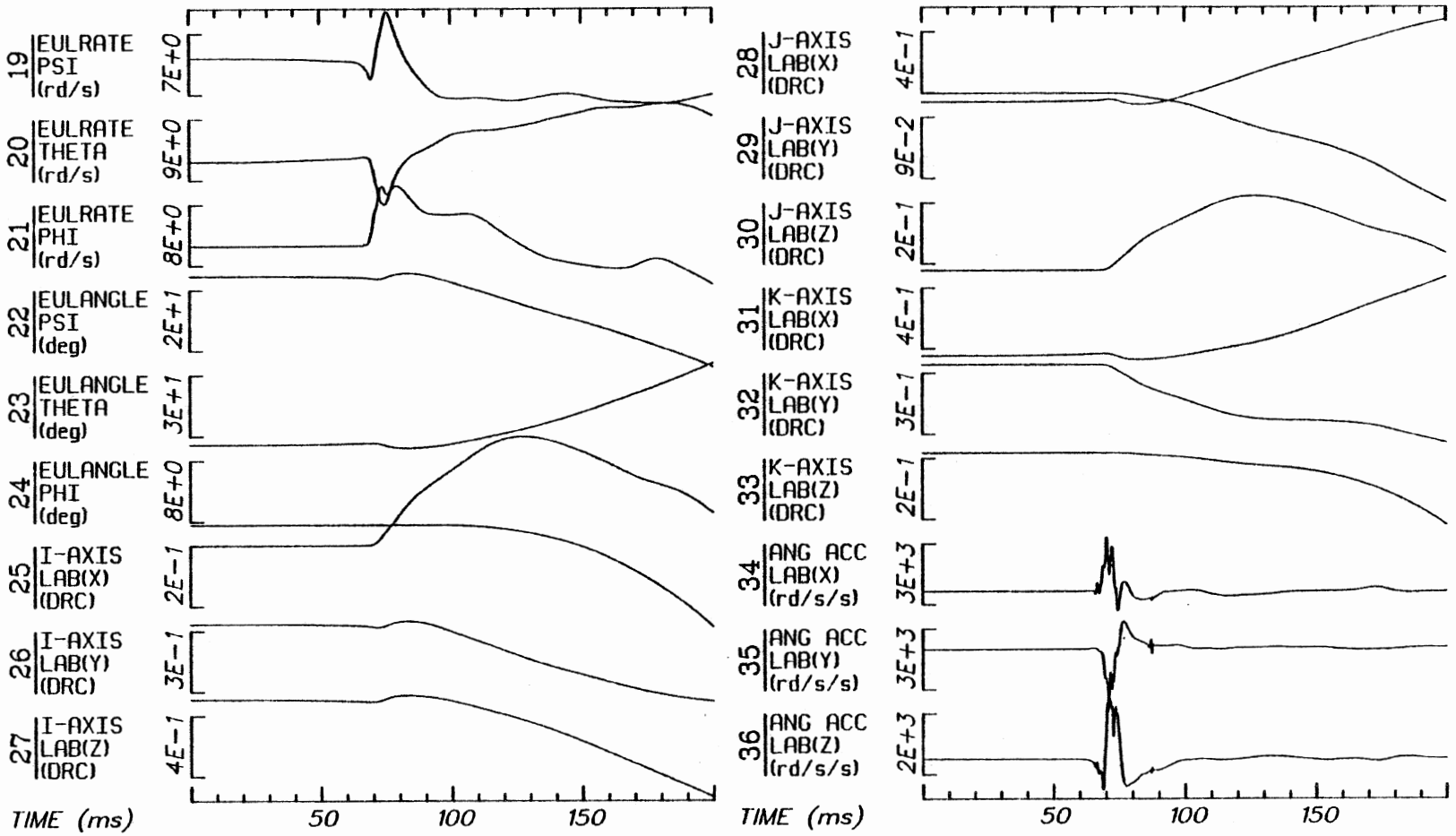

Run ID: 82E067 Disk: 82E067.3 File: 1 Date: MAY 12, 1985 Sheet: 2

Filter:1600*4C

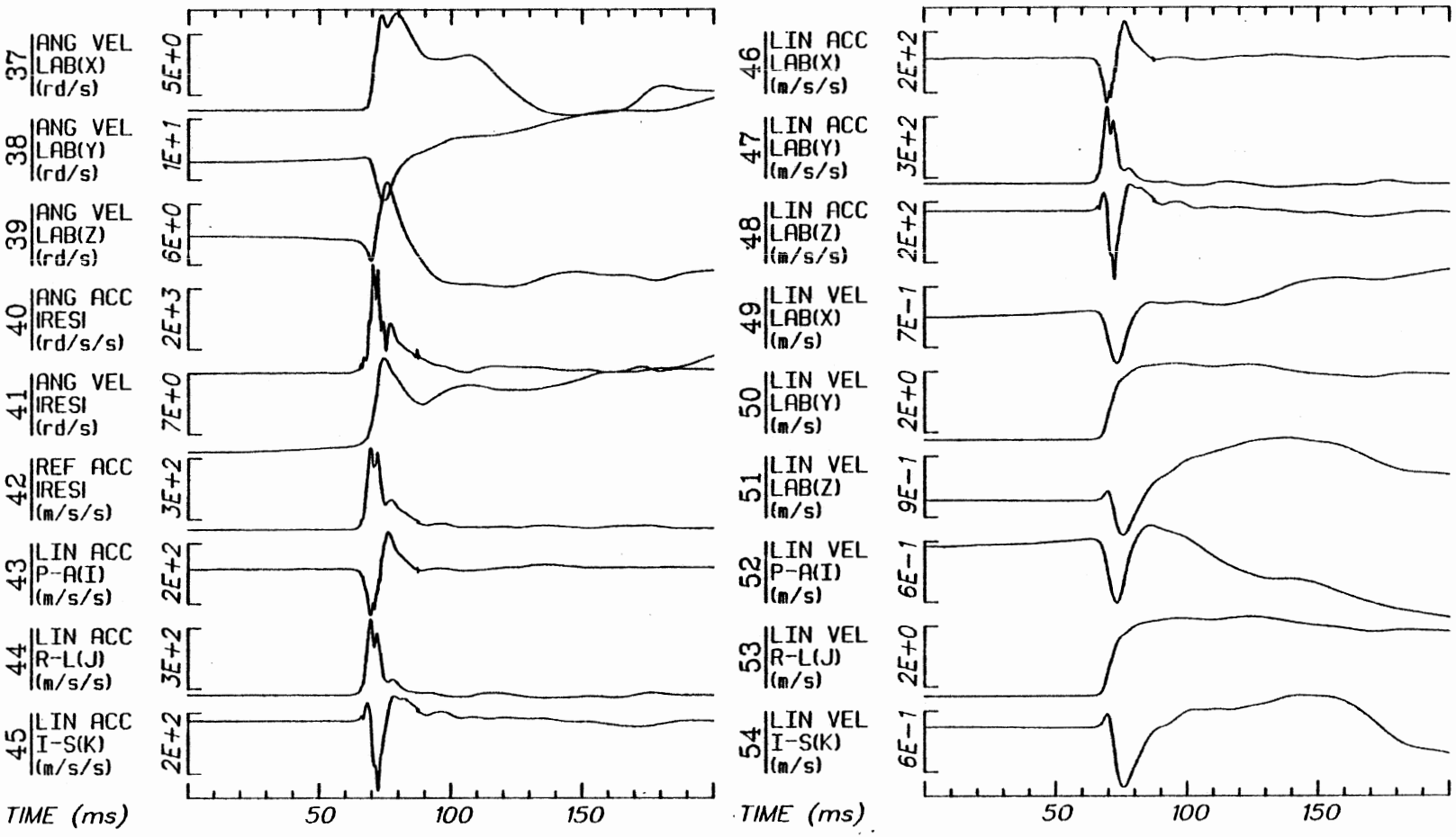

Run ID: 82E067 Disk: 82E067.3 File: 1 Date: MAY 12, 1985 Sheet: 3

Filter:1600*4C

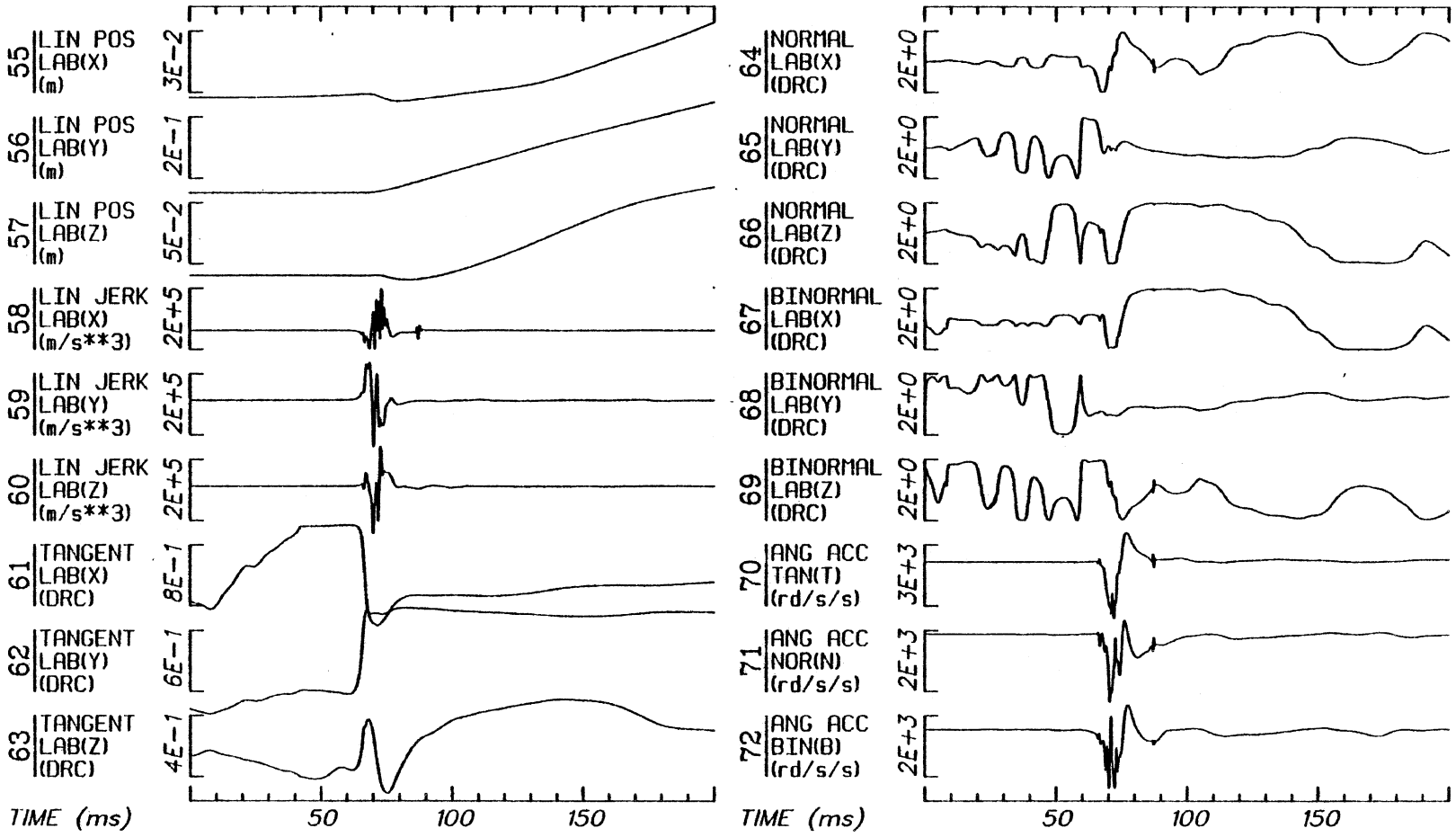

Run ID: 82E067 Disk: 82E067.3 File: 1 Date: MAY 12, 1985 Sheet: 4

Filter:1600*4C

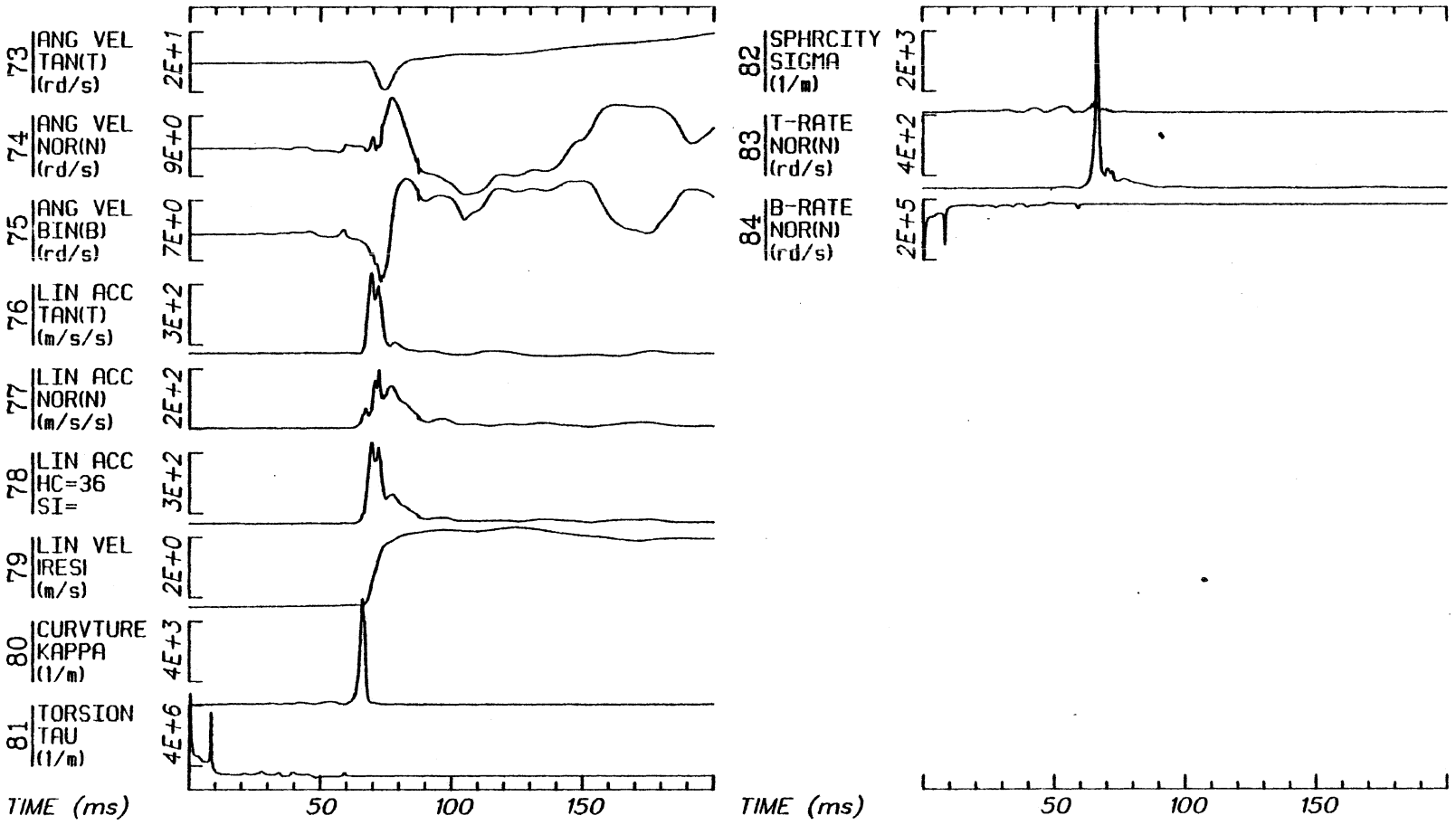

Run ID: 82E067 Disk: 82E067.3 File: 1 Date: MAY 12, 1985 Sheet: 5

Filter:1600*4C

Run ID: 82E071 *Filter:1600*4C Smooth: 3SD*

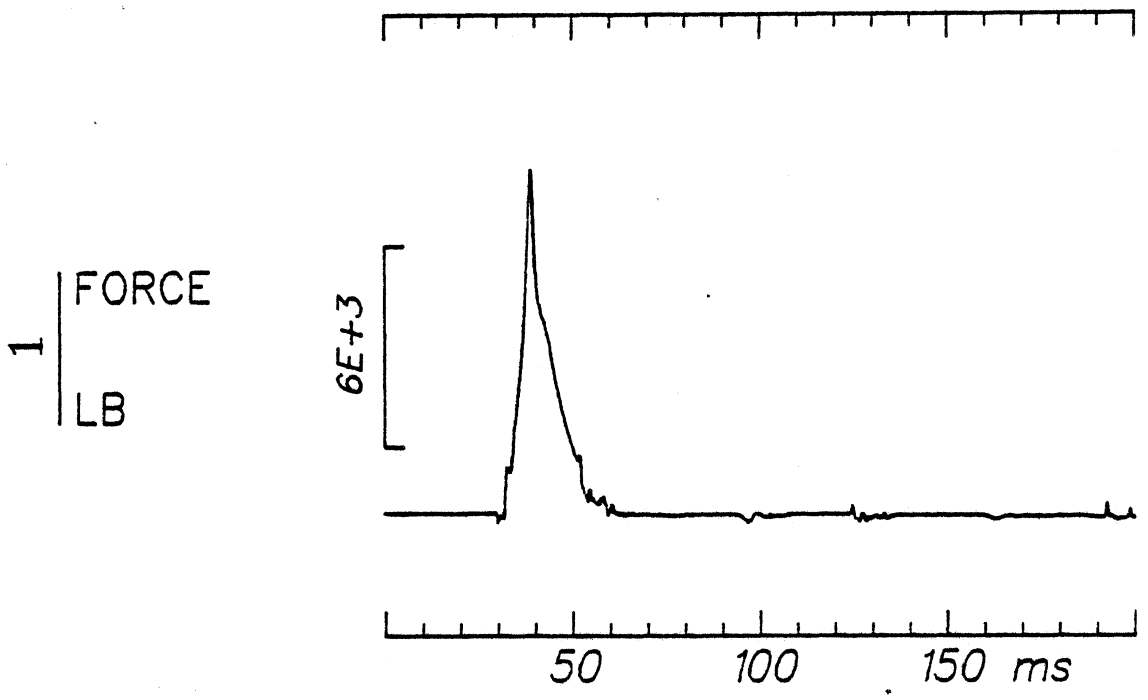

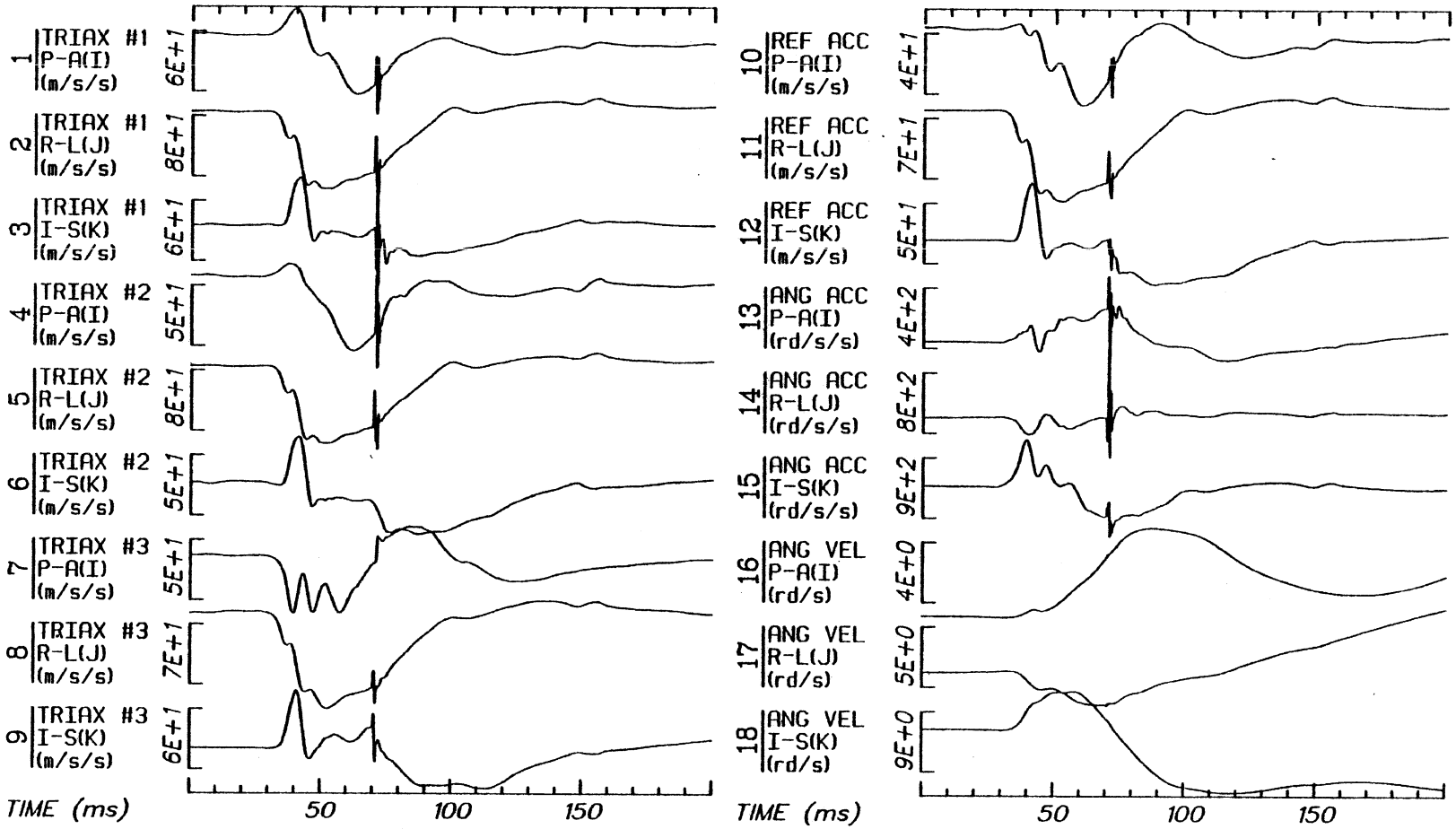

Run ID: 83E087 Disk: 83E087.3 File: 1 Date: MAY 11, 1985 Sheet: 1

Filter:1600*4C

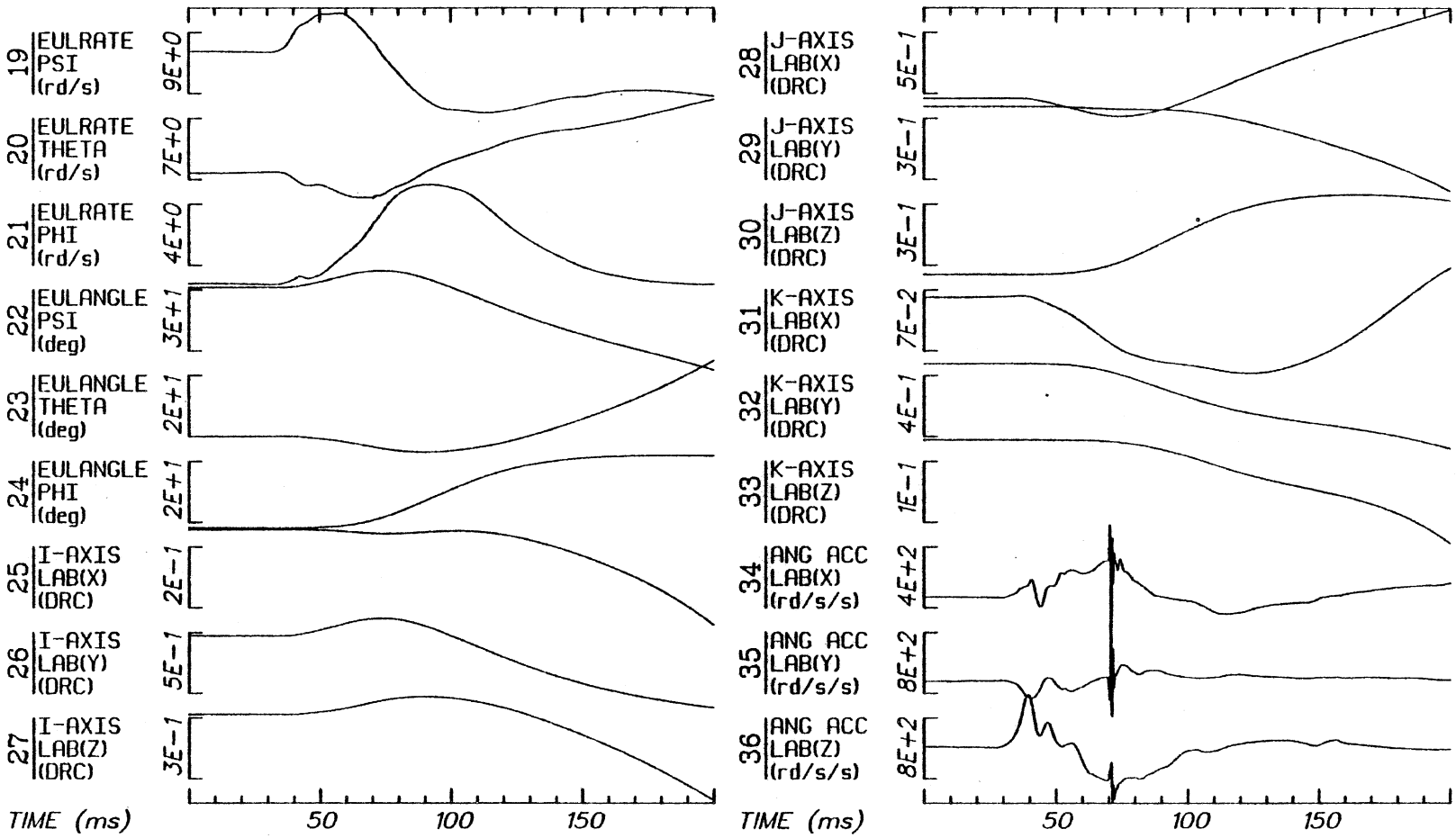

Run ID: 83E087 Disk: 83E087.3 File: 1 Date: MAY 11, 1985 Sheet: 2

Filter:1600*4C

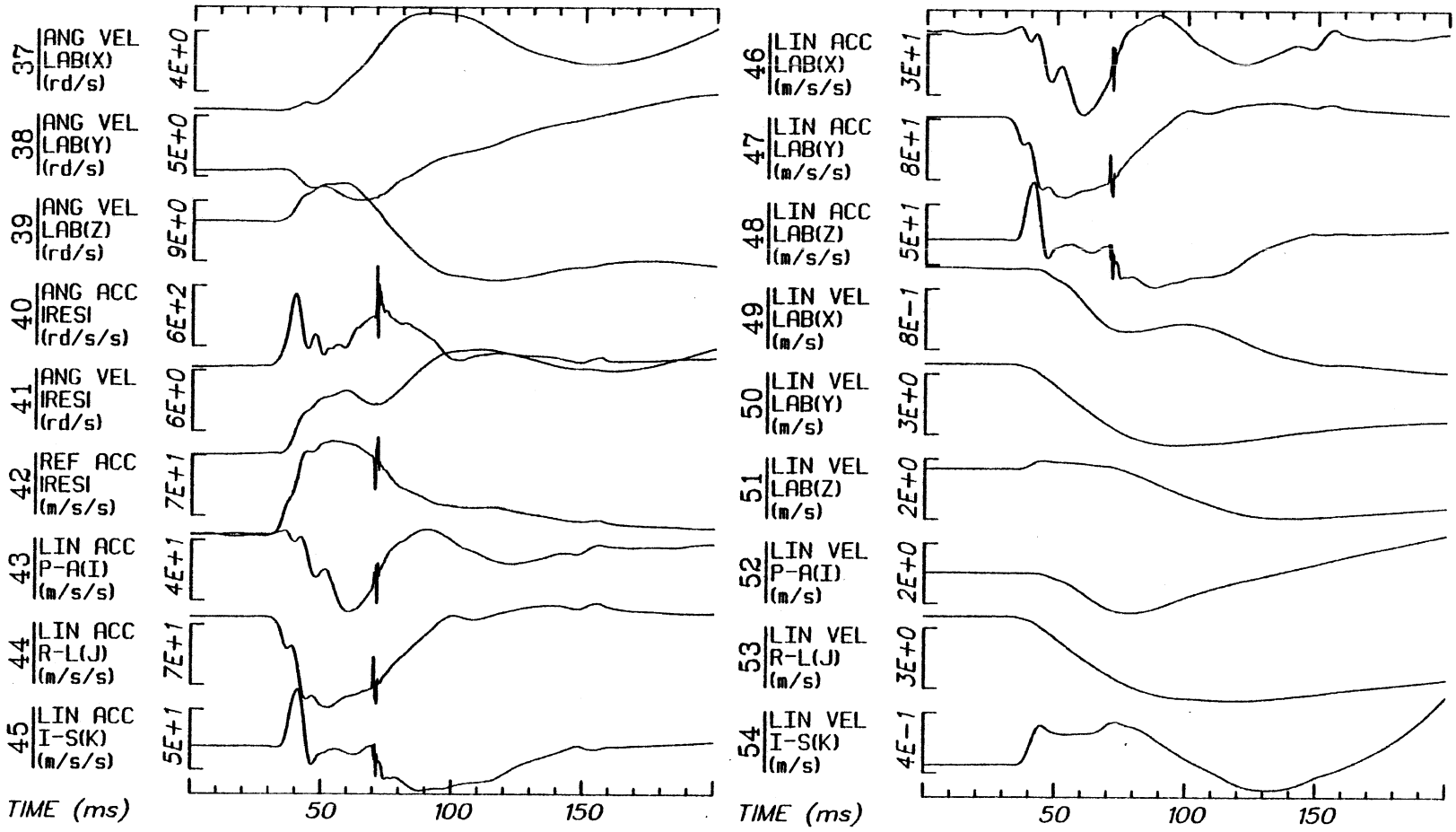

Run ID: 83E087 Disk: 83E087.3 File: 1 Date: MAY 11, 1985 Sheet: 3

Filter:1600*4C

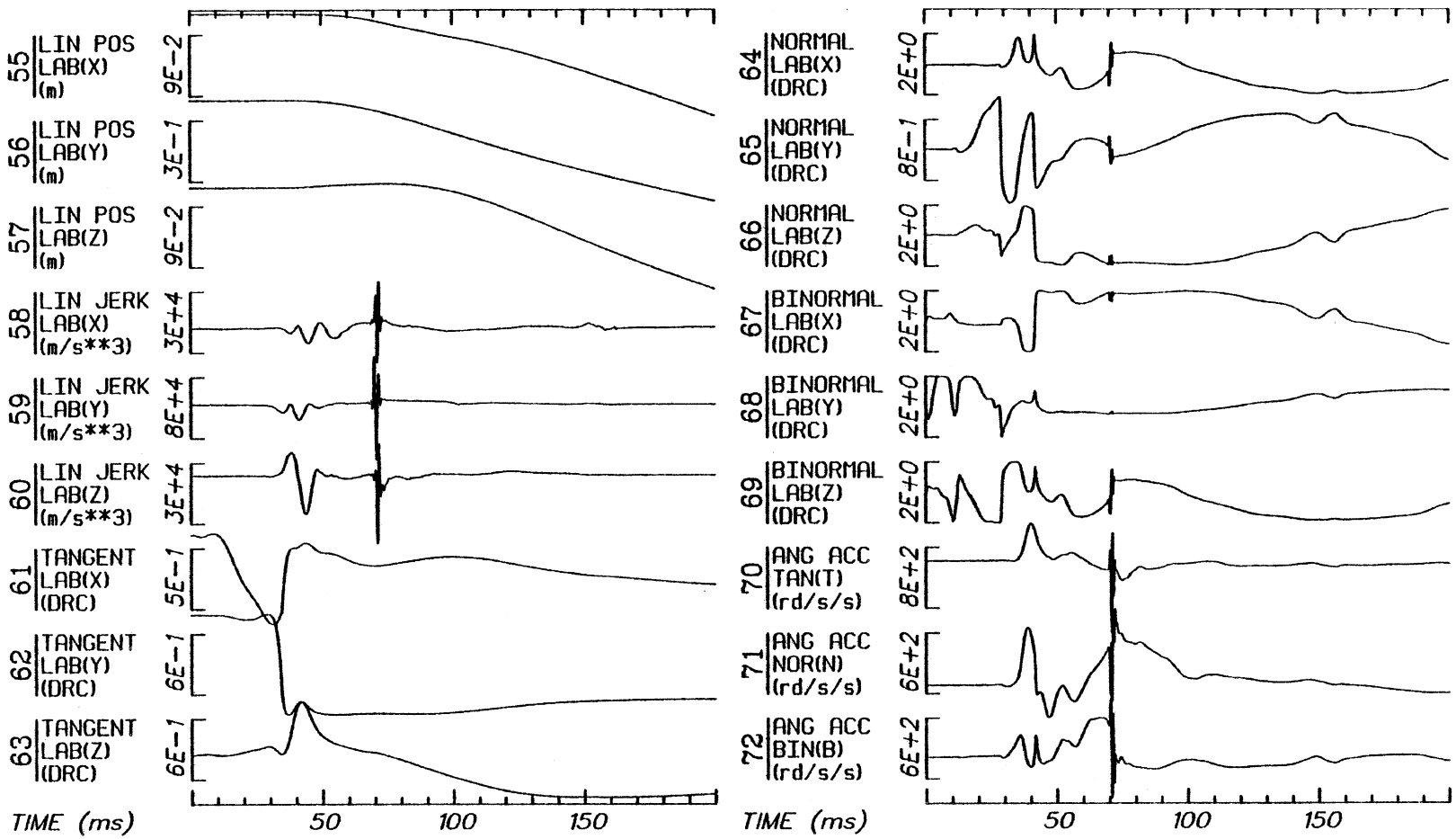

Run ID: 83E087 Disk: 83E087.3 File: 1 Date: MAY 11, 1985 Sheet: 4

Filter:1600*4C

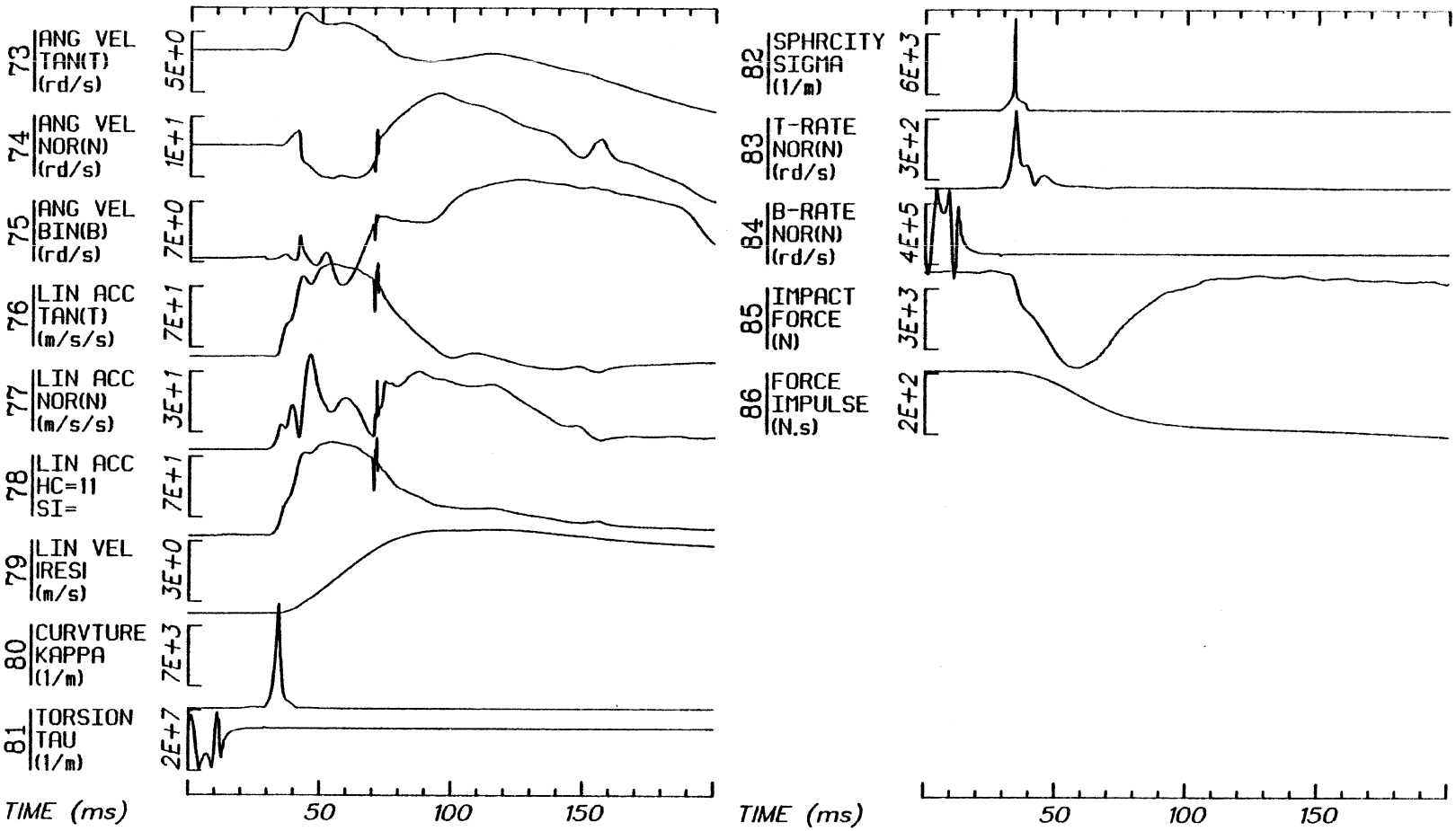

Run ID: 83E087 Disk: 83E087.3 File: 1 Date: MAY 11, 1985 Sheet: 5

Filter:1600*4C

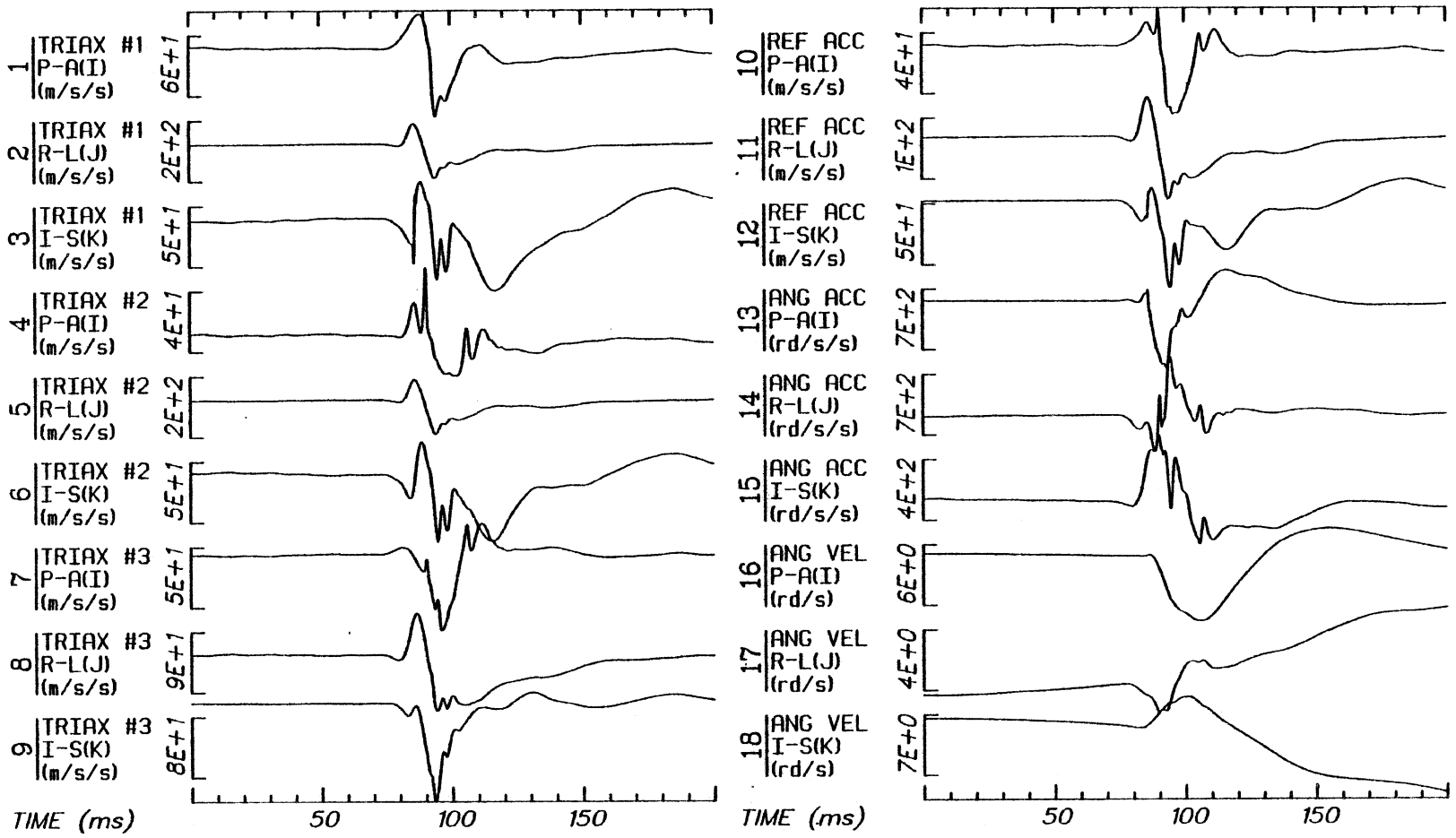

Run ID: 83E088 Disk: 83E088.3 File: 1 Date: MAY 11, 1985 Sheet: 1

Filter:1600*4C

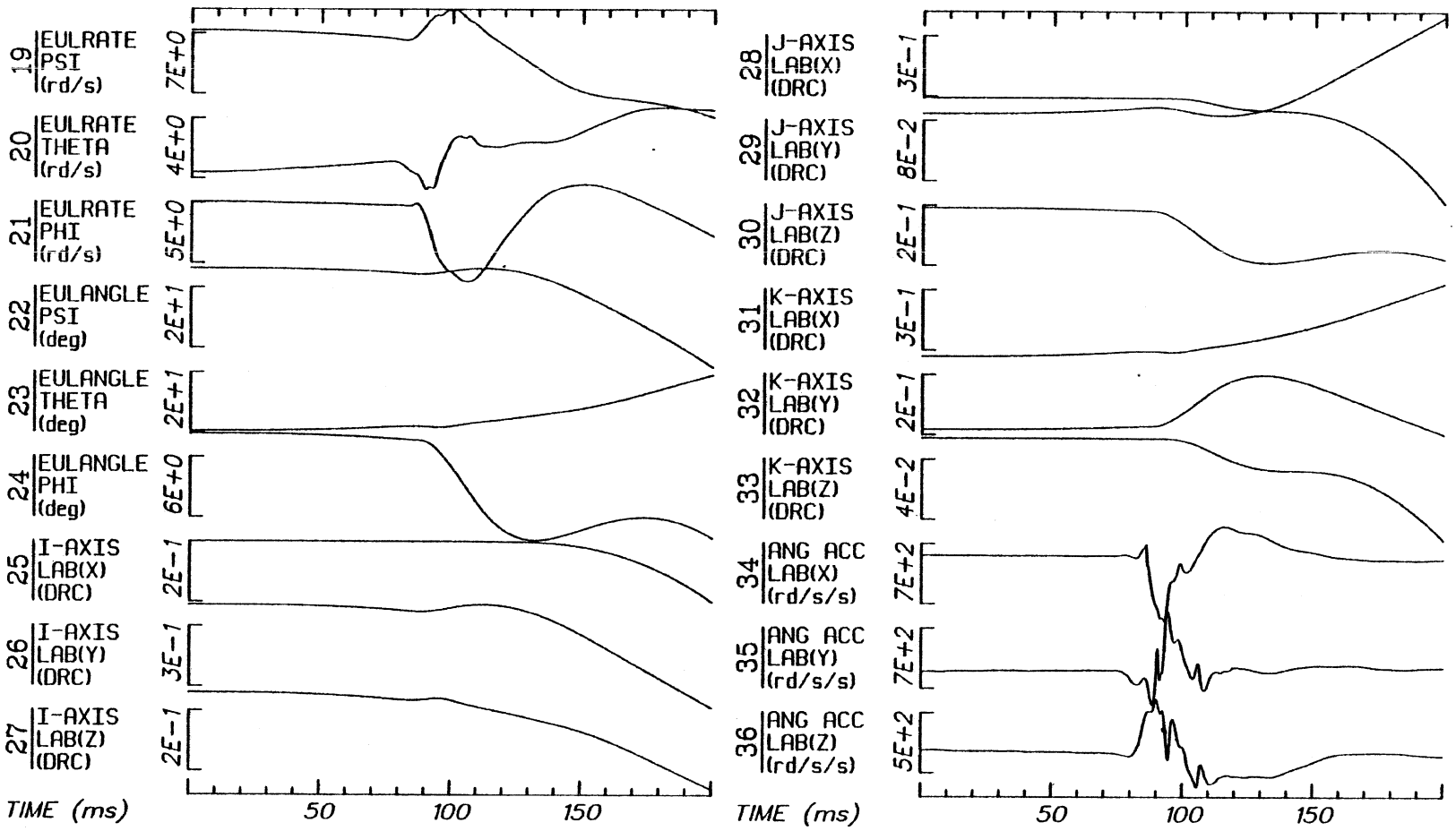

Run ID: 83E088 Disk: 83E088.3 File: 1 Date: MAY 11, 1985 Sheet: 2

Filter:1600*4C

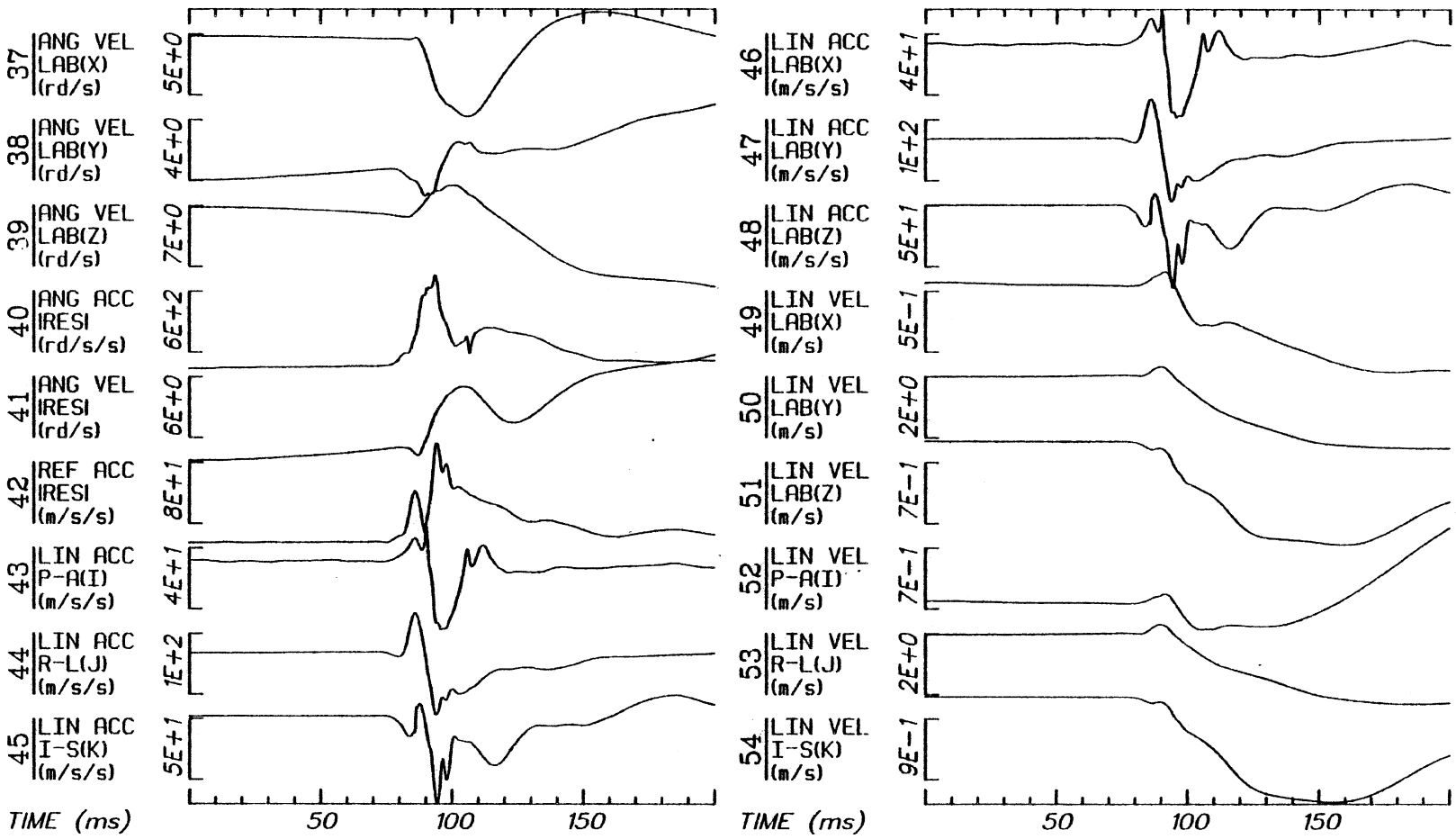

Run ID: 83E088 Disk: 83E088.3 File: 1 Date: MAY 11, 1985 Sheet: 3

Filter:1600*4C

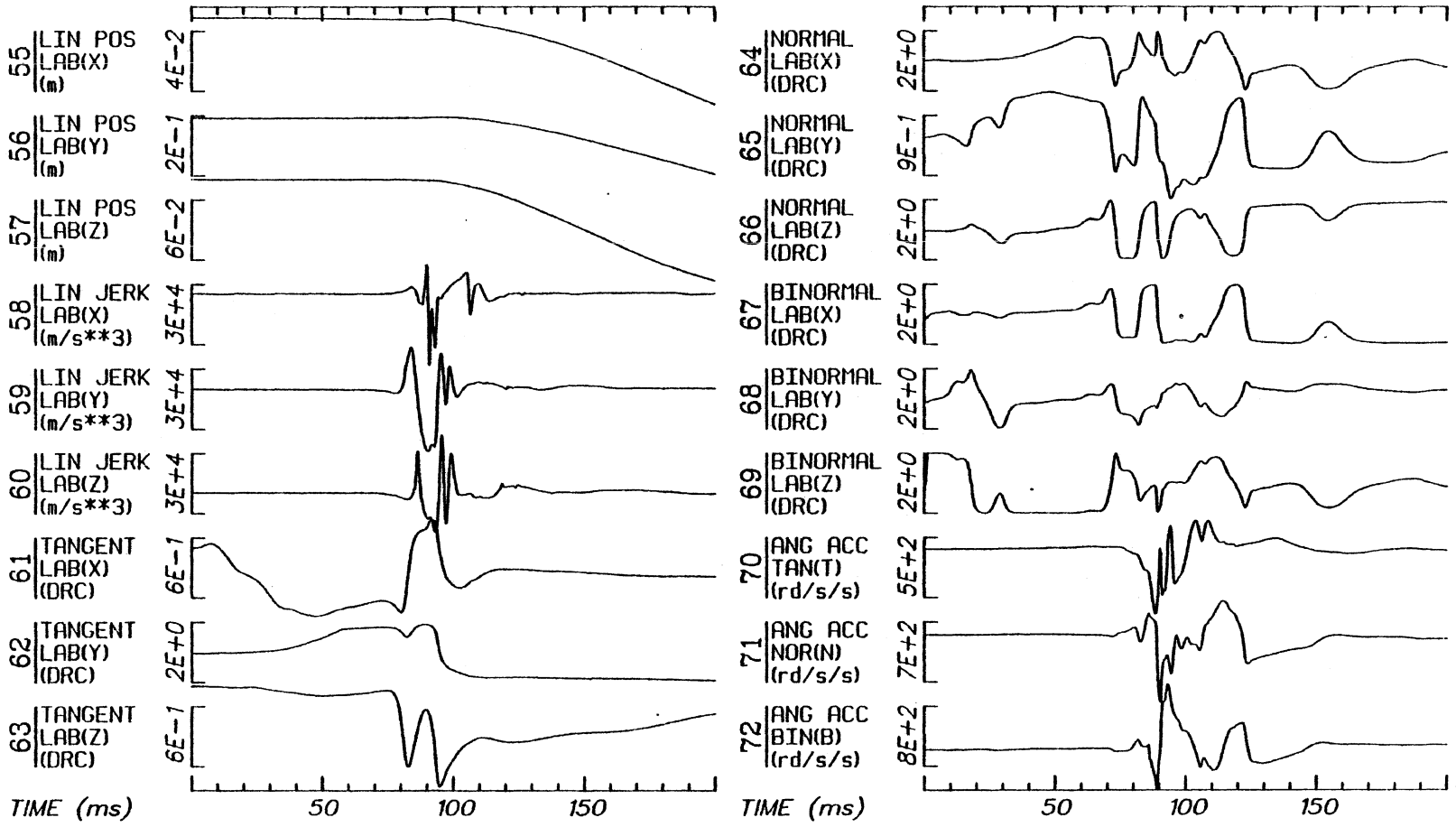

Run ID: 83E088 Disk: 83E088.3 File: 1 Date: MAY 11, 1985 Sheet: 4

Filter:1600*4C

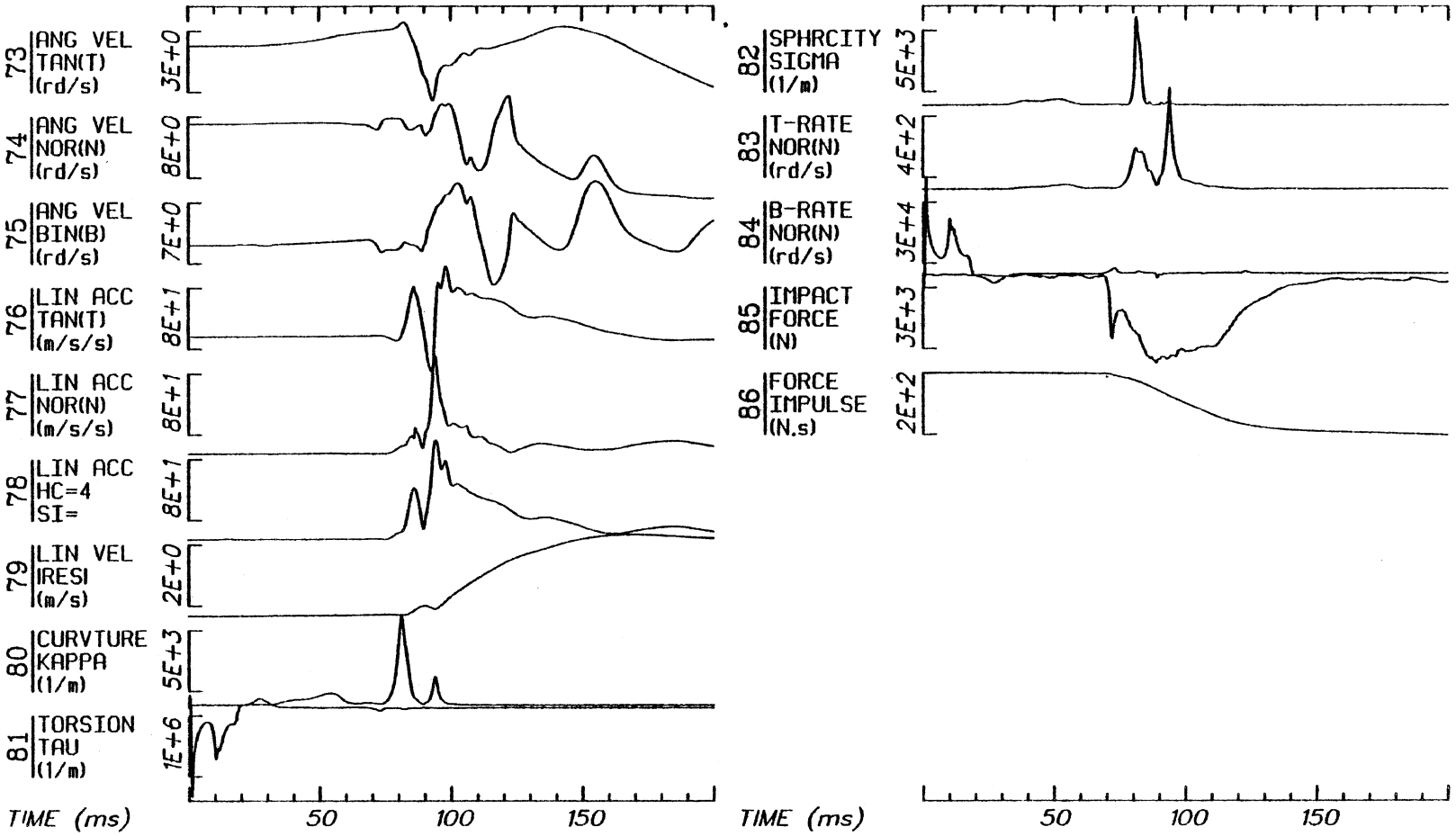

Run ID: 83E088 Disk: 83E088.3 File: 1 Date: MAY 11, 1985 Sheet: 5

Filter:1600*4C

Run ID: 83E091 *Filter:1600*4C Smooth: 3SD*

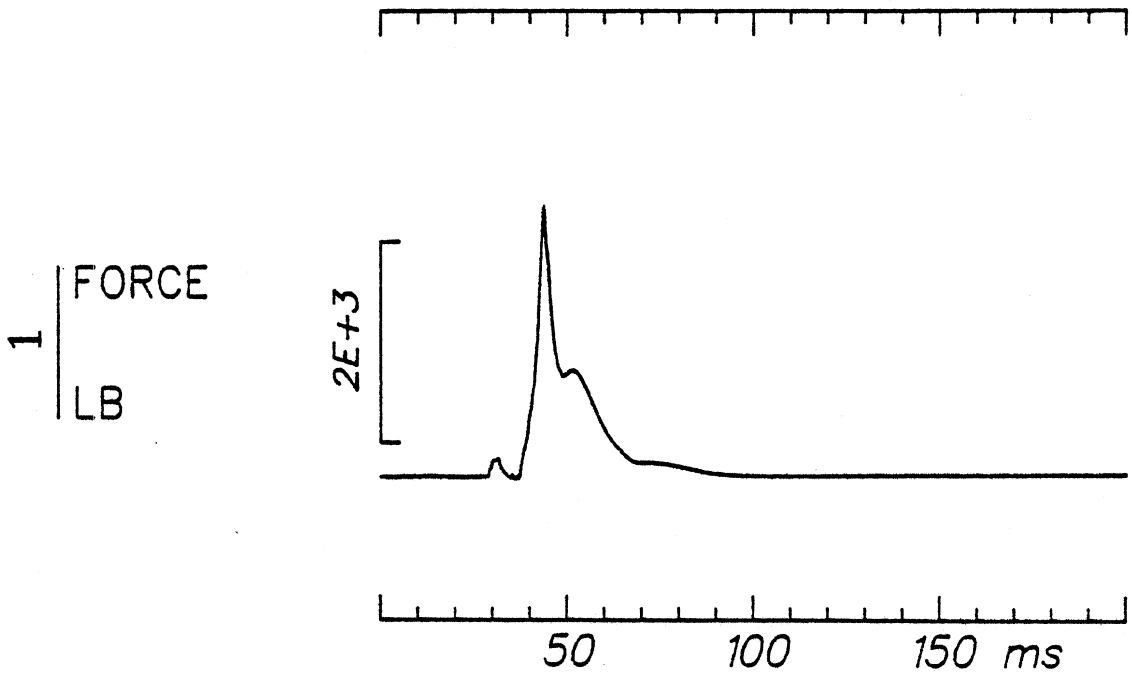

Run ID: 83E093 *Filter:1600*4C Smooth: 3SD*

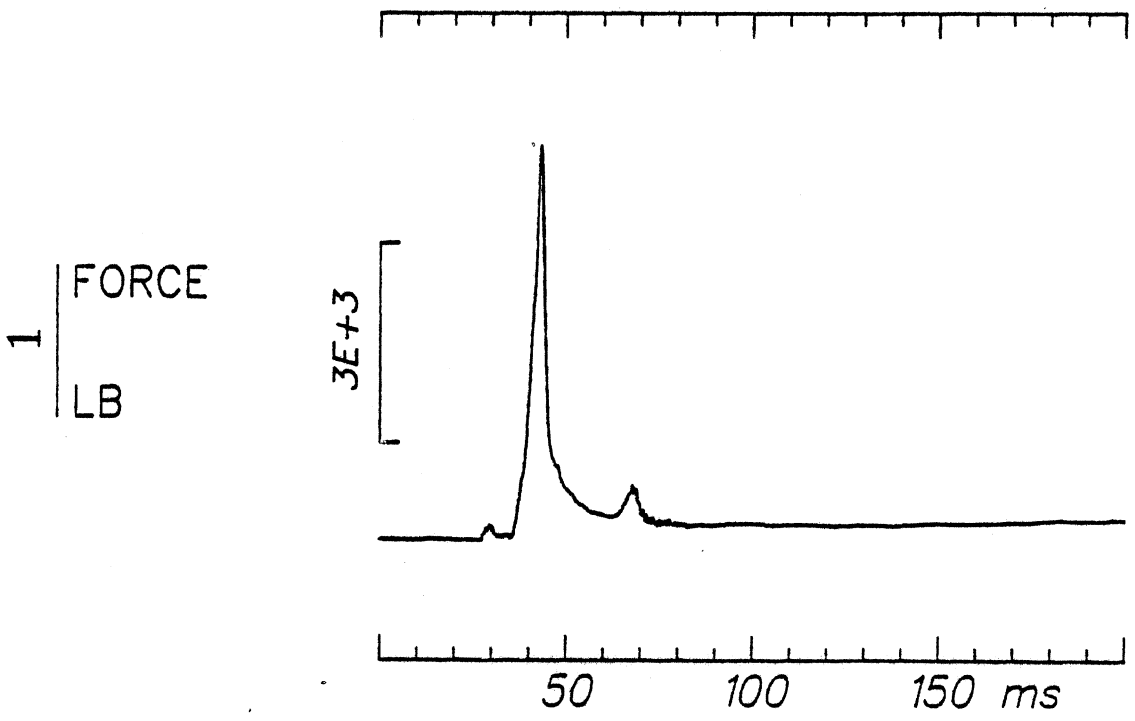

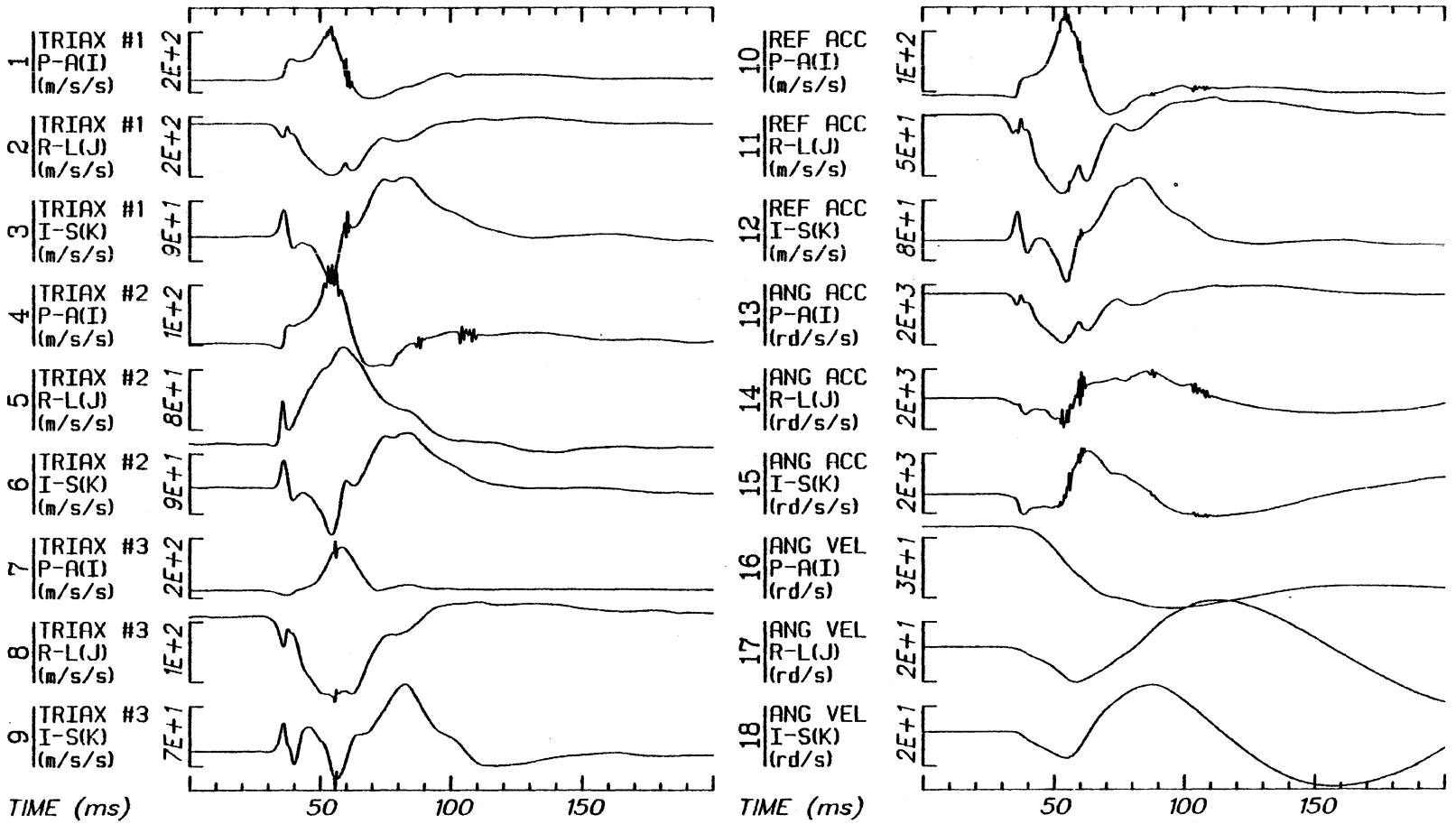

Run ID: 83E109 Disk: 83E109.3 File: 1 Date: MAY 11, 1985 Sheet: 1

Filter:1600*4C

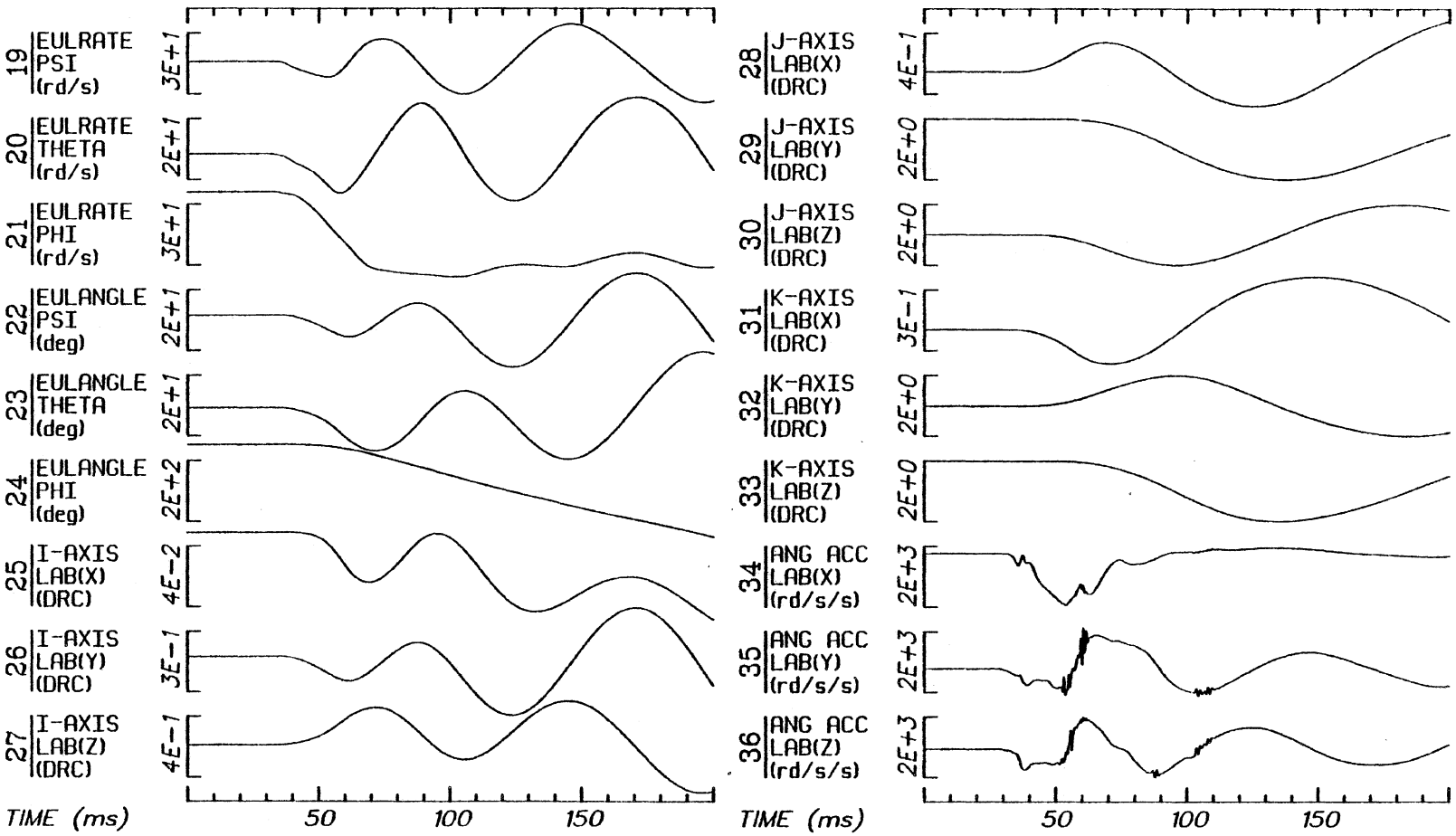

Run ID: 83E109 Disk: 83E109.3 File: 1 Date: MAY 11, 1985 Sheet: 2

Filter:1600*4C

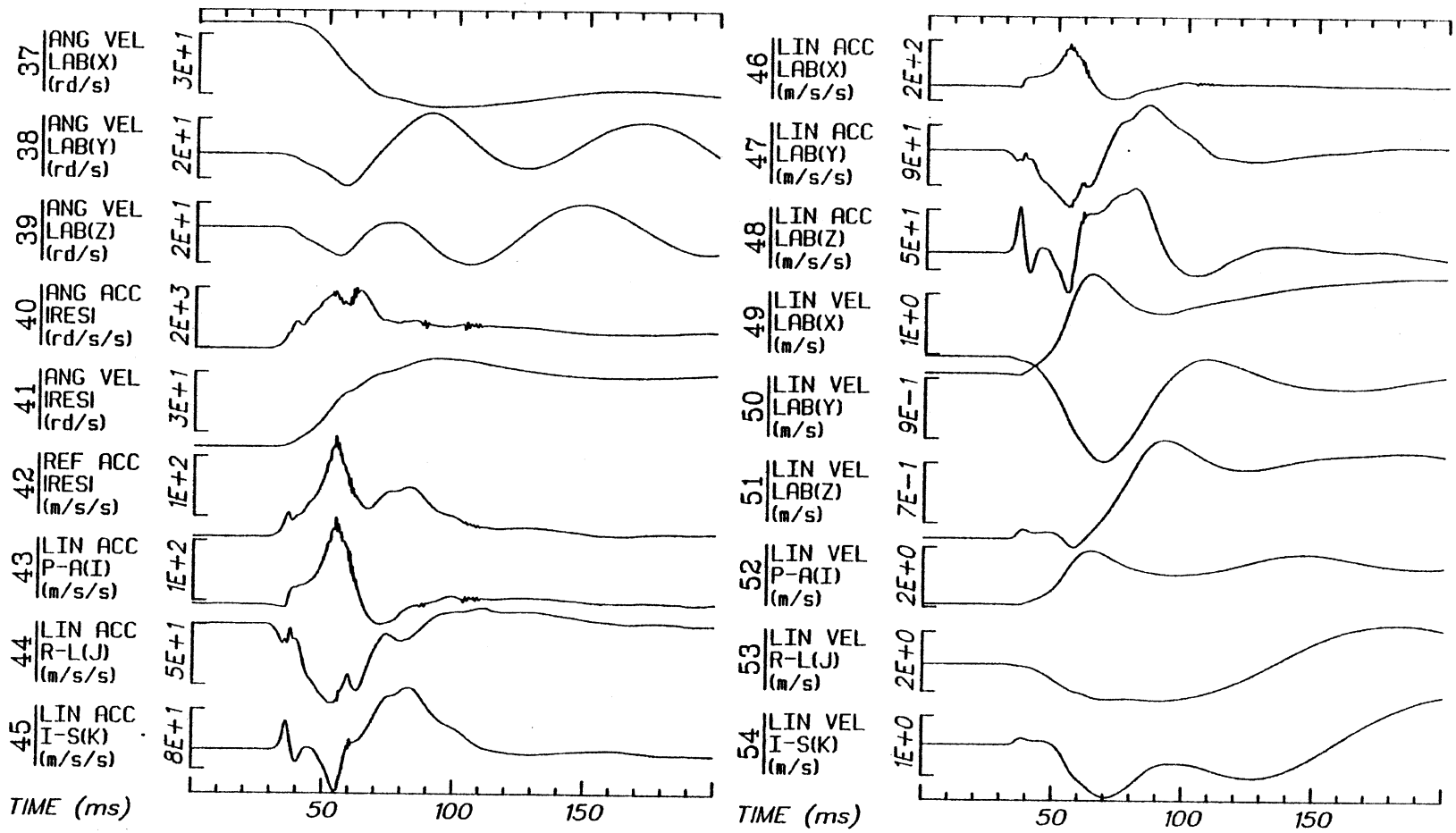

Run ID: 83E109 Disk: 83E109.3 File: 1 Date: MAY 11, 1985 Sheet: 3

*Filter:1600*4C*

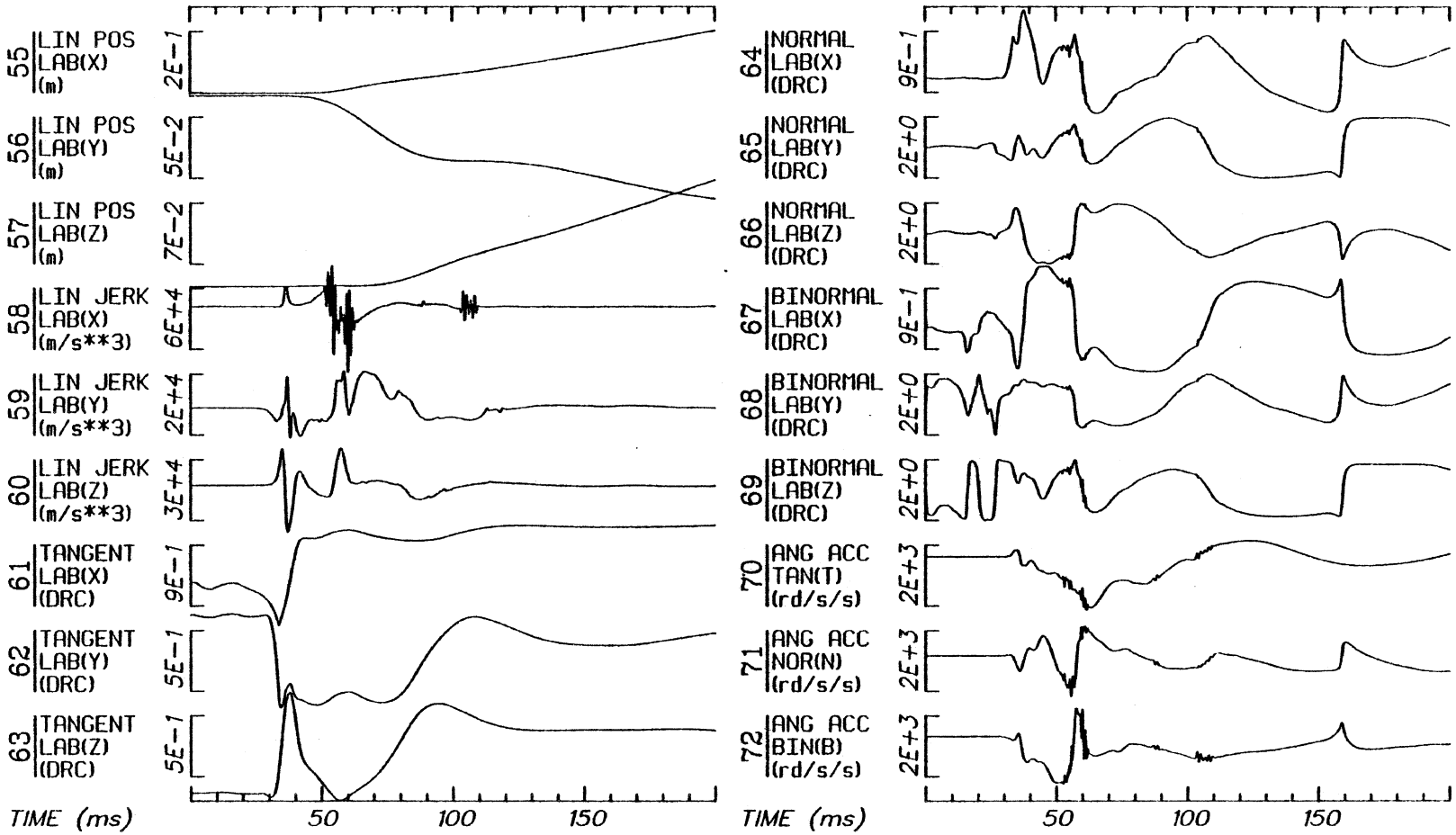

Run ID: 83E109 Disk: 83E109.3 File: 1 Date: MAY 11, 1985 Sheet: 4

Filter:1600*4C

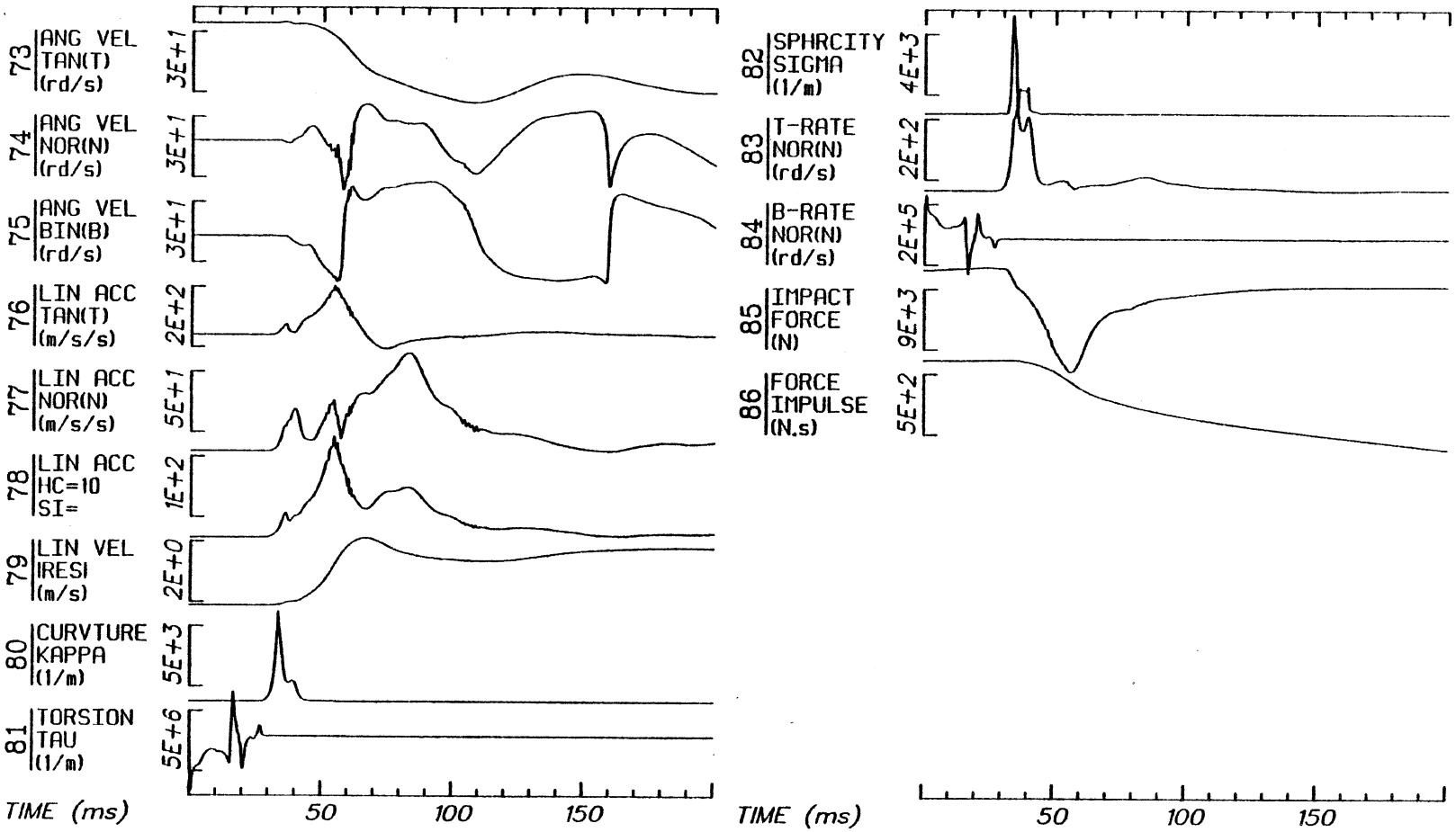

Run ID: 83E109 Disk: 83E109.3 File: 1 Date: MAY 11, 1985 Sheet: 5

*Filter:1600*4C*